

For Reference

NOT TO BE TAKEN FROM THIS ROOM

Ex LIBRIS
UNIVERSITATIS
ALBERTAENSIS



SPECIAL COLLECTIONS

UNIVERSITY OF ALBERTA LIBRARY

REQUEST FOR DUPLICATION

I wish a photocopy of the thesis by

A.V. Gopala Krishnayya (author)

entitled Analysis of Cracking of Earth Dams

The copy is for the sole purpose of private scholarly or scientific study and research. I will not reproduce, sell or distribute the copy I request, and I will not copy any substantial part of it in my own work without permission of the copyright owner. I understand that the Library performs the service of copying at my request, and I assume all copyright responsibility for the item requested.

SPECIAL COLLECTIONS
UNIVERSITY OF ALBERTA LIBRARY

REQUEST FOR REPRODUCTION

I wish a photograph of the thesis by

(author) _____

entitled _____

a copy is for the sole purpose of private scholarly or scientific study
and research. I will not reproduce, sell or distribute the copy I request,
and I will not copy any substantial part of it in my own work without per-
mission of the copyright owner. I understand that the library performs
a service of copying at my request, and I assume all copyright responsi-
bility for the item requested.



Digitized by the Internet Archive
in 2022 with funding from
University of Alberta Libraries

THE UNIVERSITY OF ALBERTA

RELEASE FORM

NAME OF AUTHOR A.V. GOPALAKRISHNAYYA
TITLE OF THESIS ANALYSIS OF CRACKING OF EARTH DAMS
.....
UNIVERSITY UNIVERSITY OF ALBERTA
DEGREE FOR WHICH THESIS WAS PRESENTED Ph.D.
YEAR THIS DEGREE GRANTED 1973

Permission is hereby granted to THE UNIVERSITY OF ALBERTA LIBRARY to reproduce single copies of this thesis and to lend or sell such copies for private, scholarly or scientific research purposes only.

The author reserves other publication rights, and neither the thesis nor extensive extracts from it may be printed or otherwise reproduced without the author's written permission.

THE UNIVERSITY OF ALBERTA

PLEASE FOLD

NAME OF AUTHOR
ANALYST OF DRAWINGS OR PHOTO DATA
TITLE OF THESIS
UNIVERSITY OF ALBERTA
UNIVERSITY

DEGREE FOR WHICH THESIS WAS SUBMITTED
YEAR THIS DEGREE GRANTED
1973

Permission is hereby granted to the University of
ALBERTA LIBRARY to reproduce single copies of this
thesis and to lend or sell such copies for private,
scholarly or scientific research purposes only.
The author reserves other publication rights, and
neither the thesis nor extensive extracts from it may
be printed or otherwise reproduced without the author's
written permission.

DATE
1973

THE UNIVERSITY OF ALBERTA

ANALYSIS OF CRACKING OF EARTH DAMS

by



ADDANKI VENKATA GOPALAKRISHNAYYA

A THESIS

SUBMITTED TO THE FACULTY OF GRADUATE STUDIES AND RESEARCH
IN PARTIAL FULFILMENT OF THE REQUIREMENTS FOR THE DEGREE
OF DOCTOR OF PHILOSOPHY

DEPARTMENT OF CIVIL ENGINEERING

EDMONTON, ALBERTA

SPRING, 1973

THE UNIVERSITY OF ALBERTA

FACULTY OF GRADUATE STUDIES AND RESEARCH

The undersigned certify that they have read, and recommend to the Faculty of Graduate Studies and Research for acceptance, a thesis entitled "ANALYSIS OF CRACKING OF EARTH DAMS" submitted by Addanki Venkata Gopalakrishnayya in partial fulfilment of the requirements for the degree of Doctor of Philosophy.

ABSTRACT

This dissertation deals with the finite element analysis of cracking of earth dams. The principal objectives of this investigation are (1) to contribute to an understanding of the tensile behaviour of a low-plastic core soil which has a high susceptibility to tensile cracking, (2) to study the relative importance of the factors that influence the analysis of cracking of earth dams, and (3) to develop analytical procedures for prediction and control of tensile cracks that are likely to develop during and at the end of the construction period.

The indirect tension test (Brazilian test) was used to conduct laboratory tensile studies on Mica Till. A procedure was developed to determine the tensile stress-strain relationship based on the results of the biaxial, indirect tension test.

The laboratory studies showed that a core material of low plasticity has a very low tensile strength which, for the purpose of analysis of cracking of earth dams, can be ignored. A rapid increase in flexibility of soil in tension was accompanied by a rapid decrease in tensile strength when water content was increased beyond the standard Proctor optimum. However, with the addition of a small percentage of bentonite to till it was possible to increase the flexibility of the mixture without an appreciable reduction of its tensile strength. An increase in the compactive effort increased the

tensile strength of till and decreased its flexibility, for water contents well below the Proctor optimum. For water contents above optimum, the tensile strength and the stiffness of soil were slightly decreased with the increase of compactive effort. The rate of tensile loading had a considerable influence on the tensile characteristics of till. Rates of loading mobilizing the minimum tensile strength and tensile failure strain were observed.

From the finite element analysis conducted with two and three dimensional modelling of earth dams, it has been observed that the construction step sequence, the non-linear stress-strain relationships of soil, and the boundary conditions associated with the three dimensionality of a dam are the most important factors to be properly simulated in the analysis for reasonable predictions of cracking of earth dams. Such simulation procedures were developed and their usefulness in practice was tested by analyzing a case study of cracking at Duncan Dam. The predicted location of cracks and sequence of their occurrence showed reasonable agreement with the field observations.

The analytical procedure developed can also be used as a design tool to study the influence of different factors on control of cracking of earth dams. A method is indicated for controlling tensile cracks in an earth dam, built in a narrow valley with rigid abutments and on incompressible foundations. The method consists of performing analyses with non-homogeneous modelling of the core material of the

dam to specify the placement conditions of core material
for an effective control on the development of tensile cracks.

ACKNOWLEDGEMENTS

The work reported in this thesis was carried out in the Department of Civil Engineering, University of Alberta, under the supervision of Dr. Z. Eisenstein.

The author expresses his sincere gratitude to Dr. Eisenstein for his guidance, help, and encouragement throughout the period of this study.

The author's sincerest thanks are due to Professor N.R. Morgenstern and Professor D.W. Murray with whom he had many stimulating and highly rewarding discussions. The suggestions given by Professor S. Thomson on the form of presentation of the thesis are highly appreciated.

The author is grateful to Dr. R.M. Hardy for providing access to the detailed field observations at Duncan Dam and to both the Montreal Engineering Co. Ltd. and the British Columbia Hydro Power Authority for permission to use these data in this study.

The assistance received from Messrs. O. Wood, G. Cyre, A. Muir and R.F. Howells of the Department of Civil Engineering in the experimental and the computational work is gratefully acknowledged.

The author expresses his sincere thanks to Mr. L.M. Chizawsky of the Alberta Research Council, Highways Division, for his helpful suggestions in building the tensile clip gauges used in the experiments.

The author is highly grateful to the University of

Alberta and the National Research Council of Canada for providing him financial support throughout the period of the study.

All the research work reported in this thesis has been carried out with the assistance of grants from the National Research Council of Canada.

Acknowledgements are due to Miss Susan Schultz for typing of the thesis.

The author wishes to express his sincerest gratitude to his wife, Leela, for her encouragement throughout the period of this work.

TABLE OF CONTENTS

	Page
CHAPTER I - INTRODUCTION.....	1
1.1 Scope.....	1
1.2 Importance of the Problem of Cracking of Earth and Rockfill Dams.....	1
1.3 General Information on Cracking of Earth and Rockfill Dams.....	2
1.3.1 Factors Contributing to the Formation of Cracks.....	2
1.3.2 Types of Cracks.....	3
1.4 Usefulness of an Analysis for the Pre- diction of Cracking of Dams.....	4
1.5 Brief Review of Past Work on Cracking of Dams.....	5
1.6 Requirements of an Analysis for Pre- dicting Cracks.....	8
1.7 Objectives of the Present Investigation....	9
1.8 Scope of the Present Work.....	9
CHAPTER II - LABORATORY STUDIES ON THE TENSILE BEHAVIOUR OF SOILS.....	13
2.1 Scope.....	13
2.2 Introduction.....	13
2.3 A Brief Review of Previous Studies on the Tensile Behaviour of Soils.....	14
2.4 Different Types of Test for Tensile Testing of Soils.....	19
2.4.1 Direct or Uniaxial Tension Test....	19
2.4.2 Flexure or Beam Test.....	20
2.4.3 Indirect Tension Test or Brazi- lian Test.....	20

	Page
2.4.4 Choice of the Type of Test for Present Studies.....	22
2.5 Theoretical Consideration of the Indirect Tension Test.....	22
2.5.1 Theoretical Stress Solutions.....	22
2.5.2 Effect of Different Elastic Moduli in Tension and Compression..	25
2.5.3 Evaluation of the Tensile Stress-Strain Relationship.....	28
2.6 Experimental Set-Up for Laboratory Tensile Tests.....	30
2.6.1 Load Measuring Device.....	30
2.6.2 Tensile Deformation Measuring Device.....	31
2.7 Experimental Set-Up for Laboratory Compression Tests.....	32
2.8 Description of Laboratory Tests.....	33
2.8.1 Description of Soil Used for Tensile and Compressive Tests.....	33
2.8.2 Tests Performed.....	34
2.8.3 Soil Preparation and Compaction of the Sample for Tension and Compression Tests.....	34
2.8.4 Specimen Preparation for Tension Test.....	37
2.8.5 Tension Test Operation.....	39
2.8.6 Computation of Tensile Stress and Strain.....	39
2.9 An Example to Illustrate the Procedure of Deriving the Tensile Stress-Strain Relationship.....	42

2.10	Discussion of Tension and Compression Test Results.....	45
2.10.1	Effect of Water Content.....	46
2.10.2	Effect of Compactive Effort.....	46
2.10.3	Effect of Rate of Loading.....	47
2.10.4	Effect of Adding Bentonite.....	49
2.10.5	Comparison of Compression and Tensile Characteristics.....	51
2.11	Summary.....	51
CHAPTER III - SIMULATION PROCEDURES FOR LINEAR AND NON-LINEAR FINITE ELEMENT ANALYSES.....		92
3.1	Scope.....	92
3.2	Introduction.....	92
3.3	Use of Isotropic Elastic Theory and Its Limitations.....	93
3.4	Types of Analyses Performed.....	95
3.5	Two Dimensional Finite Element Analyses....	97
3.6	Three Dimensional Finite Element Analyses..	99
3.7	Determination of the Elastic Parameters for Non-Linear Analysis.....	100
3.8	Validity of Triaxial Test Data for Interpolating the Elastic Parameters.....	102
3.8.1	Simulation of the Drainage Conditions.....	103
3.9	Method of Deriving the Moduli of Elasticity.....	105
3.9.1	Derivation Procedure.....	106
3.9.2	Studies to Check the Accuracy of the Procedure of Derivation of Elastic Parameters.....	110

3.9.3	Effect of Intermediate Principal Stress on Stress-Strain Results....	111
3.10	Isotropic Compression.....	111
3.11	Summary.....	112
CHAPTER IV - IMPORTANCE OF CERTAIN FACTORS IN THE ANALYSIS OF CRACKING OF DAMS.....		121
4.1	Scope.....	121
4.2	Introduction.....	121
4.3	Selection of Sections for Parametric Studies.....	122
4.4	Accuracy of Two Dimensional Analyses.....	123
4.5	Influence of the Construction Step Sequence.....	124
4.6	Two Dimensional Linear, Non-Linear, and "No Tension" Analyses.....	124
4.7	Effect of the Intermediate Principal Stress.....	128
4.8	Three Dimensional Effects.....	129
4.8.1	General.....	129
4.8.2	Three Dimensional Studies.....	129
4.9	Considerations of the Flexibility of the Core to Control Cracking.....	134
4.10	Summary.....	137
CHAPTER V - ANALYSIS OF CRACKING AT DUNCAN DAM.....		157
5.1	Scope.....	157
5.2	Introduction.....	157
5.3	History of Cracking at Duncan Dam.....	158
5.3.1	Salient Features.....	158
5.3.2	Observed Differential Settlement Cracks.....	159

	Page
5.3.3 Sequence of Appearance of Cracks...	160
5.4 Analysis of Cracking.....	161
5.5 Results of Analyses.....	165
5.5.1 Three Dimensional Analysis.....	165
5.5.2 Two Dimensional Analysis.....	169
5.6 Summary.....	169
CHAPTER VI - CONCLUSIONS AND SUGGESTIONS FOR FURTHER RESEARCH.....	186
6.1 General.....	186
6.2 Criterion for Failure of Soil in Tension...	187
6.3 Tensile Characteristics of Soil.....	189
6.4 Factors Affecting the Development of Tensile Zones in Earth Dams during Con- struction.....	191
6.4.1 Single Step and Incremental Loading.....	191
6.4.2 Linear and Non-Linear Analyses.....	192
6.4.3 "No Tension" Analysis.....	192
6.4.4 Three Dimensional Effects.....	193
6.5 Control of Cracking by Non-Homogeneous Modelling.....	193
6.6 Applicability of the Analysis of Crack- ing to a Real Structure.....	194
6.7 Suggestions for Further Research.....	194
REFERENCES.....	197
APPENDIX A - COMPUTER PROGRAM FOR TWO DIMENSIONAL FINITE ELEMENT ANALYSIS.....	A.1
A.1 Scope.....	A.1
A.2 Language, Code and Limitations.....	A.1

	Page
C.3 Element Stiffness Evaluation.....	C.3
APPENDIX D - FINITE ELEMENT METHOD FOR THE ANALYSIS OF INDIRECT TENSION TEST.....	D.1
D.1 Scope.....	D.1
D.2 Basic Considerations for a Bilinear Material.....	D.1
D.3 Analysis of Indirect Tension Test.....	D.3

LIST OF FIGURES

Figure		Page
1.1	Classification of Cracks in the Core of a Dam.....	12
1.2	Basic Modes of Crack-Surface Displacements.....	12
2.1	Theoretical Solutions for Stresses along the Vertical Diameter of a Specimen Subjected to Diametral Compression.....	57
2.2	Variation of Stresses along the Horizontal Diameter of a Specimen under Diametral Compression (Comparison of Theoretical and Finite Element Solutions and Effect of Poisson's Ratio on Stress Distribution)....	58
2.3	Variation of Compressive and Tensile Stress at the Centre of Specimen with Shear Modulus for Different Ratios of E_c/E_t	59
2.4	Variation of Tensile and Compressive Stress at the Centre of Specimen under Diametral Compression with the Ratio E_c/E_t (Stresses Correspond to G/E_c equal to 0.4).....	60
2.5	Variation of Vertical and Horizontal Stress along the Horizontal Diameter of Specimen under Diametral Compression for Different E_c/E_t (Stresses Computed for G/E_c equal to 0.4).....	61
2.6	Tensile Test Set-Up with Specimen in position.....	62
2.7	View Showing Data Acquisition System and Transducer Amplifiers.....	62
2.8	Schematic Diagram Showing the Data Acquisition System and Transducer Amplifiers.....	63
2.9(a)	Details of the Clip Gauge for Tension Test (Clip Gauge Positioned on the Specimen Between Gauge Blocks).....	64

Figure		Page
2.9(b)	Details of the Clip Gauge for Tension Test (Full Bridge Circuit for the Clip Gauge).....	64
2.10(a)	A Close-Up View of Specimen with Clip Gauge in Position.....	65
2.10(b)	A Side View of Specimen with Clip Gauge in Position.....	65
2.11	Set-Up for Unconfined Compression Test....	66
2.12	A Close-Up View of the Lateral Strain Indicator.....	66
2.13	Grain Size Distribution for Mica Till.....	67
2.14	Water Content-Density Relationships for Samples of Different Sizes Prepared under Proctor Standard Compaction.....	68
2.15	Specimen with Gauge Block Jig in Position.	69
2.16	Components for Attaching Gauge Blocks to Soil Specimen.....	69
2.17(a)	Tensile Test Specimen Before and After Failure (Specimen Kept on a Stand Before Waxing).....	70
2.17(b)	Tensile Test Specimen Before and After Failure (Typical Brittle Failure of Specimen).....	70
2.18	Variation of Coefficient (C_ℓ) with E_c/E_t for Poisson's Ratio Equal to 0.365.....	71
2.19	Stress-Strain Relationship and the Variation of Lateral Strain and Poisson's Ratio with Axial Strain for Mica Till Tested under Unconfined Compression.....	72
2.20	Relationship between Tensile Stress and the Observed Tensile Strain for Mica Till.	73
2.21	Comparison of Tensile Stress-Strain Relationships Derived from Tensile Test Data of Mica Till.....	74

Figure		Page
2.22	Effect of Water Content on the Tensile Stress at Failure for Mica Till.....	75
2.23	Effect of Water Content on the Tensile Strain at Failure for Mica Till.....	76
2.24	Variation of Stiffness in Tension with Water Content for Mica Till.....	77
2.25	Water Content-Density Relationships for Mica Till at Different Compactive Efforts.	78
2.26	Variation of Tensile Strength with Water Content for Mica Till at Different Compactive Efforts.....	79
2.27	Variation of Tensile Strain at Failure with Water Content for Mica Till at Different Compactive Efforts.....	80
2.28	Variation of Stiffness in Tension with Water Content for Mica Till at Different Compactive Efforts.....	81
2.29	Effect of Rate of Loading on the Tensile Strength of Mica Till.....	82
2.30	Effect of Rate of Loading on the Tensile Strain at Failure for Mica Till.....	83
2.31	Water Content-Density Relationships of Mica Till With and Without the Addition of Bentonite.....	84
2.32	Comparison of Tensile Strength of Mica Till With and Without the Addition of Bentonite.....	85
2.33	Comparison of Tensile Strain at Failure for Mica Till With and Without the Addition of Bentonite.....	86
2.34	Comparison of Stiffness in Tension for Mica Till With and Without the Addition of Bentonite.....	87
2.35	Percent Decrease in Tensile Strength Caused by a 2% Increase in Water Content Above Optimum for Soils with Different Consistency Limits.....	88

Figure		Page
2.36	Stress-Strain Relationships of Mica Till Tested under Unconfined Compression.....	89
2.37	Variation of Tensile Failure Stress and Strain with Water Content for Mica Till Tested under Unconfined Compression.....	90
2.38	Comparison of Compressive and Tensile Characteristics of Mica Till at Different Water Contents.....	91
3.1	Triaxial Test Data for a Silty Sand Plotted in the Conventional Manner.....	114
3.2	Triaxial Test Data for a Silty Sand Plotted in Terms of Stress and Strain Invariants and Axial Strain.....	115
3.3	Finite Element Idealization of a Soil Block.....	116
3.4	Comparison of "Past Stress" and "Average Moduli" Solutions in an Incremental Analysis Performed in Five Increments.....	117
3.5	Comparison of Incremental Non-Linear Plane Strain Solutions with Different Assumptions Regarding the Intermediate Principal Stress (Analyses in Five Increments).....	118
3.6	Comparison of Incremental Non-Linear Solutions Obtained for Different Boundary Conditions (Analyses in Five Increments)..	119
3.7	Comparison of Predicted and Experimental Stress-Strain Relationship for Isotropic Compression.....	120
4.1	Section Assumed in Two Dimensional Analyses.....	139
4.2	Quadrant of Dam Assumed in Three Dimensional Analyses.....	140
4.3	Comparison of Vertical and Horizontal Displacements for Two Dimensional Single Step Analyses.....	141

Figure		Page
4.4	Comparison of Tension Zones Computed by Single Step Two Dimensional Linear Elastic Analyses.....	142
4.5	Effect of Number of Lifts on Maximum Horizontal Stress, Strain and Vertical Displacement of Two Dimensional Section...	143
4.6	Stress Strain Relationships for Silty Sand.....	144
4.7	Tensile Zones Developed for Linear Analysis After Certain Number of Lifts....	145
4.8	Comparison of Linear Analysis With and Without Removal of Tension.....	146
4.9	Tensile Zones Developed for Non-Linear Analysis After Certain Number of Lifts....	147
4.10	Comparison of Non-Linear Plane Strain Analyses with Different Assumptions Regarding the Intermediate Principal Stress (10 Lifts).....	148
4.11	Vertical Displacement Along Crest for Two and Three Dimensional Analysis, Single Lift.....	149
4.12	Horizontal Stress and Strain Along Crest for Two and Three Dimensional Analyses in Single Lift.....	150
4.13	Comparison of Results of Two and Three Dimensional Incremental Linear Analyses Performed on a Homogeneous Dam (5 Increments).....	151
4.14	Comparison of Horizontal Stresses Along Crest for Two and Three Dimensional Analyses at Different Ratio of Moduli of Core to Shell.....	152
4.15	Comparison of Displacement Pattern and Development of Tensile Cracks on the Surface of Dam for Modular Ratios of Core to Shell Equal to 10 and 0.1. Results by Three Dimensional Linear Analyses in 5 Increments.....	153

Figure		Page
4.16	Comparison of Stresses in Core and Shell Close to the Maximum Longitudinal Section of Dam for Modular Ratios of Core to Shell Equal to 10 and 0.1. Results by Three Dimensional Linear Analyses in 5 Increments.....	154
4.17	Comparison of Maximum Tensile Stresses in Core for Different Ratios of Moduli of Core to Shell.....	155
4.18	Effect of the Non-Homogeneity of Core on the Reduction of Tensile Zones.....	156
5.1	Longitudinal Section of Duncan Dam Showing Construction Sequence and Location of Cracks.....	171
5.2	A Typical Cross Section of Duncan Dam.....	172
5.3	Plan View of Duncan Dam Showing Location of Settlement Gauges and Area of Cracks...	173
5.4	Settlement Along Longitudinal Sections.....	174
5.5	Sequence of Development of Cracks.....	175
5.6	Section of Dam at a Distance of 440 Feet from Left Abutment Showing Approximate Zones in which Cracks Developed Progressively.....	176
5.7	Finite Element Idealization at Section 3 for Three Dimensional Analysis.....	177
5.8	Consolidated Undrained Triaxial Stress-Strain Relationships for the Core and Semi-Pervious Material of Duncan Dam.....	178
5.9	Consolidated Drained Triaxial Stress-Strain Relationships for Pervious Material	179
5.10	Consolidated Drained Triaxial Stress-Strain Relationships for Common Pervious Material.....	180
5.11	Grain Size Distribution Curves for Materials of Duncan Dam.....	181
5.12	Distribution of Minimum Principal Stresses and Strains Along Vertical Lines I, II, III, and IV.....	182

Figure		Page
5.13	Minimum Principal Stresses and Strains Along Two Longitudinal Sections for Three Dimensional Analysis.....	183
5.14	Finite Element Idealization Along Central Longitudinal Section for Two Dimensional Analysis.....	184
5.15	Minimum Principal Stresses and Strains Along the Central Longitudinal Section for Two Dimensional Analysis.....	185
B.1	Sequence of Calling Different Subroutines.	B.27
B.2	Approximate CPU Time for Solution of Equations in 3-D Program.....	B.28
B.3	Three Dimensional View of a Model Dam.....	B.29
B.4	Sectional Views of Model Dam.....	B.30
C.1	Eight Node Hexahedron Representation in Local and Cartesian Co-ordinates.....	C.6
D.1	Finite Element Idealization of a Quadrant of the Circular Section Analysed.....	D.4

CHAPTER I

INTRODUCTION

1.1 Scope

In this chapter the problem of cracking of earth and rockfill dams is introduced, the past work done on the topic is reviewed, and the purpose of the present work and its scope are presented.

1.2 Importance of the Problem of Cracking of Earth and Rockfill Dams

Cracking of the core of an earth or rockfill dam has been a subject of considerable importance to the designers of dams for a number of years. Cracking of several earth and rockfill dams and in some cases, subsequent failures caused by erosion of soil through the cracks have been reported in the literature (Marsal and Ramirez, 1967; Patrick, 1967; Pope, 1967; Schober, 1967; Kjaernsli and Torblaa, 1968; Gordon and Duguid, 1970; Vaughan et al., 1970). The cracking phenomenon is a matter of considerable concern because, most of these dams in which this distress occurred were built with the best available construction practices developed over recent years. The ASCE Committee on Earth and Rockfill Dams (1967) stressed the importance of research concerning cracking of the core of earth and rockfill dams. It is necessary to evolve suitable design and construction procedures for earth and rockfill dams to resist cracking. This necessity

has been strengthened further by the increasing need to utilize heterogeneous compressible foundations, irregular steep valley walls, declining quality of embankment materials at many sites, and fills of ever increasing height.

1.3 General Information on Cracking of Earth and Rockfill Dams

Covarrubias (1969) and Lowe (1970) have noted several factors that contribute to the cracking of earth and rockfill dams, the different types of cracks, and their relative importance with respect to the safety of the structure. For completeness some general information on cracking of earth and rockfill dams is discussed in the following sections.

1.3.1 Factors Contributing to the Formation of Cracks

Stress states favouring the formation of cracks in earth and rockfill dams are generally caused by any one or a combination of the factors listed below:

- (a) Excessive differential settlements caused by non-homogeneous compressible material in the foundation.
- (b) Steepness and/or irregular shape of valley walls or abutments.
- (c) Differential deformations caused within the dam due to:
 - (i) the presence of rigid structures such as conduits, concrete cut offs, etc. within the body of the dam,
 - (ii) the softening of certain materials of the dam due to saturation, and

- (iii) the large difference in stress-strain properties of materials in adjacent zones or layers within the dam.
- (d) Large rates of strain caused in the upstream shell by the rapid filling of reservoir, especially during the first filling.
- (e) Large transient stresses caused by earthquakes and other dynamic loads.
- (f) Shrinkage effects caused by excessive drying of the core of the dam for long periods either during construction or operation of reservoir.

1.3.2 Types of Cracks

The cracks occurring in earth and rockfill dams are classified in different ways. Three well-known classifications are:

- (a) Classification by the orientation of the crack (Fig. 1.1):
 - (i) Transverse cracks: are those that are perpendicular to the longitudinal axis of the dam. These could be horizontal, vertical, inclined or skewed. They provide a free path for the passage of water from the upstream to the downstream side and are considered to be the most dangerous in causing failures due to erosion in dams.
 - (ii) Longitudinal cracks: are those running in a direction, approximately parallel to the length of dam. Though these cracks do not create a free passage of

water from the upstream to downstream faces, they may however aggravate a piping failure in a dam by connecting the transverse cracks.

(b) Visible classification of the cracks (Fig. 1.1):

- (i) Interior cracks are those not visible from outside.
- (ii) Exterior cracks are those which are formed at the surface (e.g., transverse or longitudinal cracks at the crest). Interior transverse cracks are the worst type of cracks which could cause unexpected failures due to erosion in dams.

(c) Classification according to the mode of formation (Fig. 1.2):

- (i) Tensile cracks are those caused by tensile stresses.
- (ii) Shear cracks are those caused by sliding failures.
- (iii) Tearing cracks are those caused by torsional (rotational) shear failures.
- (iv) Shrinkage cracks are tension cracks formed due to shrinkage effects.

In the investigation that forms the basis of this thesis only tension cracks have been considered. Therefore, in the remainder of this report, the term 'cracking' is implied to mean 'tensile cracking'.

1.4 Usefulness of an Analysis for the Prediction of Cracking of Dams

An analysis that can reasonably predict the extent of tensile zones that are likely to develop in a dam structure during critical periods will be useful in designing and in-

strumenting the structure in a rational manner. From the performance of the structure as revealed by field observations, the analysis could be checked and causes for any discrepancies be ascertained. It is hoped that such endeavours, as the one made in this thesis, will lead to a better understanding and control of cracking of earth and rockfill dams.

1.5 Brief Review of Past Work on Cracking of Dams

A comprehensive review of investigations of the cracking of earth and rockfill dams has been made by Covarrubias (1969). These investigations, which were described in detail by Covarrubias, are mentioned only in brief here. The investigations carried out by Covarrubias (1969) and later workers have been considered in some detail for the purpose of justifying the need for the present work.

Terzaghi (1943, p. 431) observed that tensile cracks would be caused by the tensile stresses prevailing at some distance behind the face of a vertical cut in clay overlying a rigid base. The distance at which maximum tensile stress occurs and the resulting maximum depth of tension zone were estimated to be about one-half the height of the cut.

Casagrande (1950) recognized the possibilities of piping failures that could be caused by cracks in earth and rockfill dams. He suggested that enough provisions should be made in the design of dams to make the cracks self healing.

Sherard (1952), after a comprehensive study on the performance of several earth dams, some of which cracked, arrived

at criteria to classify the soils that are susceptible to cracking. These criteria were based on the grain size and consistency limits. A similar classification was also made by Tamez and Springhall (1960). From these studies it was concluded that, in general, silty soils with uniform gradation and low plasticity index are highly susceptible to cracking. Even though these criteria help to classify soils with regard to their susceptibility to cracking, they are of very limited use in the overall evaluation of the cracking potential of an earth structure.

Nonveiller and Anagnosti (1961) proposed a limit analysis for investigating horizontal cracks in a narrow vertical clay core supported by less compressible rockshells. This analysis disregards the elastic strains which by themselves could produce cracks.

Narain (1962) tried to compare the tensile strains at failure obtained by the laboratory beam tests on soils with the tensile strains computed for a number of dams which were idealized as homogeneous isotropic linearly elastic beams of uniform cross section. He concluded that when the computed tensile strains exceeded the laboratory failure tensile strains, cracks would occur in the real structure. Even though some correlations with observed cracking were made, the analysis recommended by him is not applicable for all classes of problems involving irregular valley profiles and non-homogeneous materials because of his over-simplified idealization of the real structure.

Lee and Shen (1968) analyzed the longitudinal section of dams using a finite element method to compute the horizontal stresses and strains. Results of such computations made on El Infiernillo Dam agreed well with the field observations. The analysis was performed in a single step under plane strain conditions with the appropriate linear stress-strain relationships.

Covarrubias (1969) analyzed a number of longitudinal and transverse sections representing different simple geometrical shapes of earth dams. In all cases a finite element method was used and the analyses were performed in a single step using the assumption of linear stress-strain relationships and plane strain conditions. The purpose of these analyses was to evaluate the effect of the shape of valley and compressibility of different materials in dams and foundations on the development of tensile zones. Similar analyses were conducted on the longitudinal sections of existing dams to predict transverse cracking. Reasonable correlations were obtained even though the tensile stresses and strains were over-estimated due to the single step linear elastic analysis used.

Dolezalova (1970) considered the effect of steepness of a triangular valley on the formation of tension zones to predict transverse tensile cracking. A finite difference method was used to perform a linear elastic analysis in a single step and in a number of steps under plane strain conditions. These analyses have the same disadvantages mentioned

before in addition to the lesser adaptability of the finite difference technique to more complex problems.

Strohm and Johnson (1971) included the construction step sequence and non-linear material behaviour in the finite element analyses they have conducted for different valley profiles under plane strain conditions. These studies revealed, that by introducing the realistic non-linear material properties and the construction step sequence, the extent of tensile zones computed was very much smaller than that obtained by a single step linear analysis. In addition the principal stress ratios computed by the incremental non-linear analysis are closer to reality than the ones obtained by a single step linear analysis.

1.6 Requirements of an Analysis for Predicting Cracks

For a successful prediction of cracking of an earth structure particular attention has to be paid to the following:

- (1) The idealization of the structure for the analysis has to be such that the geometry of the structure, the boundary and body forces, the boundary displacement conditions, and the construction sequence are represented as close to the prototype as possible.
- (2) The material properties and the stress-strain relationships used in the analysis should be such that they lead to the proper simulation of the deformational behaviour of the structure.
- (3) The tensile behaviour of the materials of the structure

should be known so that the results of analysis are interpreted properly for the prediction of cracking.

1.7 Objectives of the Present Investigation

Since a procedure satisfying the requirements stated in Section 1.6 is not available yet to deal with the problem of cracking of earth dams, the present investigation was undertaken with the following objectives:

- (1) To conduct laboratory studies that contribute to an understanding of the tensile behaviour of soils,
- (2) to conduct analytical studies that contribute to an understanding of the influence of certain factors on cracking phenomena and to the development of a procedure for a reasonable prediction of the cracking of earth dams, and
- (3) to suggest a design procedure that contributes to the minimization of the possibilities of cracking of earth dams.

1.8 Scope of the Present Work

- (1) Laboratory studies on tensile behaviour of soils are restricted to a mountain till that represents a typical core material generally used for the dams constructed in western Canada. The influence of the most important factors, namely the water content at failure, the compactive effort, the rate of loading, and the addition of bentonite to till, on the tensile characteristics of

soil has been investigated. The laboratory studies are described in Chapter II.

- (2) Suitable simulation procedures for linear and non-linear finite element analyses for two and three dimensional conditions have been developed. These procedures are described in Chapter III.
- (3) Parametric studies to investigate the influence of construction sequence, non-linear stress-strain relationships of materials, and three dimensional effects on the development of tensile cracks during or at the end-of-construction period have been conducted. Studies on the first two factors namely, the construction sequence and non-linear material properties are extensions of the work done by Strohm and Johnson (1971). The other critical states, such as the first filling of reservoir, or an earthquake, have not been investigated. All the studies in this work are restricted to tensile cracking. Cracking due to shrinkage effects and shear is not considered. All the parametric studies are described in Chapter IV.
- (4) A design procedure that takes into account the redistribution of stresses due to non-homogeneity of the materials of the dam, has been suggested to minimize the transverse tensile cracks near the abutments. This procedure has been described in Chapter IV.
- (5) The simulation procedure that utilizes the analytical tools developed in Chapter III has been applied to a case study for verifying its usefulness in practice.

This case study is presented in Chapter V.

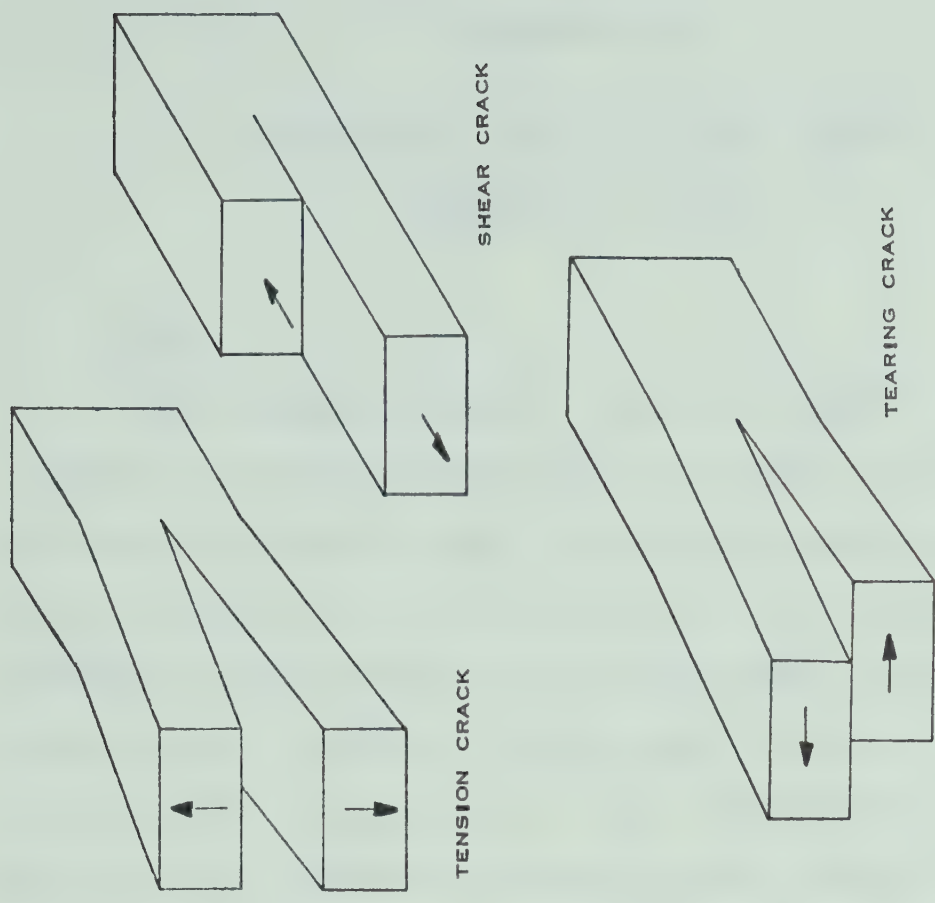


FIG. I.2 BASIC MODES OF CRACK-SURFACE DISPLACEMENTS [AFTER COVARRUBIAS, 1969]

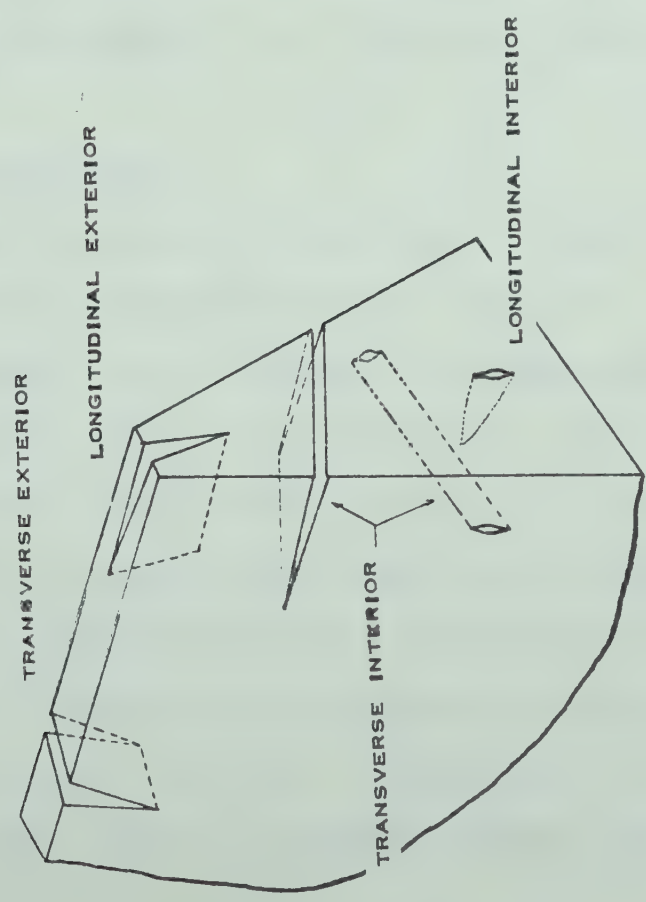


FIG. I.1 CLASSIFICATION OF CRACKS IN THE CORE OF A DAM [AFTER COVARRUBIAS, 1969]

CHAPTER II

LABORATORY STUDIES ON THE TENSILE BEHAVIOUR OF SOILS

2.1 Scope

This chapter discusses the usefulness of the laboratory studies on the tensile behaviour of soils for the analysis of cracking of earth dams. Laboratory tensile studies on soils by the previous investigators are briefly reviewed. Different tensile test methods applicable to soils are examined and the indirect tension test procedure used in the present work is described. Tests performed to evaluate the influence of different factors on the tensile behaviour of a typical core material are described and the results discussed.

2.2 Introduction

When compared to the extent of work done on the shear strength and the deformational behaviour of soils, the amount of research directed towards an understanding of the tensile behaviour of soils is very meagre. This is mainly due to the generally low tensile strength of soils. Although it is reasonable to assume zero tensile strength for soils in the analysis and design of earth dams, a knowledge of the behaviour of soil in tension is still required for an effective control of cracking of earth dams. Laboratory tests were undertaken to study the tensile behaviour of Mica Till, a soil represent-

ing typical core materials generally used for dams in western Canada. The effects of the moisture content, the strain rate, the compactive effort, and the addition of bentonite to till on the flexibility characteristics of till were examined.

2.3 A Brief Review of Previous Studies on the Tensile Behaviour of Soils

A systematic study on the tensile strength of compacted soils, by testing relatively large specimens under direct tension, was reported by Tschebotarioff et al. (1953). The soil sample had the shape of a briquette, similar to the one normally used in testing cement mortar in tension. The specimen was 52" in total length and 3" in thickness. The width was reduced from 18" at the ends to 6" at the test section, which had a length of 16". The specimen, compacted by standard proctor tampers, was supported horizontally on ball bearings to avoid friction. The important findings of this study were as follows:

- (1) The tensile strength and the strain at failure of a clay depended on the type of clay mineral in the soil.

Montmorillonite exhibited the highest tensile strength and tensile strain at failure whereas the corresponding quantities for kaolinite were the lowest.

- (2) The tensile strength was affected by the water content, the time elapsed between mixing and testing and the rate of strain.
- (3) The addition of bentonite to sand increased the tensile

strength of bentonite by about 50% when the mixture had a composition of about 15% bentonite and 85% sand.

Further addition of sand decreased both the tensile strength and the tensile strain at failure of the mixture.

From the preceding observation one can expect the possibility of considerably improving the tensile behaviour of a relatively non-plastic soil such as till by the addition of an optimum quantity of bentonite.

Narain (1962) studied the tensile behaviour of six soil types of which five were obtained from earth embankments with known construction conditions. The sixth soil was a limestone clay of relatively high plasticity that had a plasticity index of 45% and a liquid limit of 72%. The soils from embankments varied from non-plastic to a plasticity index of 16. For a given soil type, relationships were obtained between the tensile strain at the initiation of cracking and the compactive effort, moulding water content and the rate of loading. All the tensile tests were performed on soils moulded into beams 3" wide, 2.75" deep and 22.125" long. The soil was compacted in ten equal horizontal layers with an actuated vibrator having a 2.5" square base plate, weighing 16 lbs. Different compactive efforts could be simulated by adjusting the time of compaction. Loss of moisture from the specimen was prevented by coating the specimen with a layer of 50% petrowax plus 50% petrolatum oil. The beams were loaded at the centre by adding dead weights at rates that caused failure in 2 days to 6 months. From the deflections of beams obtained by cathe-

tometer observations of tungsten pins inserted into the beams, the tensile stresses and strains were computed. The computation of stresses and strains was based on a solution obtained, using the elastic theory, for a rectangular beam with known displacement boundary conditions. The rupture of beam invariably occurred near the midspan after the formation of the first crack. Parallel compression tests were conducted on all the soils to compare their behaviour in compression with that in tension. The main conclusions drawn from these tests were as follows:

- (1) The ratio of tensile strains at cracking to the compressive strain at failure varied widely from 0.01 to 0.1 with no consistent pattern, indicating that compression tests are of little value in assessing the tensile strains in soils at cracking.
- (2) An increase of moulding water content from 2% to 3% dry of optimum to nearly optimum substantially increased the flexibility of soil. At comparable moisture contents with respect to the optimum, an increase of compactive effort substantially decreased the flexibility.
- (3) Clays of high plasticity are, in general, more flexible than clays of low plasticity. However, the flexibility of soils with low plasticity could not be correlated with their plasticity characteristics.
- (4) Rapid straining of soils caused failure at lower tensile strains and stresses compared to those obtained from slow rates of testing.

Inglis and Frydman (1963) examined the suitability of the different tensile test methods for soils. Direct tension tests, indirect tension tests and flexure tests were performed on soil specimens of different sizes and different compositions. In order to cover a wide range of strengths in the specimens tested, Portland cement was added to kaolin and sand in varying small amounts. It was concluded that an indirect test would be useful and sensitive for stabilized materials as extreme as kaolin and uniformly graded coarse sand. Simplicity in test operation, low variability, and sharp failure were observed. The length of the specimen did not affect the test results significantly indicating that relatively thin specimens could be tested with minimum compaction inhomogeneities.

Hasegawa and Ikeuty (1966) tested a soil with a plastic limit of 80%, a liquid limit of 98%, and an optimum water content of 82% in direct tension, using briquette shaped specimens, similar to those used by Tschebotarioff et al. (1953) but of much smaller dimensions. The overall length of the specimen was 19 cm. with a middle test section of 2 cm. x 2 cm. in cross section and 7 cm. in length. The tensile load was transmitted to the specimen through thin steel plates embedded into the specimen at the enlarged ends during compaction. The specimen was kept horizontal and the friction was avoided by floating the specimen on mercury. The tensile strain was measured by observing through a cathetometer, the movement of two ceramic marks, kept initially at a distance

of 5 cm. apart. The failure took place perpendicular to the axis of loading but at different locations along the length of the specimen, sometimes occurring even at the ends. A maximum strain of 5.5% was measured for the soil tested. A decrease of tensile strength and increase of failure strain with the increase in moisture content were observed.

Narain and Rawat (1970) tested six soil types, covering a wide range of plasticity characteristics, under a diametral compression to determine their tensile strength at different moulding water contents. The specimen, 4" dia. x 4.6" in size, was supported on 5/8" wide and 1/4" thick rubber strips for even distribution of the load along its length. The good reproducibility of the results reported, indicates the suitability of the indirect tension test (Brazilian test) for compacted soils. Comparison of the ratio of unconfined compressive strength to the tensile strength at the optimum water content for different soils tested showed that the ratio was less for the more plastic soils.

Fang and Chen (1971) developed a new simple test, known as the double punch test, for testing soils in tension. The test consists of loading a cylindrical soil specimen by applying two steel punches at the centre on both top and bottom surfaces of the specimen. A simple formula, based on the theory of plasticity was developed for computing the tensile strength of soils. The test results for various materials including concrete, mortar, soil, and bituminous concrete were compared with those of the indirect test and good agreement

among the results were reported. However the measurement of tensile strain during a double punch test on soil specimen appears to be difficult.

2.4 Different Types of Test for Tensile Testing of Soils

Based on the experiences reported in previous investigations on tensile testing of soil, stabilized soil, concrete, rock and bituminous concrete, a general evaluation of the common tensile test methods appears to be possible.

2.4.1 Direct or Uniaxial Tension Test

A direct tension test, although quite simple in interpretation, is rather difficult to apply to soils and other materials which have a low tensile strength. The main difficulty arises in the satisfactory application of load to the ends of the specimen. A number of methods such as freezing the ends of specimen (Haefeli, 1951), cementing the ends of specimen to loading blocks with a quick-setting polyester resin (Bofinger, 1970), enlarging the ends of the specimen to form a briquette (Tschebotarioff et al., 1953) and embedding loading plates in the enlarged ends of specimen (Hasegawa and Ikeuty, 1966) were adopted. Slight eccentricities in loading, stress concentrations at the ends, and compaction planes in the case of cylindrical specimens (Ingles and Frydman, 1963) affect the reproducibility of test results to a considerable extent. When soils are to be tested at high water contents or when the dimensions of the specimen are large, the horizon-

tal application of load is preferred. This necessitates an elaborate arrangement for the application of load without friction and eccentricity (e.g., Tschebotarioff et al., 1953).

2.4.2 Flexure or Beam Test

This test is considerably easier to conduct than the direct tension test. The preparation of the specimen and the application of load do not require as much care. To some extent the loading conditions in this type of test are similar to the field loading conditions of an earth dam which, for purpose of analysis, can be considered as a beam (Narain, 1962). However, as the failure is induced at the surface, skin effects produced by the uneven distribution of compaction pressures, especially in soils of low plasticity tend to influence the results to a large extent (Ingles and Frydman, 1963). Since a part of cross section of the beam passes into the plastic range, the stress distribution in the specimen is not defined. Hence the tensile strength computed by the simple bending theory will be in error. However, Bofinger (1970), using a theory that accounts for a different moduli in tension and compression and plastic behaviour of soil, obtained extreme fibre flexural stresses which are not markedly different from the strengths of soil-cement specimens obtained by direct tension tests.

2.4.3 Indirect Tension Test or Brazilian Test

An indirect tension test that involved loading of a cir-

cular cylinder or disc with compressive loads along two diametrically opposite generators, was developed by Carneiro and Barcellos (1953) in Brazil and also by Akazawa (1953) in Japan. A relatively uniform tensile stress perpendicular to and along the diametral plane containing the applied load usually causes splitting failure along the loaded plane (Fig. 2.1). The test was originally developed for concrete and mortar specimens, however its use has been found satisfactory for materials such as rock (Mellor and Hawkes, 1971), stabilized soils (Thompson, 1965), bituminous mixtures (Breen and Stephens, 1966) and soils (Narain and Rawat, 1970). Based on the previous investigations it is generally recognized that an indirect tension test has the following advantages:

- (1) Specimen preparation and its handling are considerably easier.
- (2) Equipment needed for the test is similar to that of a compression test.
- (3) Failure is relatively insensitive to the surface conditions and compaction planes of the specimen and is initiated in a region of relatively uniform tensile stress.
- (4) Variation of the test results is low.
- (5) For brittle materials and when performed properly, the test is capable of giving a good measure of uniaxial tensile strength (Mellor and Hawkes, 1971).

However, since the formula used to compute the tensile stress in the test is based on the assumption of homogeneous, isotropic elastic material there will be an error in the estimate

of tensile strength of real materials. In addition the relationship between the tensile stress and tensile strain cannot be obtained directly because of the biaxial stress conditions of the test (Bofinger, 1970).

2.4.4 Choice of the Type of Test for Present Studies

The simplicity in preparation and handling of test specimens and the consistency of test results lead to the adoption of the indirect tension test in this investigation. The error caused in the estimate of tensile strength of materials whose moduli differ in tension and compression is examined in Section 2.5.2. A procedure to derive the tensile stress-strain relationship is indicated in Section 2.5.3.

2.5 Theoretical Consideration of the Indirect Tension Test

2.5.1 Theoretical Stress Solutions

Hertz (1883) obtained a stress solution for a disc or cylinder compressed normally by line loads along diametrically opposite generators. Later, a number of investigators (e.g., Timoshenko and Goodier, 1951; Wright, 1955; Frocht, 1957) considered the same problem. Hondros (1959) gave a complete stress solution for the case where the load is distributed over finite arcs, valid for conditions of both plane stress and plane strain. Colback (1966) observed that the presence of a diametrical fracture plane originating from centre is essential if the test is to be accepted as valid. Favourable

conditions for the acceptability of the test are generally obtained by distributing the applied load over small areas. A distributed load, when applied over a length less than a tenth of the diameter of the specimen, prevents local compressive failure without significantly altering the stress conditions at the centre of specimen that are valid for a line load. Fig. 2.1 compares the theoretical distribution of vertical and horizontal principal stresses along the vertical or loading diameter for conditions of line loading and distributed loading over an arc of length equal to 1/12 of the diameter of the specimen. The two principal stresses along the vertical diameter for distributed loading are given by Hondros (1959) as:

$$\sigma_{\theta} = + \frac{P}{\pi R t \alpha} \left\{ \frac{[1 - (r/R)^2] \sin 2\alpha}{1 - 2(r/R)^2 \cos 2\alpha + (r/R)^4} - \tan^{-1} \left[\frac{1 + (r/R)^2}{1 - (r/R)^2} \tan \alpha \right] \right\} \quad (2.1a)$$

$$\sigma_r = - \frac{P}{\pi R t \alpha} \left\{ \frac{[1 - (r/R)^2] \sin 2\alpha}{1 - 2(r/R)^2 \cos 2\alpha + (r/R)^4} + \tan^{-1} \left[\frac{1 + (r/R)^2}{1 - (r/R)^2} \tan \alpha \right] \right\} \quad (2.1b)$$

where P is the applied load, R is the radius of the specimen, t is the thickness of the specimen, 2α is the angular distance over which P is assumed to be distributed radially (normally $\leq 15^\circ$), and r is the distance from the centre of the specimen (Fig. 2.1). At the centre of specimen the stresses are given by:

$$\sigma_{\theta} = + \frac{P}{\pi R t} \left(\frac{\sin 2\alpha}{\alpha} - 1 \right) \quad (2.2a)$$

$$\sigma_r = - \frac{P}{\pi R t} \left(\frac{\sin 2\alpha}{\alpha} + 1 \right) \quad (2.2b)$$

For line loading the stresses along vertical diameter are given (Frocht, 1957) by:

$$\sigma_{\theta} = + \frac{P}{\pi R t} \quad (2.3a)$$

$$\sigma_r = - \frac{P}{\pi R t} \left\{ \frac{4}{[1 - (r/R)^2]} - 1 \right\} \quad (2.3b)$$

It will be noted that, for $\alpha \leq \tan^{-1}(1/10)$, both Eqs. 2.2 and 2.3 give the same stresses at centre, viz.,

$$\sigma_{\theta} = \frac{P}{\pi R t} \quad (2.4a)$$

$$\sigma_r = - \frac{3P}{\pi R t} \quad (2.4b)$$

Fig. 2.1 shows that a distributed load gives a finite value of compressive stress at the point of load application whereas the compressive stress in the case of a line load is infinite. Because of the stress condition that exists at the centre ($3\sigma_{\theta} + \sigma_r = 0$) the initiation of tensile failure for a brittle material, according to Griffith's criterion, should occur at the centre of the specimen. The tensile stress corresponding to the initiation of failure at centre is then

equal to the uniaxial tensile strength of the material. When the load P_f corresponding to the failure is known, the tensile strength of the material tested can be obtained from:

$$\sigma_t = \frac{P_f}{\pi R t} \quad (2.5)$$

It is interesting to note that an identical formula for the failure tensile stress could be derived assuming the material to be perfectly plastic (Chen, 1970).

2.5.2 Effect of Different Elastic Moduli in Tension and Compression

In the derivation of the stress solution discussed in the previous section it was assumed that the elastic moduli in tension and compression were equal. In general, for materials of very low tensile strength it is observed that the modulus in tension is considerably smaller in magnitude than that in compression. Bofinger (1970) observed that for an inactive clay (liquid limit 53% and plastic limit 20%) when stabilized with 6 to 10% ordinary Portland cement, the ratio of modulus in compression to that in tension varied from 7.5 to 11.1. Because of different elastic moduli in compression and tension, the tensile strength of the material estimated with the use of the Eq. 2.5 will be higher than the correct value. A numerical solution that considers different elastic moduli in tension and compression has been obtained here with the use of the finite element method. When moduli differ in tension and compression the material can be considered as bilinear

and the solution technique by successive approximations suggested by Wilson (1963) can be used to obtain a numerical solution to the problem. The stress-strain relationship for a bilinear material is of orthotropic form and can be written in terms of principal coordinate system for plane stress condition as:

$$\begin{Bmatrix} \sigma_t \\ \sigma_c \\ 0 \end{Bmatrix} = \frac{1}{1-\nu_t\nu_c} \begin{bmatrix} E_t & \nu_c E_t & 0 \\ \nu_t E_c & E_c & 0 \\ 0 & 0 & G \end{bmatrix} \begin{Bmatrix} \epsilon_t \\ \epsilon_c \\ 0 \end{Bmatrix} \quad (2.6a)$$

where σ_t the tensile principal stress
 σ_c the compressive principal stress
 ϵ_t the tensile principal strain
 ϵ_c the compressive principal strain
 E_t the modulus in tension
 E_c the modulus in compression
 ν_t the Poisson's ratio associated with tension
 ν_c the Poisson's ratio associated with compression
 G the shear modulus prescribed independently.

From symmetry considerations of the constitutive matrix given above

$$\nu_c E_t = \nu_t E_c \quad (2.6b)$$

Writing $E_c/E_t = n$ and $G = gE_c$ the constitutive matrix can be expressed as:

$$[\bar{c}] = E_c \begin{bmatrix} \frac{1}{n-v_c^2} & \frac{v_c}{n-v_c^2} & 0 \\ \frac{v_c}{n-v_c^2} & \frac{n}{n-v_c^2} & 0 \\ 0 & 0 & g \end{bmatrix} \quad (2.7)$$

The constitutive matrix $[\bar{c}]$ is defined if E_c , v_c , n and g are prescribed. For an isotropic material the extreme values of g corresponding to Poisson's ratios of zero and 0.5 are 0.5 and 0.33 respectively. As g is an independently prescribed quantity it is reasonable to assume that about 0.4 represents approximately an average condition for soils that have different moduli in tension and compression. However, solutions for different values of g ranging from 0.2 to 0.5 are obtained. The variation of n is considered from 1 to 15. The finite element procedure is given in detail in Appendix D. Fig. 2.2 compares the finite element solution with the theoretical solution for the distribution of tensile and compressive stresses along the horizontal diameter of the specimen. A close agreement between the solutions can be noticed. Finite element solutions for $E_c/E_t = 10$ and $g = 0.4$ are also shown in Fig. 2.2 for two values of v_c namely 0.10 and 0.35. An increase in compressive stress and decrease in tensile stress when compared to the isotropic case, at the centre of the specimen can be seen. The solution is little affected by the value of Poisson's ratio used in the analysis as can be seen from Fig. 2.2. Fig. 2.3 gives the tensile and compressive

stress at the centre of specimen obtained by the finite element method for different values of E_c/E_t and g . The stresses are not significantly sensitive to the variation of g especially over the range between 0.3 and 0.5. Hence it is reasonable, in the absence of a correct estimate of g , to assume that the variation of the stresses at centre as dictated by the ratio E_c/E_t for an average value of g equal to 0.4 serves the purpose of evaluating an indirect tension test. Based on this, the variations of the tensile and compressive stresses at the centre with the ratio E_c/E_t for the value of $g = 0.4$ is plotted in Fig. 2.4. This plot was used in subsequent computations (Section 2.9). The distribution of the tensile and compressive stresses along the horizontal diameter of the specimen for various values of E_c/E_t is shown in Fig. 2.5.

2.5.3 Evaluation of the Tensile Stress-Strain Relationship

Since the indirect tension test involves a biaxial stress state at the centre of the specimen, the tensile strain obtained from the test includes that caused by the compressive stress in the vertical direction. To obtain the tensile stress-strain relationship it is necessary to deduct the tensile strain due to the compressive stress from the observed tensile strain. As the tensile stress at failure for soils is generally low, the compressive stress that exists at the centre of the specimen while it fails in tension is also low, this being equal to three times the tensile stress at failure. For the range of this low compressive stress an appropriate

compression modulus (E_c) and a Poisson's ratio (ν_c) can be obtained by conducting an unconfined compression test on the same soil. The observed tensile strain at the centre of specimen in an indirect tension test can be expressed for plane stress condition as:

$$\epsilon_{xc} = \frac{\sigma_{xc}}{E_t} + \nu_c \frac{\sigma_{yc}}{E_c} \quad (2.8)$$

where σ_{xc} , σ_{yc} represents respectively the tensile and compressive stress at the centre, ϵ_{xc} the observed tensile strain at centre and E_t the modulus in tension. The tensile strain due to tensile stress alone can be obtained from:

$$\frac{\sigma_{xc}}{E_t} = \epsilon_{xc} - \nu_c \frac{\sigma_{yc}}{E_c} \quad (2.9)$$

Initially, as E_t is not known, σ_{xc} and σ_{yc} can be computed for $E_c/E_t = 1$. From tensile stress-strain relationship obtained after the first trial, E_t is derived and the ratio E_c/E_t computed. In the second trial the appropriate values of σ_{xc} and σ_{yc} are derived from Fig. 2.4 for the known E_c/E_t and used in Eq. 2.9 to obtain the new tensile stress-strain relationship. Now the E_t can be derived from the present tensile stress-strain relationship and the E_c/E_t can be recomputed and compared with previous value of E_c/E_t . The procedure can be repeated until close agreement is achieved between the successive values of E_c/E_t . An example illustrating the procedure appears in Section 2.9.

2.6 Experimental Set-Up for Laboratory Tensile Tests

2.6.1 Load Measuring Device

Since the tensile stress to be measured for soils is small, the load measuring device should be sufficiently sensitive to record small loads. The system should be rigid causing negligible deformation in the load measuring device. The recording equipment should be such that it is possible to record measurements of load and deformation at close intervals. This will lead to a precise evaluation of the stress-strain relationship especially at the failure of specimen.

All tensile tests were performed on a strain controlled loading machine having various constant speeds including a minimum of 0.000013"/minute. The load was measured by a sensitive, 300 lb. capacity tension-compression miniature transducer load cell, (Fig. 2.6) manufactured by Intertechonology Ltd., Don Mills, Ontario. The load cell is temperature compensated, has 50% over load capacity, and could be operated satisfactorily in a moist room at 95% relative humidity and at a temperature of 45°F to reduce the loss of moisture from the specimen. The load cell is supplied with 10 volts d.c. and the output is picked on one of the channels of the d.c. strain gauge control (Figs. 2.7 and 2.8). The channels were scanned and recorded by a Hewlett-Packard data acquisition system (Figs. 2.7 and 2.8). The readings could be taken at intervals of time ranging from 1 second to 1 hour. The minimum load that could be recorded with the system is 0.1685 lbs., equivalent to 0.01 millivolts.

2.6.2 Tensile Deformation Measuring Device

Tensile deformation measurement in soils is rather involved because of the difficulty in attaching the tensile deformation measuring device to the soil specimen and the need to measure extremely small tensile deformations. In the present studies a clip gauge shown in Figs. 2.9, 2.10(a) and 2.10(b) was used to measure the displacement between two brass gauge blocks attached to the specimen on either side of its centre by means of Phenyl Salicylate. Similar clip gauges were successfully used in the past by the Alberta Research Council, Highways Division, Edmonton to obtain the tensile deformations of soil-cement specimens.

The clip gauge consists of two arms of $1\frac{1}{4}$ " long, $\frac{1}{4}$ " wide and 0.015" thick "feeler gauge" material firmly soldered to two brass blocks as shown in Fig. 2.9(a). The two arms were provided with brass knife edge points at their ends so that the clip gauge sits snugly between the grooved sides of the gauge blocks (Fig. 2.10(a)). The brass ends of the clip gauge were kept at a fixed distance apart on either end of a spacer by means of a screw and a pin (Fig. 2.9(a)). The thickness of the spacer selected was such that a distance of 0.915" between the ends of knife edge points was obtained in the unstrained state. When the gauge sits within the grooves of the gauge blocks the distance between the knife edge points is 0.84" so that a maximum tensile strain of 8.92% can be read over the entire range of the clip gauge. A distance greater than 0.915" was not found to be desirable as in this

case the two arms of clip gauge in the initial strained position, exerted excessive pressure on the gauge blocks causing them to come off the specimen. The two cantilever arms, which tend to reach the unstrained position as the specimen undergoes tensile deformation, were fitted with two Budd's metal film strain gauges (type C6-111, gauge factor 2.4, 120 ohms) to measure the tensile deformation (Fig. 2.9(a)). To achieve a maximum signal output, one of the gauges was fixed on the compression side of one arm while the other was on the tension side of the other arm. Two resistors of 120 ohms each were put into the circuit to make it a full bridge circuit (Fig. 2.9(b)). The transducer amplifier indicator (Figs. 2.7 and 2.8) supplies 3 volts a.c. at 3kHz to the strain gauge circuit, receives back the a.c. signal from the circuit, amplifies and converts into a d.c. signal which is read by the data acquisition system. As the tensile deformations were to be read from both ends of the specimen, two clip gauge units with two transducer amplifier indicators have been used (Figs. 2.7 and 2.8). The minimum tensile strain that could be read with the set up used is 0.002%, equivalent to 0.01 millivolts. A L.V.D.T. (linear variable differential transformer) of 6 volts was fixed to the loading head (Fig. 2.10(b)) to check the rate of loading of the specimen.

2.7 Experimental Set-Up for Laboratory Compression Tests

The unconfined compression tests were conducted on the same loading machine with the same load cell used for the ten-

sile tests. The tests were performed on 4" dia. x 8" long samples with lateral strain measurement (Fig. 2.11). The lateral strain measuring device used is a modification of the lateral strain indicator described by Bishop and Henkel (1962) for performing compression test on 4" dia. samples under zero lateral strain. The modification was the replacement of the diaphragm-mercury indicator by an L.V.D.T. of 24 volts with a thin wire tied to the lower end of the core while the upper end was supported by a spring (Fig. 2.12). The relative movement of two curved metal pads which bear lightly on the surface of the sample is magnified twice by the hinged ring which embraces the sample and is imparted to the thin wire, stretching across the two ends of the ring (Fig. 2.12). The wire causes the vertical movement of the core of L.V.D.T. equivalent to twice the amount of the lateral displacement of the specimen. Lateral strains are measured here to compute the Poisson's ratio during the unconfined compression of the specimen. The vertical displacement of the specimen is measured by a 6 volt L.V.D.T. attached to the loading plunger of the triaxial cell as shown in Fig. 2.11.

2.8 Description of Laboratory Tests

2.8.1 Description of Soil Used for Tensile and Compressive Tests

Mica Till was used in all tensile and compressive tests to represent the tensile and compressive stress-strain characteristics of a typical brittle core material of an earth dam.

Some tension tests were performed on Mica Till mixed with 6% bentonite to study the effect of adding a plastic material to the core material. Mica Till tested, has the following properties:

Liquid limit	18.2%
Plastic limit	14.7%
Plasticity index	3.5
Proctor maximum dry density (material passing #4 sieve)	132.0 pcf
Proctor optimum water content (material passing #4 sieve)	9.2%

The gradation curve for Mica Till for sizes less than 3/4" is shown in Fig. 2.13. Mica Till mixed with 6% commercial bentonite (liquid limit 59%, plastic limit 87%, and activity 5.6) has the following properties:

Liquid limit	42.0%
Plastic limit	21.2%
Plasticity index	20.8
Proctor maximum dry density (material passing #4 sieve)	126.0 pcf
Proctor optimum water content (material passing #4 sieve)	10.8%

2.8.2 Tests Performed

Fifty-two tension tests and four unconfined compression tests were performed altogether as detailed in Table 2.1.

2.8.3 Soil Preparation and Compaction of the Sample for Tension and Compression Tests

The till obtained from borrow area of Mica dam had a

water content of about 12%. The soil was forced through a #4 sieve and the material passing the sieve was air dried for a week. The dried soil was stored in plastic bags. Twenty-six hundred grams of the air dried soil was mixed with the required quantity of distilled water by weight in a mechanical mixer for 3 minutes. The soil thus mixed was forced through a #4 sieve to remove all lumps. A uniform mixture was achieved without difficulty because of the non-plastic nature of soil. However, when 6% bentonite was mixed with Mica Till it was relatively difficult to force the soil through a #4 sieve when the water content was well above optimum. In such cases the lumps were broken by hand. The loss of water during mixing and compaction was compensated by adding about 0.5% more water than required. The soil mixed with water was kept in a moisture proof plastic bag and stored for 24 hours in a moist room.

The soil was compacted in a mould 4" in diameter and 1.53" high fitted with a collar. An automatic compactor with a hammer weighing 5.5 lbs. and a height of fall 12" was used for compacting the specimen. A specimen of 4" diameter and 1.53" was obtained after trimming. Three such specimens were obtained from each batch of 2600 grams of air dried soil. All the tensile test specimens were prepared using dynamic compaction. The effect of type of compaction such as kneading or vibratory compaction was not studied. The number of blows was maintained at 25 for M, B and T series of the tests (Table 2.1) and varied only for the C series in which the

effect of compactive effort was studied. Greater compactive effort was simulated by increasing the number of blows while the height of fall and the weight of the hammer were kept constant at 12" and 5.5 lbs. respectively. The thickness of sample selected was 1/3 the height of the standard proctor sample. A sample 4" dia. x 1.53" was preferred over the full proctor sample (4" dia. x 4.59") for the following reasons:

- (1) The quantity of soil to be handled for each specimen is smaller.
- (2) Non-homogeneity caused due to compaction of standard proctor sample in three layers is avoided.
- (3) For the evaluation of tensile strains a plane stress condition can be assumed with the size of sample selected while it is neither a plane strain nor a plane stress condition for the full proctor sample. Also a plane stress condition simplifies the evaluation of tensile strain when modulus in compression differs from that in tension (Sections 2.5.2, 2.9, and Appendix D). In the case of a plane strain analysis the Poisson's ratio associated with the third direction also enters the constitutive matrix.
- (4) A thinner specimen would lead to a better correspondence between the tensile deformations measured on the two ends of the specimen.

For the compression tests the soil mixed with water as described above, was compacted in a 4" diameter by 8" high, 3 part split mould in 5 equal layers. Twenty-five blows of

a standard 5.5 pound hammer with a 12" drop were given on each layer.

The compaction curves obtained on different size samples are compared in Fig. 2.14. A close agreement among the moisture-density relationships can be noted.

2.8.4 Specimen Preparation for Tension Test

The compacted soil specimen for a tension test was weighed for the determination of its density. Two gauge blocks are fixed to both ends of the specimen to receive the tensile clip gauges. To facilitate correct location of the gauge blocks at both ends of the specimen, a gauge-block locating jig, from here on in referred to as jig, was used. The jig as shown in Fig. 2.16 had four straight edges fixed to a brass disc of 4" diameter. The disc had two square holes to receive the two gauge blocks of $3/8"$ x $3/8"$ size separated by a fixed distance of 0.84". Two straight edges were fixed on the ends of the diameter joining the gauge blocks while the other two were fixed on the ends of the diameter perpendicular to the former. The soil specimen was kept on a wooden block with two holes to receive the gauge blocks, the jig was placed on the specimen and the four generators on the circumference of the specimen were marked along the four straight edges of the jig (Figs. 2.15 and 2.16). Marking the generators facilitated the setting of gauge blocks on the other end of the specimen exactly in opposite positions and at the same gauge length of 0.84". After marking the generators a few

drops of phenyl salicylate at 200°F temperature were dropped into the square holes and the gauge blocks were set in position by lightly pressing them into the molten liquid. The jig was removed from the specimen without disturbing the blocks. In a few minutes the liquid set and held the gauge blocks firmly to the specimen. To the other end of the specimen also the gauge blocks were attached in a similar manner after turning the specimen upside down and orienting it properly so that the lines marked previously coincided with the straight edges of the jig. Any phenyl salicylate that entered the grooves of the gauge blocks was removed with a sharp knife. The specimen was then held on a stand (Fig. 2.17(a)) and dipped into a mixture of 50% petrowax and 50% petrolatum kept in a molten condition at about 55°C. A thin and pliable coat of the mixture thus formed not only prevents the loss of moisture from the specimen but also forms a protective coat to prevent the edges from spalling. The specimen thus prepared was cured in the moist room for about 2 weeks before testing.

Before performing the tensile test the wax covering the gauge blocks of the specimen was removed to insert the knife edge points of the clip gauge into the grooves of the gauge blocks. A strip of wax along the thickness of the specimen was removed at both ends of the vertical diameter so that the surface of soil was in direct contact with the loading strips. The loading strips used were butyl rubber 0.385" wide and 0.185" thick. From the preliminary tests it was

found that the type of rubber used was neither too soft nor too rigid for the proper distribution of load to the samples tested. The width chosen for the loading strips was slightly less than a tenth of the diameter of the sample so that the theoretical stress distributions at the centre of the specimen for a concentrated load was valid. A greater width for the loading strip causes the specimen to mobilize greater resistance than that needed to cause the initial fracture. A typical brittle failure observed in all the tension tests performed is shown in Fig. 2.17(b).

2.8.5 Tension Test Operation

All the tension tests were performed in the moist room at 45°F and 95% relative humidity. The variations in temperature and the relative humidity were $\pm 2^\circ\text{F}$ and $\pm 5\%$ respectively. The purpose of conducting the test in a moist room was to avoid loss of moisture from the specimen especially during long term tests. The specimen was properly positioned in the loading machine before the application of the load as shown in Figs. 2.10(a) and 2.10(b). While the load was applied to the specimen the load cell, the two strain gauges and the L.V.D.T. readings were recorded on a paper by the data acquisition system at an interval of time, set on the digital clock.

2.8.6 Computation of Tensile Stress and Strain

The readings obtained in volts and millivolts on the recording paper were converted to the proper units by using

the appropriate calibration factors determined prior to testing. It was assumed that a tensile crack was initiated at the peak load and the tensile stress at failure was computed using Eq. 2.5. From the tensile deformations recorded at peak load from both ends of the specimen the tensile strains were computed and were averaged. The resulting strain was taken as the average observed tensile strain at failure. The average tensile strain was observed over a gauge length of 0.84". To obtain the tensile strain at the centre of the specimen, the average observed tensile strain has to be multiplied by a coefficient which can be evaluated from the tensile strain distribution on the horizontal diameter of the specimen. This tensile strain distribution can in turn be computed from the stress distribution shown in Fig. 2.5. For the plane stress condition the horizontal tensile strain at a distance r from the centre can be expressed as:

$$\epsilon_x = \frac{\sigma_x}{E_t} + \frac{\nu_c}{E_c} \sigma_y$$

or

$$\frac{\pi R t}{P} \epsilon_x E_t = \sigma_x \frac{\pi R t}{P} + 3 \nu_c \frac{E_t}{E_c} \sigma_y \frac{\pi R t}{3P} \quad (2.10)$$

The tensile strain at the centre can be expressed as:

$$\epsilon_{xc} = \frac{\sigma_{xc}}{E_t} + \frac{\nu_c}{E_c} \sigma_{yc}$$

or

$$\frac{\pi R t}{P} \epsilon_{xc} E_t = \sigma_{xc} \frac{\pi R t}{P} + 3 \nu_c \frac{E_t}{E_c} \sigma_{yc} \frac{\pi R t}{3P} \quad (2.11)$$

From Eqs. 2.10 and 2.11

$$\frac{\epsilon_x}{\epsilon_{xc}} = \frac{\sigma_x \frac{\pi R t}{P} + 3 \nu_c \frac{E_t}{E_c} \sigma_y \frac{\pi R t}{3P}}{\sigma_{xc} \frac{\pi R t}{P} + 3 \nu_c \frac{E_t}{E_c} \sigma_{yc} \frac{\pi R t}{3P}} \quad (2.12)$$

Using Eq. 2.12 and Fig. 2.5 $\frac{\epsilon_x}{\epsilon_{xc}}$ along the horizontal diameter can be computed for a given value of ν_c and E_c/E_t . From the distribution of $\frac{\epsilon_x}{\epsilon_{xc}}$ along the horizontal diameter the central tensile strain, ϵ_{xc} , can be related to the strain ϵ_{xl} , observed over a length l as:

$$\epsilon_{xl} = \frac{\epsilon_{xc} \int_{-l/2}^{l/2} \frac{\epsilon_x}{\epsilon_{xc}} \cdot dr}{l} \quad (2.13)$$

or

$$\epsilon_{xc} = C_l \times \epsilon_{xl} \quad (2.14)$$

where

$$C_\ell = \frac{\ell}{\int_{-\ell/2}^{\ell/2} \frac{\epsilon_x}{\epsilon_{xc}} \cdot dr} \quad (2.15)$$

The variation of coefficient C_ℓ determined by graphical integration of Eq. 2.15 for $\nu_c = 0.365$, $\ell = 0.84"$, and for E_c/E_t ranging from 1 to 15 is shown in Fig. 2.18. The use of this coefficient in the evaluation of the tensile stress-strain relationship is shown in Section 2.9.

The terms pertaining to the tensile strain used in all the subsequent sections mean as follows: Observed tensile strain is the tensile strain computed from the tensile deformation measured over a gauge length of 0.84". Average observed tensile strain is the tensile strain obtained by averaging the observed tensile strains computed for both ends of the specimen. Observed central tensile strain is the tensile strain at the centre of the specimen obtained by multiplying the average observed tensile strain by a coefficient (Eq. 2.15). Tensile strain ("true" tensile strain) is the strain caused at the centre of the specimen by the tensile stress alone. This strain is obtained by deducting from the observed central tensile strain, the tensile strain caused by the compressive stress at the centre of specimen.

2.9 An Example to Illustrate the Procedure of Deriving the Tensile Stress-Strain Relationship

As mentioned in Section 2.5.3, in a biaxial indirect tension test, the observed central tensile strain consists of

strains due to both tensile and compressive stress at the centre of the specimen. The following example illustrates the procedure for deriving the tensile stress-strain relationship (Section 2.5.3).

An unconfined compression test performed on a 4" dia. x 8" sample with lateral strain measurement yielded the results presented in Fig. 2.19. The water content at failure was 10.65%, about 1.5% greater than the optimum. The compressive stress-strain relationship and the Poisson's ratio, computed from measured lateral and axial strains throughout the test, are shown in Fig. 2.19. An increase in Poisson's ratio with axial strain can be noticed. A tension test was also performed on 4" dia. x 1.53" sample at the same rate of loading (0.005"/min.) as that used in the compression test. The results of the tension test are shown in Fig. 2.20 and Table 2.2. The water content at failure (10.68%) was almost the same as that obtained in the compression test. The tensile stress was computed using Eq. 2.4(a). This formula is valid when the modulus in compression is equal to that in tension. In Fig. 2.20 the tensile stress is plotted against the observed tensile strains, computed from the measured tensile deformation on both ends of the specimen over a gauge length of 0.84". In the same figure the relationship between the tensile stress and the average of the observed tensile strains is also shown.

The relationship between the tensile stress and tensile strain is obtained using the following steps (Table 2.3):

- Step 1: A representative value for E_c and ν_c is chosen from the compression test results for the range of compressive stress realized in the tension test. For the example considered, the failure tensile stress from Fig. 2.20 is 0.525 psi and the corresponding compressive stress at the centre of specimen would be 1.575 psi, i.e., three times the tensile stress. From Fig. 2.19 representative values for E_c and ν_c can be selected for a range of compressive stress between zero and 1.575 psi. These are 260.9 psi and 0.365 respectively.
- Step 2: The relationship between central tensile stress and central observed tensile strain, shown by a solid line in Fig. 2.21, is derived by multiplying the observed average tensile strain, shown by a solid line in Fig. 2.20, by a coefficient equal to 1.048. This coefficient, corresponding to $E_c/E_t = 1$, is obtained from Fig. 2.18 in which the value of coefficient is plotted against E_c/E_t for a ν_c equal to 0.365.
- Step 3: From the relationship between central tensile stress and the observed central tensile strain the relationship between the tensile stress and the tensile strain, for $E_c/E_t = 1$ is obtained. This relationship is shown by a solid line passing through solid circles in Fig. 2.21. This relationship is obtained by deducting the tensile strain at the centre caused by

the compressive stress from the observed central tensile strain (Eq. 2.9, Section 2.5.3).

Step 4: The secant modulus (E_t) at 2/3 of the failure tensile stress is obtained from the tensile stress-strain relationship derived in Step 3. The value is 31.99 psi (Table 2.3) and the corresponding ratio of E_c/E_t is 8.16.

The relationship in Step 3 is obtained for $E_c/E_t = 1$, whereas the actual E_c/E_t computed from the relationship is equal to 8.16. Steps 2, 3 and 4 are repeated for the $E_c/E_t = 8.16$, making use of Figs. 2.18 and 2.4, and the new value of E_c/E_t is computed. The procedure is repeated until the values of E_c/E_t obtained in two successive cycles of computation agree reasonably with each other (Table 2.3). In this example the final relationship between tensile stress and strain, derived for a value of $E_c/E_t = 11.64$, gives $E_c/E_t = 12.10$ which is reasonably close to 11.64. Further calculations are not necessary because the corresponding change in the final tensile stress-strain relationship is negligible. In Fig. 2.21 the final tensile stress-strain relationship is shown by a solid line through squares.

2.10 Discussion of Tension and Compression Test Results

Since the tensile deformations were measured on the same gauge length in all the tests performed, the influence of various factors has been studied in terms of the observed failure strains instead of "true" tensile failure strains.

Similarly the tensile strength of the soil as influenced by different factors was computed using the formula given by Eq. 2.5. Since the purpose of the present study was mainly to compare the influence of different factors on the tensile characteristics of soil, the somewhat simplified approach adopted here was considered to be appropriate enough to bring out the salient points.

2.10.1 Effect of Water Content

The tensile strength of the low-plastic till tested, decreases with an increase in water content at failure (Fig. 2.22). The observed average tensile strain at failure on the other hand increases with the increase in water content at failure (Fig. 2.23). The increase in strain becomes disproportionately high at water contents greater than the optimum. Assuming for the present studies, the ratio of the failure tensile stress to the observed average tensile strain as a measure of stiffness of the soil in tension it can be seen from Fig. 2.24 that the stiffness decreases with an increase in the water content at failure.

2.10.2 Effect of Compactive Effort

As stated in Section 2.8.3, the amount of compactive effort was varied by changing the number of blows. The weight of the hammer (5.5 lbs.) and the height of fall (12") were constant for all the tests. The water content-dry density relationships obtained for 25, 50 and 70 blows are shown

in Fig. 2.25. The tensile stress at failure increases with the compactive effort for water contents below the optimum and decreases slightly with the compactive effort for water contents above the optimum (Fig. 2.26). The observed average tensile strain at failure and the stiffness of the soil in tension are plotted against water content at failure in Figs. 2.27 and 2.28 respectively. Increasing the compactive effort for water contents greater than about 7% causes a decrease in the stiffness of the soil in tension. This appears to be due to the effect of some softening induced by over compacting the non-plastic Mica Till at water contents above and close to the optimum. However, increasing the compactive effort at water contents well below the optimum increases the stiffness as well as the tensile strength of soil.

2.10.3 Effect of Rate of Loading

The effect of rate of loading on the tensile strength and on the observed average tensile strain at failure is shown for water contents at 9% and 10.4% in Figs. 2.29 and 2.30. Both the tensile strength and the strain at failure attain the minimum values at a certain rate of loading depending on the water content at failure. Tschebotarioff et al. (1953) reported a decrease in tensile strength and tensile strain at failure with an increase of the duration of the test. The test duration for the tests conducted by Tschebotarioff et al. (1953) ranged approximately from 5 to 430 minutes. Narain (1962) reported an increase in the tensile strength and ten-

sile strain at failure with the increase of the test duration. The duration of tests conducted by Narain (1962) ranged from 2 days to 6 months. The two opposite effects of test duration on the tensile characteristics of compacted soils reported by Tschebotarioff et al. (1953) and Narain (1962) appear to be mainly due to the different ranges of test durations used in the experiments. The test durations of the present tension tests cover the range of test durations reported by Tschebotarioff et al. (1953) and extend to the lowest of the range reported by Narain (1962). From Figs. 2.29 and 2.30 it can be seen that the duration of test has a significant effect on the tensile characteristics of a compacted soil. The critical rate of loading at which the minimum tensile strength is mobilized is almost the same as that needed to produce the minimum tensile strain at failure. However the critical rate of loading is influenced by the water content at failure (Figs. 2.29 and 2.30). From a practical point of view, it can be concluded that a fairly rapid loading, comparable to the test durations lasting between 1 to 2 days, causes conditions favourable to the formation of cracks. Considering only the effect of rate of loading, it is unlikely that extremely rapid or extremely slow rates of loading would cause tensile failures in compacted soils of low to medium plasticity. By conducting a number of representative laboratory tension tests at different rates of loading it appears possible to define the minimum tensile strength and the minimum tensile strain at failure for a given compacted soil of the type tested here.

2.10.4 Effect of Adding Bentonite

As a means of increasing the flexibility of the core of an earth dam a small percentage of bentonite may be added to the almost non-plastic till. For example, in the case of Duncan Dam (Chapter V) about 6% bentonite was added to the core material. To study the effect of adding the bentonite, tension tests were conducted on a mixture of Mica Till and 6% by weight of commercial bentonite. Fig. 2.31 shows the water content-dry density relationships for Mica Till with and without bentonite. Addition of 6% bentonite decreased the maximum dry density by 6 pcf and increased the optimum water content by 1.6%. The liquid limit and plasticity index are also increased by 23.8% and 17.3 respectively.

The effect of water content at failure on the tensile strength of Mica Till is shown in Fig. 2.32 with and without bentonite. A significant difference between the variation of the tensile strength for water contents below optimum is evident. For Mica Till without bentonite the tensile strength decreases steadily with the water content while for Mica Till with 6% bentonite the tensile strength increases up to the optimum water content and then decreases beyond the optimum.

The tensile strain at failure increases with water content at failure both for Mica Till and Mica Till with bentonite (Fig. 2.33). However the increase in failure strain is more rapid in the case of Mica Till for water contents greater than optimum. To achieve the required flexibility,

the soil mixed with bentonite requires a higher percentage of water than that needed for a soil without bentonite. The stiffness of Mica Till with and without bentonite is shown against the tensile strength in Fig. 2.34. For Mica Till without bentonite a decrease in stiffness is followed by a decrease in tensile strength. On the other hand for Mica Till with bentonite a decrease in stiffness up to the optimum water content is followed by a slight increase in tensile strength. Beyond the optimum moisture content, the tensile strength decreases with the stiffness. Comparing the two soils at a given stiffness it will be noted that till with bentonite has a greater tensile strength than till without bentonite. The decrease in tensile strength for water contents beyond the optimum is more rapid in the case of Mica Till without bentonite than that with bentonite. The addition of bentonite to till makes it possible to increase the flexibility without appreciably decreasing the tensile strength. In Fig. 2.35, the percent decrease in tensile strength that occurs with an increase of water content of 2% above the optimum for different soils is shown. The results for soils from A to F were obtained from the work of Narain and Rawat (1970). The results for soils G and H are from the present work. As can be seen from Fig. 2.35, the percent decrease in tensile strength is more for soils of low plasticity than that of soils of high plasticity.

2.10.5 Comparison of Compression and Tensile Characteristics

The stress-strain relationship obtained from unconfined compression tests on Mica Till are shown in Fig. 2.36. The variation of the compressive strength and strain at failure with water content is shown in Fig. 2.37. A comparison of compression and tensile characteristics of Mica Till appears in Fig. 2.38. The ratio of compressive strength to tensile strength increases with the water content. This is due to the fact that the reduction of tensile strength with water content is more rapid than that of compressive strength. The ratio of compressive failure strain to the tensile failure strain decreases initially and stays relatively constant for water contents greater than 7%. The secant moduli, assumed here as the ratio of the failure stress to failure strain, are also compared in Fig. 2.38. The ratio of secant moduli increases with the water content. This increase is mainly due to the greater percent reduction of tensile strength with water content as compared to the percent reduction of compressive strength (Figs. 2.22 and 2.37).

2.11 Summary

Soils are extremely weak in tension. The tensile strength of an earth dam core, comprised of soils of low to medium plasticity, can be assumed to be zero for purposes of design and analysis. The tensile strength measured here for a till of low plasticity, compacted at a water content 1.5% greater than the optimum, is only about 0.5 psi. Considering

different methods of tensile testing, the Brazilian or the indirect tension test offers the maximum facility for testing soils in tension. However, because of the biaxial stress state that exists, the interpretation of the test becomes somewhat involved. When the moduli in tension and compression are not equal, as is usually the case for soils of low to medium plasticity, the theoretical stress solutions obtained under isotropic conditions over-estimate the tensile strength of the material. Numerical solutions, using the finite element method, for cases involving different moduli in tension and compression, have been obtained in this report to estimate the tensile strength of soils. By conducting parallel unconfined compression tests, the relationship between tensile stress and tensile strain can be determined from the data of an indirect tension test.

At water contents greater than the optimum the flexibility of a soil increases accompanied by a considerable decrease in tensile strength. The percent decrease of the tensile strength is higher for a less plastic soil compared to that of a more plastic soil. Addition of bentonite with the appropriate water content aids in increasing the flexibility of the soil, at the same time without a considerable reduction in the tensile strength. For a compacted till of low plasticity, the rate of loading has a significant influence on the tensile strength mobilized at failure and the associated tensile strain. Rates of loading comparable to a laboratory test duration of one to two days appears to be critical for

the type of soil tested in this investigation.

The ratio of unconfined compressive strength to the tensile strength increases with the water content. The ratio for the soil tested varied from 11 to 31.2 for water contents 3.56% below optimum to 1.45% above optimum respectively.

As the water content increases, for a low plastic soil the tensile strength decreases very rapidly while the reduction in compressive strength is comparatively less. The ratio of modulus in compression to that in tension also increases with the water content. The ratio for the till tested varied from 2.68 to 15.40 for water contents 3.56% below the optimum to 1.45% above the optimum.

TABLE 2.1
DETAILS OF TENSION AND COMPRESSION TESTS PERFORMED

Name of the Series and Type of Test	Purpose	Name of Sample	Percent Water Added at the Time of Mixing	Rate of Test (inches/min.)	Number of Blows Per Layer Administered by a 5.5 lb. Hammer with 12" Fall	Number of Samples Tested
M Tension	To study the influence of water content	M5/1, M5/2, M5/3	5.5	0.005	25	3
		M6/1, M6/2	6.5	0.005	25	2
		M6/3	6.0	0.005	25	1
		M7/1, M7/2	7.5	0.005	25	2
		M9/1, M9/2, M9/3	9.5	0.005	25	3
C Tension	To study the influence of compactive effort	M11/1, M11/2, M11/3	11.0	0.005	25	3
		C6/50	6.0	0.005	50	1
		C6/70	6.0	0.005	70	1
		C7/50	7.5	0.005	50	1
		C7/70	7.5	0.005	70	1
		C9/50	9.5	0.005	50	1
		C9/70	9.5	0.005	70	1
T Tension	To study the influence of the rate of loading	C11/50	11.0	0.005	50	1
		C11/70	11.0	0.005	70	1
		S21, S22, S23	9.5	0.001300	25	3
		S31, S41, S51	9.5	0.000100	25	3
		S61, S62, S63	9.5	0.000013	25	3
		T21, T22, T23	11.0	0.001300	25	3
		T31, T41, T51	11.0	0.000100	25	3
B Tension	To study the influence of adding 6% bentonite	T61, T62, T63	11.0	0.000013	25	3
		B6/1, B6/2, B6/3	6.6	0.005	25	3
		B8/1, B8/2, B8/3	8.6	0.005	25	3
		B10/1, B10/2, B10/3	10.6	0.005	25	3
		B12/1, B12/2, B12/3	12.6	0.005	25	3
UC Unconfined Compression	To compare the behaviour of soil in tension and compression	UC6	6.0	0.005	25	1
		UC7	7.5	0.005	25	1
		UC9	9.5	0.005	25	1
		UC11	11.0	0.005	25	1
Total Number of Tests:		Tension	52			
		Compression	4			

TABLE 2.2
COMPUTATION OF TENSILE STRESS AND STRAIN FROM EXPERIMENTAL DATA

Load Cell Reading in Milli- volts	Load in Millivolts	Tensile stress in psi (2) x 1.75	Strain Gauge Reading from Bottom End of Specimen in Millivolts	Observed Tensile Strain from Bottom End in Millivolts	Observed Tensile Strain from Bottom End in Percent (5)x0.1417	Strain Gauge Reading from Top End of Specimen in Millivolts	Observed Tensile Strain from Top End of Specimen in Millivolts	Observed Tensile Strain from Top End in Percent (8)x0.259	Average Observed Tensile Strain [(6)+(9)]/2
(1)	(2)	(3)	(4)	(5)	(6)	(7)	(8)	(9)	(10)
1.58	0.05	0	1.55	0	0	50.40	0	0	0
1.63	0.08	0.088	2.76	1.21	0.171	49.47	0.93	0.241	0.206
1.66	0.08	0.140	3.46	1.91	0.271	49.02	1.38	0.357	0.314
1.68	0.10	0.175	4.12	2.57	0.364	48.62	1.78	0.461	0.413
1.70	0.12	0.210	4.52	2.97	0.421	48.42	1.98	0.513	0.467
1.72	0.14	0.245	5.51	3.96	0.561	47.90	2.50	0.648	0.605
1.74	0.16	0.280	6.73	5.18	0.734	47.30	3.10	0.803	0.769
1.76	0.18	0.315	8.04	6.49	0.920	46.68	3.72	0.963	0.942
1.78	0.20	0.350	9.94	8.39	1.189	45.85	4.55	1.178	1.184
1.80	0.22	0.385	11.40	9.85	1.396	45.26	5.14	1.331	1.364
1.82	0.24	0.420	14.47	12.92	1.831	44.09	6.31	1.634	1.733
1.84	0.26	0.455	17.18	15.63	2.215	43.07	7.33	1.898	2.057
1.86	0.28	0.490	21.27	19.72	2.794	41.46	8.94	2.315	2.555
1.88	0.30	0.525	24.58	23.03	3.263	40.28	10.12	2.621	2.942
1.86	0.28	0.490	35.99	34.44	4.880	35.32	15.08	3.906	4.393

Note: Bottom or top end refer to the position of the specimen while it was compacted.

TABLE 2.3
DETERMINATION OF TENSILE STRESS-STRAIN RELATIONSHIP

$E_c/E_t = 1.0$					$E_c/E_t = 8.16$					$E_c/E_t = 11.64$				
Tensile Stress at Centre of Specimen	Observed Average Strain Over a Length of 0.84"	Observed Tensile Strain at Centre of Specimen	Tensile Strain Due to Compressive Stress Alone	(psi) (1)	Observed Tensile Strain at Centre of Specimen	Tensile Strain Due to Compressive Stress Alone	(psi) (2)	(3)	(4)	Observed Tensile Strain at Centre of Specimen	Tensile Strain Due to Compressive Stress Alone	(psi) (3)	(4)	(5)
0.088	0.206	0	0.037	0	0.216	0	0.061	0.221	0.046	0	0.175	0	0.223	0
0.140	0.314	0.329	0.059	0.270	0.337	0.073	0.098	0.337	0.073	0.341	0.078	0.341	0.341	0.174
0.175	0.413	0.433	0.073	0.360	0.444	0.091	0.123	0.444	0.091	0.448	0.097	0.448	0.448	0.263
0.210	0.467	0.489	0.088	0.401	0.502	0.109	0.147	0.502	0.109	0.506	0.117	0.506	0.506	0.351
0.245	0.505	0.534	0.103	0.531	0.550	0.128	0.172	0.550	0.128	0.556	0.136	0.556	0.556	0.389
0.280	0.769	0.806	0.118	0.688	0.826	0.146	0.196	0.826	0.146	0.834	0.156	0.834	0.834	0.520
0.315	0.942	0.987	0.132	0.855	1.012	0.164	0.221	1.012	0.164	1.022	0.175	1.022	1.022	0.673
0.350	1.184	1.241	0.147	1.094	1.272	0.182	0.245	1.272	0.182	1.284	0.194	1.284	1.284	0.827
0.385	1.364	1.429	0.162	1.267	1.465	0.200	0.270	1.465	0.200	1.479	0.214	1.479	1.479	1.092
0.420	1.733	1.816	0.176	1.640	1.861	0.219	0.294	1.861	0.219	1.879	0.233	1.879	1.879	1.265
0.455	2.057	2.156	0.191	1.965	2.209	0.237	0.319	2.209	0.237	2.231	0.253	2.231	2.231	1.646
0.490	2.555	2.678	0.206	2.472	2.744	0.255	0.343	2.744	0.255	2.771	0.272	2.771	2.771	1.578
0.525	2.942	3.083	0.220	2.863	3.160	0.273	0.368	3.160	0.273	3.191	0.292	3.191	3.191	2.499
0.490	4.393	4.604	0.206	4.398	4.718	0.255	0.343	4.718	0.255	4.764	0.272	4.764	4.764	2.899

$E_c = 260.9$ psi; $\nu_c = 0.365$

At 2/3 of the maximum tensile stress:

$$E_t = \frac{100 \times 0.35}{1.094} = 31.99 \text{ psi}$$

and $E_c/E_t = 8.16$.

$E_c = 260.9$ psi; $\nu_c = 0.365$

At 2/3 of the maximum tensile stress:

$$E_t = \frac{100 \times 0.245}{1.090} = 22.47 \text{ psi}$$

and $E_c/E_t = 11.64$.

$E_c = 260.9$ psi; $\nu_c = 0.365$

At 2/3 of the maximum tensile stress:

$$E_t = \frac{100 \times 0.235}{1.090} = 21.56 \text{ psi}$$

and $E_c/E_t = 12.10$.

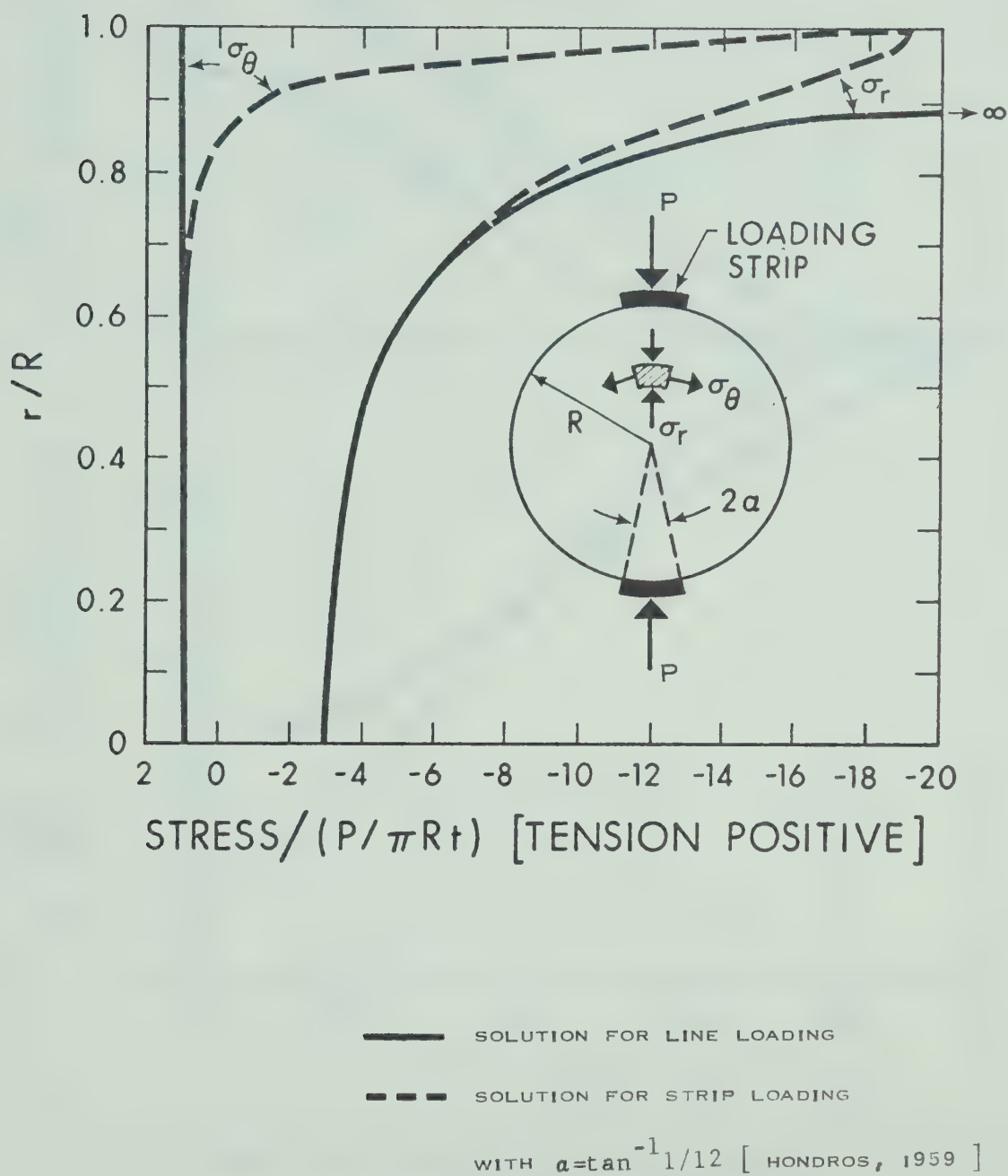


FIG. 2.1 THEORETICAL SOLUTIONS FOR STRESSES ALONG THE VERTICAL DIAMETER OF A SPECIMEN SUBJECTED TO DIAMETRAL COMPRESSION

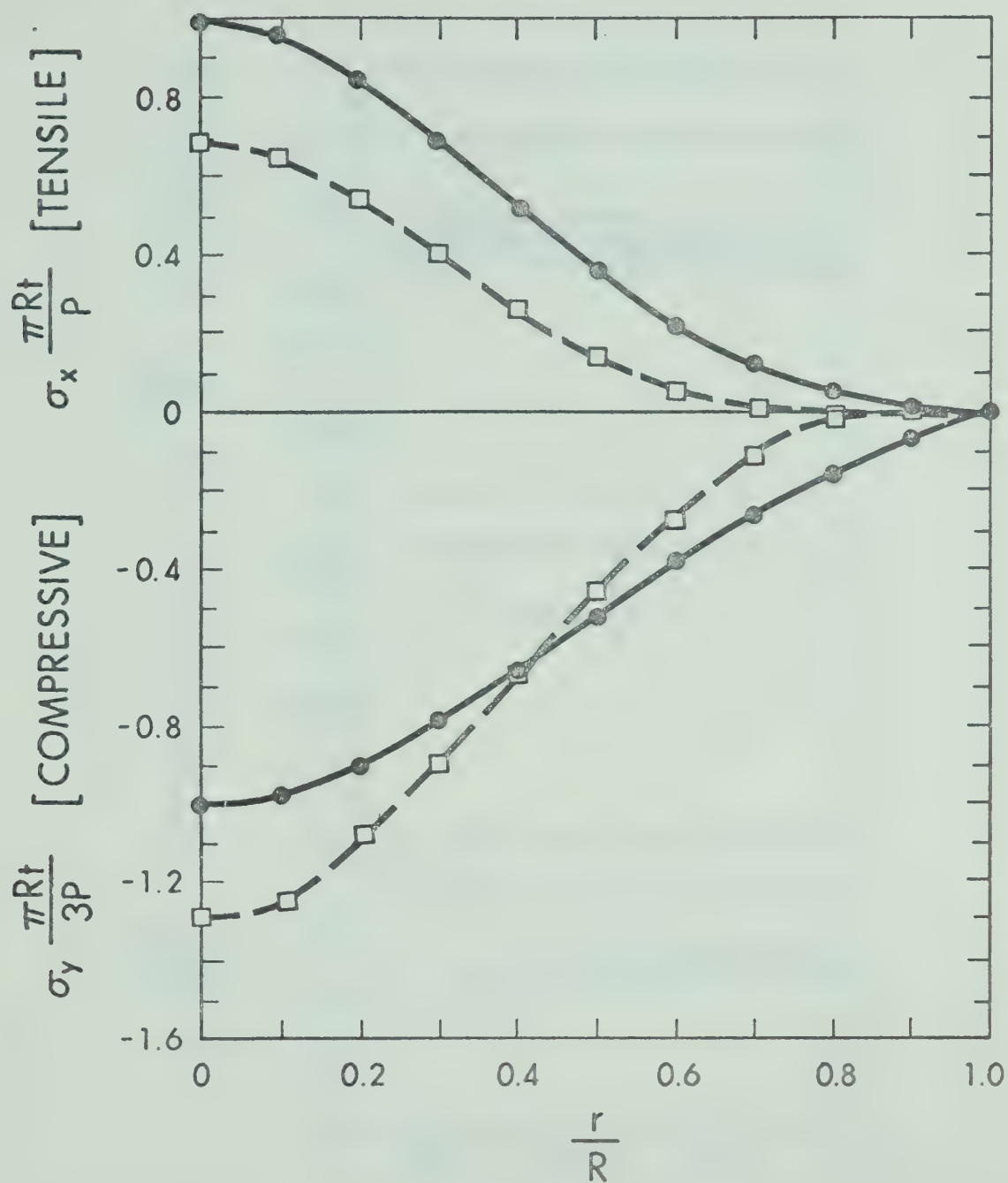


FIG. 2.2 VARIATION OF STRESSES ALONG THE HORIZONTAL DIAMETER OF A SPECIMEN UNDER DIAMETRAL COMPRESSION [COMPARISON OF THEORETICAL AND FINITE ELEMENT SOLUTIONS AND EFFECT OF POISSON'S RATIO ON STRESS DISTRIBUTION]

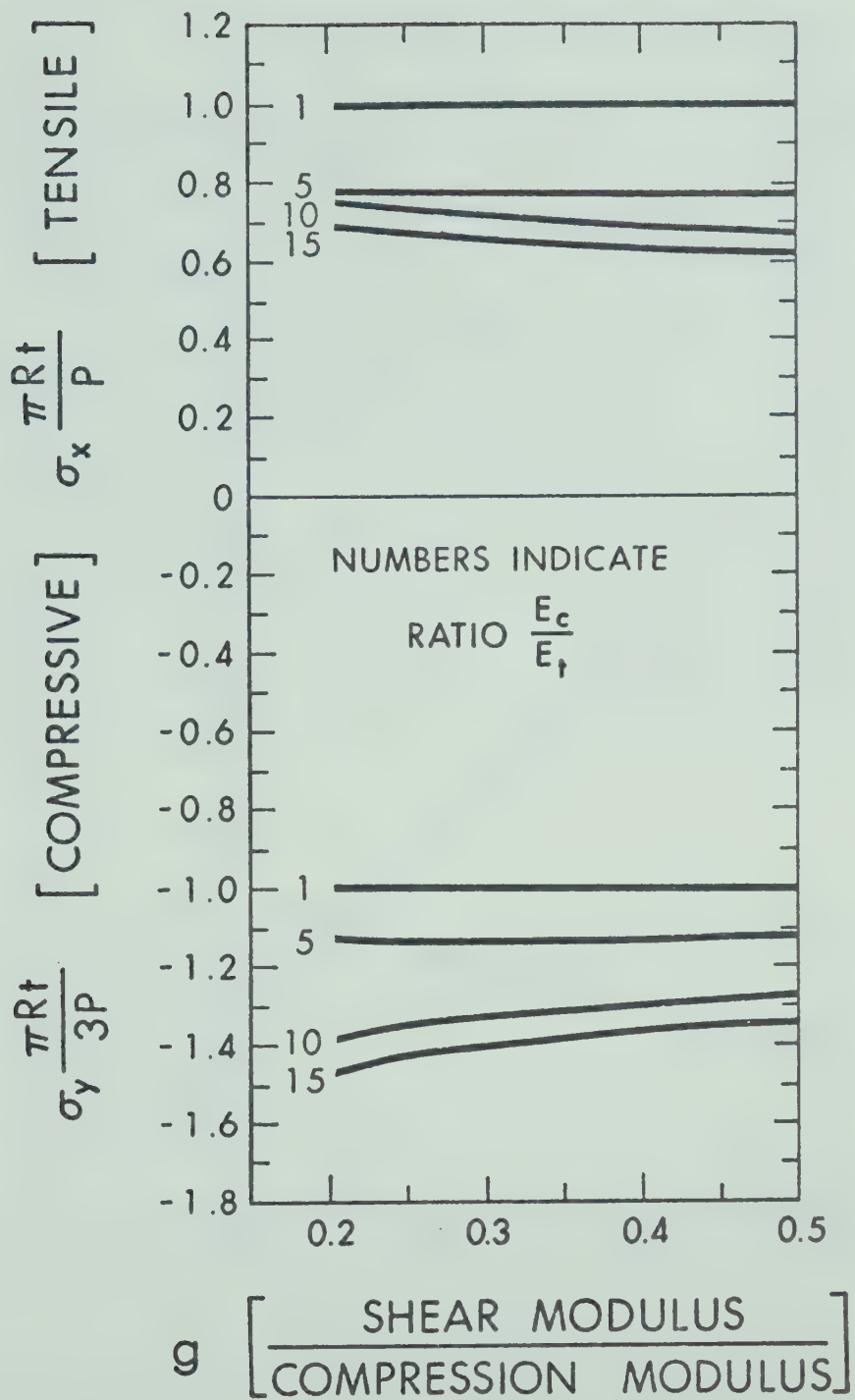


FIG. 2.3 VARIATION OF COMPRESSIVE AND TENSILE STRESS AT THE CENTRE OF SPECIMEN WITH SHEAR MODULUS FOR DIFFERENT RATIOS OF E_c/E_t

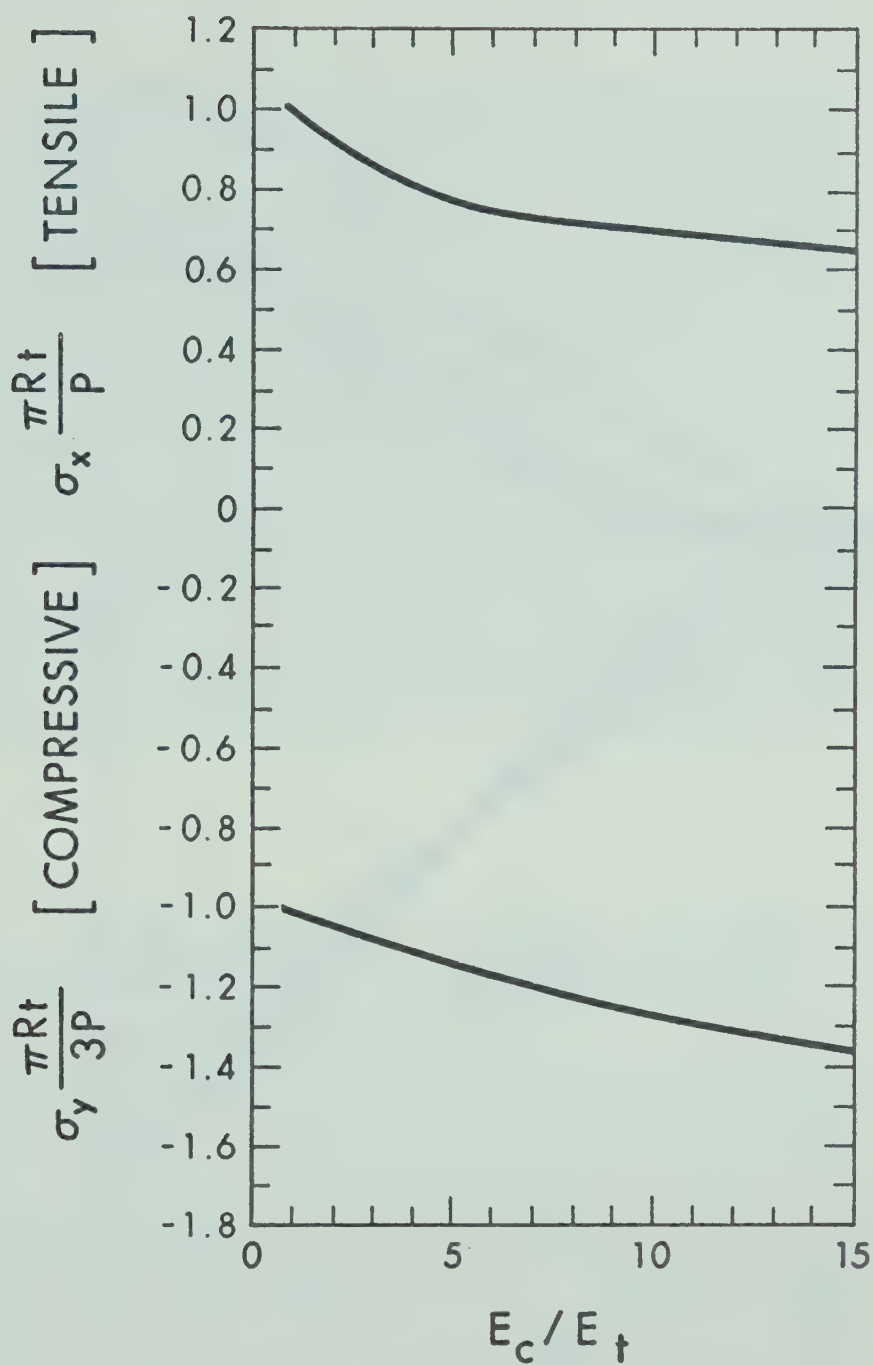


FIG. 2.4 VARIATION OF TENSILE AND COMPRESSIVE STRESS AT THE CENTRE OF SPECIMEN UNDER DIAMETRAL COMPRESSION WITH THE RATIO E_c/E_t [STRESSES CORRESPOND TO G/E_c EQUAL TO 0.4]

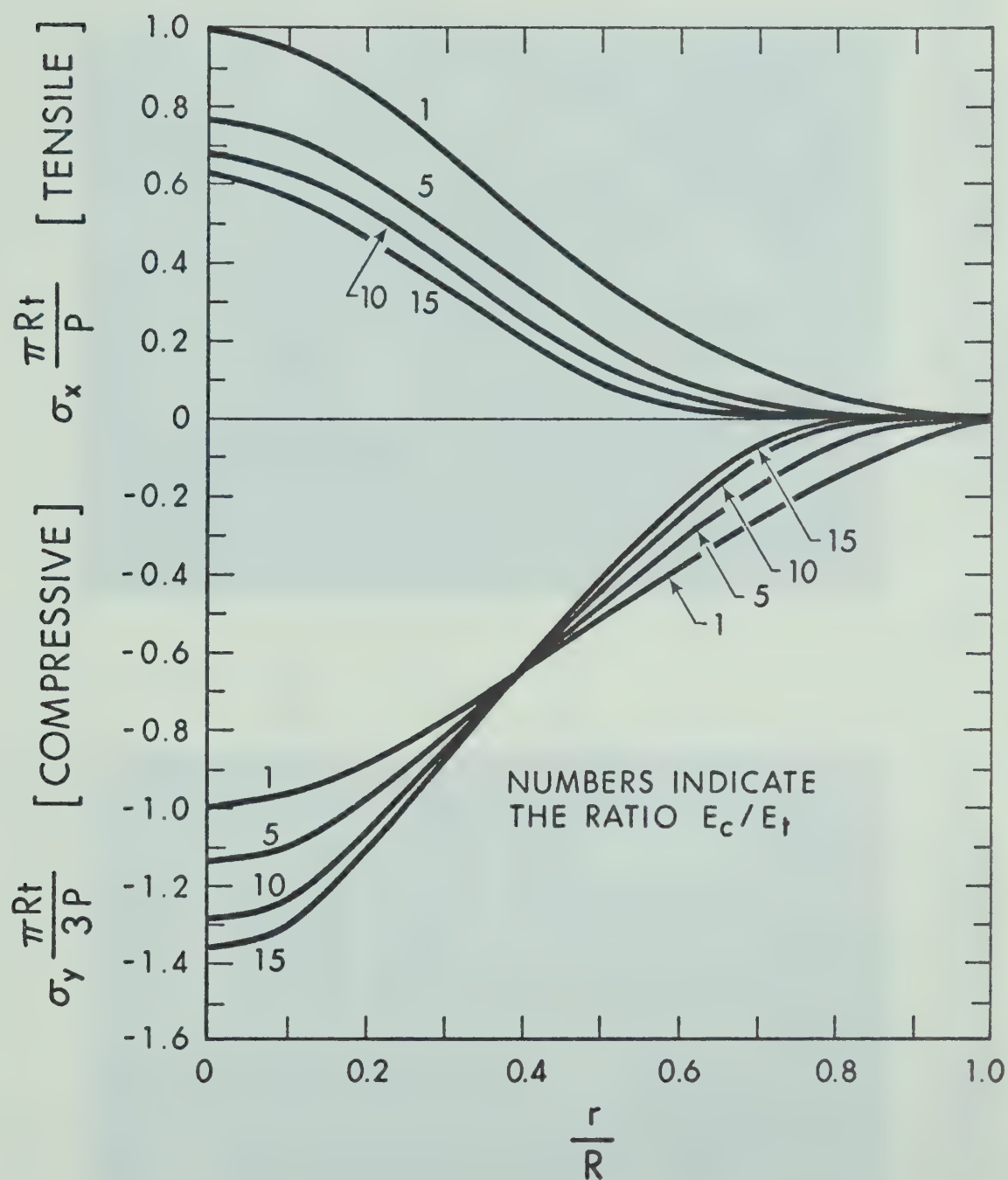


FIG. 2.5 VARIATION OF VERTICAL AND HORIZONTAL STRESS ALONG THE HORIZONTAL DIAMETER OF SPECIMEN UNDER DIAMETRAL COMPRESSION FOR DIFFERENT E_c/E_t RATIOS [STRESSES COMPUTED FOR G/E_c EQUAL TO 0.4]

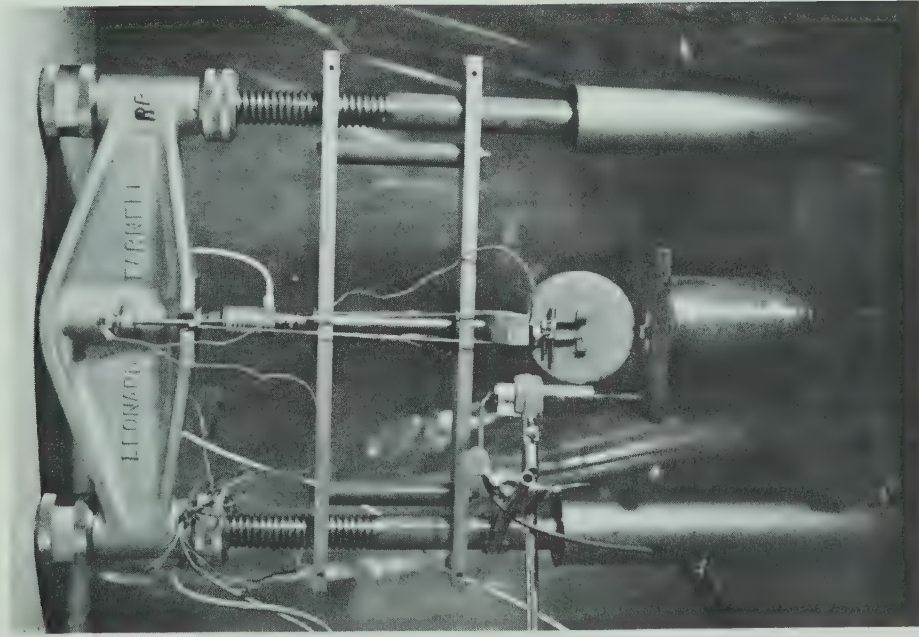


FIG. 2.6 TENSILE TEST SET-UP WITH SPECIMEN IN POSITION

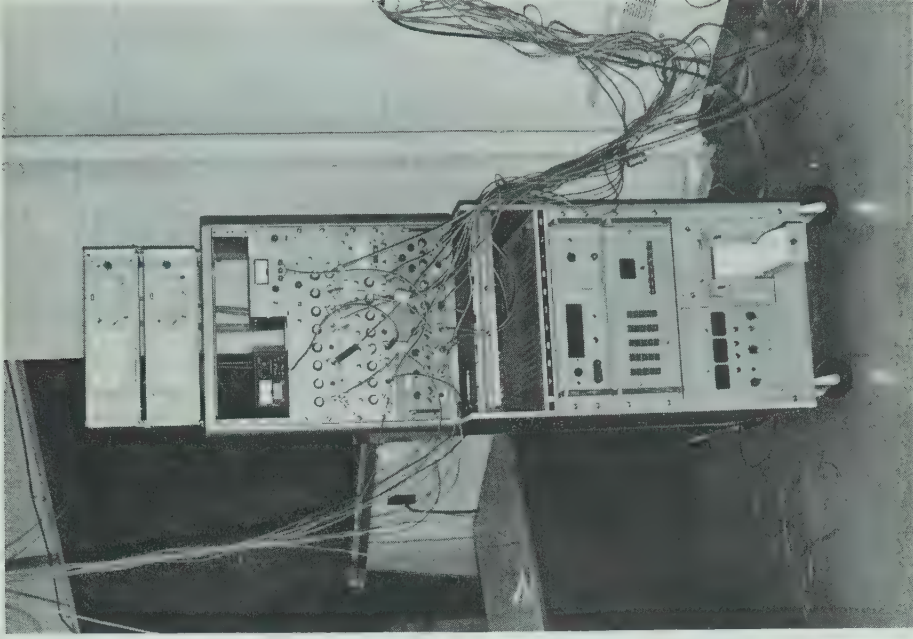


FIG. 2.7 VIEW SHOWING DATA ACQUISITION SYSTEM AND TRANSDUCER AMPLIFIERS

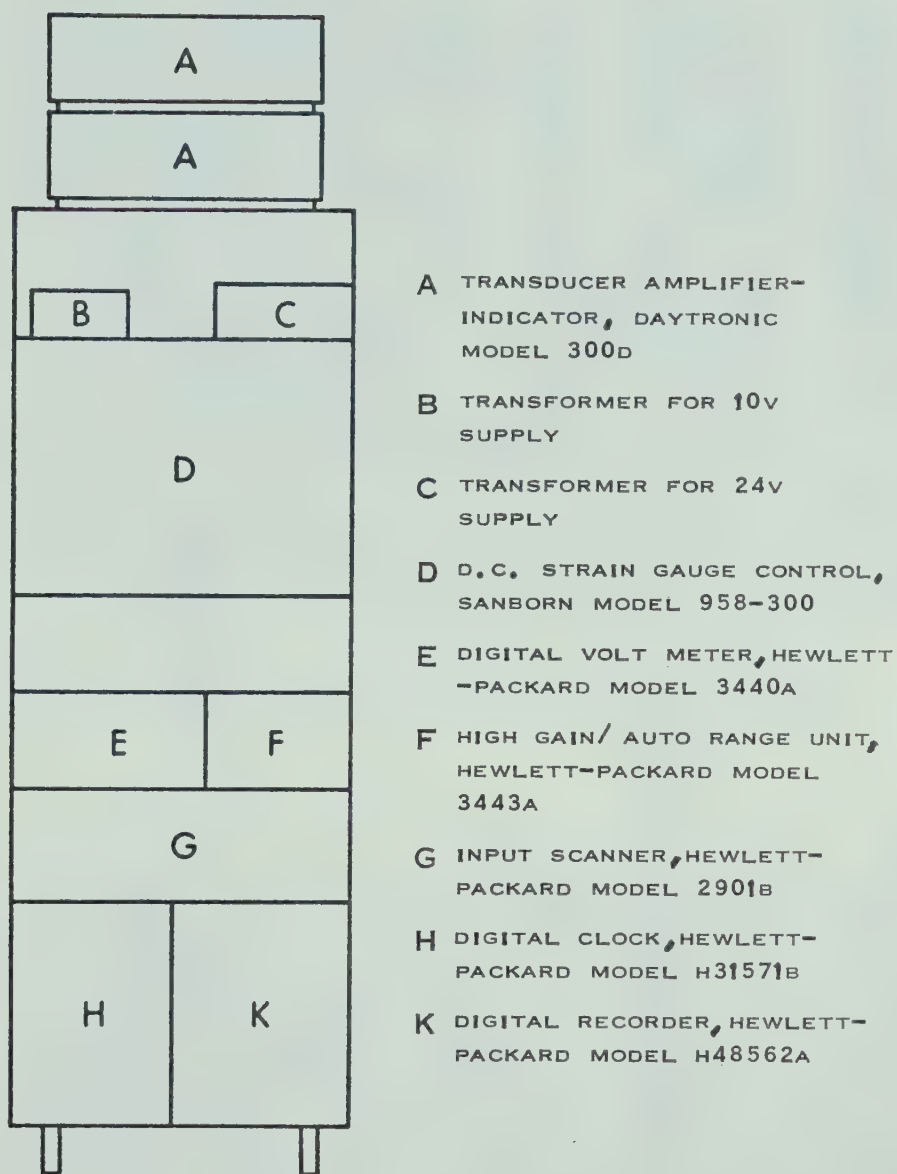
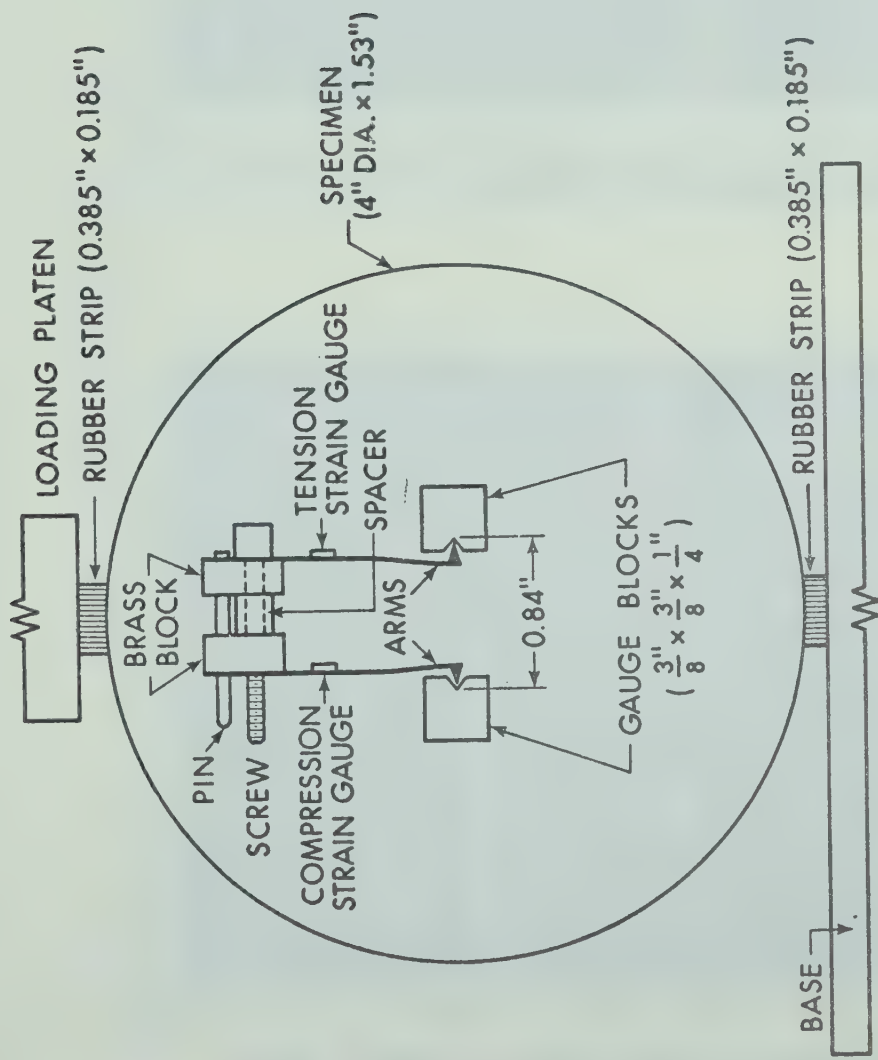
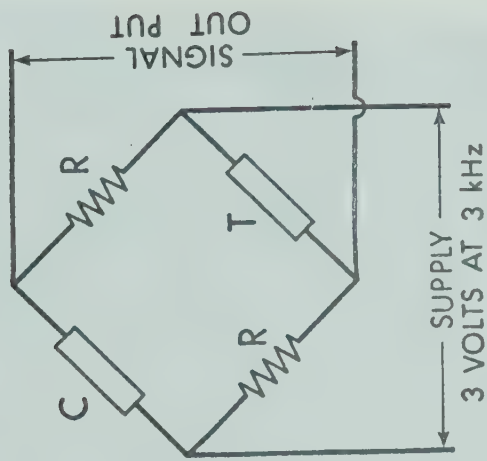


FIG. 2.8 SCHEMATIC DIAGRAM SHOWING THE DATA ACQUISITION SYSTEM AND TRANSDUCER AMPLIFIERS



[A] CLIP GAUGE POSITIONED ON THE SPECIMEN BETWEEN GAUGE BLOCKS



- C COMPRESSION STRAIN GAUGE
- T TENSION STRAIN GAUGE
- R RESISTOR (120 Ohms)

[B] FULL BRIDGE CIRCUIT FOR THE CLIP GAUGE

FIG. 2.9 DETAILS OF THE CLIP GAUGE FOR TENSION TEST

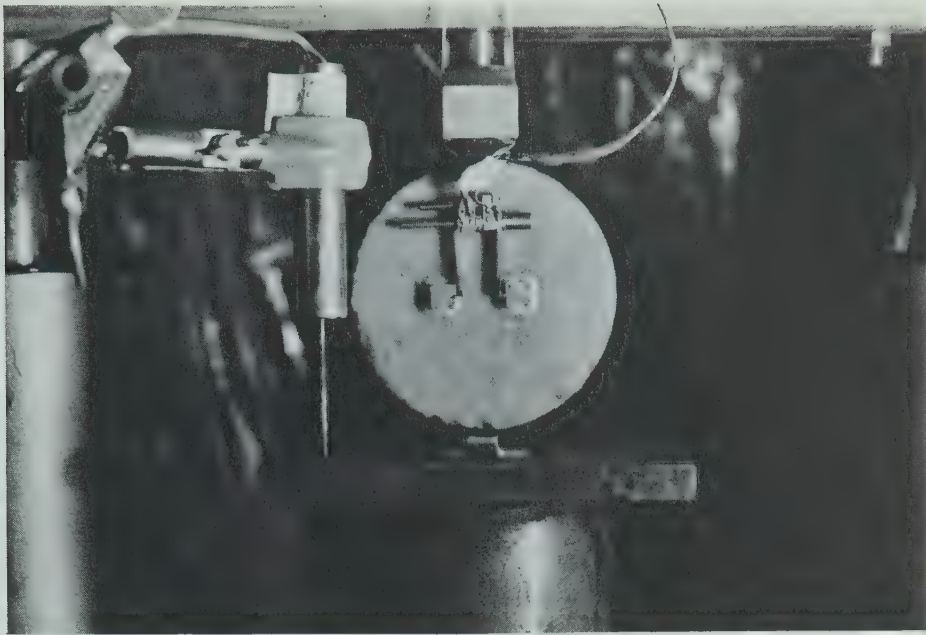


FIG. 2.10[A] A CLOSE-UP VIEW OF SPECIMEN
WITH CLIP GAUGE IN POSITION

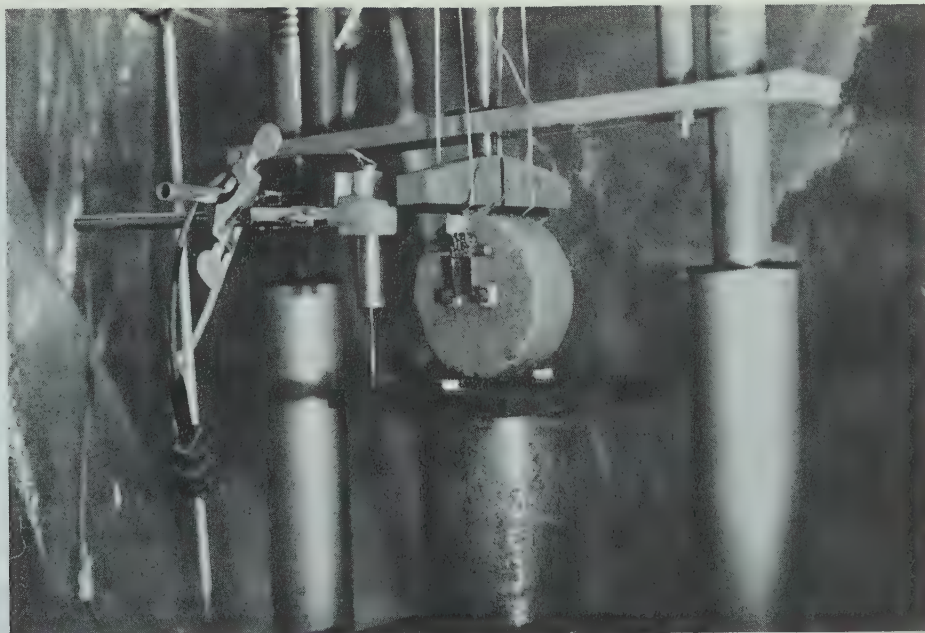


FIG. 2.10[B] A SIDE VIEW OF SPECIMEN WITH
CLIP GAUGE IN POSITION

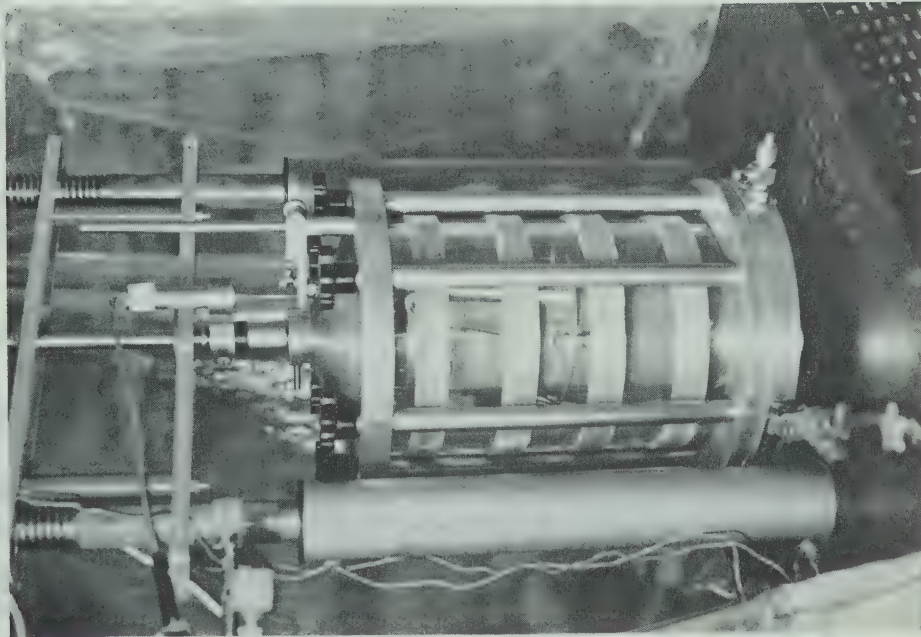


FIG. 2.11 SET-UP FOR UNCONFINED
COMPRESSION TEST

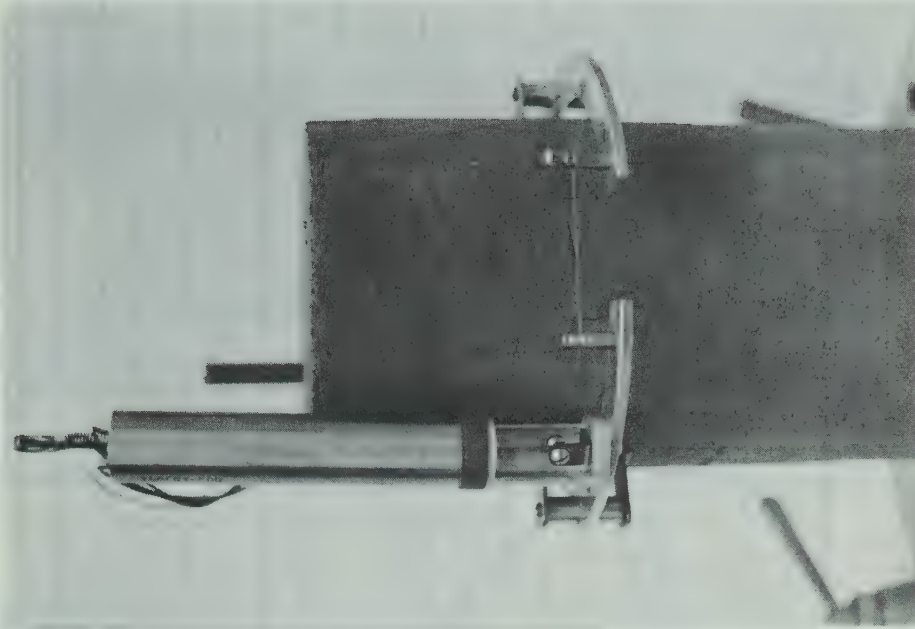


FIG. 2.12 A CLOSE-UP VIEW OF THE
LATERAL STRAIN INDICATOR

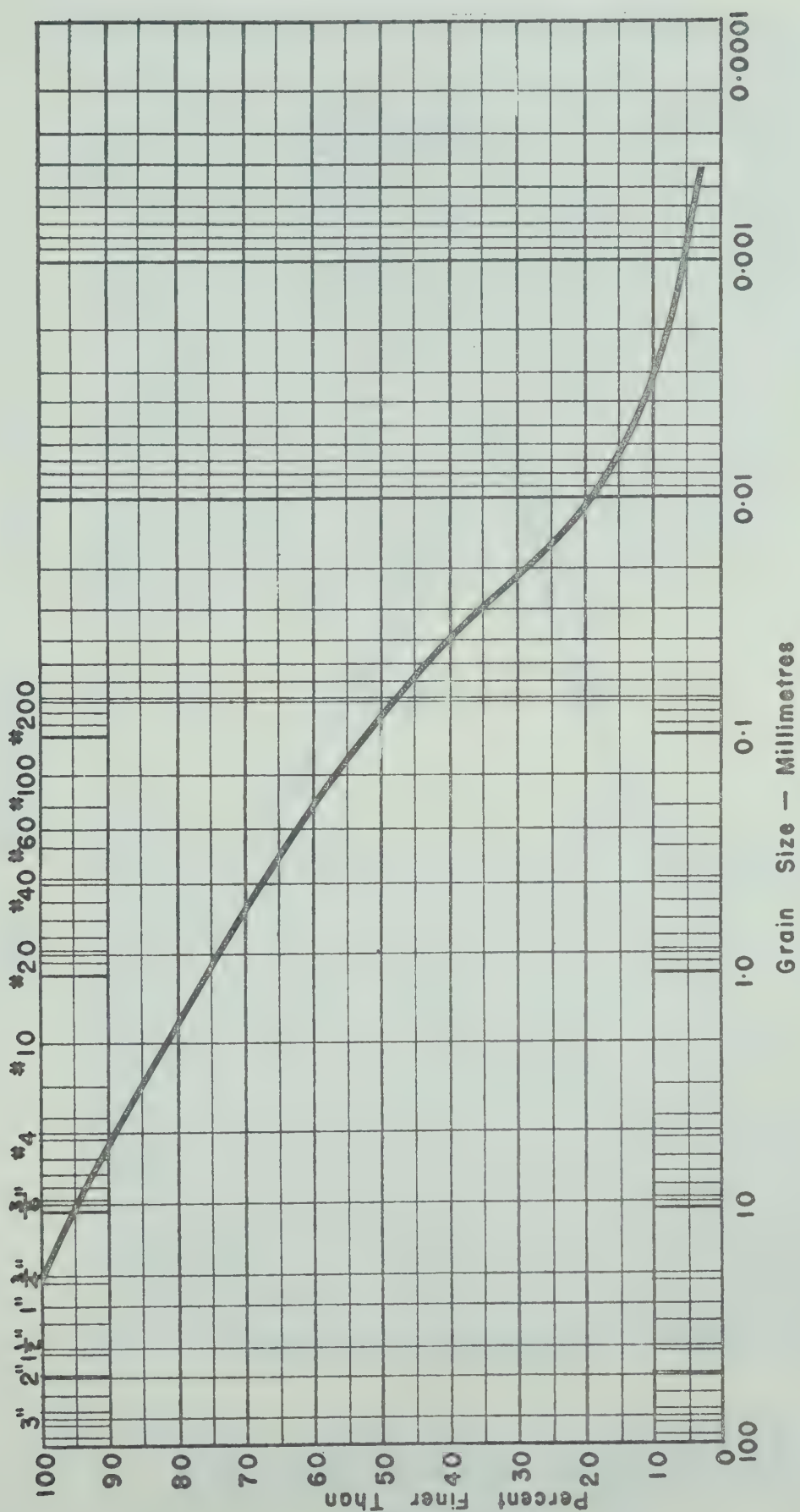


FIG. 2.13 GRAIN SIZE DISTRIBUTION FOR MICA TILL

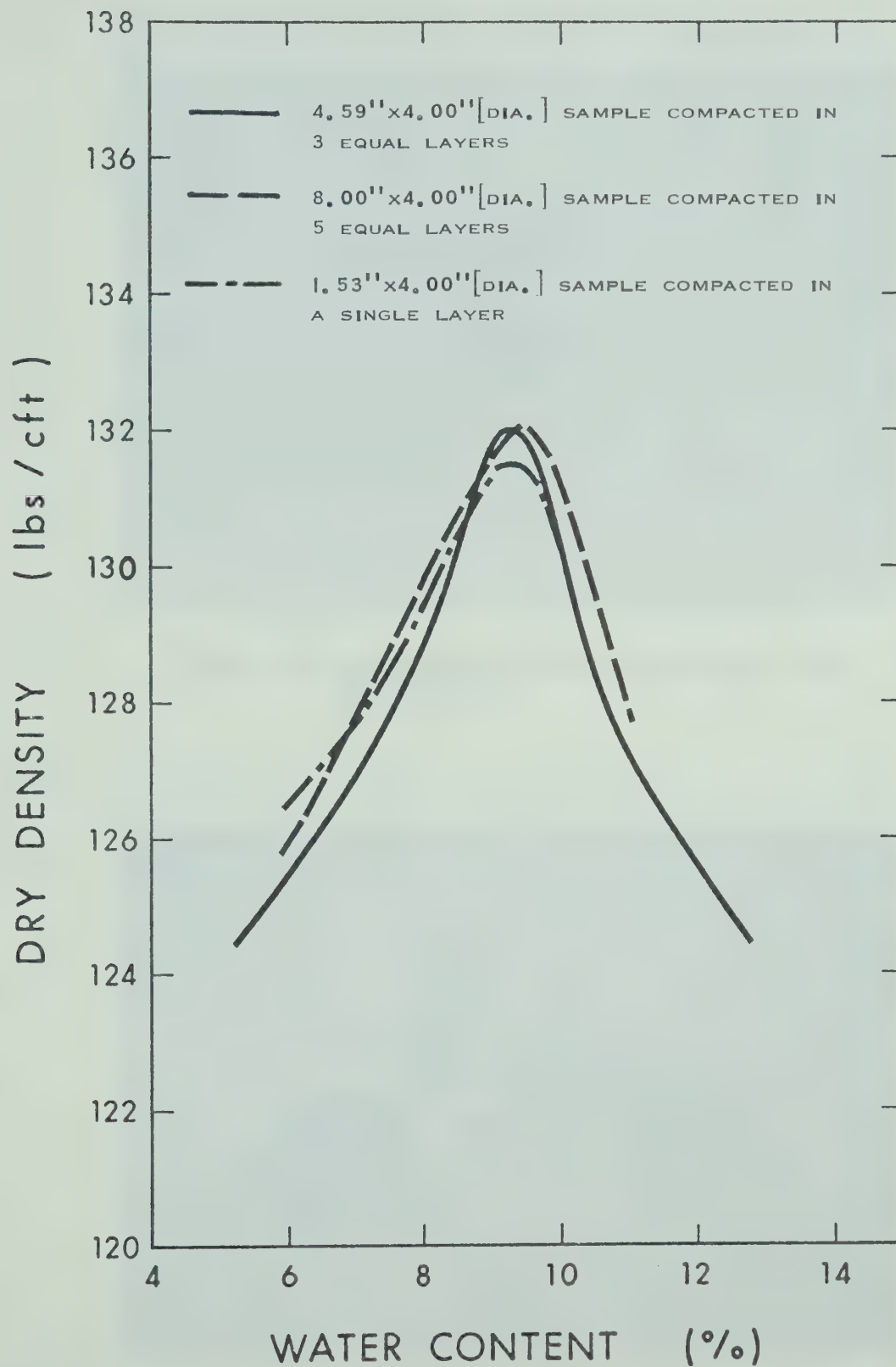


FIG. 2.14 WATER CONTENT-DENSITY RELATIONSHIPS FOR SAMPLES OF DIFFERENT SIZES PREPARED UNDER PROCTOR STANDARD COMPACTION



FIG. 2.15 SPECIMEN WITH GAUGE BLOCK JIG
IN POSITION

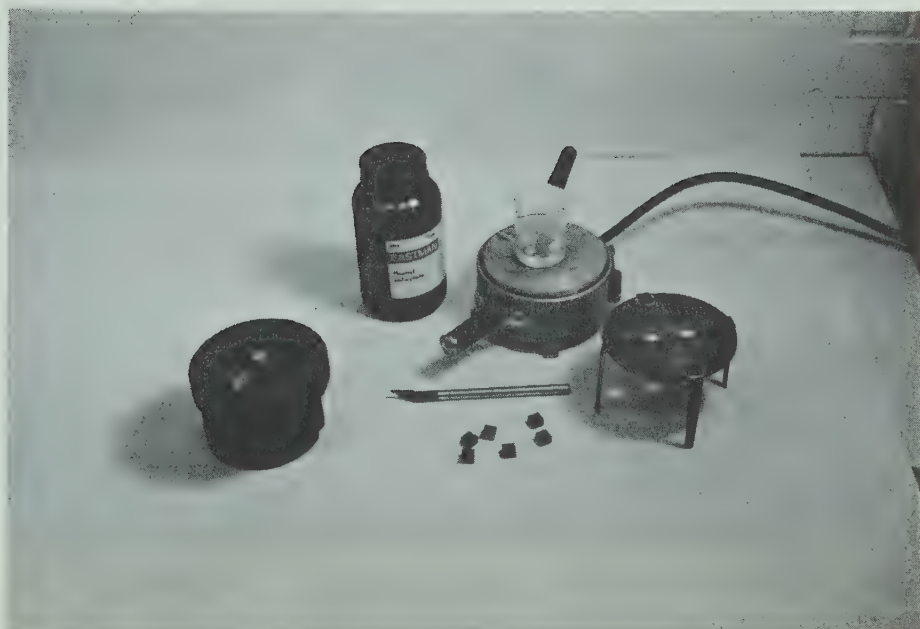
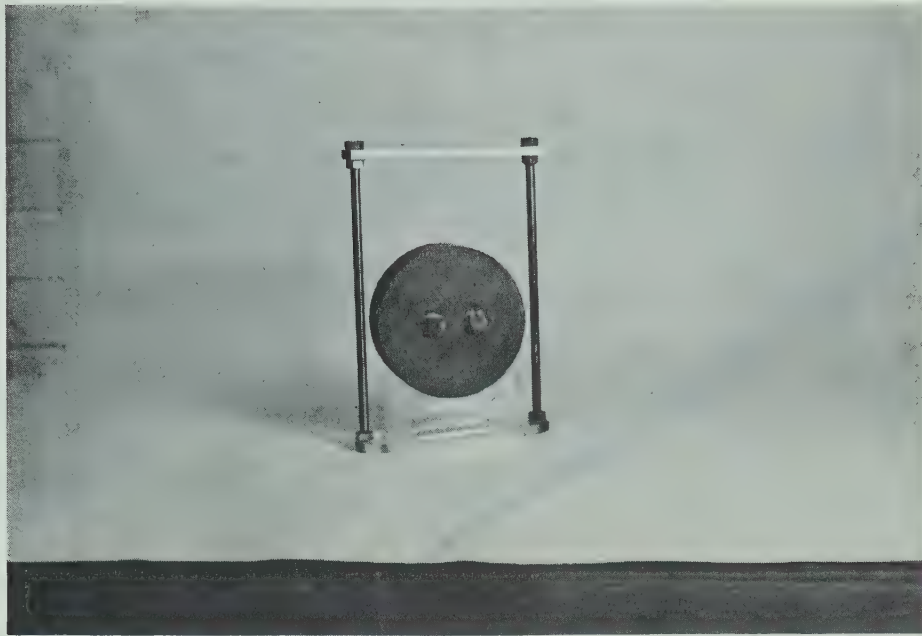
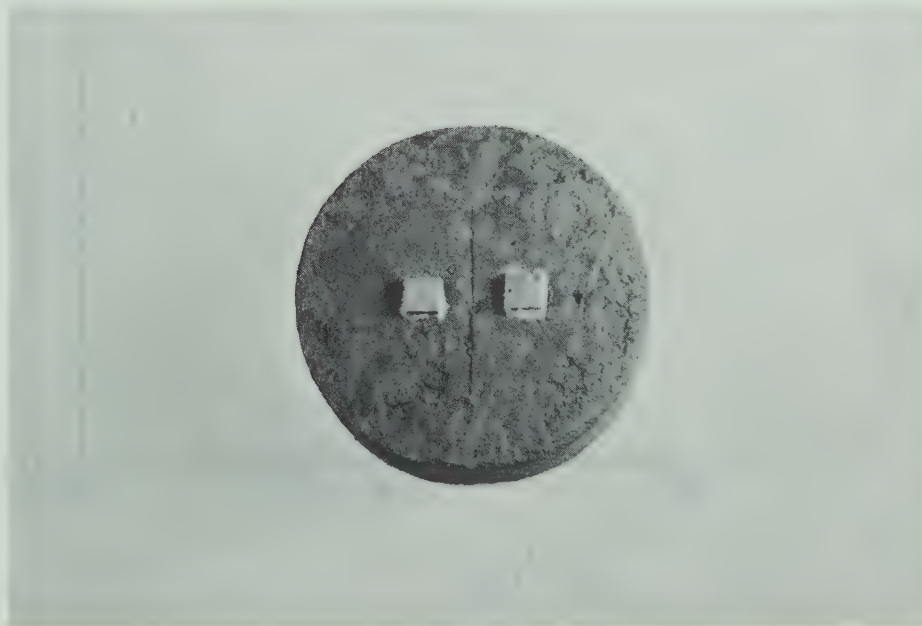


FIG. 2.16 COMPONENTS FOR ATTACHING GAUGE
BLOCKS TO SOIL SPECIMEN



[A] SPECIMEN KEPT ON A STAND BEFORE
WAXING



[B] TYPICAL BRITTLE FAILURE OF SPECIMEN

FIG. 2.17 TENSILE TEST SPECIMEN BEFORE AND
AFTER FAILURE

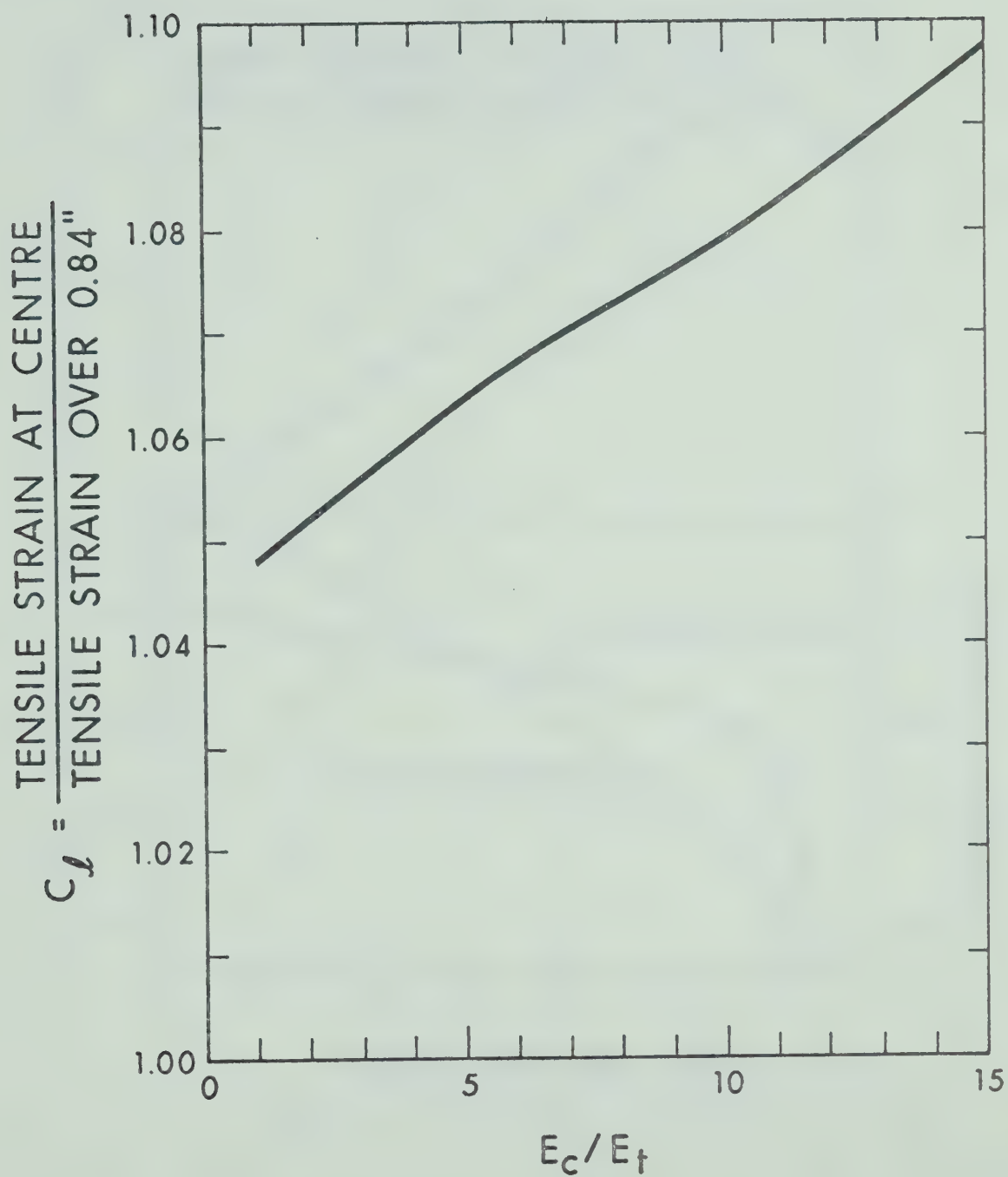


FIG. 2.18 VARIATION OF COEFFICIENT $[C_l]$ WITH E_c/E_t
FOR POISSON'S RATIO EQUAL TO 0.365

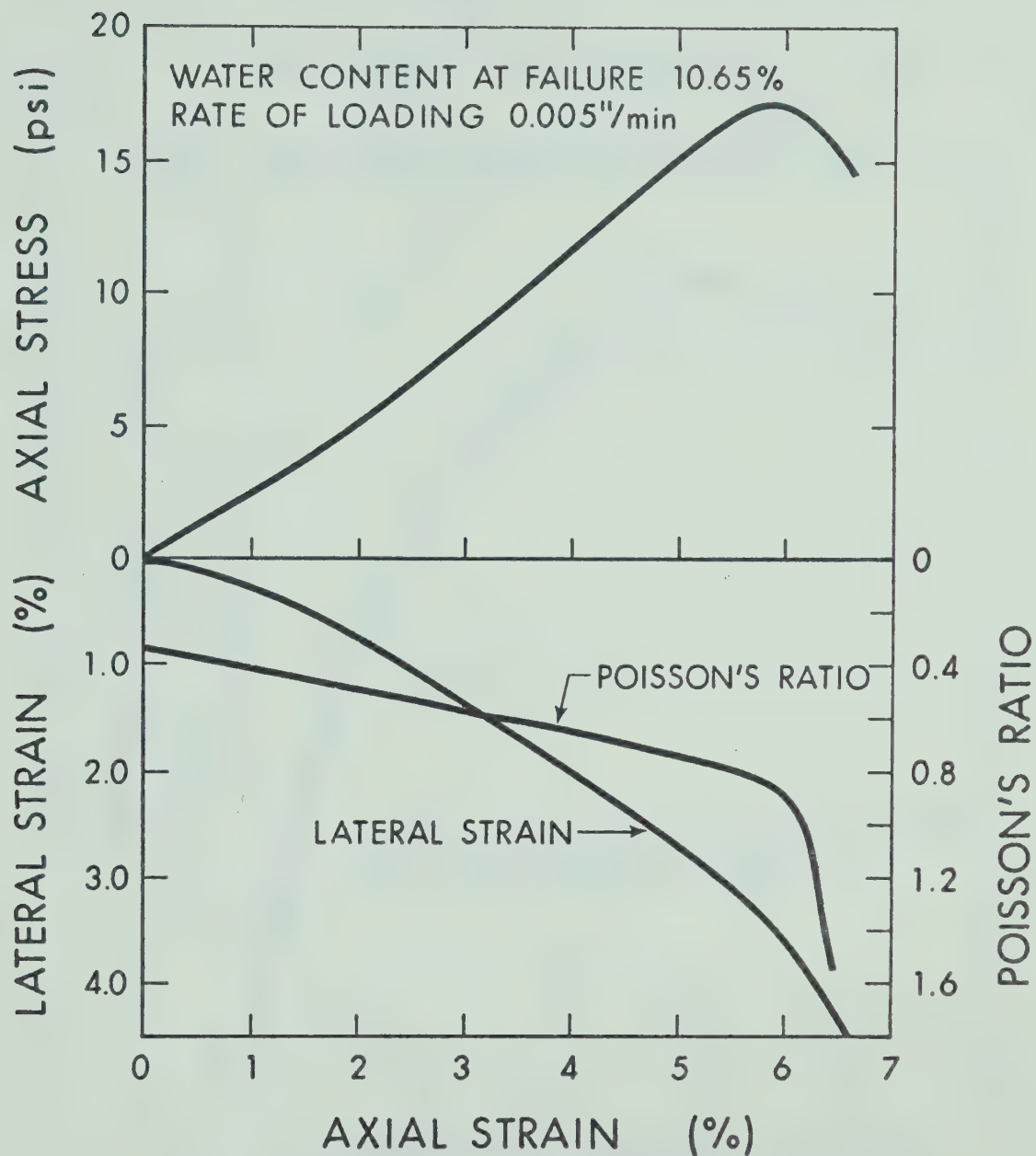


FIG. 2.19 STRESS-STRAIN RELATIONSHIP AND THE VARIATION OF LATERAL STRAIN AND POISSON'S RATIO WITH AXIAL STRAIN FOR MICA TILL TESTED UNDER UNCONFINED COMPRESSION

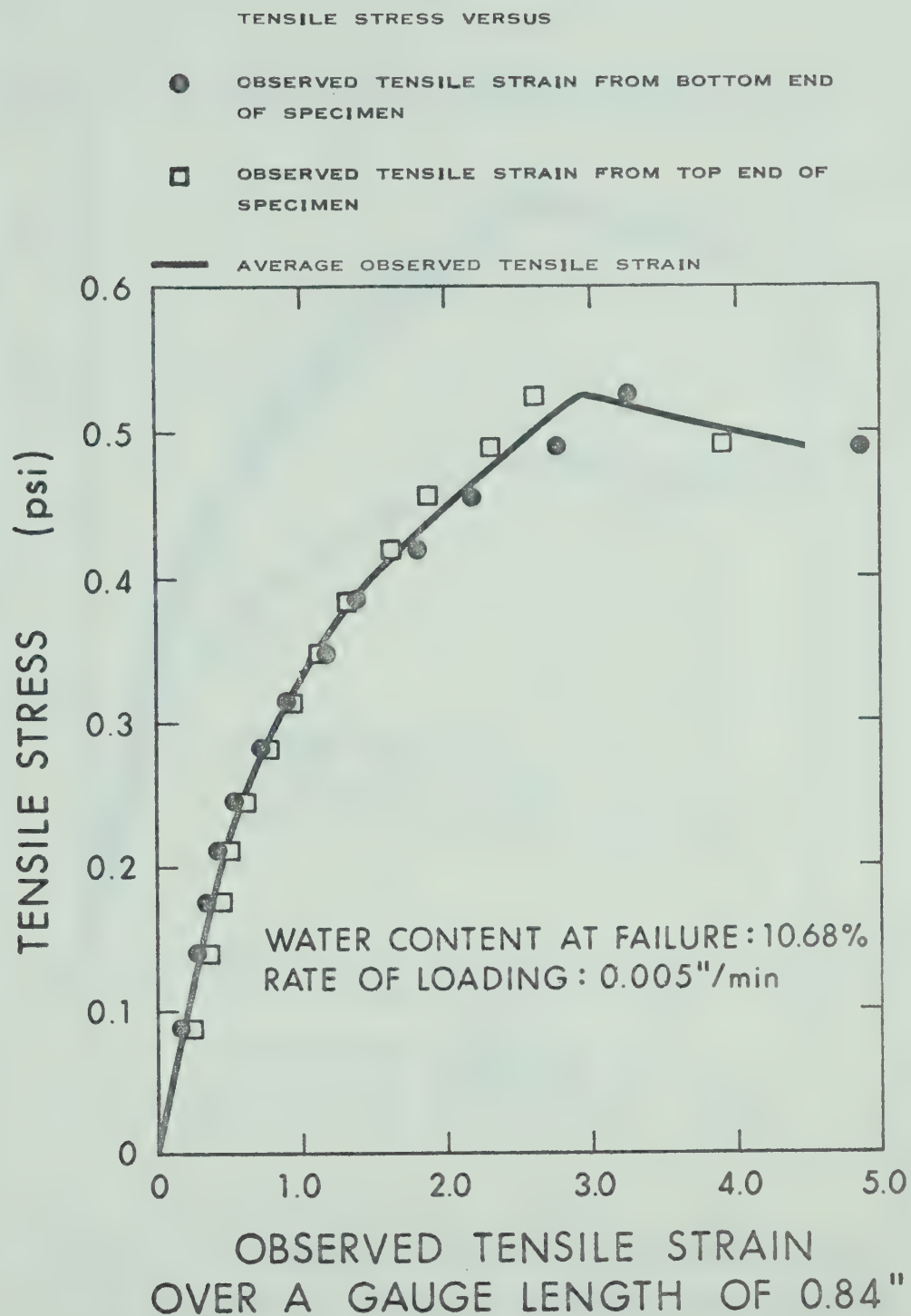
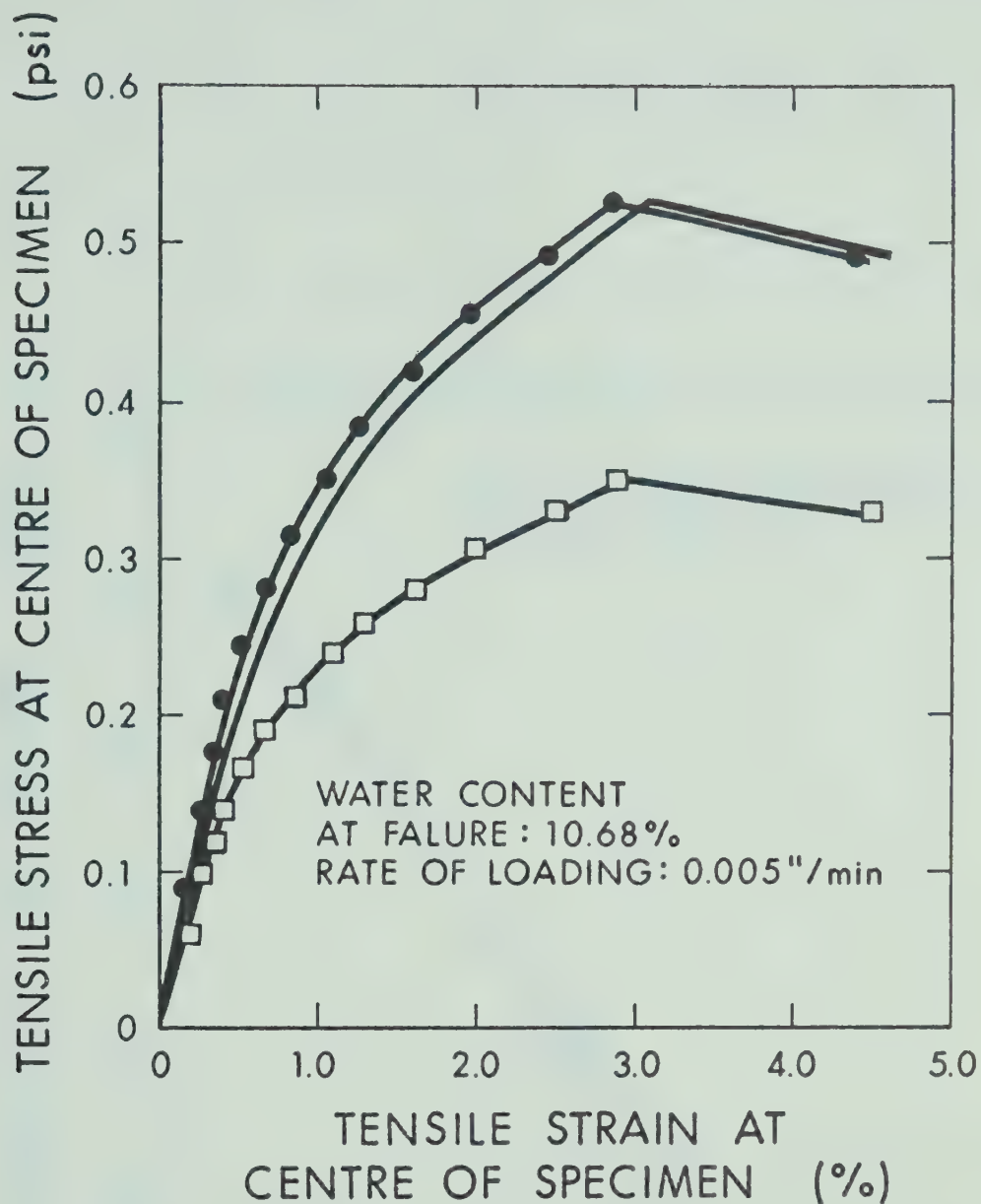


FIG. 2.20 RELATIONSHIP BETWEEN TENSILE STRESS AND THE OBSERVED TENSILE STRAIN FOR MICA TILL



- OBSERVED TENSILE STRAIN AT CENTRE
- TENSILE STRAIN AT CENTRE WITH E_c/E_t EQUAL TO 1.0
- TENSILE STRAIN AT CENTRE WITH E_c/E_t EQUAL TO 11.64

FIG. 2.21 COMPARISON OF TENSILE STRESS-STRAIN RELATIONSHIPS DERIVED FROM TENSILE TEST DATA OF MICA TILL

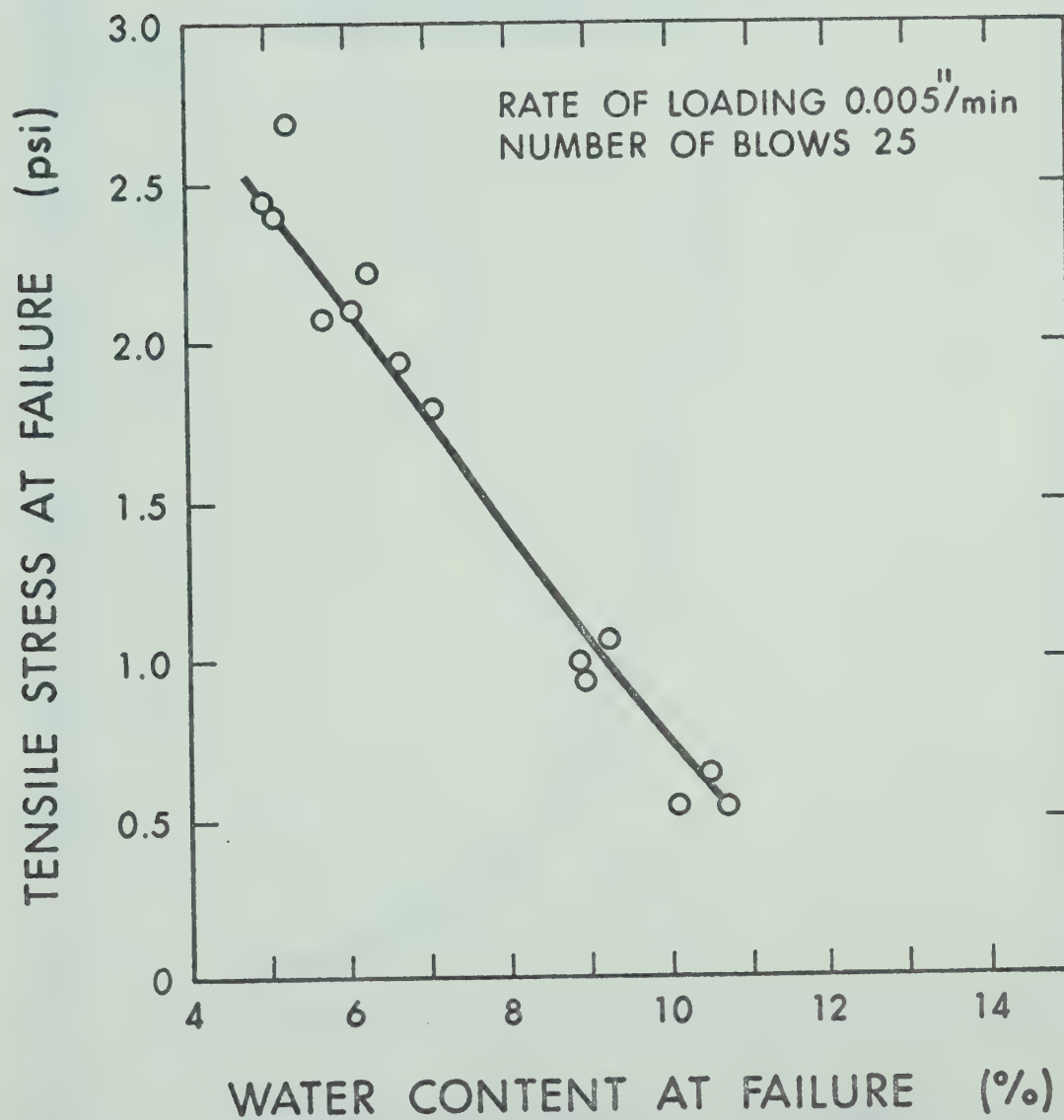


FIG. 2.22 EFFECT OF WATER CONTENT ON THE TENSILE STRESS AT FAILURE FOR MICA TILL

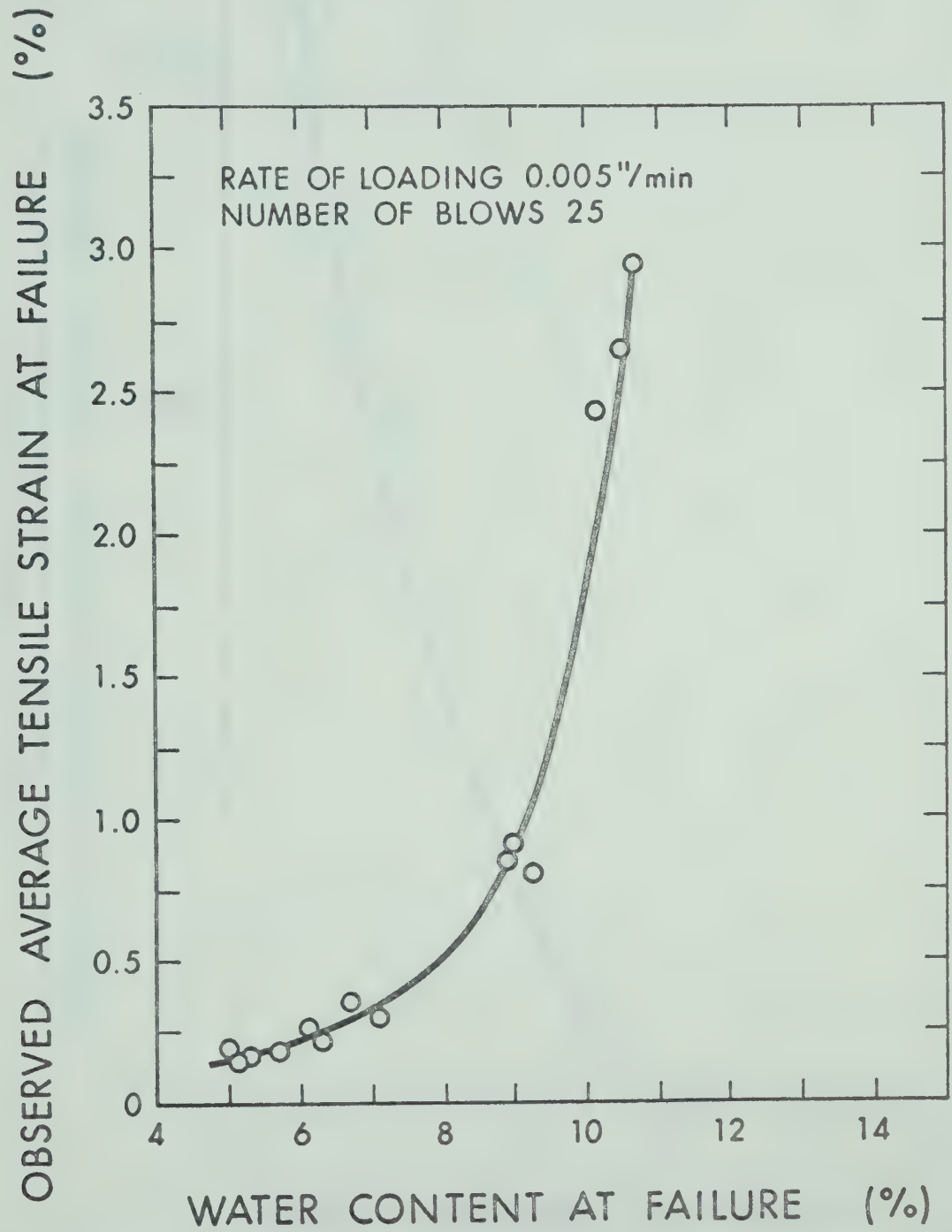


FIG. 2.23 EFFECT OF WATER CONTENT ON THE TENSILE STRAIN AT FAILURE FOR MICA TILL

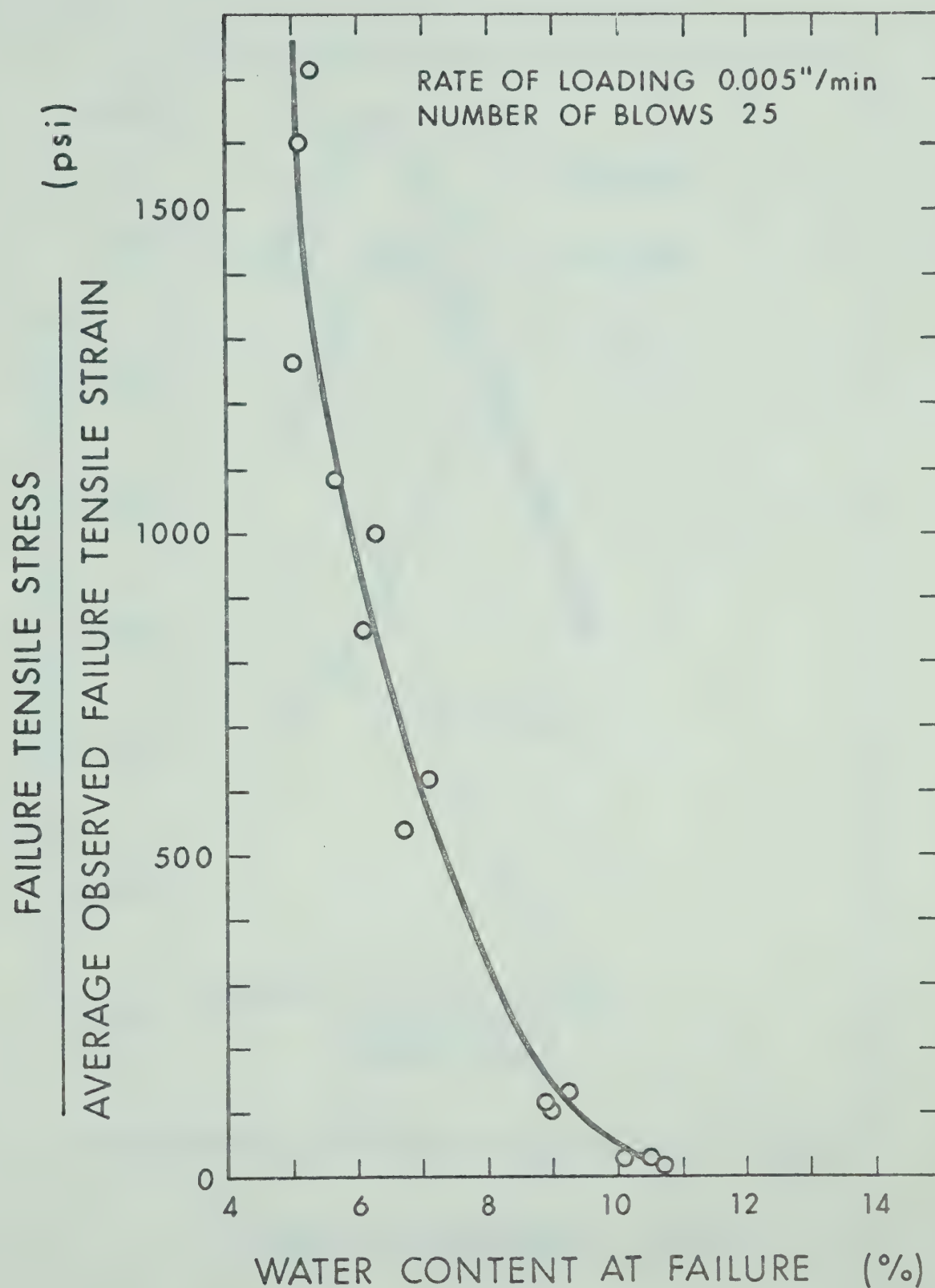


FIG. 2.24 VARIATION OF STIFFNESS IN TENSION WITH WATER CONTENT FOR MICA TILL

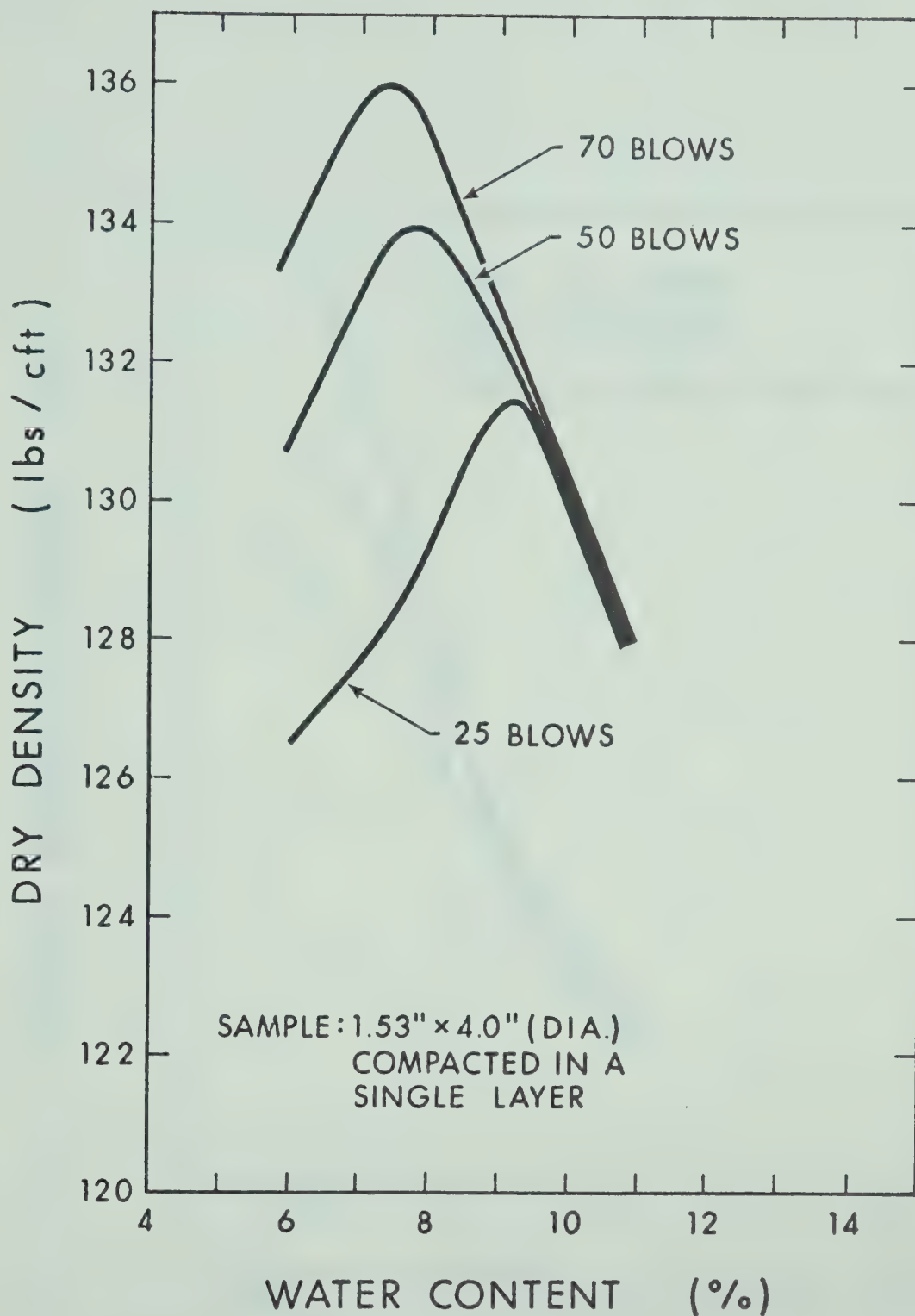


FIG. 2.25 WATER CONTENT-DENSITY RELATIONSHIPS FOR MICA TILL AT DIFFERENT COMPACTIVE EFFORTS

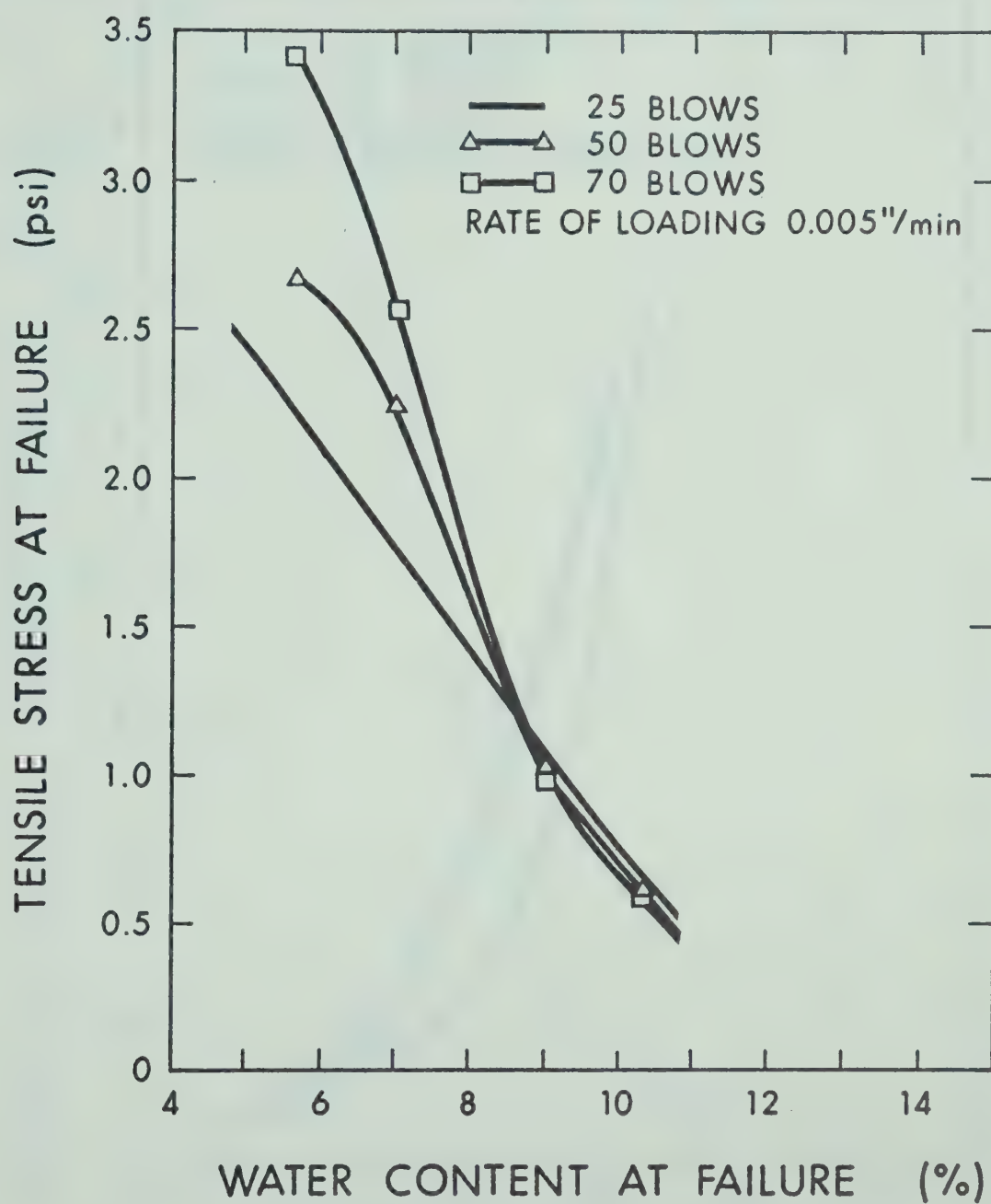


FIG. 2.26 VARIATION OF TENSILE STRENGTH WITH WATER CONTENT FOR MICA TILL AT DIFFERENT COMPACTIVE EFFORTS

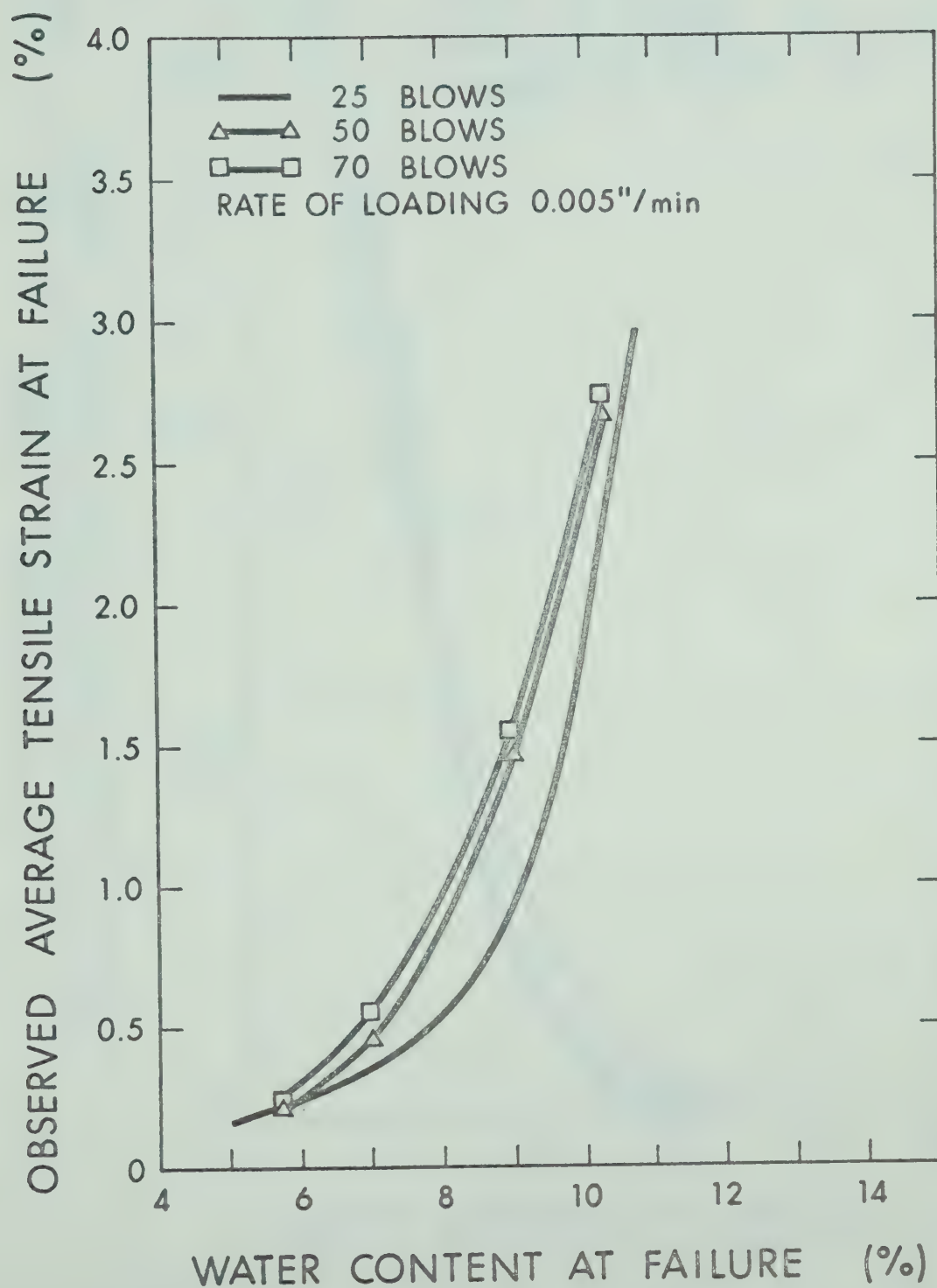


FIG. 2.27 VARIATION OF TENSILE STRAIN AT FAILURE WITH WATER CONTENT FOR MICA TILL AT DIFFERENT COMPACTIVE EFFORTS

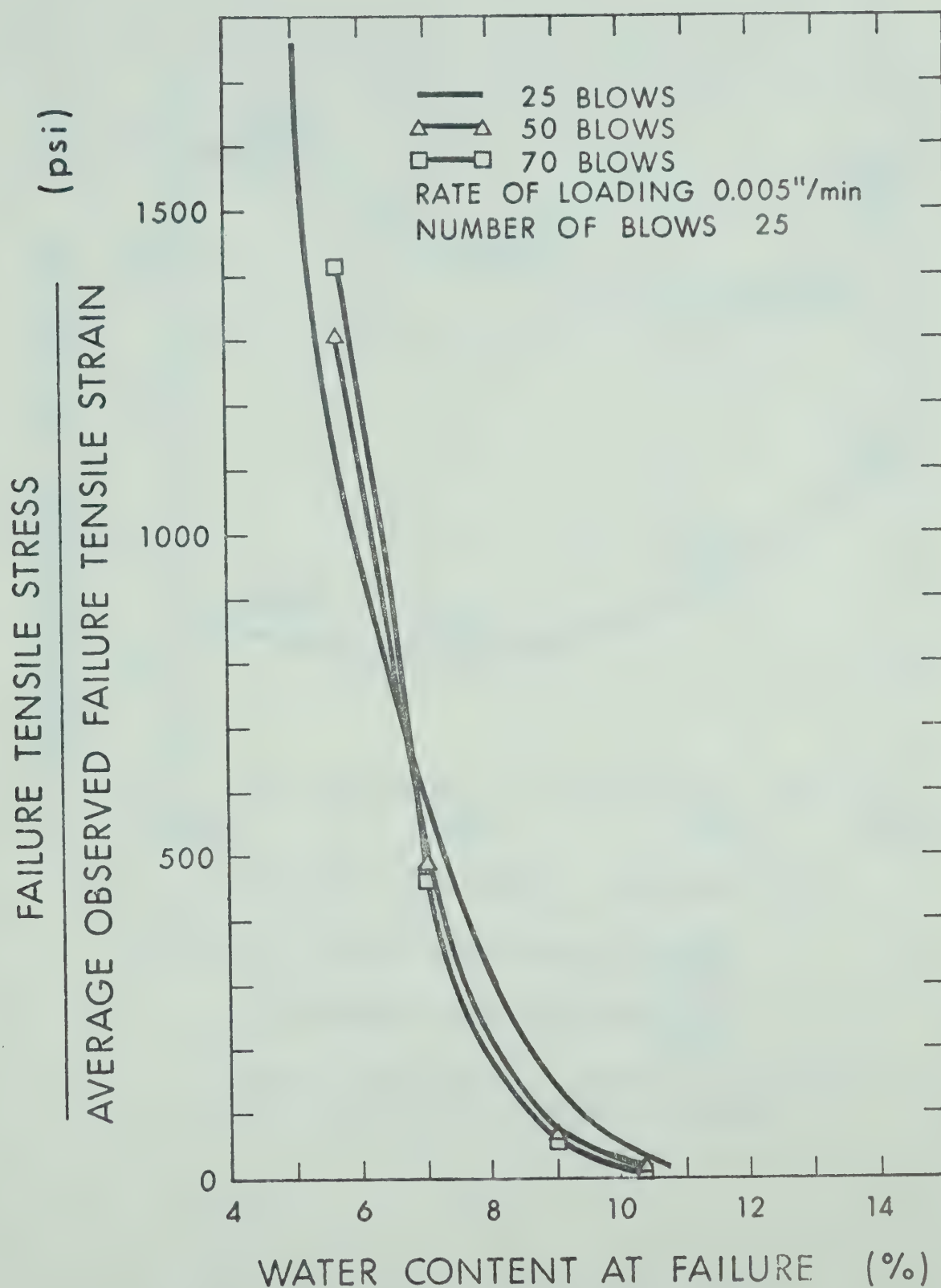
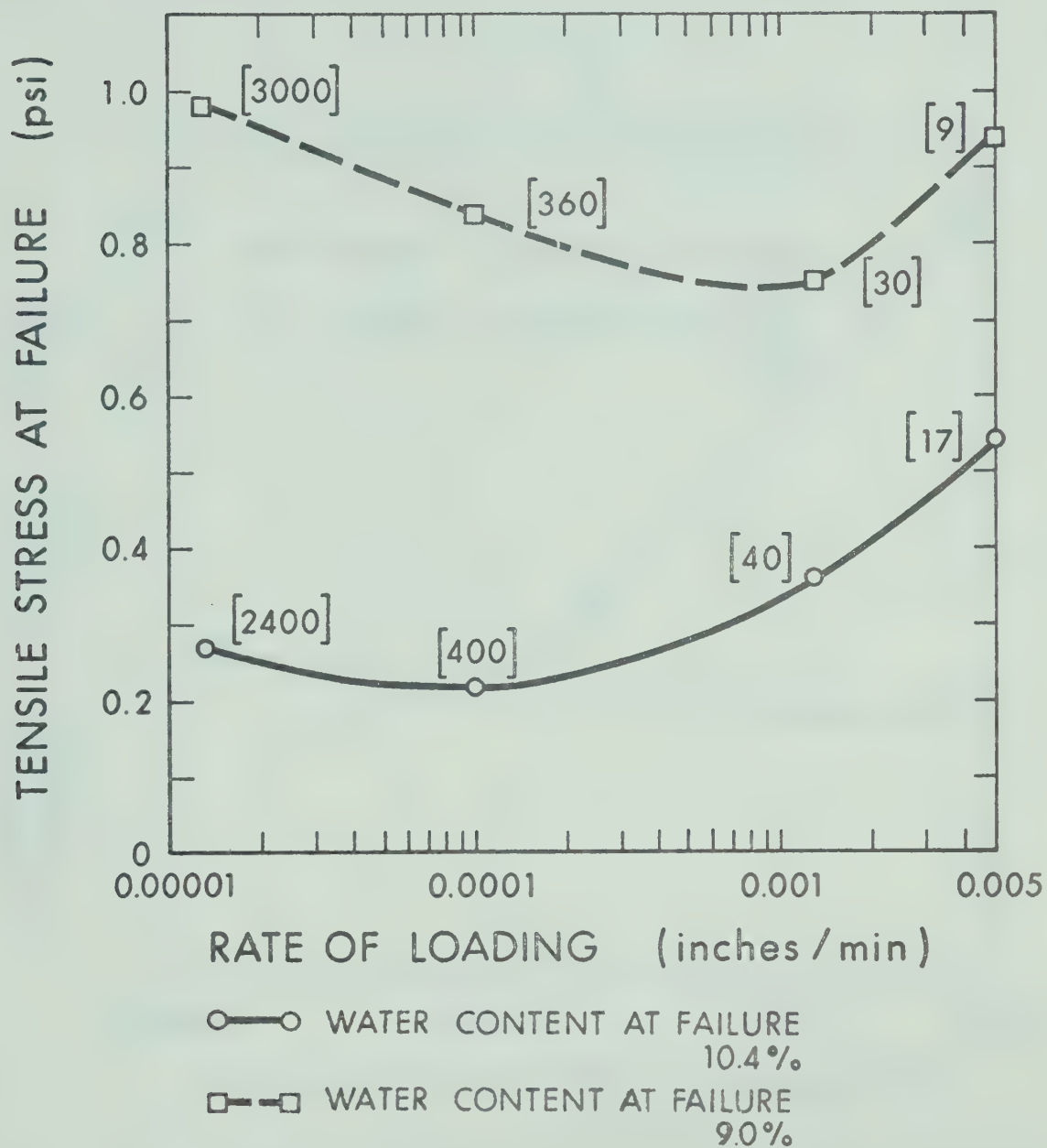


FIG. 2.28 VARIATION OF STIFFNESS IN TENSION WITH WATER CONTENT FOR MICA TILL AT DIFFERENT COMPACTIVE EFFORTS



NUMBERS WITHIN BRACKETS INDICATE THE APPROXIMATE TIME IN MINUTES FOR THE FAILURE OF SPECIMEN

FIG. 2.29 EFFECT OF RATE OF LOADING ON THE TENSILE STRENGTH OF MICA TILL

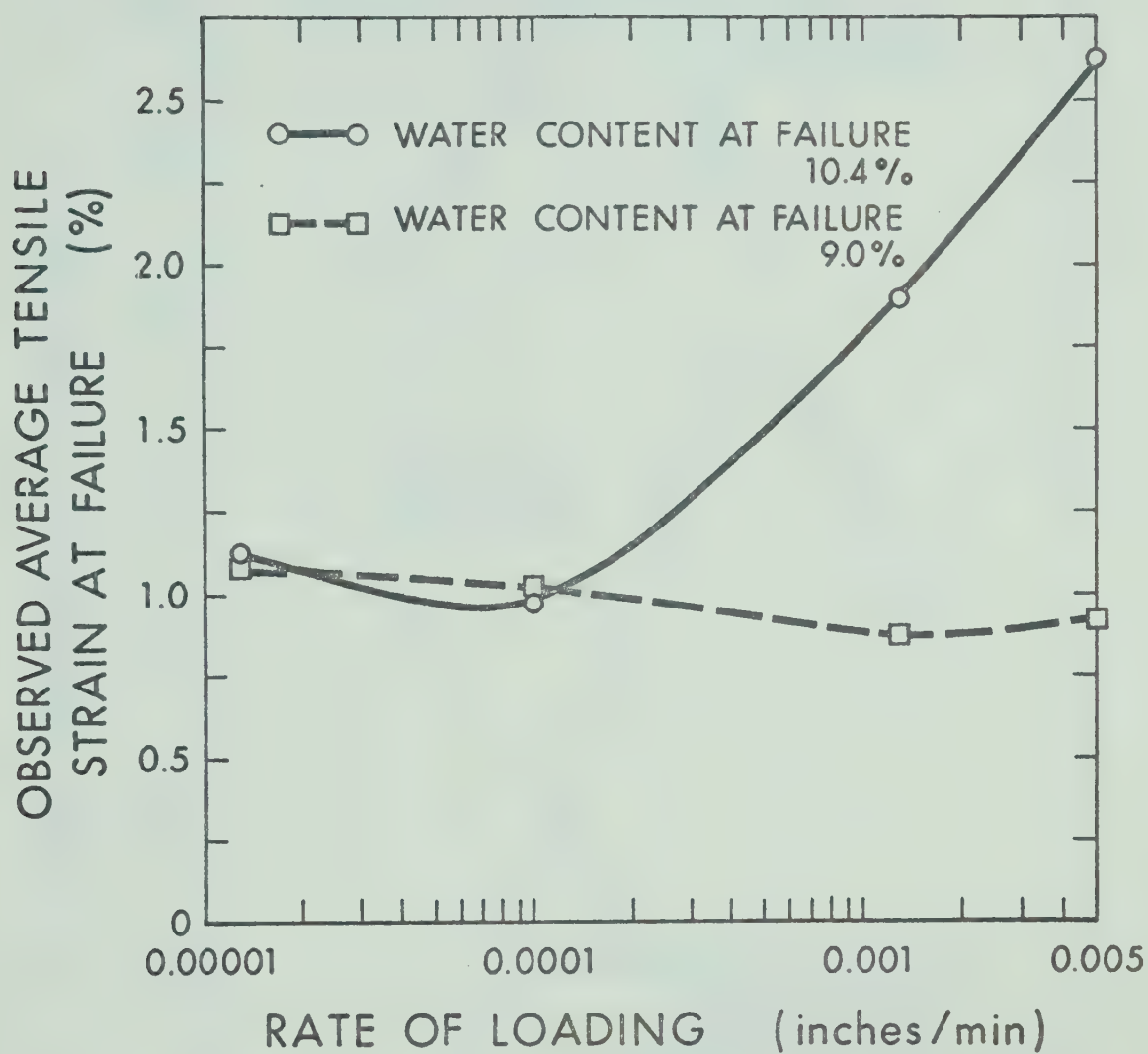


FIG. 2.30 EFFECT OF RATE OF LOADING ON THE TENSILE STRAIN AT FAILURE FOR MICA TILL

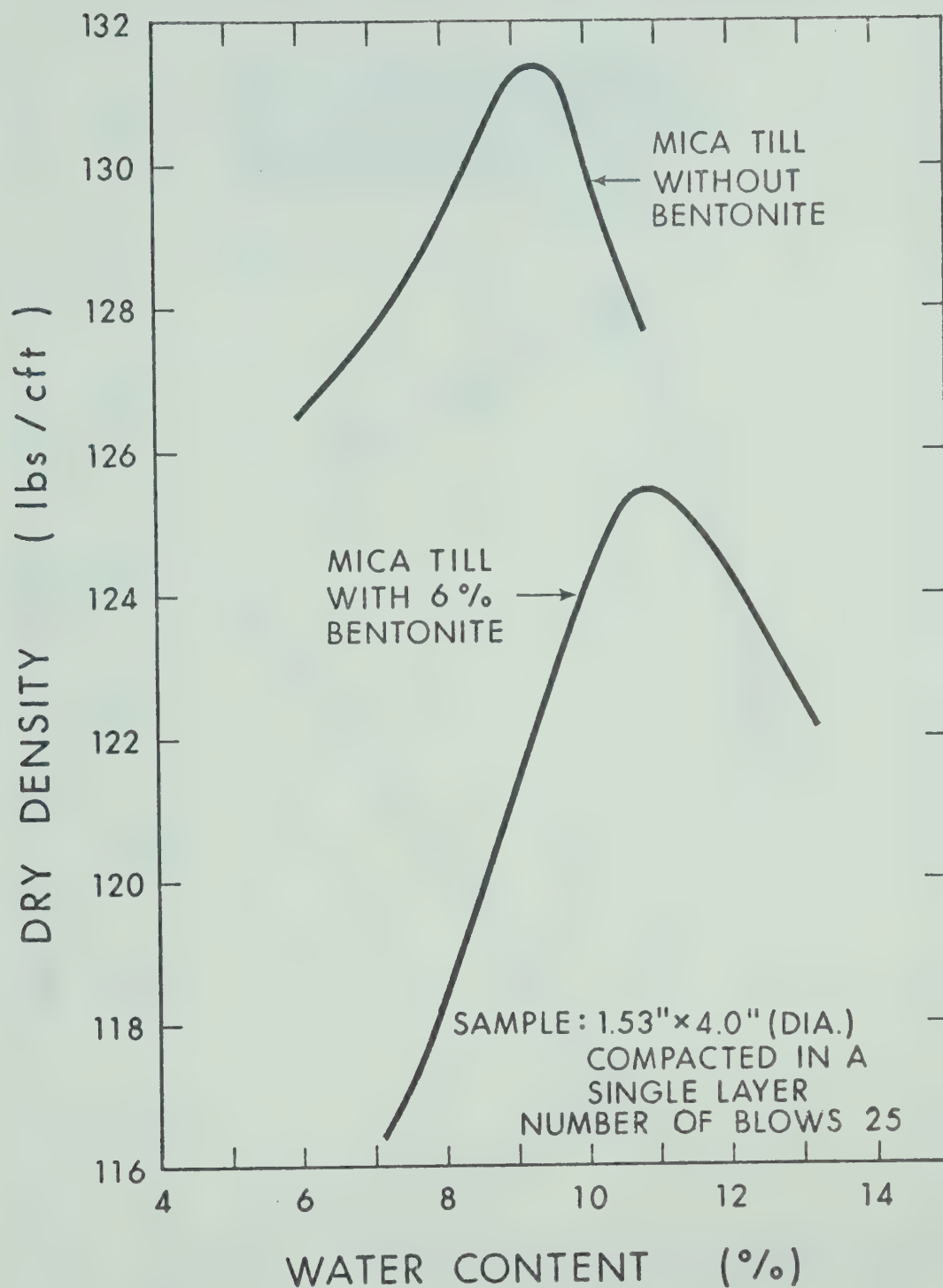


FIG. 2.31 WATER CONTENT-DENSITY RELATIONSHIPS OF MICA TILL WITH AND WITHOUT THE ADDITION OF BENTONITE

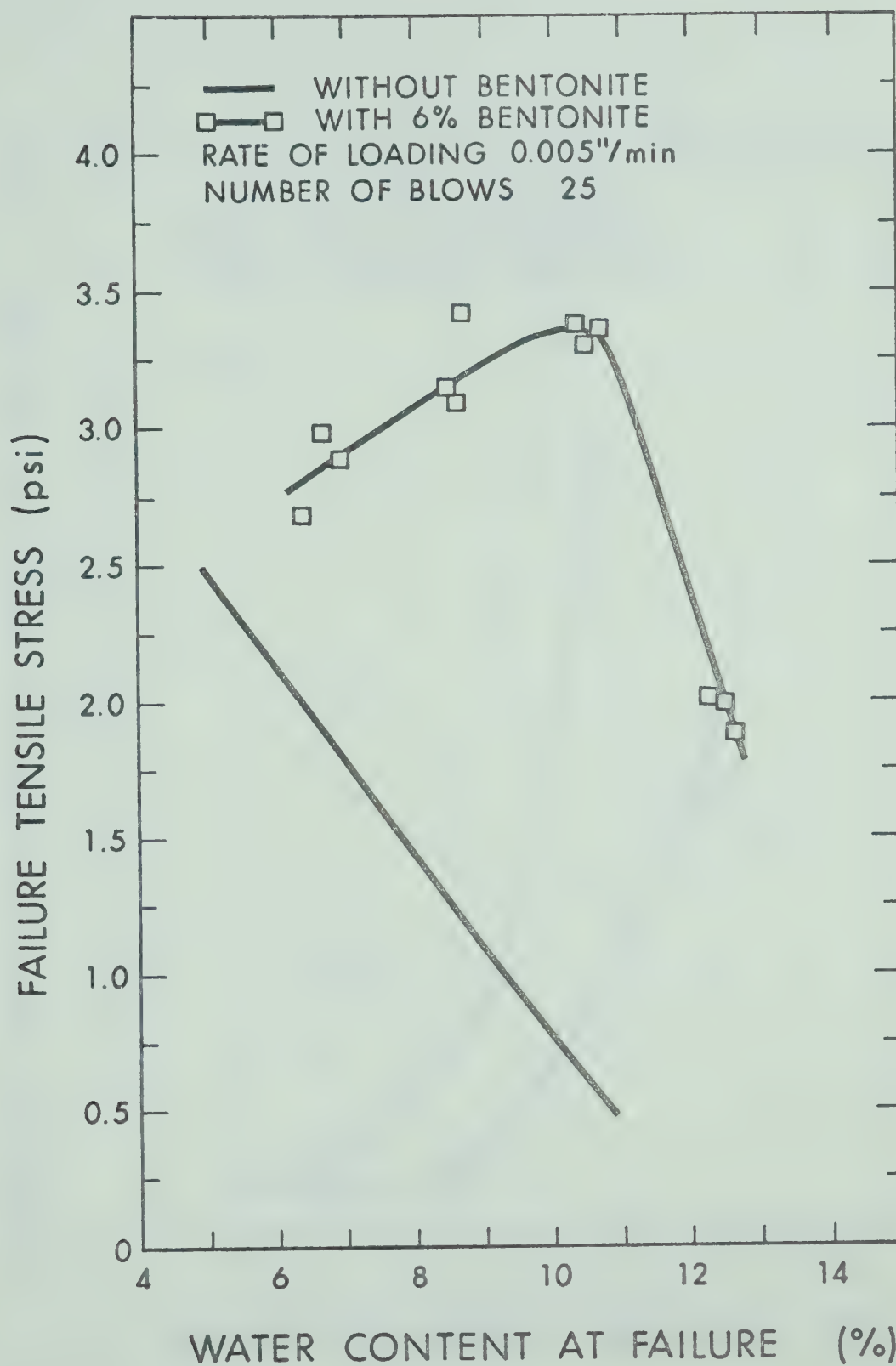


FIG. 2.32 COMPARISON OF TENSILE STRENGTH OF MICA TILL WITH AND WITHOUT THE ADDITION OF BENTONITE

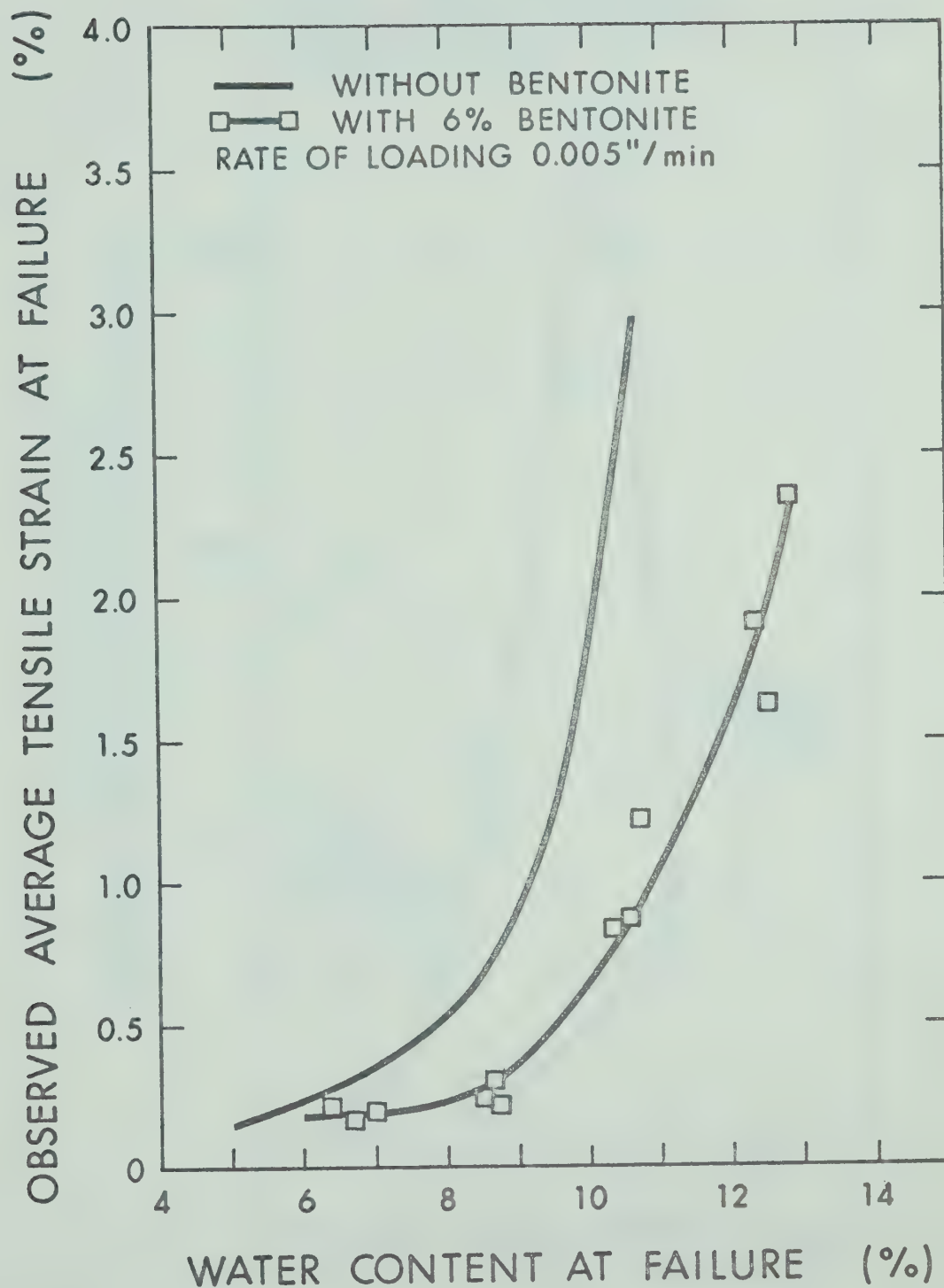


FIG. 2.33 COMPARISON OF TENSILE STRAIN AT FAILURE FOR MICA TILL WITH AND WITHOUT THE ADDITION OF BENTONITE

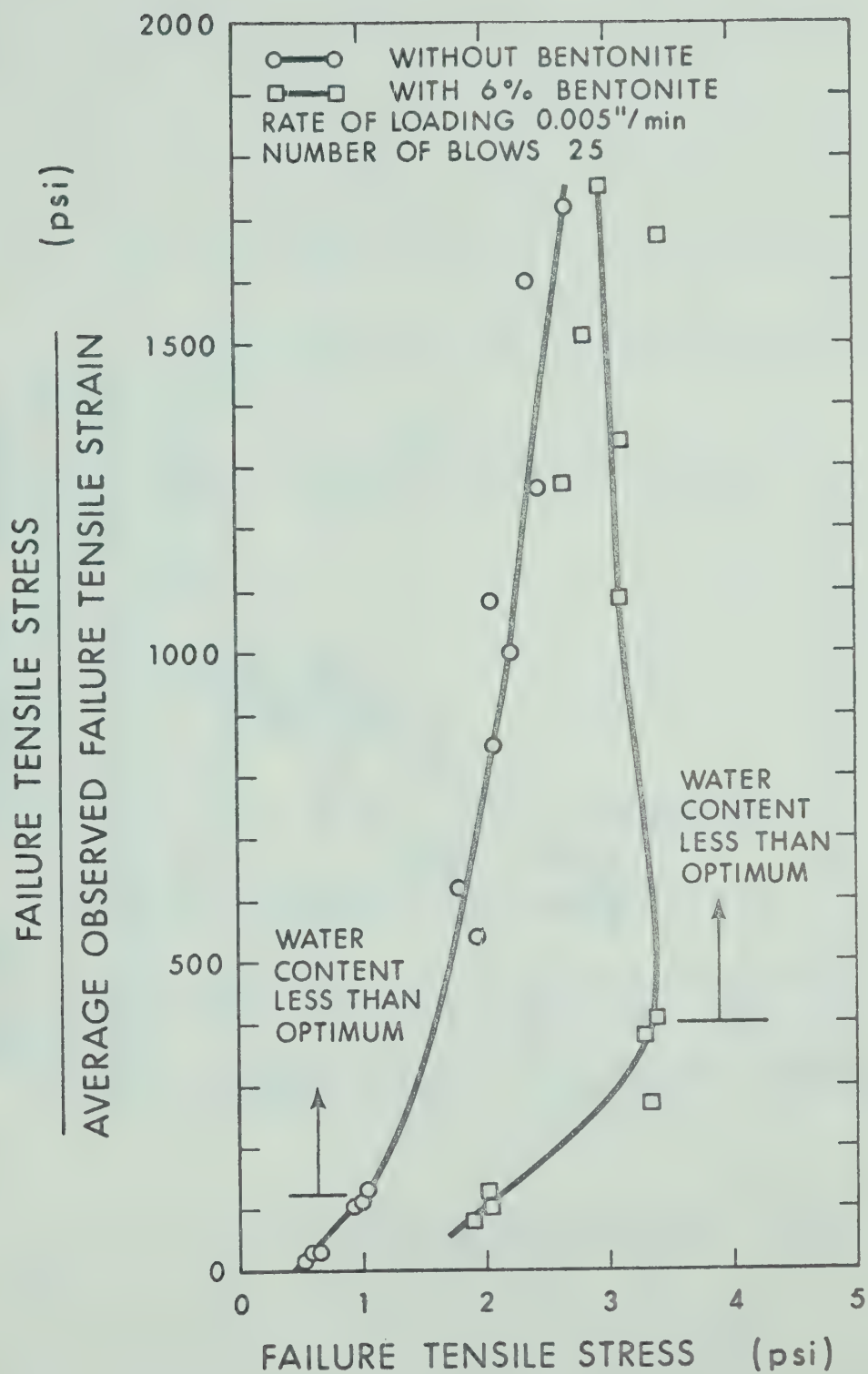
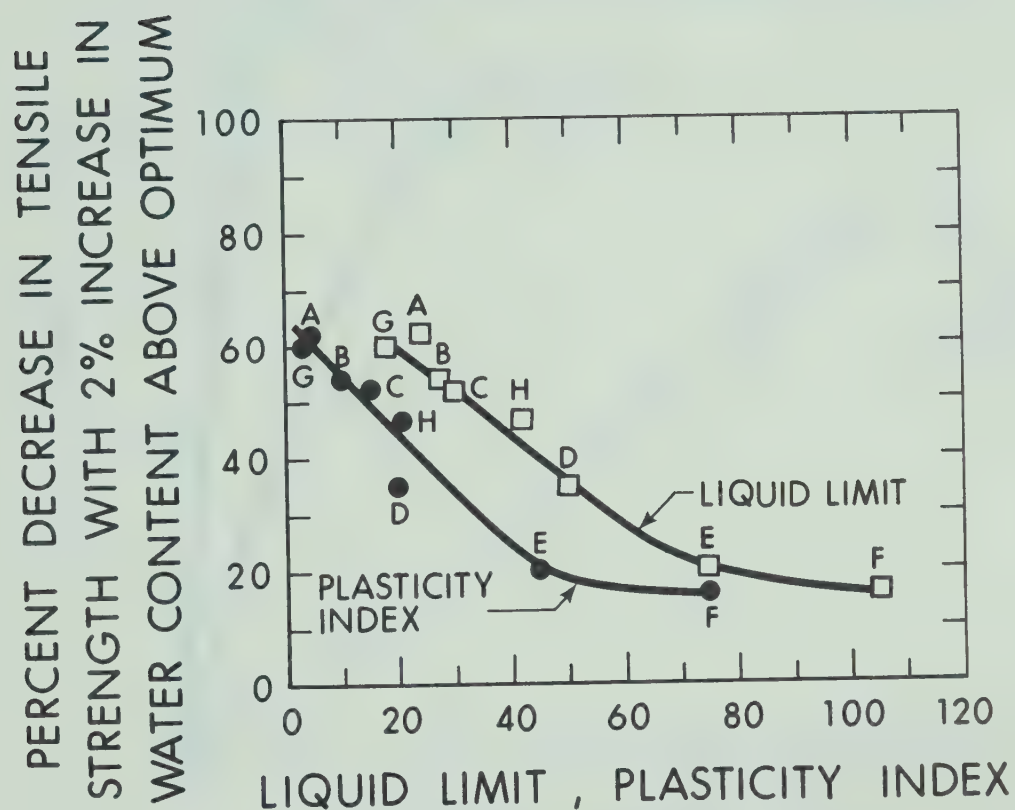


FIG. 2.34 COMPARISON OF STIFFNESS IN TENSION FOR MICA TILL WITH AND WITHOUT THE ADDITION OF BENTONITE



A TO F SOILS FOR WHICH THE DATA IS AFTER
NARAIN AND RAWAT [1970]

G MICA TILL

H MICA TILL WITH 6% BENTONITE

FIG. 2.35 PERCENT DECREASE IN TENSILE STRENGTH CAUSED BY A 2% INCREASE IN WATER CONTENT ABOVE OPTIMUM FOR SOILS WITH DIFFERENT CONSISTENCY LIMITS

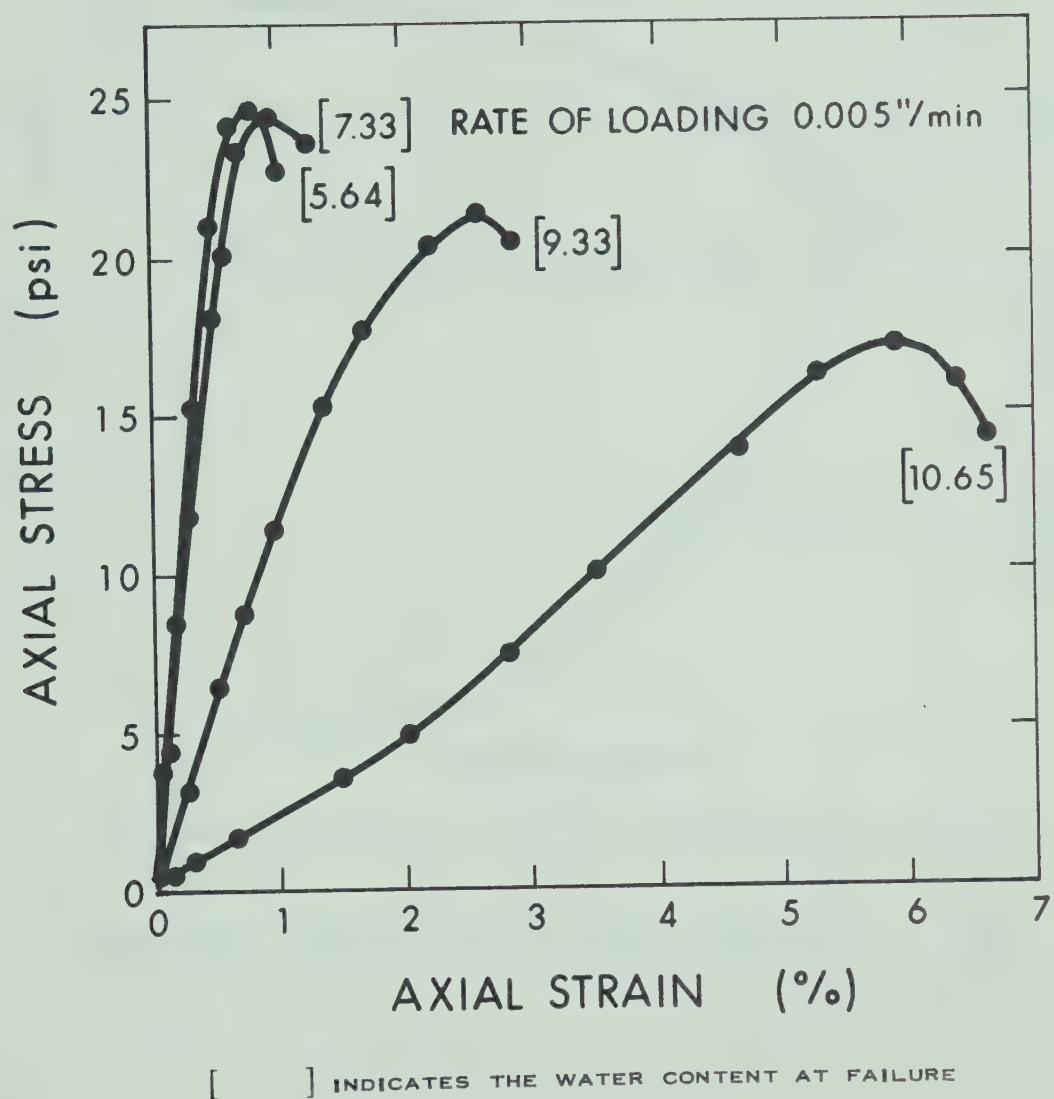


FIG. 2.36 STRESS-STRAIN RELATIONSHIPS OF MICA TILL TESTED UNDER UNCONFINED COMPRESSION

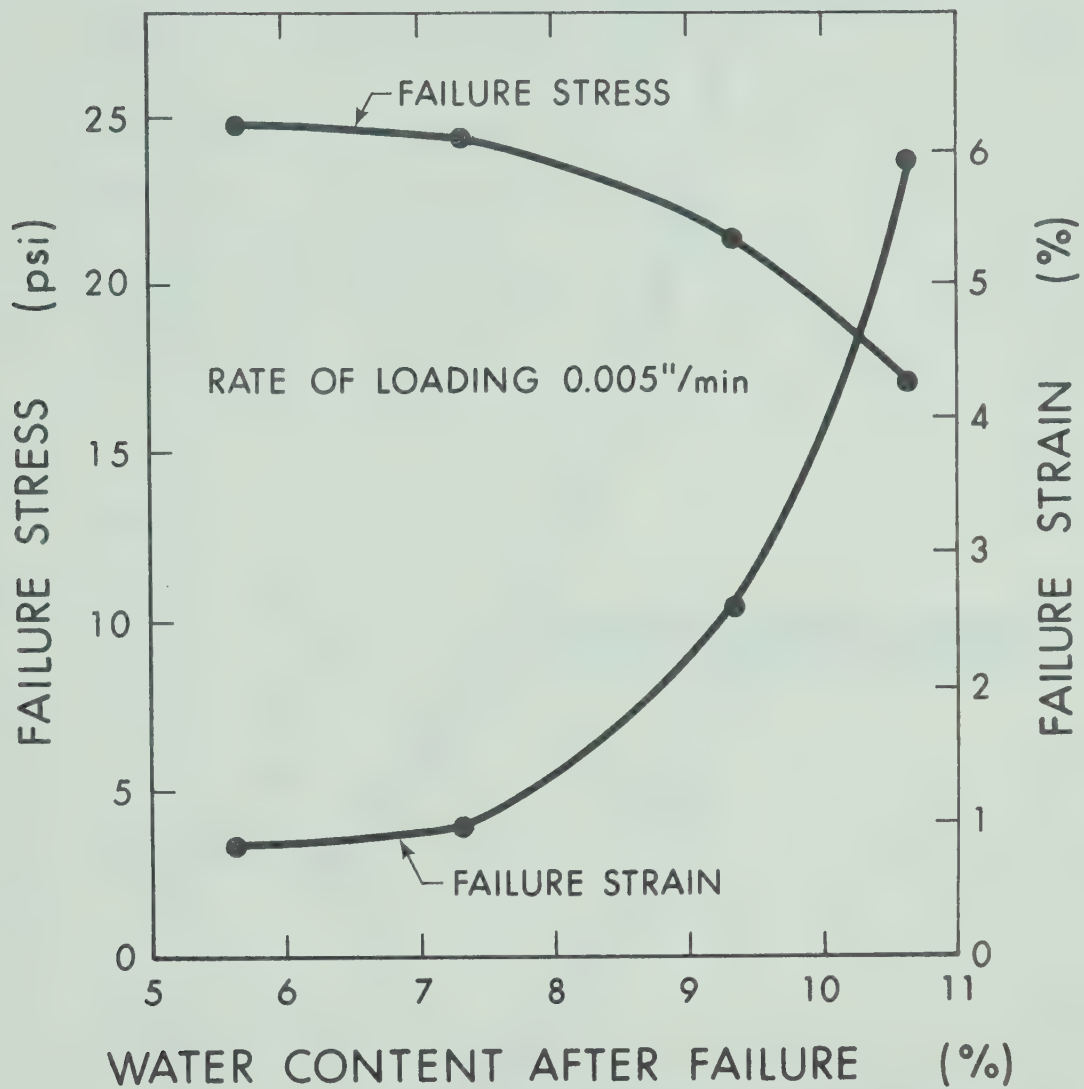


FIG. 2.37 VARIATION OF THE FAILURE STRESS AND STRAIN WITH WATER CONTENT FOR MICA TILL TESTED UNDER UNCONFINED COMPRESSION

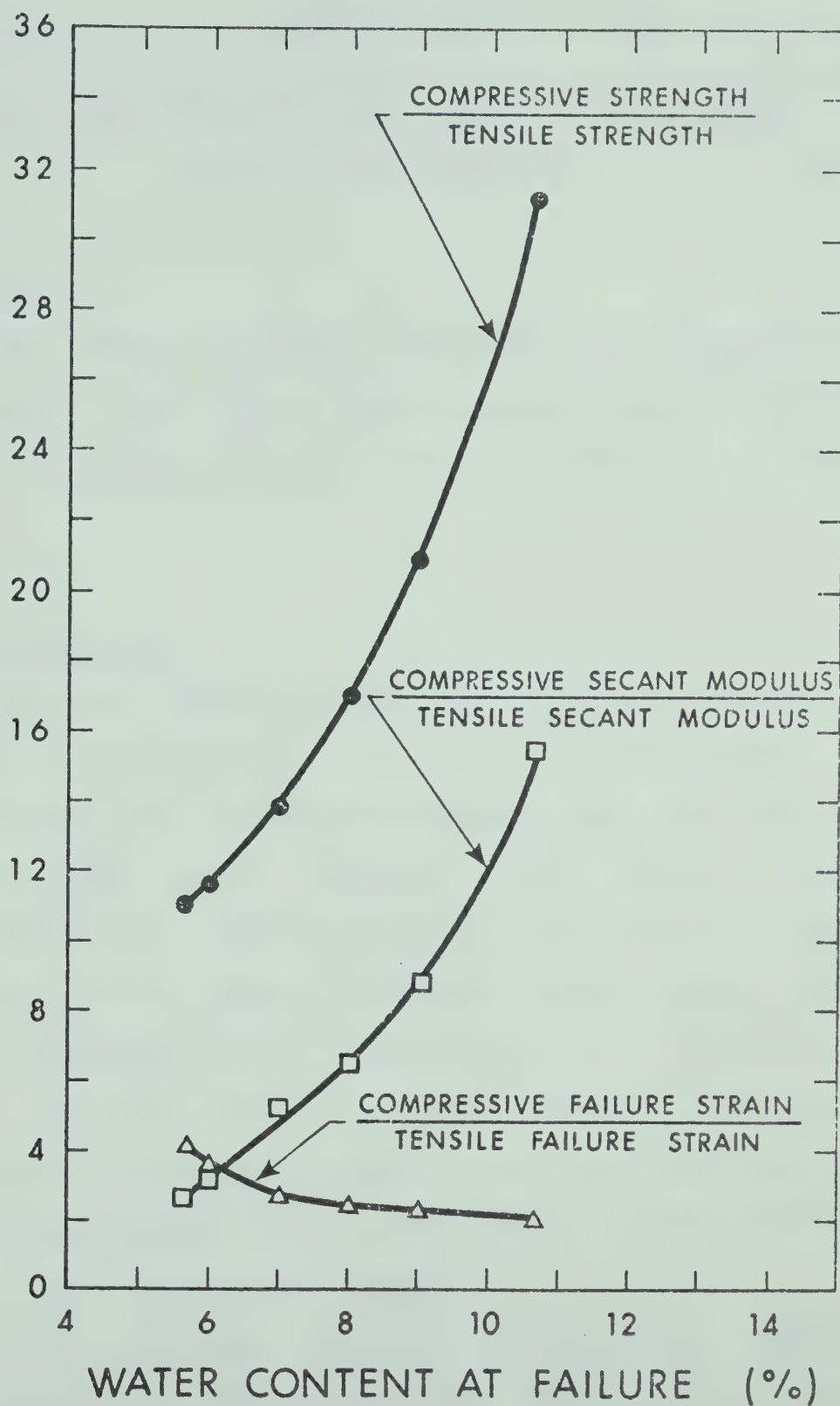


FIG. 2.38 COMPARISON OF COMPRESSIVE AND TENSILE CHARACTERISTICS OF MICA TILL AT DIFFERENT WATER CONTENTS

CHAPTER III

SIMULATION PROCEDURES FOR LINEAR AND NON-LINEAR FINITE ELEMENT ANALYSES

3.1 Scope

This chapter discusses the simulation procedures developed for the finite element analyses and the validity of their application to the problem of cracking of earth dams.

3.2 Introduction

Classical theory of elasticity, with the assumptions of isotropy, homogeneity, linear elastic stress-strain relationships, and simplified boundary conditions has been used in the past (e.g., Jurgensen, 1934; Terzaghi, 1943; Scott, 1963; Harr, 1966) to obtain closed form solutions for a certain limited number of boundary value problems, concerned with the determination of stress and strain fields in soil masses. Since the ideal conditions assumed in obtaining such solutions are rarely satisfied in practical problems, these analytical procedures can be used only to a very limited extent in the field of soil mechanics.

Finite difference numerical analyses (e.g., Bishop, 1952; Dolezalova, 1970) that assume linear elastic stress-strain relationships, were used for solving some boundary value problems concerned with earth dams.

The finite element method, which has more flexibility than other methods for dealing with complex boundary conditions, non-homogeneous materials, and non-linear stress-strain relationships, has been in active use for some ten years. It has been shown by a number of workers (e.g., Clough and Woodward, 1967; Girjavallabhan and Reese, 1968; Kulhawy et al., 1969; Chang and Duncan, 1970; Desai and Reese, 1970; Kulhawy and Duncan, 1970) that with a proper application of the finite element method one can obtain reasonably good solutions for problems concerned with the stresses and strains in soil masses. It is evident that success in obtaining a good solution depends to a considerable extent on close simulation of field behaviour of the structure. At present, research on the application of finite element method to soil problems is largely directed towards developing suitable simulation procedures to obtain close agreement between the results of analysis and field or experimental observations. In the present investigation, the finite element method has been used because of its capabilities.

3.3 Use of Isotropic Elastic Theory and Its Limitations

The stress-strain relationships for soils are non-linear, partially inelastic, and depend on stress path and stress level. Geometric anisotropy and stress-induced anisotropy are quite common in soils. Volume changes take place not only due to changes in all around pressure but also due to factors such as pure shear and rotation of principal stress

axes.

A theory that completely describes the deformation properties of soils is not available yet, although the application of such a theory in the analysis is highly desirable (Scott and Ko, 1969). Some attempts have been made to introduce volume changes due to shear into the analysis (e.g., Chang et al., 1967; Smith and Kay, 1971). The limitations that exist in the experimental determination of soil parameters needed for the application of more complex non-linear theories, seriously limit, at present, the finite element analysis. Until sufficient progress in the development of suitable laboratory procedures for obtaining stress-strain relationships under conditions that simulate field behaviour of soil is achieved, the use of simple isotropic elastic theory appears to be reasonable. The parameters needed for such a theory are easily obtained from conventional laboratory tests. Perhaps the most significant disadvantage, from a practical engineering point of view, in using the small-strain isotropic elastic theory to represent soil behaviour is that it cannot account for the dilatancy effect of soils (Scott and Ko, 1969).

Despite these limitations successful solutions using isotropic elastic theory have been reported in literature (e.g., Clough and Woodward, 1967; Girjavallabhan and Reese, 1968; Kulhawy et al., 1969; Chang and Duncan, 1970; Desai and Reese, 1970; Kulhawy and Duncan, 1970). These solutions are based on the assumption of a piecewise linearity between the

stress and strain. The appropriate stress-strain relationships used in the analyses were derived from conventional triaxial tests. A conventional triaxial test refers here to a test in which the deviatoric stress is increased under a constant cell pressure.

Based on the comments of the previous paragraphs, isotropic elastic theory for small strains has been applied to the finite element analyses performed in this work. Piecewise linearity between stress and strain has been assumed during each increment of the load. The appropriate stress-strain relationships, dependent on stress level, have been derived from the conventional triaxial tests. The volume change data of the triaxial tests has been used to derive the second parameter needed.

3.4 Types of Analyses Performed

Different types of finite element analyses, pertaining to the studies on cracking of earth dams, were performed in this work. Explanatory definitions of the analyses are given with each type:

- (1) Linear analysis is an analysis in which the two elastic parameters defined either by K and G or by E and ν are maintained constant in the analysis.
- (2) Non-linear analysis is an analysis in which the loads are applied in a number of small increments. A piecewise linear relationship between stress and strain has been assumed during each increment of the load. The

elastic parameters during a certain increment of load are defined either by K and G or by E and ν . The displacements, stresses and strains determined in each increment of loads are accumulated to obtain the total values corresponding to all increments of loads.

- (3) Single step linear analysis is an analysis in which the loads are applied instantaneously and the analysis is performed with constant values of elastic parameters defined either by K and G or by E and ν .
- (4) Incremental linear analysis is an analysis in which loads are applied in a number of small increments with the elastic parameters used in all the increments remaining constant.
- (5) "No tension" analysis is an analysis in which soil is considered incapable of sustaining tension and the tensile principal stresses are removed by replacing them by equivalent nodal forces. The "no tension" analysis procedure has been elaborated in detail by Zienkiewicz et al. (1968).

In all types of analyses listed above Poisson's ratio is not allowed to exceed 0.49. Generally the results of an analysis obtained for Poisson's ratio exceeding 0.49 and very close to 0.5 are not accurate (Herrmann, 1964). For Poisson's ratio equal to 0.5 the analysis cannot be performed as some elements of the constitutive matrix become infinite. These limitations are inherent in the formulation based on the minimum potential energy principle. Using a variational principle

which is equivalent to the elastic field equations expressed in terms of the displacements and a function of mean pressure, Herrmann (1964) showed that sufficiently accurate results can be obtained for all values of Poisson's ratio ranging from 0 to 0.5. The formulation proposed by Herrmann (1964) is particularly suited to incompressible materials such as rubber. Such a formulation is not used in this work for two reasons:

- (1) For soils which dilate during shear, Poisson's ratio exceeds the permissible value of 0.5 hence volume change behaviour of such a soil cannot be represented by a value of Poisson's ratio equal to 0.5.
- (2) By limiting Poisson's ratio to 0.49, reasonably good correlations between the results of analysis and field or experimental observations have been achieved in a number of cases (e.g., Girjavallabhan and Reese, 1968; Kulhawy et al., 1969; Chang and Duncan, 1970; Kulhawy and Duncan, 1970) involving nearly incompressible soils ($\nu \approx 0.5$).

3.5 Two Dimensional Finite Element Analyses

The two dimensional finite element analyses in this work were performed by using the computer program given in Appendix A. In this program constant strain triangular elements each having six degrees of freedom are used. More refined elements such as quadrilateral elements, each having four constant strain triangular elements (Covarrubias, 1969) or two linear

strain triangular elements are possible (Felippa, 1966). However the results obtained using constant strain triangular elements for the cases considered in this work are in good agreement with those of Covarrubias (1969) who used more refined quadrilateral elements along with constant strain triangular elements. The comparison of results appears in Section 4.4 of Chapter IV. The equations are solved by Gauss-Seidel iterative procedure. The original computer program which could perform a linear single step analysis was developed by Wilson (1963). The program was modified to incorporate the following additional facilities:

- (1) the automatic generation of element and nodal data,
- (2) the performance of an incremental analysis with an option to analyze each step once or twice,
- (3) the calculation of elastic parameters from the laboratory test data needed for each increment of loads,
- (4) the performance of a "no tension" analysis.

The iterative method of solution of equations, used in the program is particularly suitable for the "no tension" analysis, because it involves an iterative procedure. Since the element stiffness formulation for a constant strain triangle is well known it will not be discussed here. Details regarding the computer program for two dimensional finite element analysis are in Appendix A.

3.6 Three Dimensional Finite Element Analyses

The three dimensional analyses were performed using a computer program (Appendix B) developed by the author. In this program, isoparametric hexahedral elements, each having twenty-four degrees of freedom, are used. Each element is specialized to represent triangular prisms and tetrahedra (Appendix B). The equations are solved in blocks using the direct Gaussian elimination method and the necessary integrations for the evaluation of element stiffness and stresses are performed numerically by using Gaussian quadrature formulae. The program includes facilities that:

- (1) automatically generate nodal and element data,
- (2) perform a single step linear analysis,
- (3) perform an incremental analysis with an option to analyze each step once or twice,
- (4) calculate elastic parameters for each increment of loads from the laboratory test data.

Provision for "no tension" analyses has not been made due to the excessive amount of computation effort needed for the iterative procedure in a three dimensional analysis.

The selection of isoparametric hexahedral elements for the three dimensional analysis is based on the comparative studies on three dimensional finite elements conducted by Clough (1969). His conclusions regarding the performance of the various types of three dimensional elements are as follows:

- (1) the isoparametric hexahedral elements are distinctly

superior to any tetrahedron assemblages, both with respect to the individual element properties and in application to idealized structural systems. Also the isoparametric elements have the advantage of isotropy whereas the stiffness of the tetrahedron assemblages are slightly different along their three axes.

- (2) based on the comparative efficiency studies of 8 node and 20 node isoparametric hexahedral elements, it is recommended that an 8 node element be used in standard three dimensional programs for analysis of general elastic solids and the 20 node element be applied primarily in systems or local regions when the plate bending mechanism is likely to dominate the behaviour.

From the preceding conclusions it can be seen that an 8 node isoparametric hexahedral element would be well suited for the analysis of earth dams in which shear effects dominate the behaviour of the structure.

The details regarding the main features of the program, its limitations and the computation time needed are discussed in Appendix B. The element stiffness formulation for the isoparametric hexahedral element used in this work is discussed in Appendix C.

3.7 Determination of the Elastic Parameters for Non-Linear Analysis

Since an incremental loading procedure is used to simulate the construction sequence of an earth dam, the elastic

parameters to be used during each increment of the load are to be calculated from laboratory or field test data. The elastic parameters are either K and G or E and ν . Generally two approaches are possible to feed the test data into the computer for the evaluation of the parameters. In one approach the test data is supplied in digital form and in the other it is supplied in functional form.

In the digital form, a number of closely spaced points on a stress-strain curve are given as input. Hence the modulus calculated by considering two adjacent points (by chord slope) approximates the tangent modulus. Because of their dependency on the stress level, the relationships between stress and strain must be supplied at a number of closely spaced values of stress levels. From the set of data supplied in digital form the moduli are calculated at the required stress level.

In the second approach, the stress-strain relationships are supplied in functional form assuming either hyperbolic stress-strain relationships (Kulhawy et al., 1969; Duncan and Chang, 1970) or using mathematical spline functions (Desai, 1971). The hyperbolic representation involving the use of a small number of parameters with identifiable physical significance has the advantage that it is easier to compare the properties of different soils, and to develop experience and judgment in terms of the parameters (Duncan and Chang, 1972). However, in general, it involves greater approximations to the measured stress-strain behaviour than those obtained by

the spline function representation (Desai, 1971; Duncan and Chang, 1972). In the present work the digital form was used because, although it may involve more computation time for interpolation than other methods, no approximation of the stress-strain relationships is necessary.

3.8 Validity of Triaxial Test Data for Interpolating the Elastic Parameters

The conventional triaxial tests are performed by increasing the deviatoric stress with constant cell pressure. Several other stress paths consistent with the type of problem considered can be simulated in the triaxial tests. However, because of the axisymmetric conditions maintained in triaxial tests the behaviour of the soil under plane strain or general three dimensional conditions cannot be simulated. To simulate such conditions a plane strain test apparatus or a "true" triaxial test apparatus in which stresses and strains can be controlled in all three directions is needed. Since the data from such tests are not readily available, the conventional triaxial tests may continue to find their application in the analyses, at least for some years to come. Triaxial data obtained from tests performed on representative soil samples with the proper simulation of stress paths and drainage conditions could be of a considerable value in reasonably predicting the deformations and stresses. However research is needed to develop suitable laboratory tests, the data from which can be used in the analyses for reasonably

accurate predictions. On the other hand if the conventional triaxial test data obtained under a particular stress path are used for problems involving different types of stress paths, the results predicted by the analysis are bound to be inaccurate for some cases. Duncan and Chang (1972), based on the investigations conducted under different stress paths, indicated that the simple incremental procedures using the conventional triaxial test data result in a reasonably good prediction of strains for unloading-reloading stress-paths and for a range of stress-paths in the primary loading range. However the predictions are poor for primary loading under constant or nearly constant stress-ratios (σ_3/σ_1) and for certain other types of stress paths.

In the present work only the conventional triaxial test data have been used for the following reasons:

- (1) Data from either plane strain tests or "true" triaxial tests are not available.
- (2) As the present work is primarily concerned with the evaluation of tension zones caused by tensile stresses, it is to be expected that the stresses computed would be less sensitive to the changes in the derived elastic parameters than the computed displacements or strains.

3.8.1 Simulation of the Drainage Conditions

Duncan (1972) and Lowe (1972) discussed the importance of a proper simulation of the drainage conditions in the finite element analysis. The data from the unconsolidated undrained

tests are used to simulate the undrained conditions while the consolidated drained test data are used for the fully drained conditions. However, the simulation of partial drainage conditions in the analysis is rather difficult. Because of the uncertainty involved in the evaluation of the amount of drainage that occurs in the field, the laboratory test results simulating a partial drainage condition will be of limited value. Chang and Duncan (1970) performed two types of analyses for an excavation problem involving a partial drainage in the clayey soil. In one of the analyses no drainage was assumed to occur within the clayey soils while in the other full drainage was assumed to occur in all types of soils. The extreme drainage conditions assumed in the two analyses resulted in two sets of displacements that bounded the observed displacements.

In earth dams with relatively thin cores of low plastic till a certain amount of drainage is normally expected to occur within the impervious and semi-pervious zones during the period of construction. The stress-strain relationships used in the analysis are to be derived from the laboratory tests that simulate the proper stress paths and the partial drainage, consistent with the field conditions. For the purpose of the present investigation such tests were not performed. Instead the results from the consolidated undrained tests were used to simulate the behaviour of the impervious and the semi-pervious materials (Chapter V). It was believed that such an approach would simulate a condition that lies between the

two extreme possibilities of the fully drained and the undrained conditions.

3.9 Method of Deriving the Moduli of Elasticity

The derivation of the moduli proposed in this work consists of converting the conventional triaxial test data to a form involving the three stress invariants, the axial strain, and the octahedral shear strain. The elastic parameters based on the three stress invariants are computed in the finite element analysis for each element. The proposed method has the following advantages:

- (1) Approximations involved in representing the test data are eliminated by using a digital form for the actual stress-strain relationships.
- (2) The method proposed to derive the moduli in terms of stress invariants, removes the necessity of making an assumption regarding the intermediate principal stress.
- (3) Even though the derivation procedure given here was developed for the conventional triaxial tests, the generality of the use of stress invariants can easily be applied with suitable modifications to other types of tests (e.g., triaxial tests with different stress paths, plane strain tests, etc.).

One obvious disadvantage of the method is that it involves greater computational effort than other methods that consider functional form of representing the test data. However, the time involved in the calculations is a minor part

of that needed for the solution of equations in the finite element analysis. In the subsequent sections the procedure of derivation of moduli and its accuracy are discussed.

3.9.1 Derivation Procedure

From the deviatoric stress versus axial strain (ϵ_1) and volumetric strain (ϵ_v) versus axial strain relationships of the triaxial test results, two plots can be generated. The first plot is the octahedral shear stress (τ_{oct}) versus axial strain for a set of chosen values of $J_3/(\sigma_{oct})^2$ where J_3 is the third stress invariant and σ_{oct} is the octahedral normal stress. The dimensions of $J_3/(\sigma_{oct})^2$ is that of stress. To determine the octahedral shear (τ_{oct}) and $J_3/(\sigma_{oct})^2$ one has to consider the three stress invariants in order that the three principal stresses are uniquely represented. The second plot is the octahedral shear strain (γ_{oct}) plotted against the axial strain. Fig. 3.1 shows a typical conventional plot of the triaxial test data obtained by performing consolidated undrained triaxial tests on a silty sand representing the semi-pervious material of Duncan Dam (Chapter V). The net volumetric expansion is neglected as shown by the dotted lines. Fig. 3.2 shows the relationships between τ_{oct} and ϵ_1 and γ_{oct} and ϵ_1 for a set of chosen values of $J_3/(\sigma_{oct})^2$. For clarity the relation between γ_{oct} and ϵ_1 is shown only for two values of $J_3/(\sigma_{oct})^2$ (0 psi and 80 psi). The triaxial data are given as data input to the computer program and the conversion to the stress invariant form is a

part of the program.

The following expressions were used to calculate the stress invariants and γ_{oct} from the conventional triaxial test data:

$$\sigma_{oct} = (\sigma_1 + 2\sigma_3)/3 \quad (3.1)$$

$$\tau_{oct} = (\sqrt{2}/3)(\sigma_1 - \sigma_3) \quad (3.2)$$

$$J_3 = \sigma_1(\sigma_3)^2 \quad (3.3)$$

$$\gamma_{oct} = (\sqrt{2}/3)(3\varepsilon_1 - \varepsilon_v) \quad (3.4)$$

The following procedure was used for the determination of the elastic parameters:

- (1) The three stress invariants were computed from the three known principal stresses in an element. For a two dimensional plane strain analysis, the intermediate principal stress was computed from

$$\sigma_2 = \nu(\sigma_1 + \sigma_3)$$

where ν was a trial value of Poisson's ratio (say 0.35). Since ν in turn depends on the stress condition, an iterative method was used.

- (2) For the values of τ_{oct} and $J_3/(\sigma_{oct})^2$ computed, the incremental ratio, $(\Delta\tau_{oct}/\Delta\varepsilon_1)$ was interpolated from the τ_{oct} versus ε_1 plot. Similarly from the γ_{oct} versus ε_1 plot,

the incremental ratio, $(\Delta\gamma_{\text{oct}}/\Delta\epsilon_1)$ is interpolated for the same value of $J_3/(\sigma_{\text{oct}})^2$ and the corresponding axial strains used for interpolating $(\Delta\tau_{\text{oct}}/\Delta\epsilon_1)$. The shear modulus was obtained from:

$$G = (\Delta\tau_{\text{oct}}/\Delta\epsilon_1)/(\Delta\gamma_{\text{oct}}/\Delta\epsilon_1) \quad (3.5)$$

Since the value $(\Delta\gamma_{\text{oct}}/\Delta\epsilon_1)$ obtained above corresponds to a particular constant value of σ_3 in the triaxial test, Poisson's ratio was computed from:

$$\nu = (3/2/2)(\Delta\gamma_{\text{oct}}/\Delta\epsilon_1) - 1 \quad (3.6)$$

and was limited to a maximum of 0.49. The bulk modulus was computed from:

$$K = G(2/3)(1 + \nu)/(1 - 2\nu) \quad (3.7)$$

When one of the principal stresses becomes negative (tensile) it was artificially set to zero hence $J_3/(\sigma_{\text{oct}})^2$ should be zero. Under isotropic compression $J_3/(\sigma_{\text{oct}})^2$ would be equal to σ_3 .

In case of a two dimensional analysis steps 1 and 2 were repeated until the intermediate principal stress values computed in two consecutive trials agree closely with each other.

The elastic parameters used in a particular increment of load can be derived from the stress state corresponding to the conditions that existed before the increment of load. The solution obtained by such a procedure was called a "past stress" solution by Kulhawy et al. (1969). Since this procedure usually gives a poor result, it was recommended that the use of the "average stress" be made for the derivation of moduli. The "average stress" was defined as the average of stresses that exist immediately before and after the load increment. A similar procedure has been used in this work to improve the solutions of the non-linear analysis. The incremental load was added to the existing load and the stresses were computed using the elastic parameters calculated on the basis of "past stresses" and these stresses are termed the "present stresses" (Kulhawy et al., 1969). The elastic parameters based on the "present stresses" were calculated. The average elastic parameters were computed from those calculated on the basis of "past stresses" and "present stresses" and were used in the reanalysis of the same increment. This procedure termed the "average moduli" procedure here, has been used in this work because of computational advantages in terms of storage. It is obvious that the "average moduli" or "average stress" procedure takes twice as much time as the "past stress" solution.

3.9.2 Studies to Check the Accuracy of the Procedure of Derivation of Elastic Parameters

To check the accuracy of the present method of derivation of elastic parameters, a weightless soil block 4" x 4" x 1" was considered to be loaded vertically, in five increments, of 20 lbs. each which cause a vertical incremental stress of 5 psi. The problem was analyzed both in two and three dimensions. The finite element idealizations for two and three dimensional analyses for a half of the soil block (because of symmetry) are shown in Fig. 3.3. The nodal loads imposed in each increment are also shown. The initial moduli for the first increment of load for all these studies were derived from the experimental data (Fig. 3.2) for the condition:

$\tau_{oct} = 0$ and $J_3(\sigma_{oct})^2 = 0$. The following cases were studied:

- (1) Plane stress analysis using the elastic parameters derived from "past stresses".
- (2) Plane stress analysis using "average moduli".
- (3) Three dimensional analysis using "average moduli" for the unconfined compression of the soil block.

Fig. 3.4 shows the comparison between the "past stress" solution and "average moduli" solution, the latter agreeing very well with the experimental curve obtained under unconfined compression (Fig. 3.1). The three dimensional analysis gives the same result as the two dimensional one for the particular case. The better accuracy of the "average moduli" approach led to its adoption in all the subsequent studies in this work unless otherwise stated.

3.9.3 Effect of Intermediate Principal Stress on Stress-Strain Results

The effects of the assumption regarding the intermediate principal stress on the stress-strain results are of interest.

The following studies have been conducted for this purpose:

- (1) Two dimensional plane strain analysis assuming that

$$\sigma_2 = \sigma_3.$$

- (2) Two dimensional plane strain analysis assuming that

$$\sigma_2 = \nu(\sigma_1 + \sigma_3).$$

- (3) Two dimensional plane strain analysis with lateral restraint in the x-direction (Fig. 3.3). This has been done merely to compare the solution with plane stress and plane strain solutions.

Fig. 3.5 indicates that the assumption $\sigma_2 = \sigma_3$ gives greater strains compared to the correct strains obtained from $\sigma_2 = \nu(\sigma_1 + \sigma_3)$. This is due to the lower moduli calculated for the former assumption. However the difference between the results is not significant for the lower range of axial strains (up to 2% for present case). Fig. 3.6 compares the results for conditions of plane stress, plane strain and plane strain with lateral restraint. The progressively increasing slope of the stress-strain curve or the "locking" effect can be seen in the case of the plane strain analysis with lateral restraint.

3.10 Isotropic Compression

Compression under an all around stress is dealt with

by considering the initial-tangent Young's moduli and Poisson's ratios at the appropriate confining stresses. In terms of stress invariants they correspond to the initial-tangent shear and bulk moduli at the appropriate confining stresses. An example of isotropic compression is shown in Fig. 3.7. The axial stress (σ_1) is plotted against axial strain (ϵ_1) both for isotropic and deviatoric compression for a silty sand tested at a water content 3% greater than the optimum in a triaxial apparatus for consolidated undrained conditions. The deviatoric compression results are shown only for σ_3 equal to 15 psi and 40 psi for clarity. The predicted isotropic compression curve obtained by using the incremental procedure described previously agrees reasonably well with the experimental curve even though the drainage condition is not the same for the isotropic and deviatoric compressions.

3.11 Summary

Satisfactory simulation procedures for two and three dimensional finite element analyses with a method of deriving moduli based on stress invariants and "average moduli" have been developed. The main limitation of the procedure is the restriction of Poisson's ratio to a maximum value of 0.49. However this is not serious because the dilatancy effects of soil become more important at comparatively large strains such as those caused due to shear failures. Since the present studies are concerned essentially with the tensile cracking of earth dams, and not with the shear failure of earth dam,

it is believed that the above limitation has no significant effect on the prediction of tensile zones in earth dams.

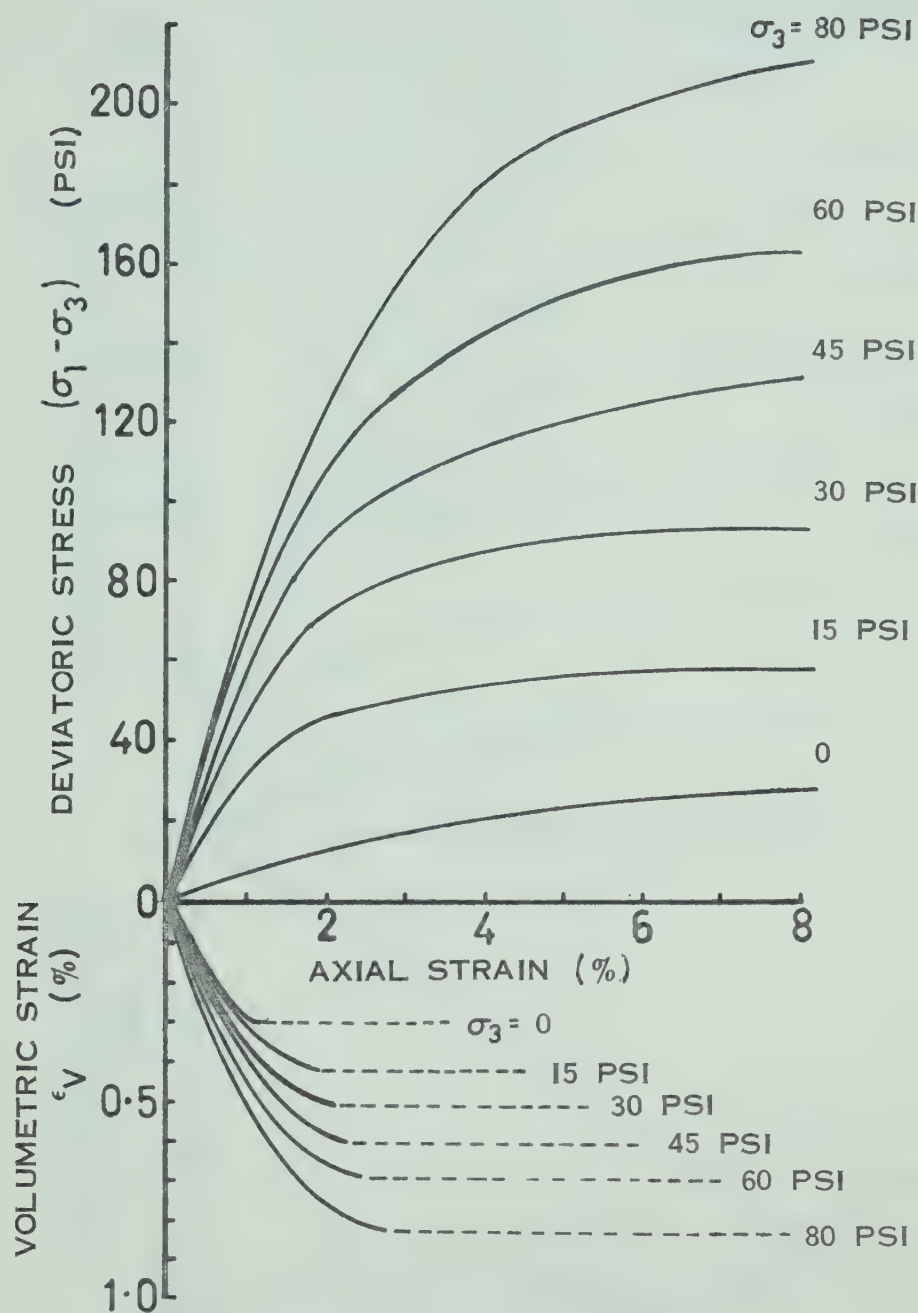


FIG. 3.1 TRIAXIAL TEST DATA FOR A SILTY SAND PLOTTED IN THE CONVENTIONAL MANNER

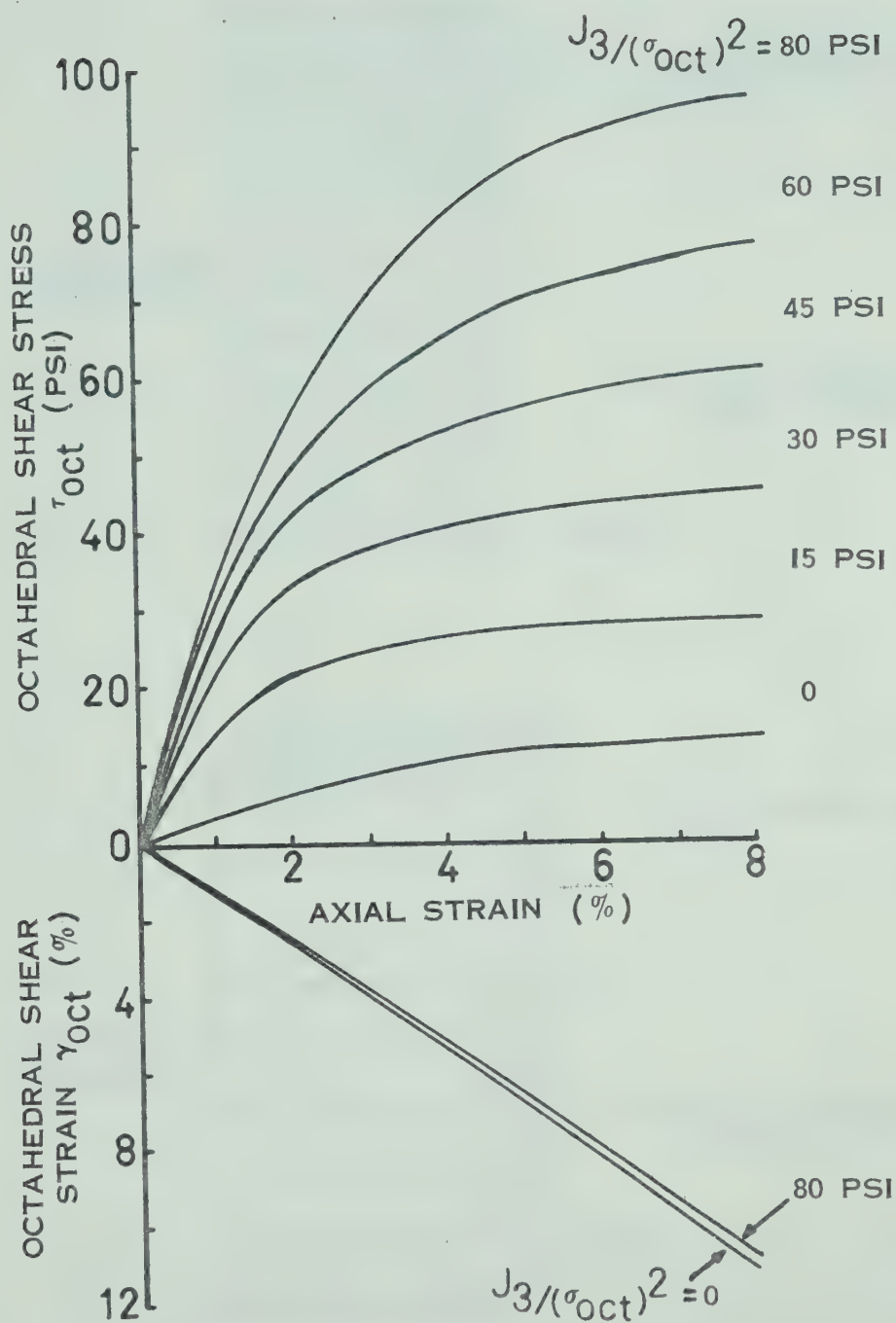


FIG. 3.2 TRIAXIAL TEST DATA FOR A SILTY SAND
PLOTTED IN TERMS OF STRESS AND STRAIN
INVARIANTS AND AXIAL STRAIN

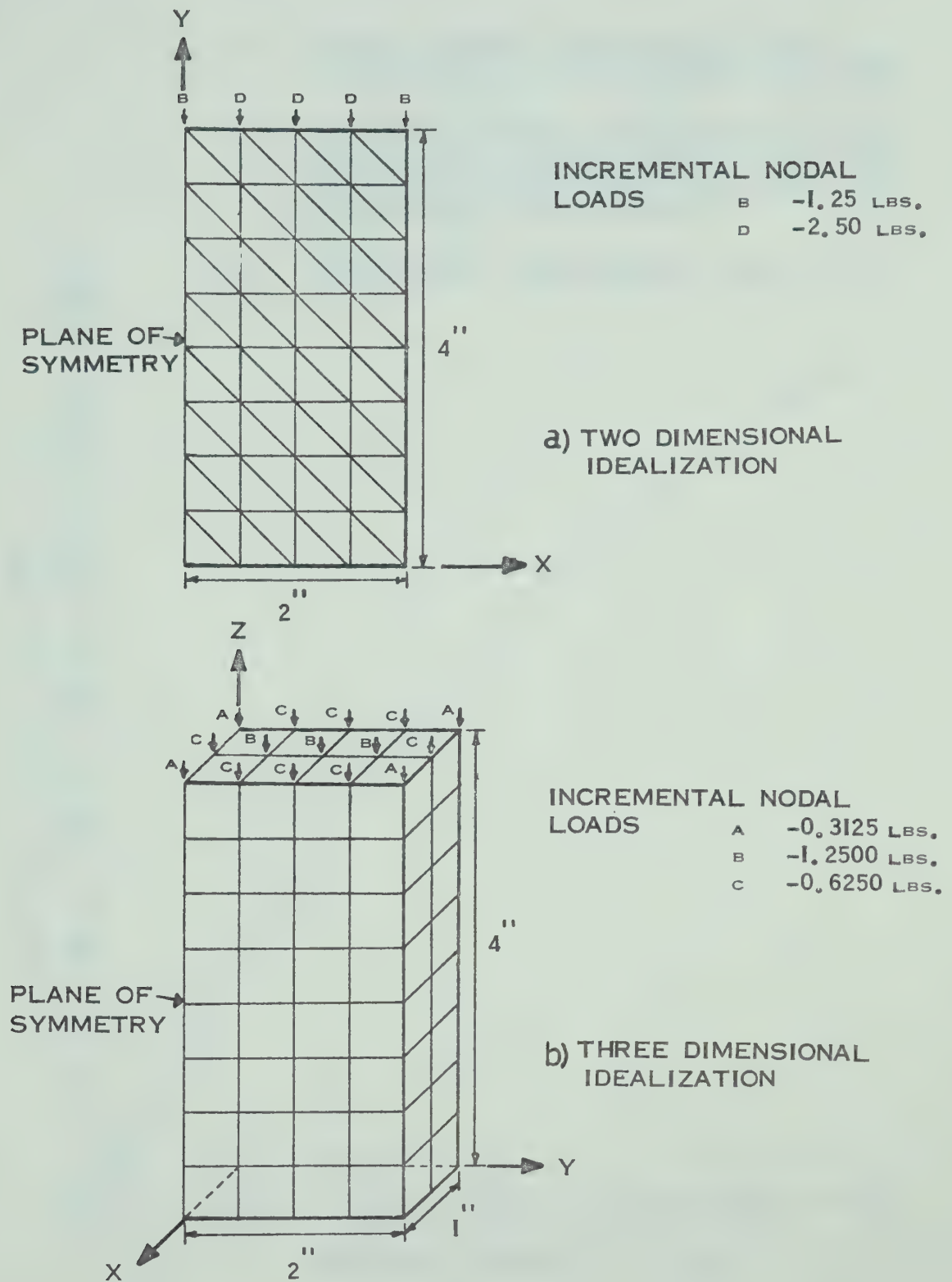


FIG. 3.3 FINITE ELEMENT IDEALIZATION OF A SOIL BLOCK

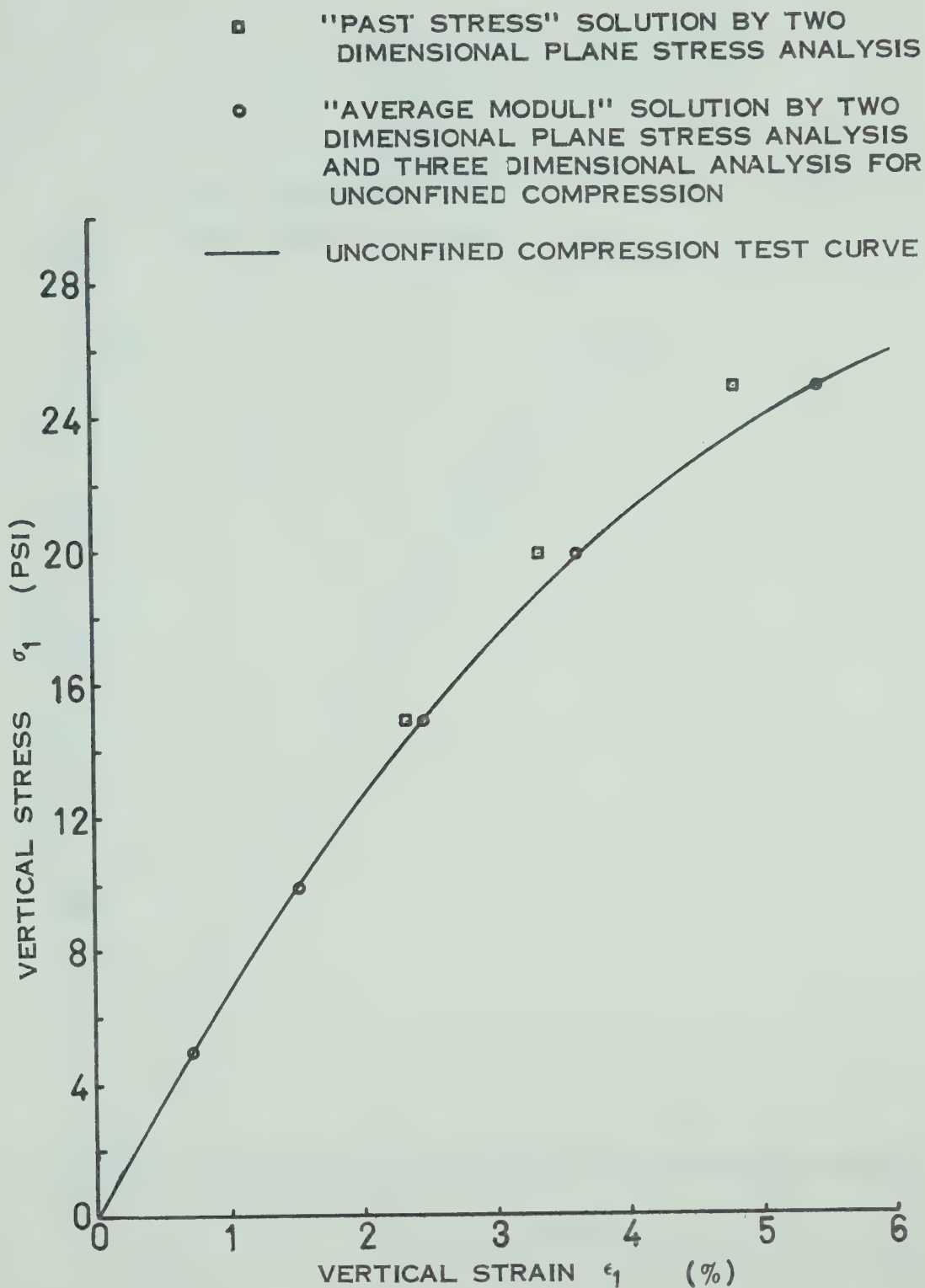


FIG. 3.4 COMPARISON OF "PAST STRESS" AND "AVERAGE MODULI" SOLUTIONS IN AN INCREMENTAL ANALYSIS PERFORMED IN FIVE INCREMENTS

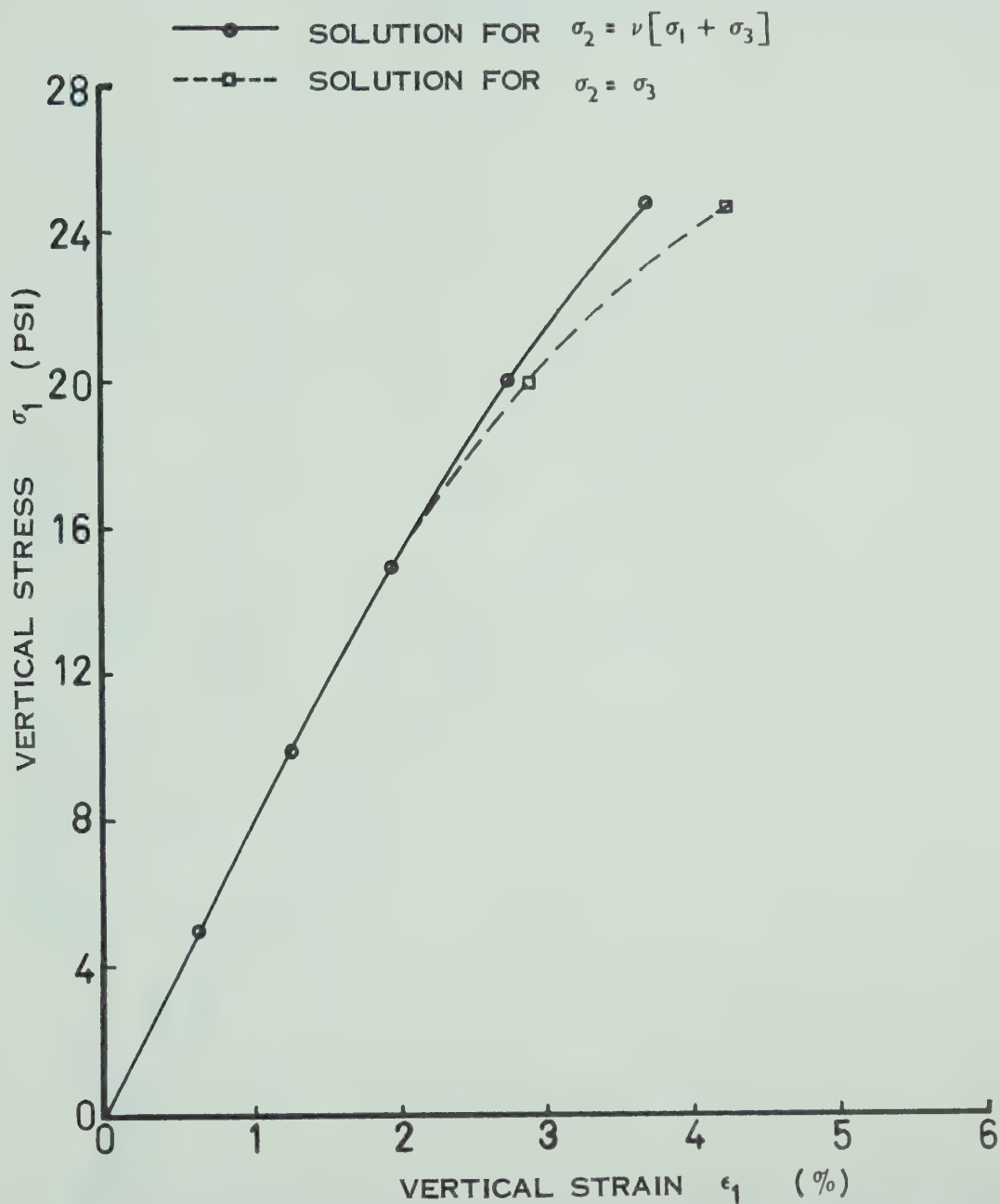


FIG. 3.5 COMPARISON OF INCREMENTAL NONLINEAR PLANE STRAIN SOLUTIONS WITH DIFFERENT ASSUMPTIONS REGARDING THE INTERMEDIATE PRINCIPAL STRESS [ANALYSES IN FIVE INCREMENTS]

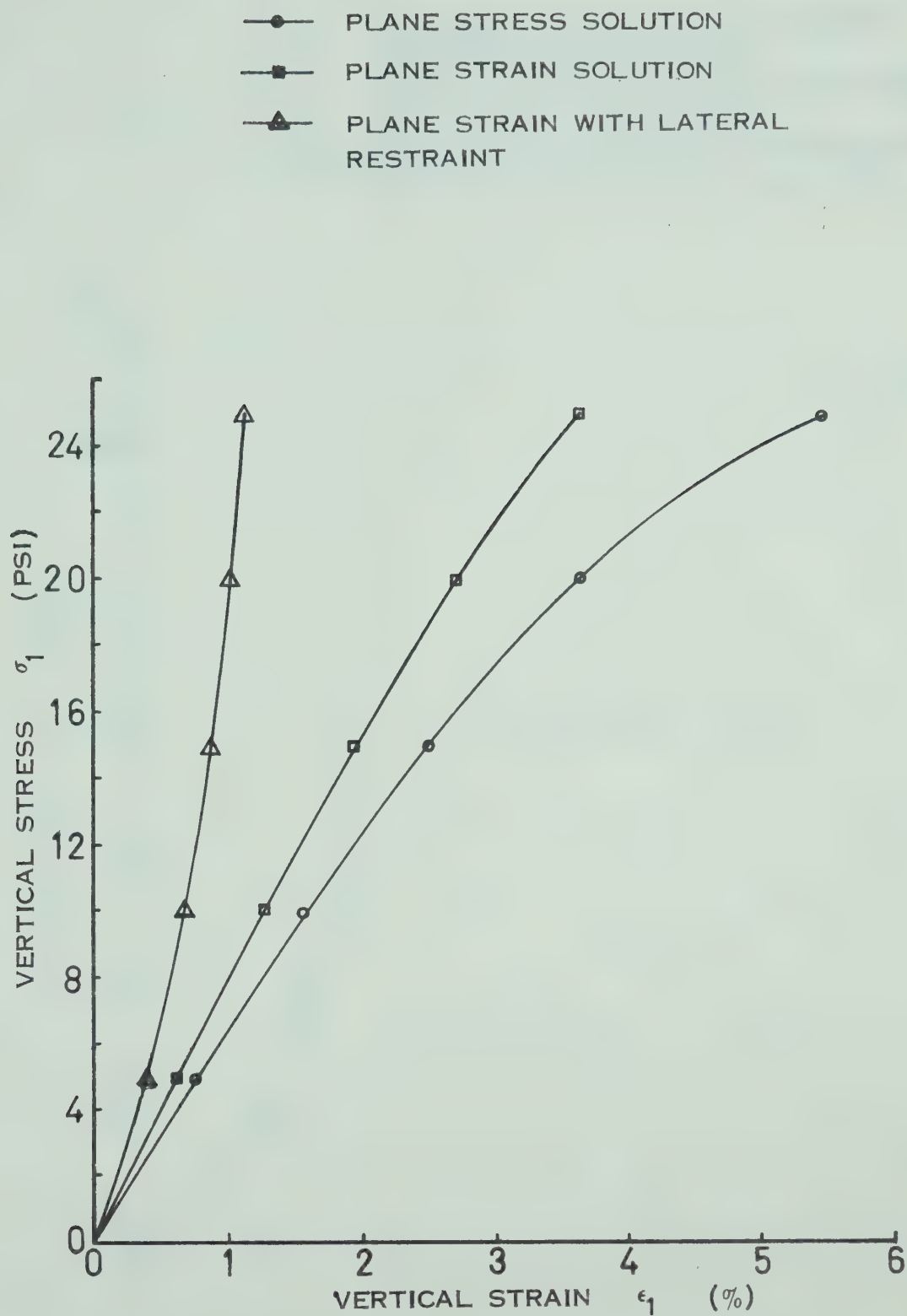


FIG. 3.6 COMPARISON OF INCREMENTAL NONLINEAR SOLUTIONS OBTAINED FOR DIFFERENT BOUNDARY CONDITIONS [ANALYSES IN FIVE INCREMENTS]

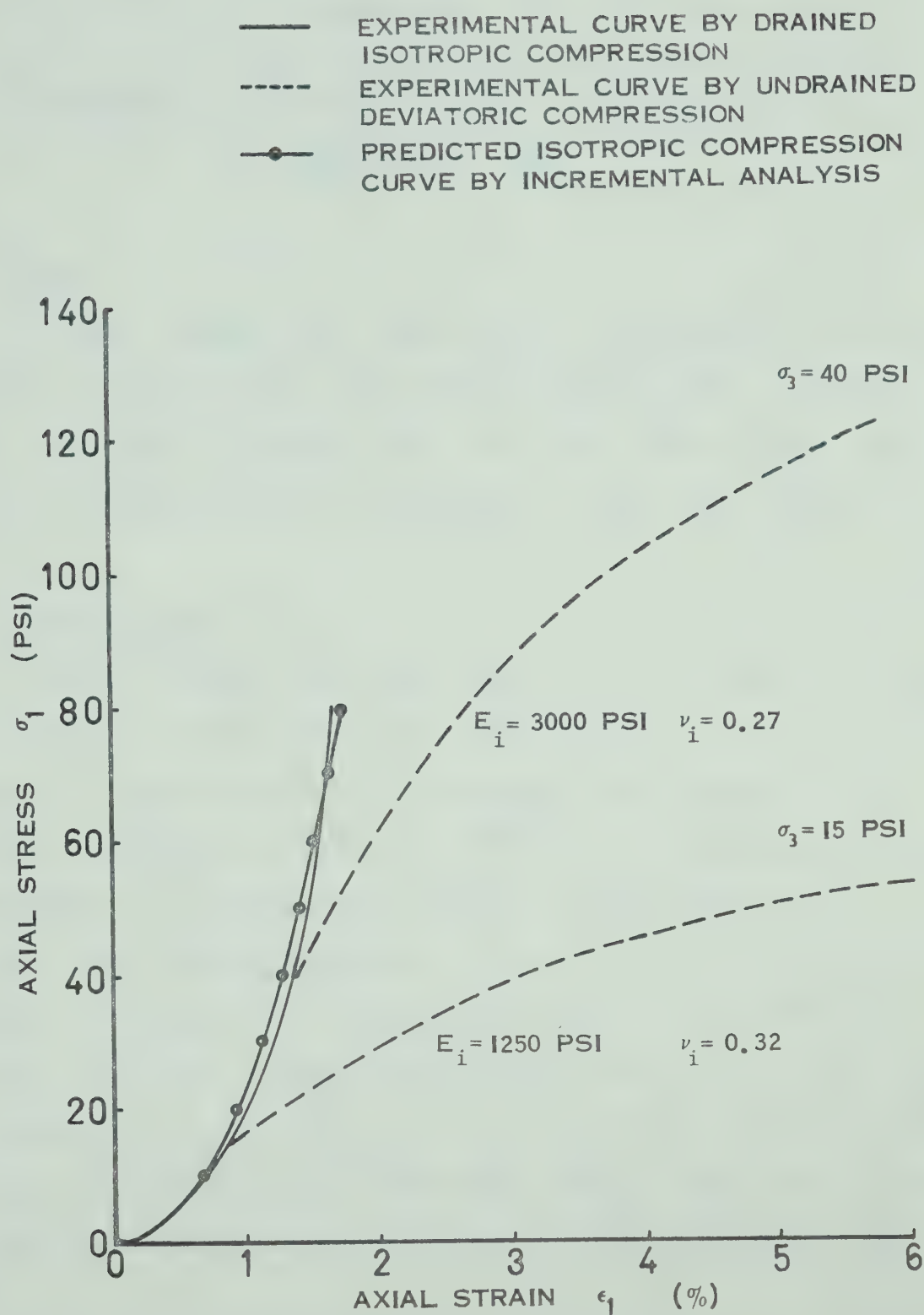


FIG. 3.7 COMPARISON OF PREDICTED AND EXPERIMENTAL STRESS-STRAIN RELATIONSHIP FOR ISOTROPIC COMPRESSION

CHAPTER IV

IMPORTANCE OF CERTAIN FACTORS IN THE ANALYSIS
OF CRACKING OF DAMS4.1 Scope

In this chapter the importance of considering the construction step sequence, non-linear stress-strain relationships, no tensile strength for soils, and three dimensional effects in the analysis of cracking of dams are discussed.

4.2 Introduction

Several factors contributing to the development of tensile cracks in earth dams were outlined in Section 1.3.1 of Chapter I. The influence of the shape (Covarrubias, 1969) and the steepness (Dolezalova, 1970) of the valley walls on the development of tension zones during the construction of a dam has been studied elsewhere. The effects of considering a number of steps that simulate the construction sequence, and the non-linear stress-strain characteristics of soil in the analysis have been discussed by Strohm and Johnson (1971). The studies conducted by Strohm and Johnson were restricted to the period during and at the end of construction of the dam.

As mentioned in Section 1.6 of Chapter I, an analysis should be able to simulate field conditions as closely as possible so that the predictions regarding cracking of dams

would be of some practical value. In order to develop a procedure for reasonable prediction of cracking it is necessary to study the influence of certain assumptions made in the analysis on the predicted results. As outlined in Section 1.8 of Chapter I the parametric studies carried out in this work are restricted to the period, during and at the end of construction of a dam. The studies are directed towards evaluating the influence of construction sequence, non-linear stress-strain relationships of soil, zero tensile strength for soil, and three dimensional effects on the predicted results. The first two factors, even though considered by Strohm and Johnson (1971) before have been studied and included in the present studies for the sake of completeness.

4.3 Selection of Sections for Parametric Studies

The section shown in Fig. 4.1 represents a half of the maximum longitudinal section passing through the centre line of an earth dam founded in a narrow, steep, symmetrical valley. The same section, though not with the same number of elements, was used in all two dimensional analyses. The abutment was assumed to be rough and rigid. The same section was also considered previously by Covarrubias (1969) and Strohm and Johnson (1971). Therefore comparison of results to test the accuracy of the present analyses was facilitated. In order to evaluate the three dimensional effects on a comparative basis, the same symmetrical triangular valley was used for the three dimensional model. In this case, the dam was

symmetrical in the transverse direction also, with a centrally located core having sides inclined at 1:10 and outer slopes of 2:1. A view of one quadrant of the three dimensional model with the type and size of the spatial elements used is shown in Fig. 4.2.

4.4 Accuracy of Two Dimensional Analyses

Since the accuracy of the finite element analysis depends to a large extent on the type of element and the number of elements chosen for the analysis, it is of interest to compare the results of the present work with other available solutions. For this purpose the section shown in Fig. 4.1 was analyzed under plane strain conditions in a single lift assuming linear stress-strain relationships. One hundred constant strain triangular elements as shown in Fig. 4.1 were chosen. The elastic parameters used are shown in Fig. 4.3. The results obtained by Covarrubias (1969) for the same problem using slightly more refined quadrilateral elements are compared with the present results in Fig. 4.3. The horizontal and vertical displacements compared at the crest of the dam are almost identical. In Fig. 4.4 the extent of tension zones computed by Covarrubias (1969), Strohm and Johnson (1971), and the present analysis are compared for the same problem. The good agreement of results shown in Fig. 4.3 and 4.4 indicates that the number and type of element selected are satisfactory for subsequent analyses on the same section to elicit parametric effects.

4.5 Influence of the Construction Step Sequence

Since an earth dam is constructed in a number of layers of small thicknesses, an analysis that simulates the construction step sequence is necessary to predict the stresses and strains in a realistic manner (Clough and Woodward, 1967; Kulhawy et al., 1969). It is not economically possible to deal with a large number of steps in an analysis. Hence it is necessary to determine the number of steps that result in reasonable prediction of stresses and strains. To assess this feature, two dimensional linear elastic analyses were performed for a different number of steps. The maximum vertical displacement at centre line of valley, the maximum horizontal tensile stress and strain at the crest are compared for different number of steps in Fig. 4.5. The vertical displacement compared includes the settlement due to self weight of each layer as it is placed. It can be seen from Fig. 4.5 that all the three quantities compared are reduced with the number of steps and the reduction becomes insignificant after ten steps. Based on these results it is considered that ten steps would be sufficient for the purpose of present parametric studies.

4.6 Two Dimensional Linear, Non-Linear, and "No Tension" Analyses

Since the deformational behaviour of soil is essentially non-linear, the computation of realistic stresses and strains requires that a non-linear stress-strain relationship be used

in the analysis, even though such relationships are employed within the framework of the theory of isotropic elasticity. In order to compare the results of linear and non-linear analyses, a typical set of conventional triaxial test results, obtained by performing consolidated undrained tests on a silty sand was selected (Fig. 4.6). The soil tested represents the semi-pervious material of Duncan Dam (Chapter V). For the purpose of linear analyses an average linear stress-strain relation that represents the stress conditions at the mid height of the dam and close to the centre line of valley is also shown in Fig. 4.6. The initial tangent Poisson's ratio corresponding to the preceding linear relation is 0.26. The curves relating volume changes to axial strain are discontinued after they become horizontal. Poisson's ratio was taken as 0.49 for subsequent stress levels. A density of 2.16 G/CM^3 was used in all analyses and the construction was simulated by ten lifts in every case. As described in Section 3.9.1 the elastic moduli were derived in terms of stress invariants and each step was analyzed twice to use the "average moduli".

The results illustrating the development of tension zones in the incremental linear analysis are shown in Fig. 4.7. Since it was assumed that soil can withstand a substantial amount of tension, it can be seen from the final stage of the analysis shown in Fig. 4.7, that a fairly large zone remains in tension. However since soils in general and the soils used in the analyses here in particular have very

low tensile strengths, it is more appropriate to ignore the tensile strength in the analysis. In other words it may be assumed that as soon as an element goes into tension cracking would take place in that element. To simulate such a condition Zienkiewicz et al. (1968) suggested a "no tension" analysis in which the tensile principal stress in an element is artificially replaced by a system of equivalent nodal forces for that element thereby the redistribution of stresses due to removal of tensile stress in an element after cracking is achieved in a number of iterations. This method of analysis is found to be more efficient than one in which the tensile element is treated as anisotropic by assigning a very low elastic modulus in the direction of the tensile principal stress and the analysis is performed iteratively. Kulhawy et al. (1969) treated a tensile failure, similar to a shear failure, by assigning a zero value of shear modulus to the element in which tensile failure occurs. Strohm and Johnson (1971) assigned an overall low Young's modulus to the element in which tension failure took place. Since a "no tension" analysis is more realistic and efficient than other methods it has been used here. After removing the tensile stress the element is assigned moduli calculated from unconfined compression test data since the confining stress is zero.

The effect of a "no tension" analysis on the development of the tensile zone, major and minor principal stresses, and the displacements is of interest. The results of incremental linear analyses performed with and without the removal of

tensile stresses are compared in Fig. 4.8. The extent of the tensile zone, as indicated by the contour of the zero minor principal stress, is smaller when tension is removed. The distribution of the minor principal stress is affected to a fair degree by the "no tension" analysis whereas the major principal stress and the vertical displacement along the centre line are relatively insensitive to the removal of tension. The variation in the distribution of the minor principal stress that occurs due to the "no tension" analysis depends to a large extent on the magnitude of the tensile stresses removed. If the tensile stresses removed are very small the "no tension" analysis does not significantly alter the results regarding the development of tension zones. In such cases analyses performed without the removal of tensile stresses may be preferred as it considerably saves the computation effort needed especially in a three dimensional analysis.

The growth of tension zones in an incremental non-linear analysis is illustrated in Fig. 4.9. It can be seen that the extent of the tension zone and the magnitude of tensile stresses developed are quite small compared to the results obtained in a linear analysis. A similar result was also obtained by Strohm and Johnson (1971). In this analysis it was assumed that the intermediate principal stress is equal to the minor principal stress (i.e., $\sigma_2 = \sigma_3$) while calculating the elastic moduli. For the elements in which tension occurs the modulus is calculated from the stress-strain curve

corresponding to unconfined conditions. A "no tension" analysis is not performed as the tensile stresses developed are very small in magnitude.

4.7 Effect of the Intermediate Principal Stress

It is of interest to assess the effect of the intermediate principal stress on the analytical results. To determine any effects the intermediate principal stress was computed from:

$$\sigma_2 = \nu(\sigma_1 + \sigma_3)$$

and its value was utilized in calculating the stress invariants for deriving the moduli. An iterative procedure was used because of the dependence of Poisson's ratio on stress. Results obtained from such an analysis are compared in Fig. 4.10 with those obtained by assuming σ_2 is equal to σ_3 . It is apparent that the intermediate principal stress has practically no effect on the horizontal stress and strain at the crest of dam. However, vertical displacements at the centre line of the valley are about 2.5% greater for the analysis in which it is assumed that σ_2 is equal to σ_3 .

The small difference between the results obtained for the plane strain cases analyzed can be attributed to the condition, close to a confined compression with relatively small vertical strains, that exists over a major portion of the valley. Under small vertical strains the effect of intermediate principal stress is not significant (Fig. 3.5, Chapter

III). Because of the closeness to confined compression $\sigma_2 \approx \sigma_3$.

4.8 Three Dimensional Effects

4.8.1 General

Finite element analyses for embankments are performed mostly for plane strain conditions even though some solutions were obtained recently by three dimensional analysis (e.g., Frazier, 1969; Lefebvre and Duncan, 1971; Palmerton, 1972). The major drawback of a three dimensional analysis is its high computational cost compared to a two dimensional analysis. However, for certain situations a three dimensional finite element analysis for an embankment structure becomes very useful and sometimes irreplaceable. A three dimensional analysis may be preferred when the complex boundary geometry and boundary conditions cannot be represented by the plane strain conditions assumed in a two dimensional analysis. Considering the complexity of the problem of cracking of earth dams founded on irregular, non-homogeneous, compressible foundations, it appears that a three dimensional analysis is more relevant than a two dimensional analysis. Under such conditions a three dimensional analysis may be justified as its cost forms only a minor part of the total cost of the project.

4.8.2 Three Dimensional Studies

Palmerton (1972) compared the results of plane strain

and three dimensional analyses performed on an earth dam located in a narrow triangular valley, similar to that in Figs. 4.1 and 4.2. The plane strain analysis was performed only on the maximum transverse section. The analyses used non-linear stress-strain relationships in the hyperbolic functional form and an incremental construction was simulated. Considerable differences in stress conditions were observed between plane strain and three dimensional analyses but the displacements predicted by both analyses were more or less similar. The differences between the stresses were mainly due to the arching action aided by the valley walls.

From these results it appears that a two dimensional analysis performed on the maximum transverse section of an earth dam founded in a symmetrical or nearly symmetrical narrow rigid valley may provide useful information regarding the displacements which can be verified easily by field observations at the maximum section.

In the present studies, the results of three dimensional analyses performed on the dam shown in Fig. 4.2 are compared with those of two dimensional analyses. For the purpose of comparison linear three dimensional analyses in single and multiple increments were performed. Linear analyses were performed to facilitate comparison of two and three dimensional analyses at the same moduli values.

Fig. 4.11 and Fig. 4.12 show the comparison of vertical displacement and horizontal stress and strain at the crest of the dam respectively. As seen from the comparison the results

obtained by plane strain and three dimensional analyses are not significantly different. The difference between the maximum vertical displacement of the crest obtained by the two types of analysis is 4.7%. Incremental linear analyses with five construction steps were performed for two and three dimensional sections shown in Figs. 4.1 and 4.2. The results of horizontal and vertical stresses in the core, and the vertical displacements at the centre line of the valley obtained by plane strain and three dimensional incremental linear analyses are compared in Fig. 4.13. The horizontal and vertical stresses near the crest obtained by both analyses are very much the same. However, significant differences in stresses are evident in the lower portion of the dam, the stresses being smaller in magnitude in the three dimensional case. The difference between the maximum vertical settlements at the centre line of the valley is about 13.6%.

From these studies it emerges that the results of plane strain analyses are useful to predict, with some reliance, the tensile stresses close to the crest of a homogeneous earth dam founded in a narrow symmetrical steep valley.

However, when the rigidity of the core differs from that of the shell the predictions by plane strain analyses lead to large errors in tensile stresses near the crest. This is revealed by the comparisons shown in Fig. 4.14. The plane strain analysis predicts much higher magnitudes of tensile stresses compared to the three dimensional analysis when the core is ten times softer than the shell. The reverse is true

when the shell is softer than core. The results are similar both in a single step and 5-step incremental analyses even though the absolute magnitude of stresses developed in the incremental analysis is considerably less.

The reason for these large differences in stresses can be understood from the displacement patterns shown in Fig. 4.15. The displacement results were obtained from three dimensional linear 5-step incremental analyses for two ratios of elastic moduli of core to shell. The ratios chosen for rigid and soft core are 10 and 0.1 respectively. The displacement of the surface points in the x-y plane are shown by dotted lines for the rigid core case and by full lines for the soft core case. The displacement vectors both in magnitude and direction and the locations of the zones in which tensile stresses develop are also shown for both cases. The following features can be observed from this figure:

- (1) For the rigid core case, the displacements in the core are away both from the crest and the abutment.
- (2) For the soft core case, the displacements in the x-direction are towards the crest, and in the y-direction they are away from the abutment.
- (3) Plane strain conditions along the maximum longitudinal section, assumed in a two dimensional analysis, will not be satisfied in both cases.
- (4) Longitudinal tensile strains produced in a core of a given flexibility close to the crest are influenced by the flexibility of shell. A shell more flexible than

core produces greater longitudinal tensile strains in core than those produced by a shell stiffer than core. For example in Fig. 4.15 the displacements shown by dotted line would increase by ten times if an analysis is performed with the modulus of core equal to 200 KG/CM^2 (same as that used for the soft core case) and with the modulus of shell equal to 20 KG/CM^2 . Larger longitudinal strains produced in a rigid core due to greater flexibility of shell result in larger tensile stresses in comparison to the case of a soft core with a rigid shell.

- (5) In a rigid core both longitudinal and transverse cracks are possible whereas in the case of a soft core the cracks that are likely to occur in the core are mainly in the transverse direction. The locations where tensile stresses developed in the transverse and longitudinal directions, for the two cases studied, are shown in Fig. 4.15.

The distribution of vertical and horizontal stresses in core and shell for two cases discussed above is shown in Fig. 4.16. Large reductions in both horizontal and vertical stresses in the soft core can be seen. Such reductions are usually the cause of hydraulic fracturing, a factor that could cause internal cracks leading to piping failures (Bjerrum, 1967; Kjaernsli and Torblaa, 1968; Sherard et al., 1972). Fig. 4.17 shows the effect of the difference in flexibilities between core and shell on the maximum tensile principal stress developed in the core. The results were

obtained by performing three dimensional linear analyses in a single step for different ratios of moduli of core to shell ranging from 0.01 to 100.0. The variation of the maximum tensile stress is predominant between ratios 0.1 to 10.0. For ratios less than 0.07, representing conditions seldom realized in practice, the computed stress may not be reliable and it is thought that the dashed line is more representative. While the result shown in Fig. 4.17 is applicable to the geometry and the conditions assumed in the analysis, it nevertheless indicates that by controlling the compaction and moisture content of shell and core, placement conditions of the fill can be specified which will contribute significantly to the design of dams against cracking.

4.9 Considerations of the Flexibility of the Core to Control Cracking

One of the common methods used to control the cracking of earth dams is to place the fill at water contents 1 to 2% greater than the optimum. It is assumed that the increase in flexibility of the core thus achieved, prevents the core from cracking due to tensile stresses. However, when the flexibility of the core is to be increased, it is necessary to distinguish between two common situations:

- (1) A dam built on a highly compressible foundation, will undergo differential settlement which causes tensile cracks in the core (e.g., Duncan Dam, Chapter V). The stresses in the core are governed mainly by the settle-

ment of the foundation and the flexibility of the core.

When the flexibility of the core is increased the tensile stresses in the critical zones are generally reduced.

- (2) The tensile zones developed in the core of a dam built in a valley with more or less rigid abutments and incompressible foundations are governed mainly by the settlement that occurs within the core. Two dimensional finite element analyses under plane strain conditions were performed on the section shown in Fig. 4.1 for the following three cases to illustrate the effect of increasing the flexibility of the core and the non-homogeneity of the core on the development of tensile zones:

- (i) A homogeneous dam (Fig. 4.18(a)) consisting of material with $E = 200 \text{ KG/CM}^2$ and $\nu = 0.35$.
- (ii) A homogeneous dam (Fig. 4.18(a)) consisting of material with $E = 100 \text{ KG/CM}^2$ and $\nu = 0.35$.
- (iii) A homogeneous dam (Fig. 4.18(b)) consisting of two materials with
 - (a) $E = 100 \text{ KG/CM}^2$ and $\nu = 0.35$ in the tensile zone as determined in case (i) or case (ii) and
 - (b) $E = 200 \text{ KG/CM}^2$ and $\nu = 0.35$ elsewhere in the dam.

Fig. 4.18(a) compares the tensile zone and the tensile strain along the crest for cases (i) and (ii). An increase in the flexibility of the core does not change the tensile stresses or the extent of the tensile zone because, for the type of

boundary considered, the stresses are independent of the values of the moduli used in the analysis. The tensile strains along the crest, on the other hand, increase with the flexibility of the core.

Fig. 4.18(b) shows the results of a finite element analysis performed on a non-homogeneous section. This section consists of two types of material. A material with a high flexibility is incorporated in the tensile zones determined previously for homogeneous section (case (i) or case (ii)), whereas material with a low flexibility is retained elsewhere in the dam. The non-homogeneity of the material in the dam causes a favourable stress redistribution, the magnitude of tensile stresses is lowered as well as reducing the extent of the tensile zone. The tensile strains along the crest are slightly more than those obtained in case (i). Introducing another type of material of higher flexibility than that corresponding to 100 KG/CM^2 into the tensile zone indicated by tensile stresses in Fig 4.18(b), further reduces the tensile stresses and the extent of tensile zone.

For the type of boundary considered above, the reduction of tensile zones or even their elimination would become possible if materials with appropriate flexibility characteristics are properly distributed within the suspected tensile zones. An overall increase in flexibility of material throughout the core, for the type of boundary considered, is of little use in controlling of tensile cracks. A finite element analysis with non-homogeneous modelling can be employed conveni-

ently, as shown, to assess the relative influence of changing the placement conditions of the fill in the critical zones of a dam.

4.10 Summary

An analysis which considers realistic boundary conditions, representative non-linear stress-strain characteristics of soils and the construction step sequence is a considerable contribution to the proper evaluation of tensile zones in earth dams both during and at the end of construction. A single step linear analysis, even though simple and straightforward, exaggerates the tensile zones and results in unrealistic displacements and stress distributions. Consideration of incremental loading is of utmost importance even for an approximate evaluation of displacements. The influence of the intermediate principal stress on the results of a plane strain analysis is small when geometry analyzed almost represents conditions of confined compression with relatively small strains. This generally occurs for a valley having a narrow profile. The removal of tensile stresses in cracked zones ("no tension" analysis) influences the results of the non-linear incremental analysis of cracking only to a minor extent. As a non-linear incremental analysis in general results in tensile stresses of low magnitude compared to those obtained by a linear incremental analysis, the redistribution of stresses caused by the removal of tensile stresses does not significantly alter the extent of tensile stresses subsequent-

ly computed in the upper layers. As the "no tension" analysis involves an iterative procedure its use in a three dimensional analysis increases the cost of computation considerably. Because of its rather minor effect on the results, and also due to the high cost of computation involved, a "no tension" analysis was not introduced into the three dimensional finite element program for the purpose of the present work. The extension of the "no tension" analysis to three dimensional problems is however possible. While a two dimensional analysis provides reasonably accurate solutions in the analysis of cracking of homogeneous earth dams founded in narrow steep valleys, significant errors could be caused when core and shell differ in their deformational properties. The tensile stresses are under-estimated when the shell is more flexible than core whereas they are over-estimated when the shell is less flexible than core. For certain boundary conditions a finite element analysis with a non-homogeneous modelling of dam may be used to assess the relative influence of changing the flexibility of the fill. Such an assessment is useful in designing dams against tensile cracking.

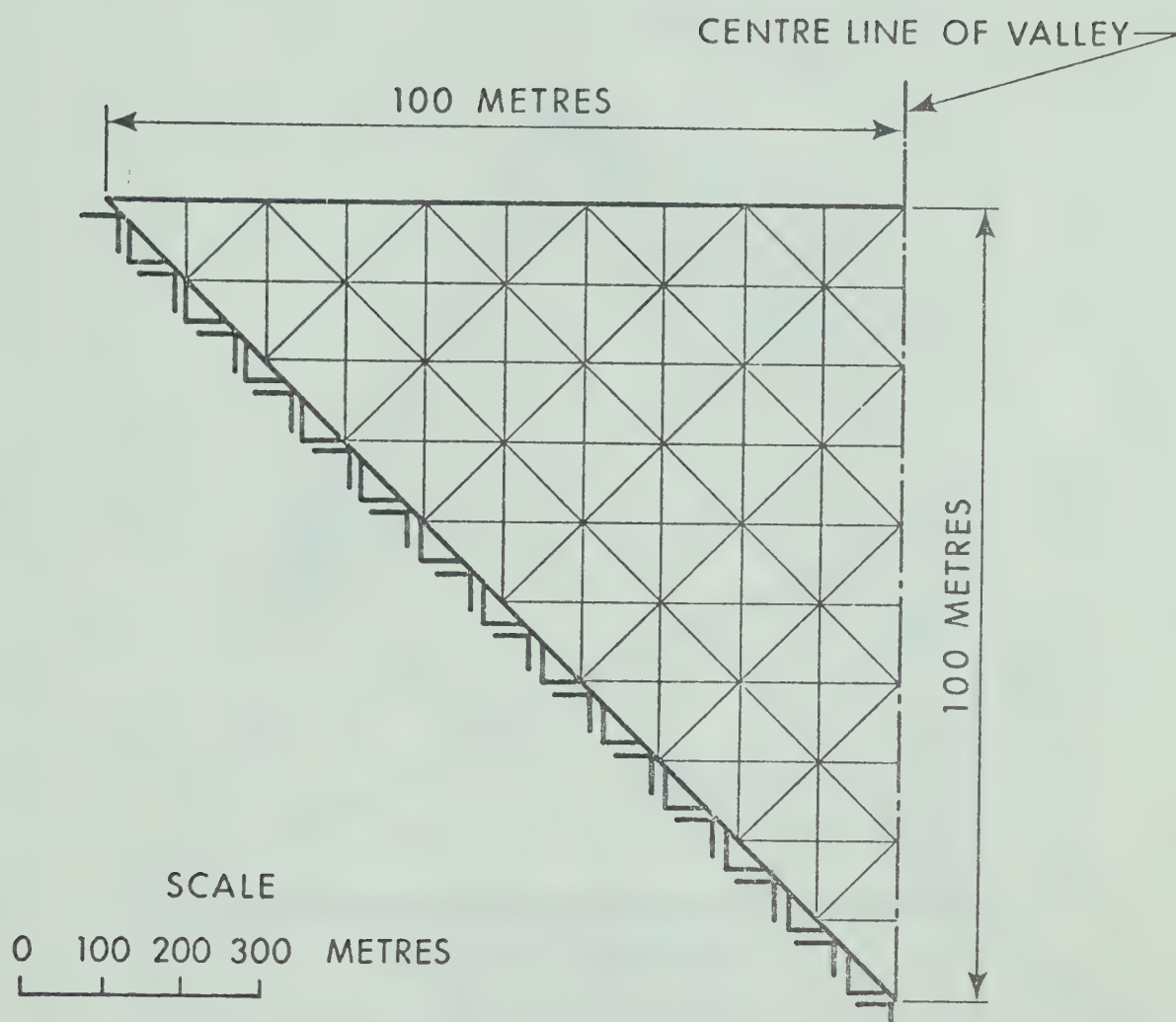


FIG. 4.1 SECTION ASSUMED IN TWO DIMENSIONAL ANALYSES

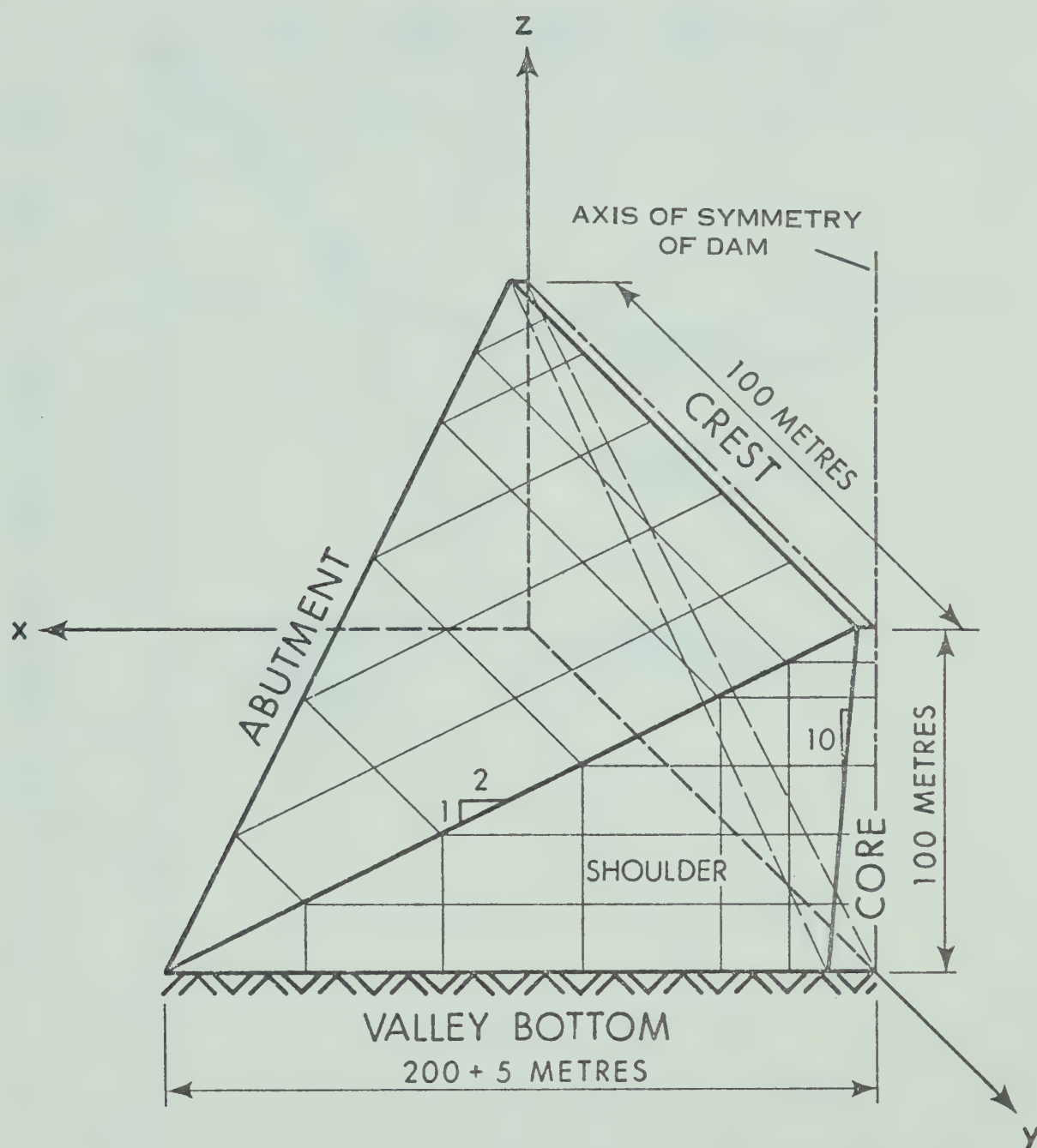


FIG. 4.2 QUADRANT OF DAM ASSUMED IN THREE DIMENSIONAL ANALYSES

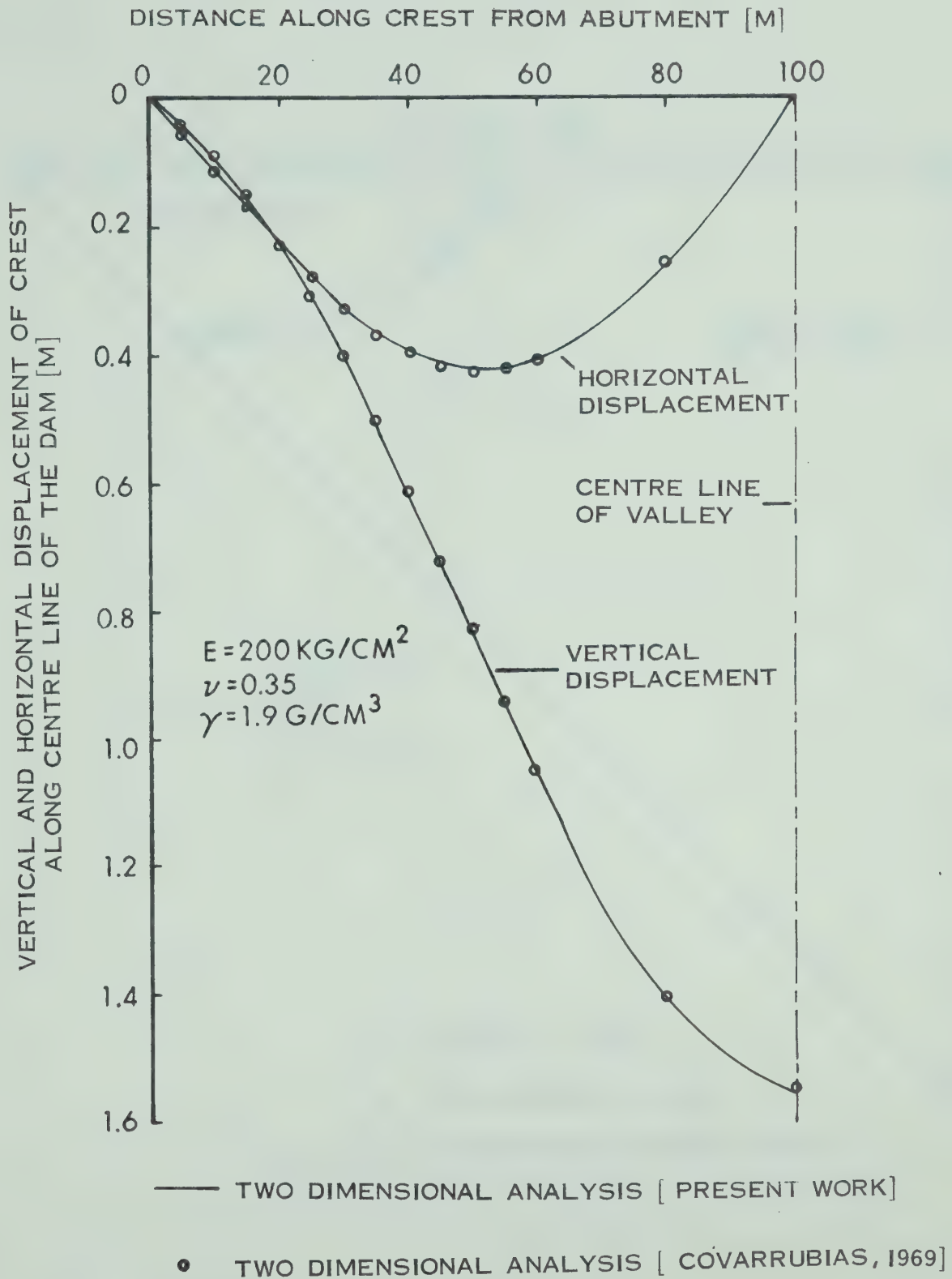


FIG. 4.3 COMPARISON OF VERTICAL AND HORIZONTAL DISPLACEMENTS FOR TWO DIMENSIONAL SINGLE STEP ANALYSES

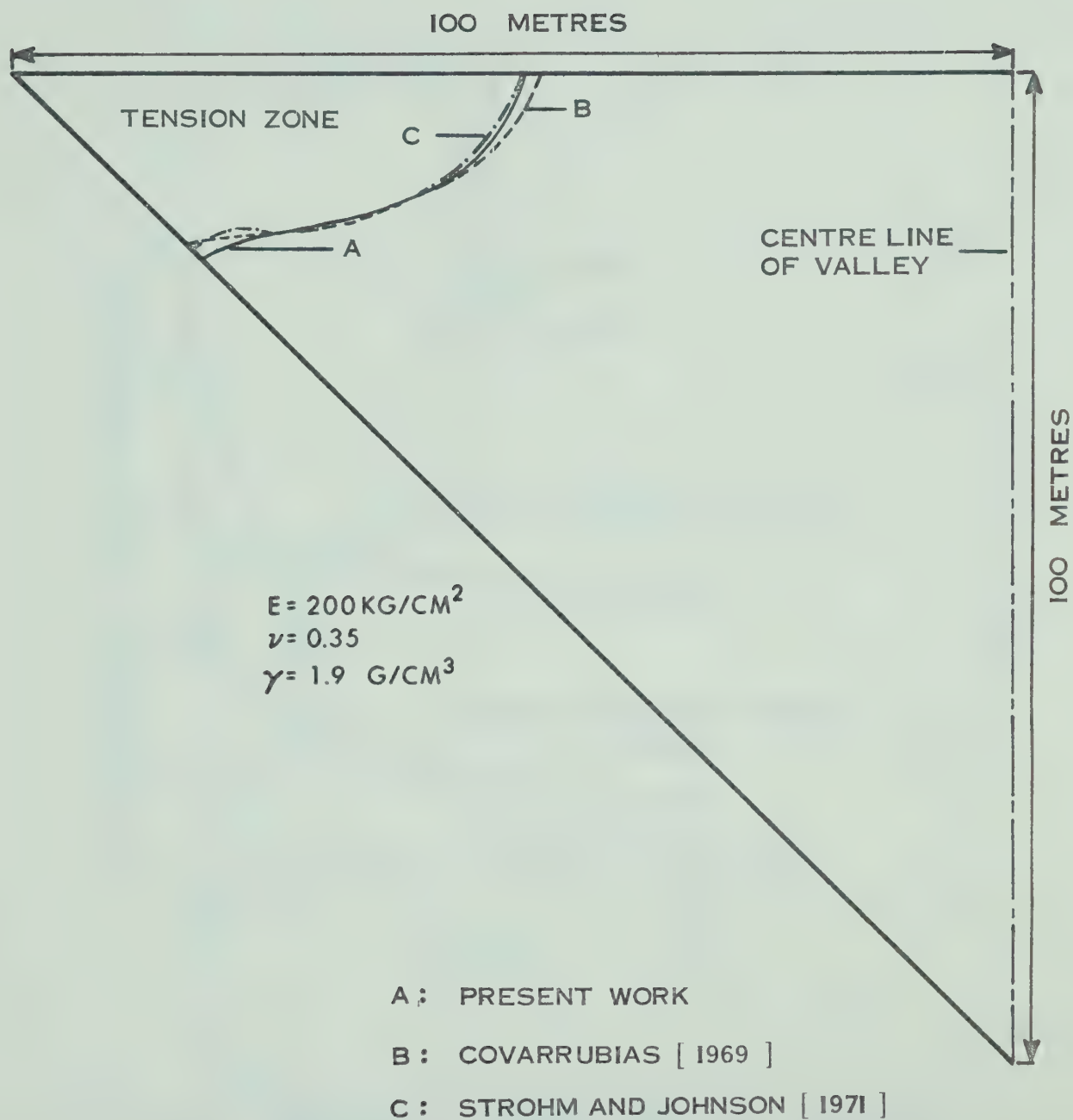


FIG. 4.4 COMPARISON OF TENSION ZONES COMPUTED BY SINGLE STEP TWO DIMENSIONAL LINEAR ELASTIC ANALYSES

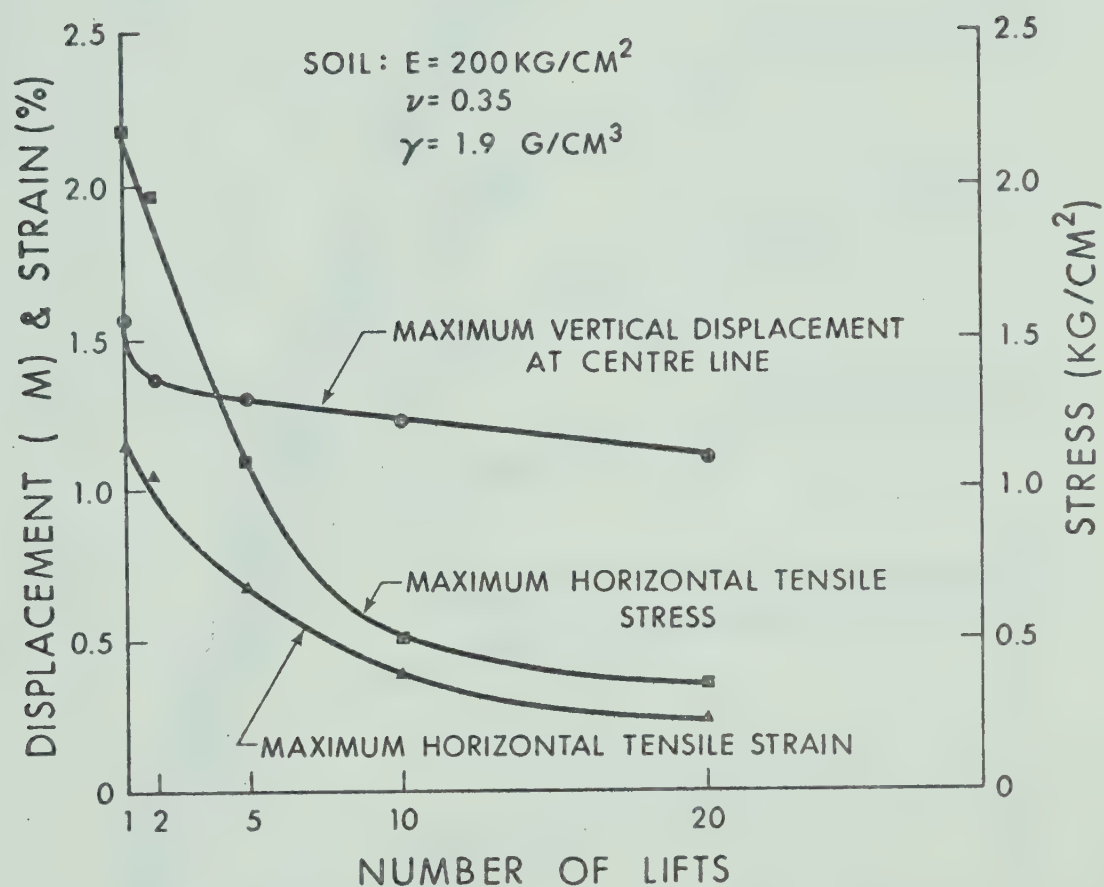


FIG. 4.5 EFFECT OF NUMBER OF LIFTS ON MAXIMUM HORIZONTAL STRESS, STRAIN AND VERTICAL DISPLACEMENT OF TWO DIMENSIONAL SECTION

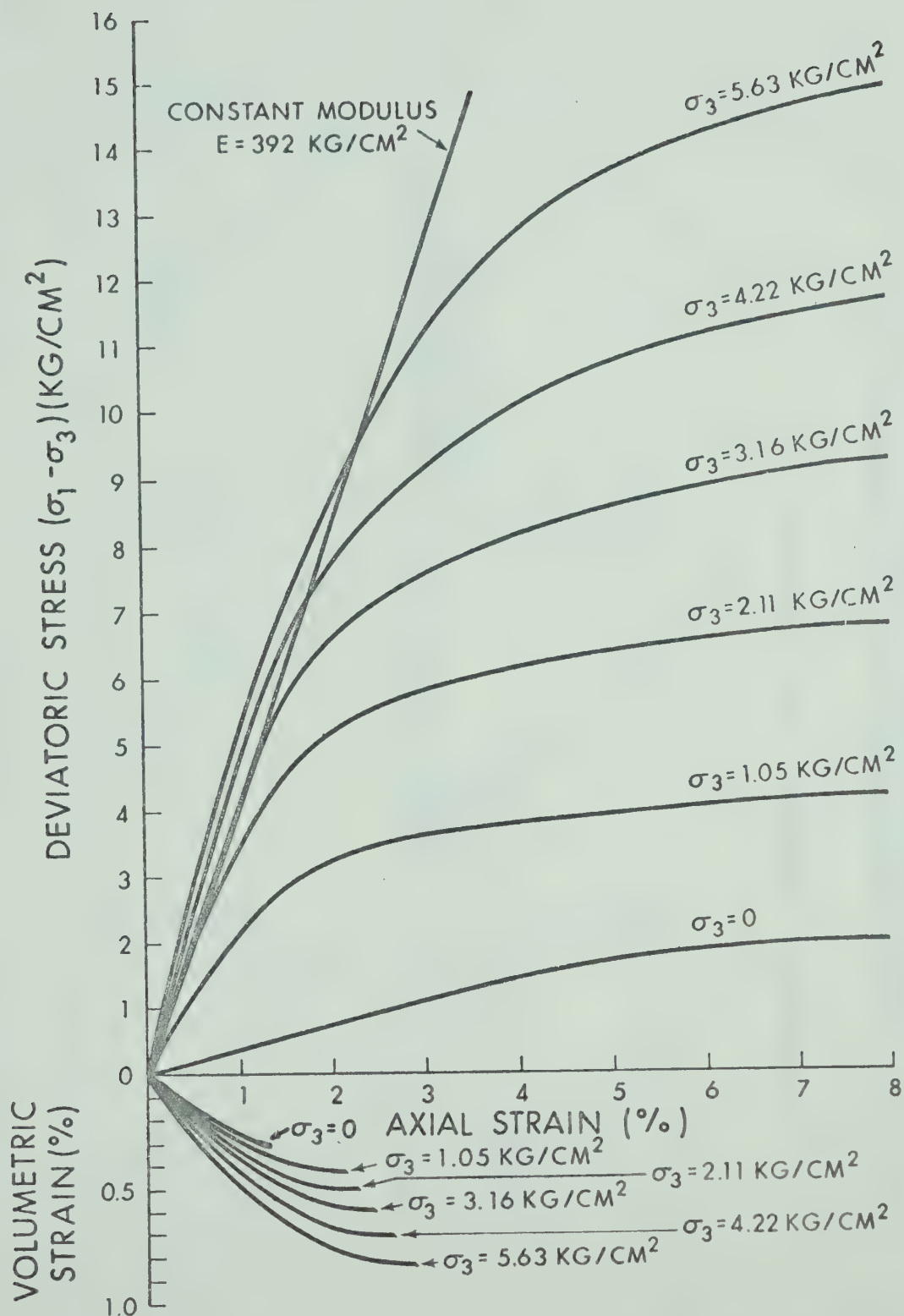


FIG. 4.6 STRESS STRAIN RELATIONSHIPS FOR SILTY SAND

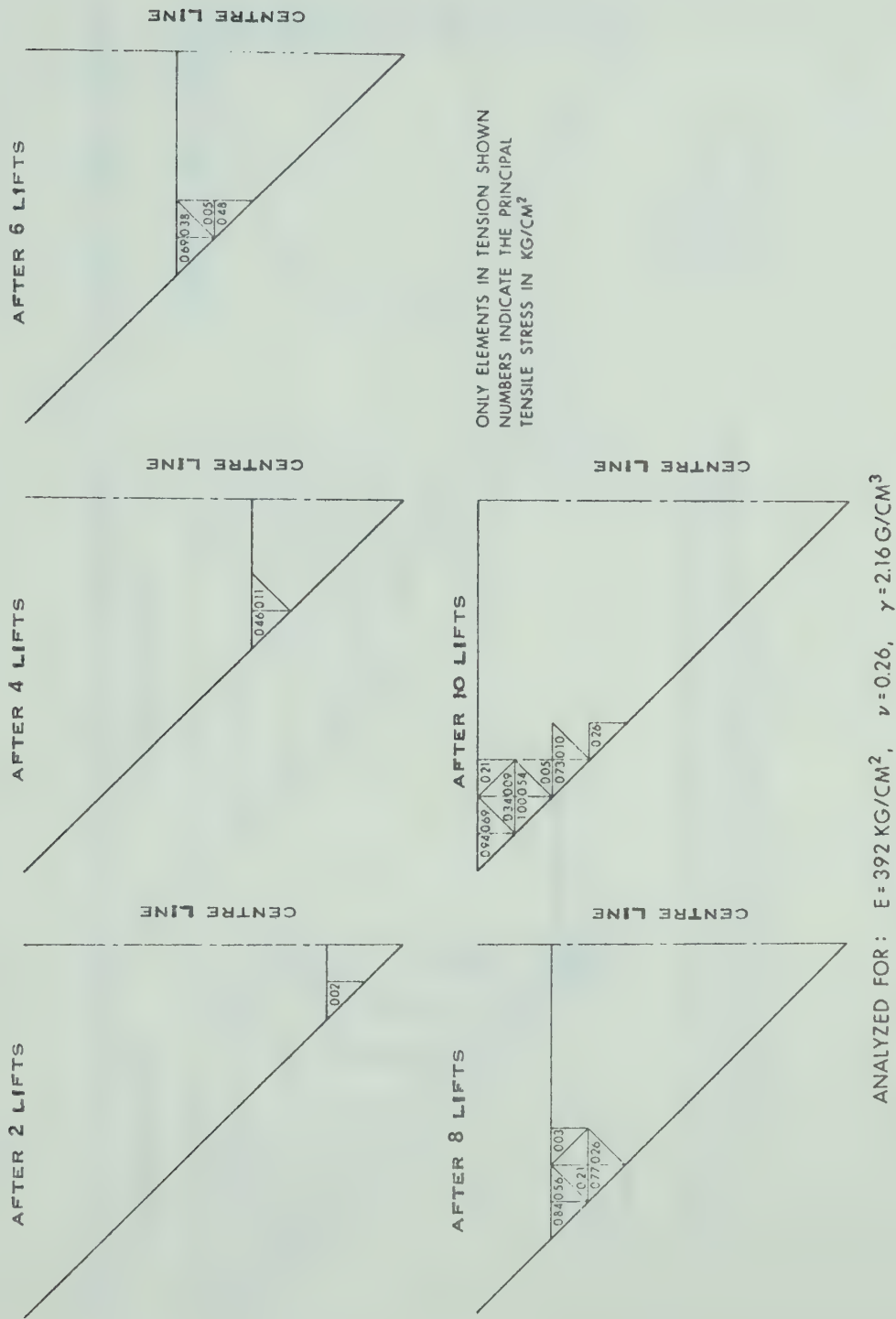


FIG. 4.7 TENSILE ZONES DEVELOPED FOR LINEAR ANALYSIS
AFTER CERTAIN NUMBER OF LIFTS

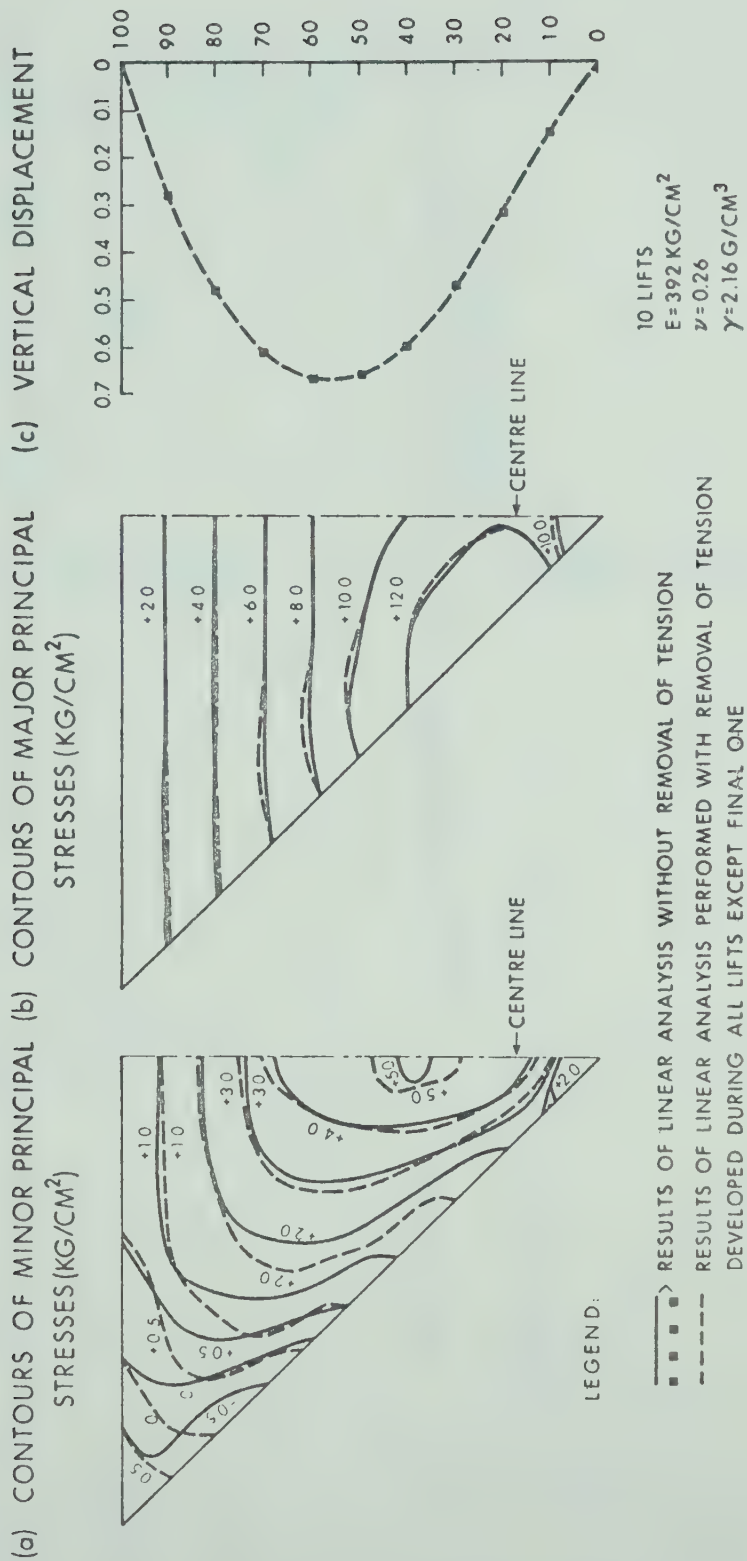


FIG. 4.8 COMPARISON OF LINEAR ANALYSIS WITH AND WITHOUT REMOVAL OF TENSION

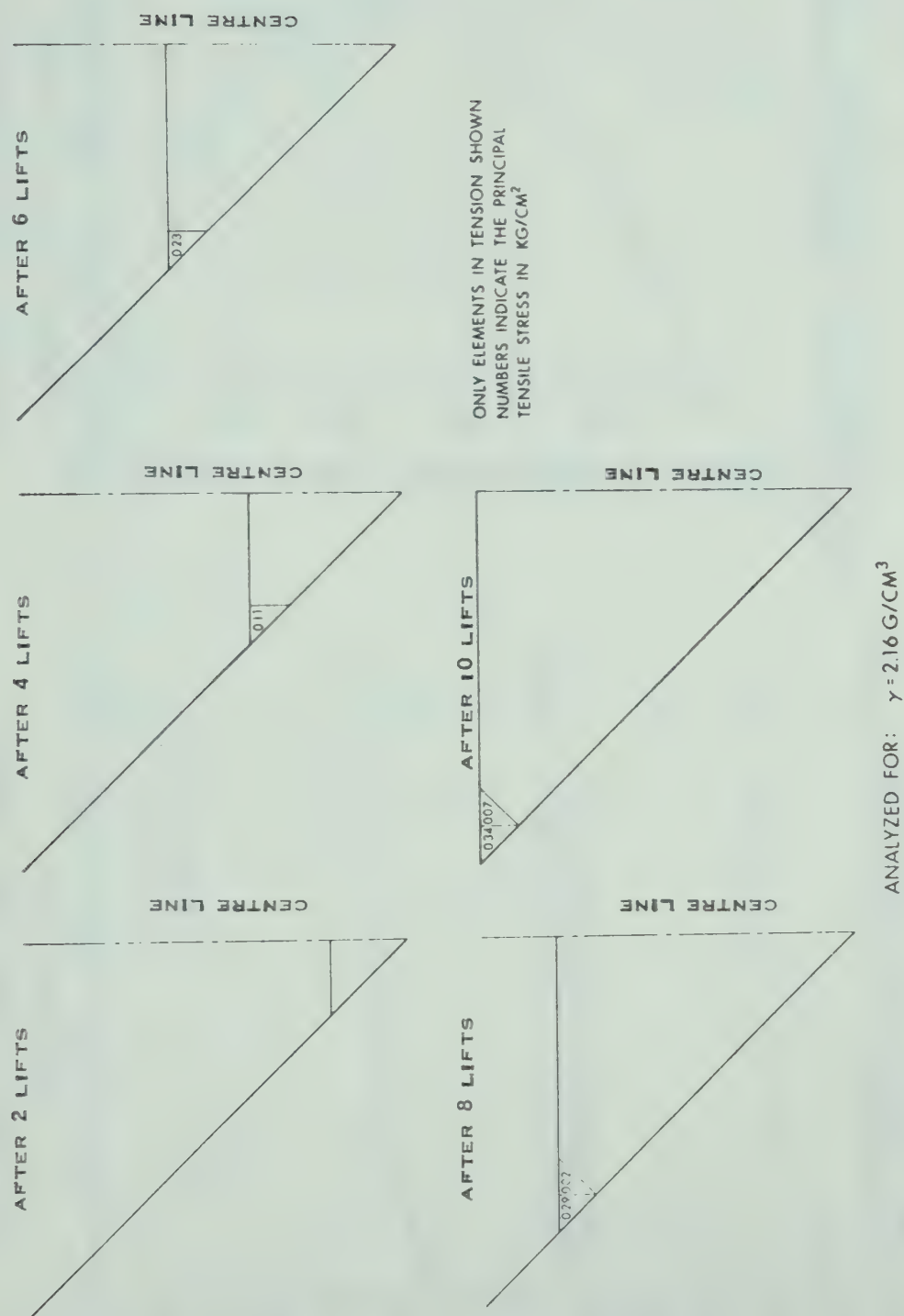


FIG. 4.9 TENSILE ZONES DEVELOPED FOR NONLINEAR ANALYSIS
AFTER CERTAIN NUMBER OF LIFTS

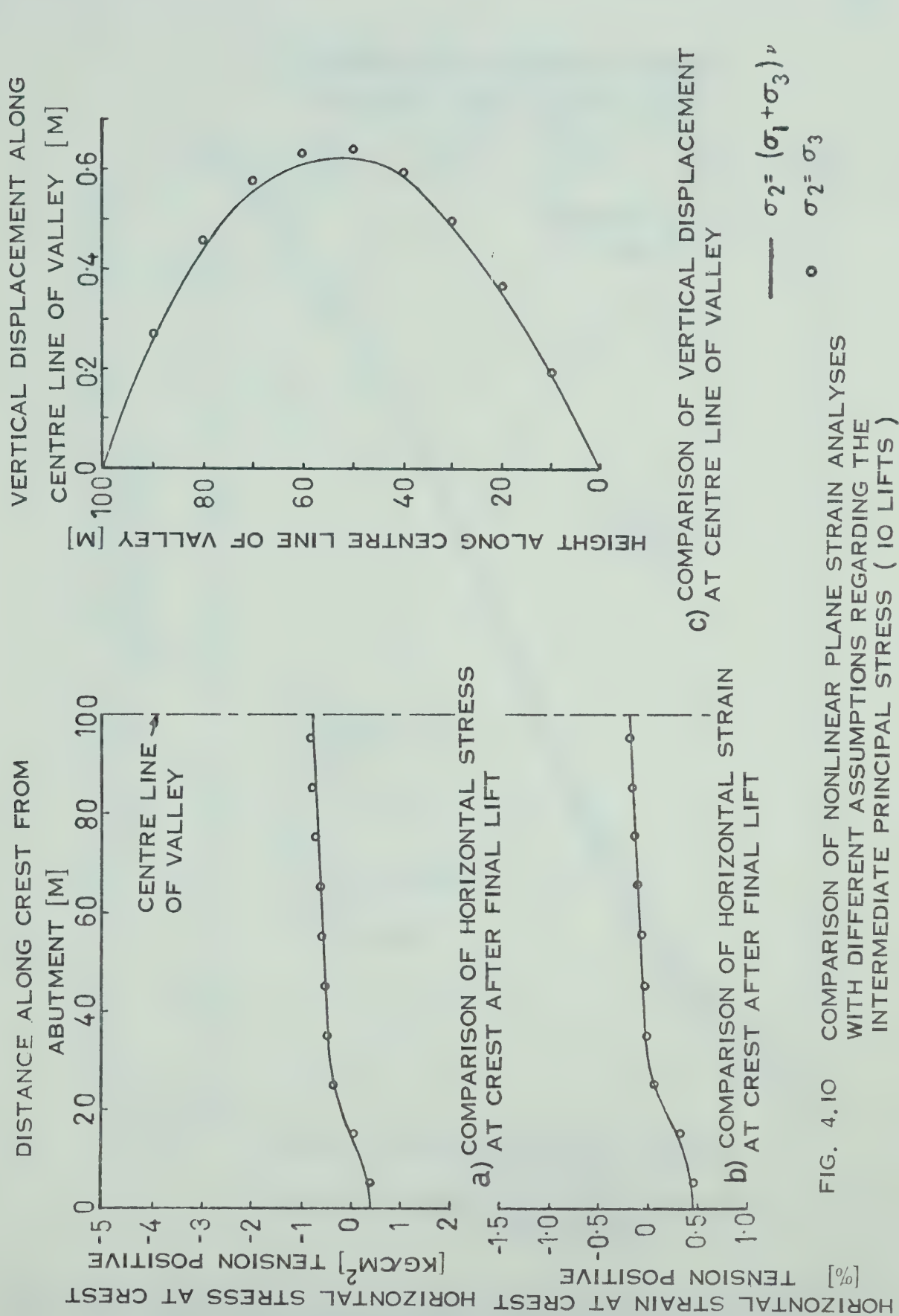


FIG. 4.10 COMPARISON OF NONLINEAR PLANE STRAIN ANALYSES WITH DIFFERENT ASSUMPTIONS REGARDING THE INTERMEDIATE PRINCIPAL STRESS (10 LIFTS)

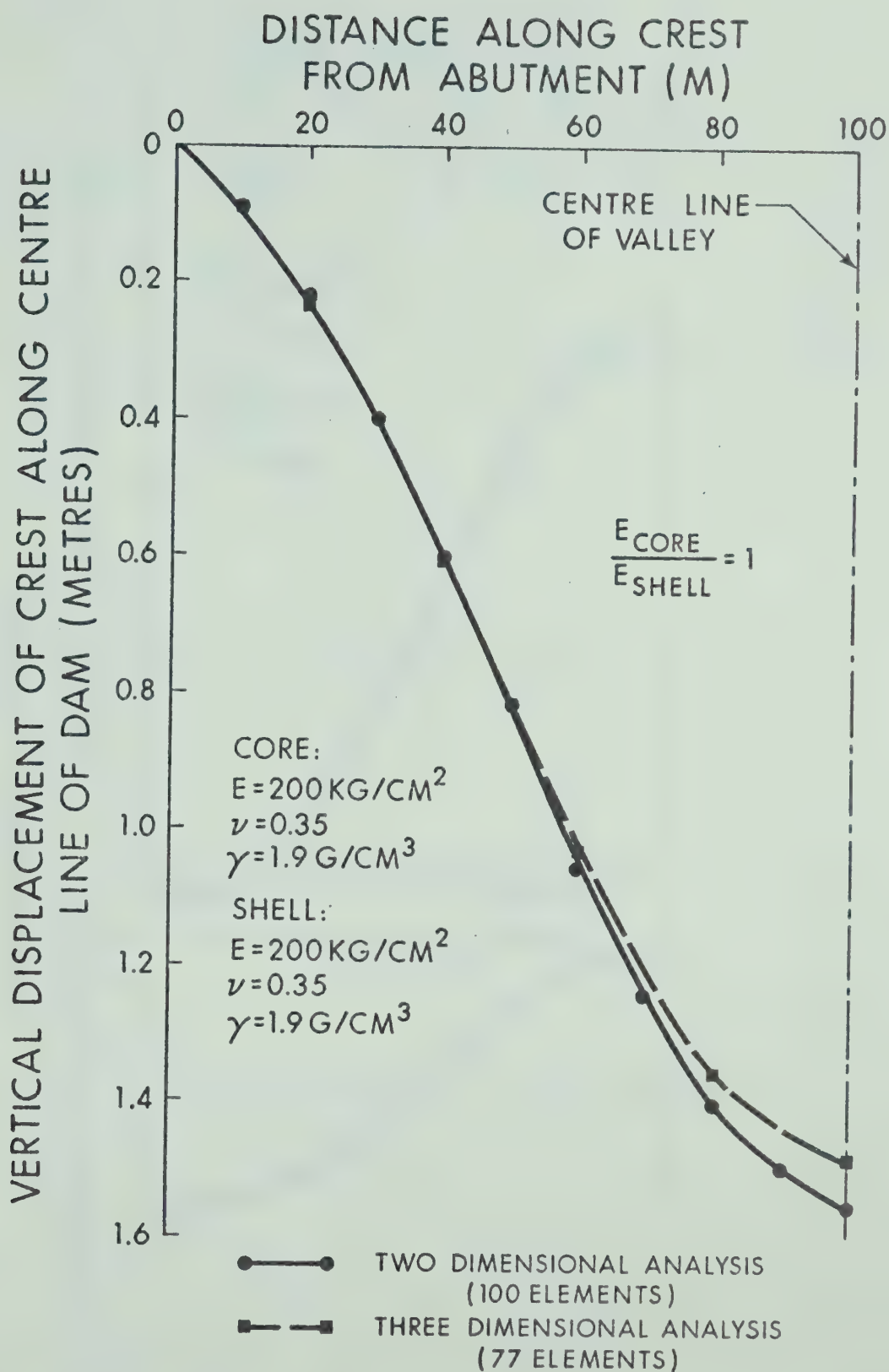


FIG. 4.II VERTICAL DISPLACEMENT ALONG CREST FOR TWO AND THREE DIMENSIONAL ANALYSIS, SINGLE LIFT

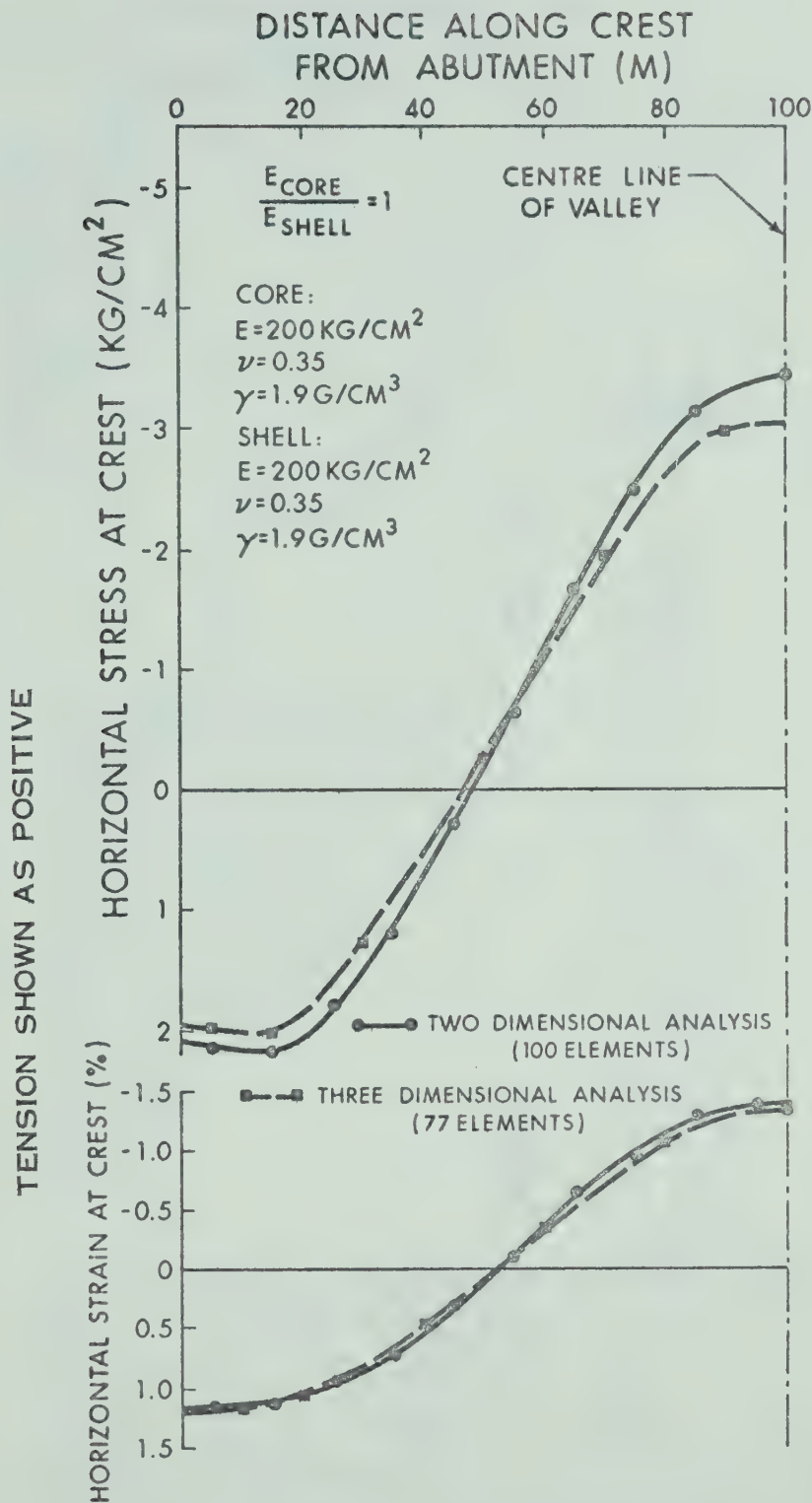


FIG. 4.12 HORIZONTAL STRESS AND STRAIN ALONG CREST
FOR TWO AND THREE DIMENSIONAL ANALYSES
IN SINGLE LIFT

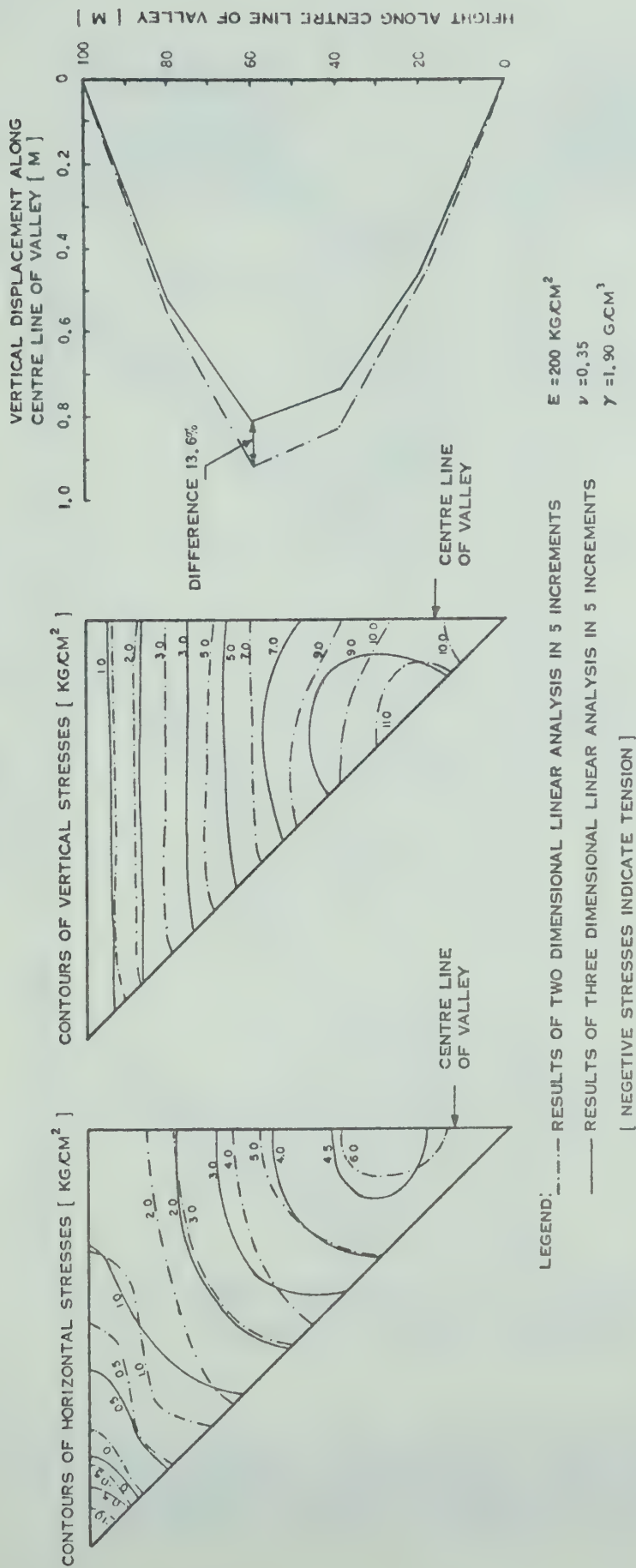


FIG. 4.13 COMPARISON OF RESULTS OF TWO AND THREE DIMENSIONAL INCREMENTAL LINEAR ANALYSES PERFORMED ON A HOMOGENEOUS DAM [5 INCREMENTS]

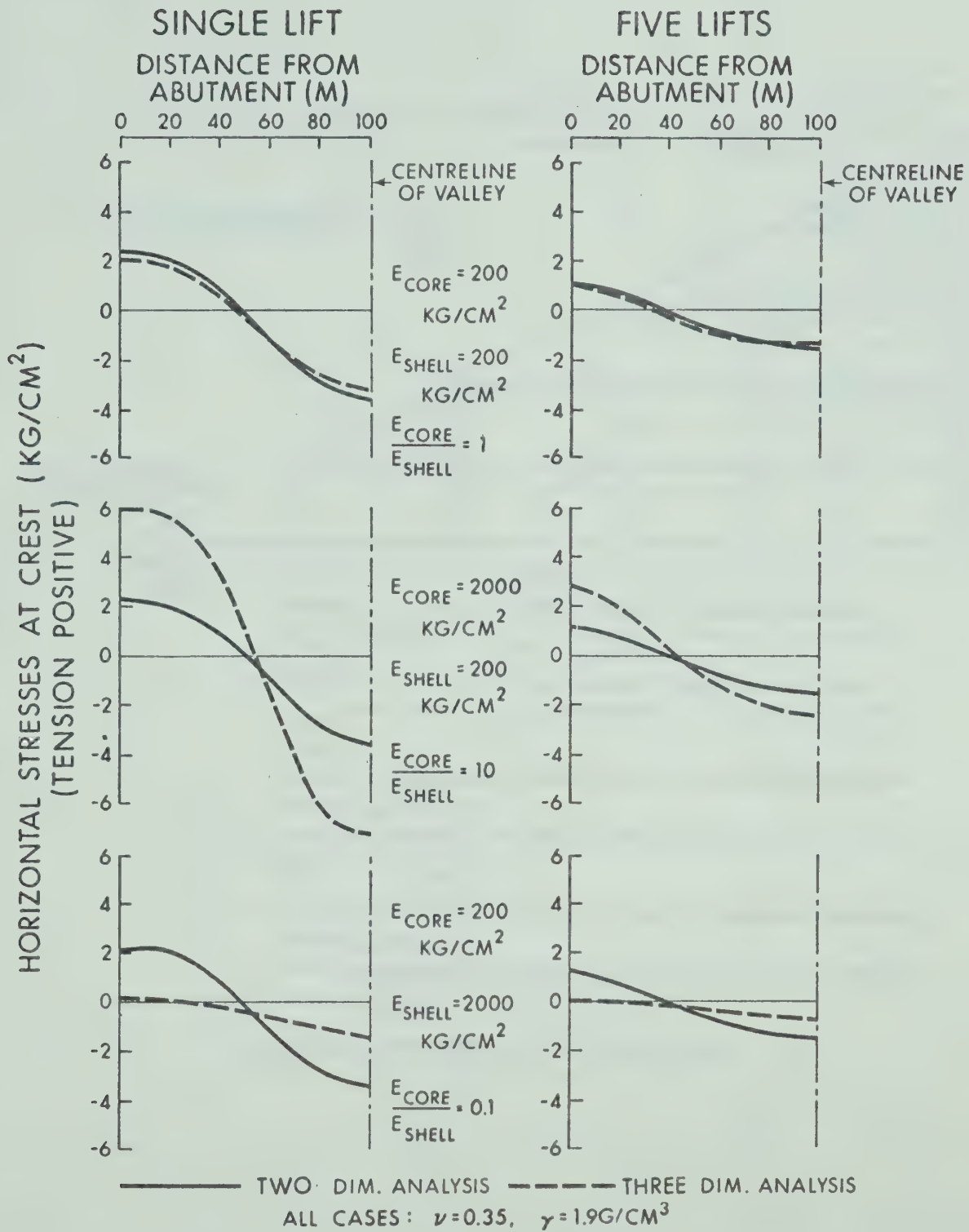


FIG. 4.14 COMPARISON OF HORIZONTAL STRESSES ALONG CREST FOR TWO AND THREE DIMENSIONAL ANALYSES AT DIFFERENT RATIO OF MODULI OF CORE TO SHELL

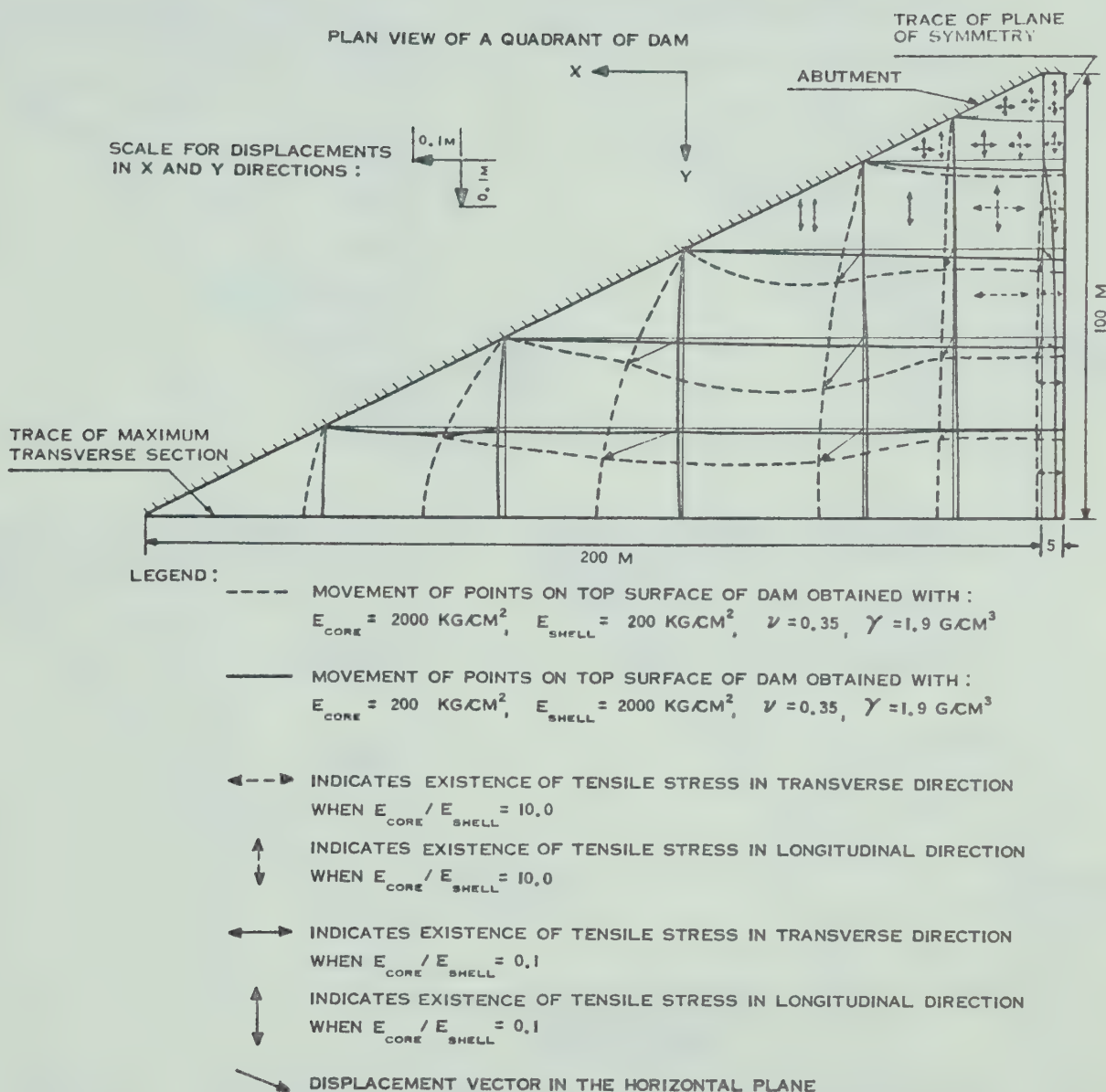


FIG. 4.15

COMPARISON OF DISPLACEMENT PATTERN AND DEVELOPMENT OF TENSILE CRACKS ON THE SURFACE OF DAM FOR MODULAR RATIOS OF CORE TO SHELL EQUAL TO 10 AND 0.1. RESULTS BY THREE DIMENSIONAL LINEAR ANALYSES IN 5 INCREMENTS

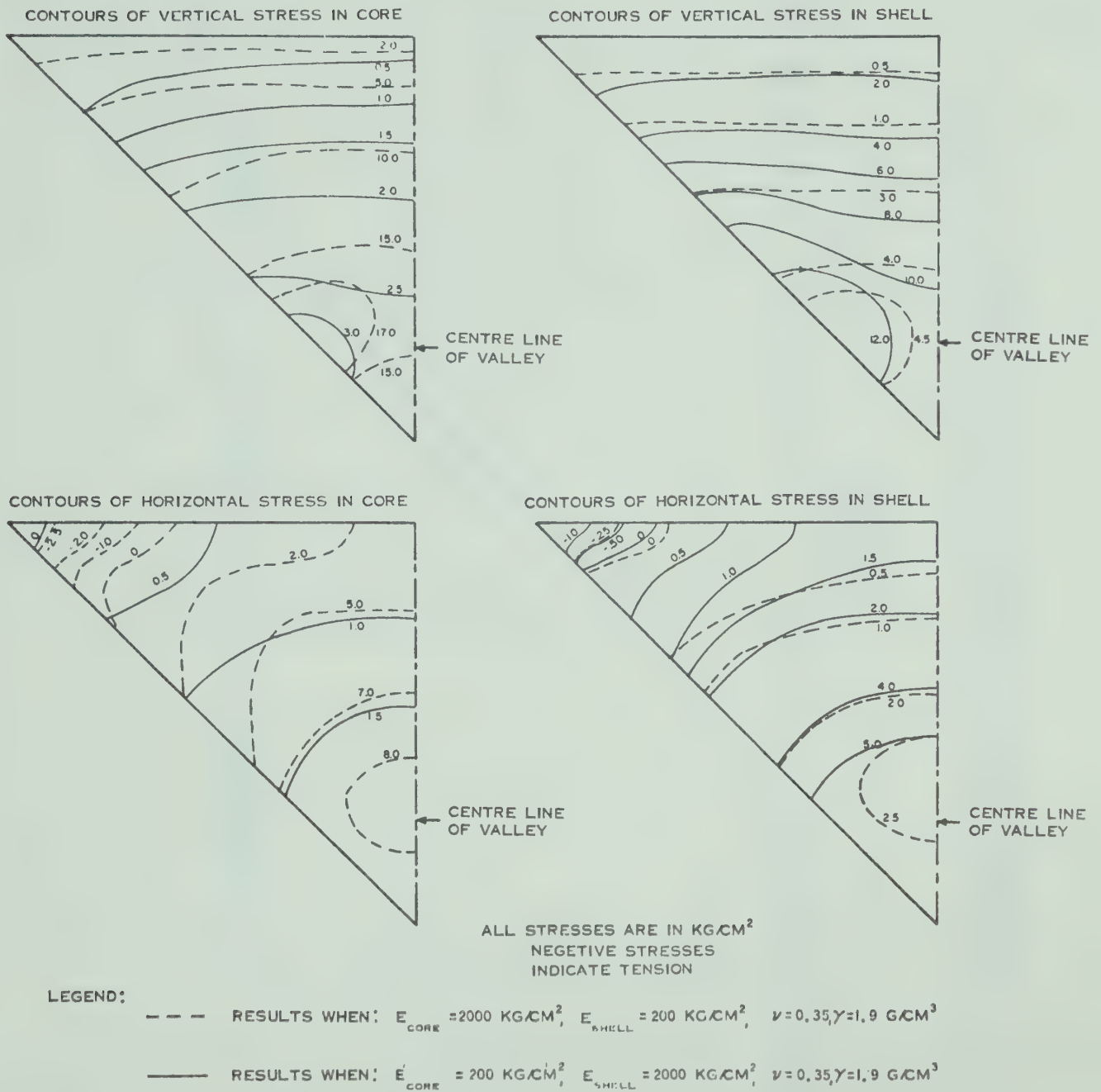


FIG. 4.16 COMPARISON OF STRESSES IN CORE AND SHELL CLOSE TO THE MAXIMUM LONGITUDINAL SECTION OF DAM FOR MODULAR RATIOS OF CORE TO SHELL EQUAL TO 10 AND 0.1. RESULTS BY THREE DIMENSIONAL LINEAR ANALYSES IN 5 INCREMENTS

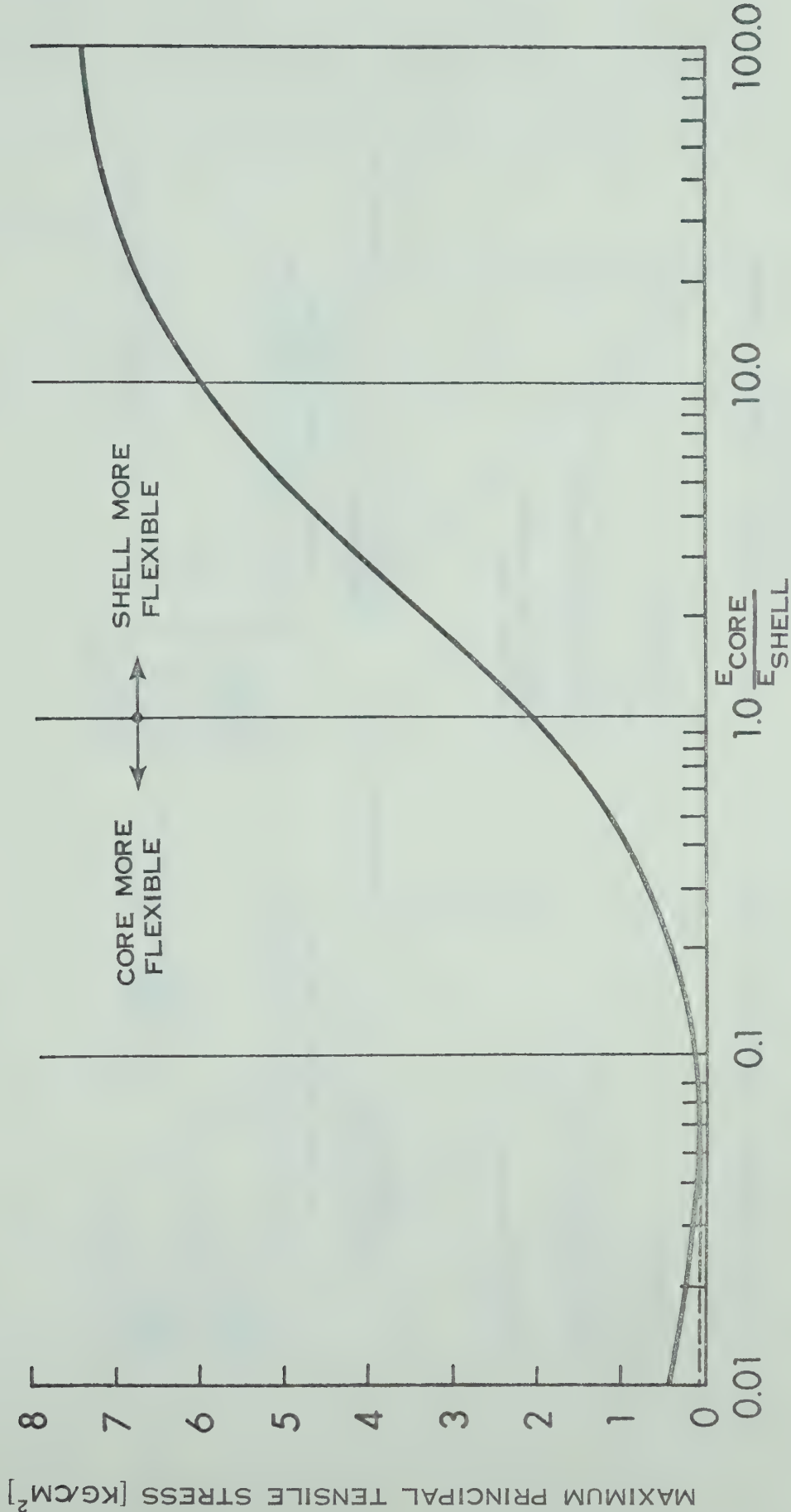


FIG. 4.17 COMPARISON OF MAXIMUM TENSILE STRESSES IN CORE FOR DIFFERENT RATIOS OF MODULI OF CORE TO SHELL

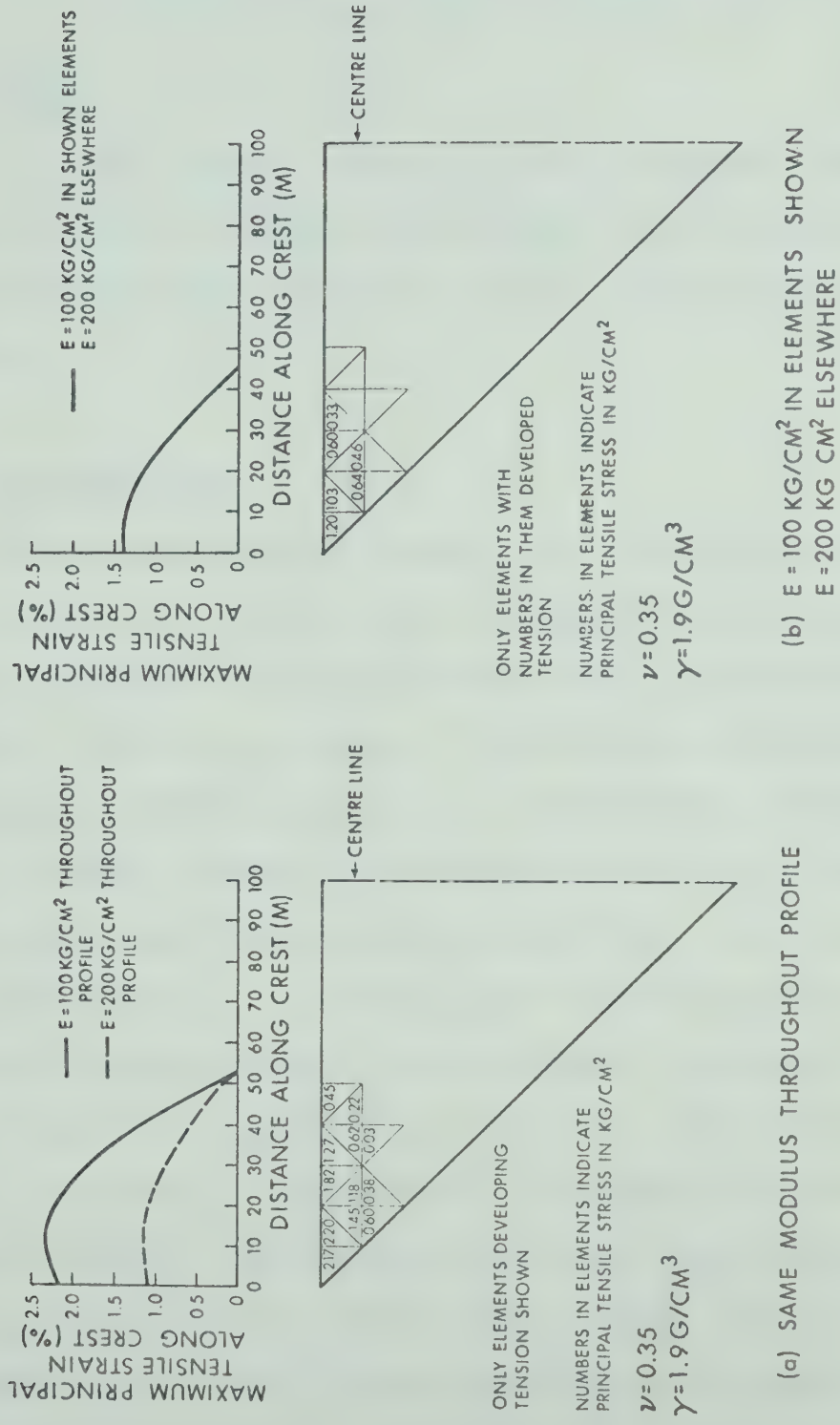


FIG. 4.18 EFFECT OF THE NONHOMOGENEITY OF CORE ON THE REDUCTION OF TENSILE ZONES

CHAPTER V

ANALYSIS OF CRACKING AT DUNCAN DAM

5.1 Scope

In this chapter the analytical procedures developed in the previous chapters are applied to the analysis of the cracking of the Duncan Dam to assess their practical application.

5.2 Introduction

As pointed out in Chapter III, any analytical procedure that attempts to model a real structure mathematically in order to predict its behaviour can only yield approximate answers. This is a result of the various simplifications introduced into the analysis in representing factors such as the complex stress-strain behaviour of soils, geometry of the structure, the boundary conditions, and the history of construction. In addition, the laboratory stress-strain data used in the analysis can sometimes introduce an appreciable error in the prediction of in-situ behaviour (Alberro, 1972; Low, 1972). These factors introduce an unknown error into the model. The magnitude of this error can be assessed by comparison with an actual case history. Hence studies of the behaviour of well documented earth structures are of utmost importance for the evaluation of analytical procedures based on the finite element method (Chang and Duncan, 1970).

The recorded behaviour of the Duncan Dam in Southern British Columbia, Canada has proved to be particularly valuable for verifying the usefulness of the proposed procedures in the analysis of cracking of earth dams.

5.3 History of Cracking at Duncan Dam

5.3.1 Salient Features

A detailed account of cracking at Duncan Dam and the remedial measures taken for its successful completion are given by Gordon and Duguid (1970). Only the features relevant to the present analysis are described here.

Duncan Dam is an earthfill dam built during 1964-1967 on the Duncan River in British Columbia, Canada. The dam makes it possible to increase the power generation at downstream plants and also provides a measure for flood control.

The dam is about 120 feet high and 2500 feet long with an upstream sloping core. It was built across a valley, underlain by sediments about 1240 feet deep infilling a canyon. The stratigraphy of the foundation, shown in Fig. 5.1, is rather irregular with deposits ranging from the relatively incompressible gravel to silty clay layers, possessing considerable compressibility. The poor foundation conditions and previous experiments with dams on deep alluvial deposits dictated the use of conservatively flat side slopes. A typical cross-section of the dam is shown in Fig. 5.2. The designers of the dam anticipated large settlements and made

provisions in the design and construction procedures to avoid excessive cracking (Gordon and Dugid, 1970). The main steps taken were the delayed placement of core-abutment ties, placement of overwet till core (1% to 2% greater than the optimum water content) and the self healing zoned section of the dam. Also the dam has been profusely instrumented with settlement gauges and piezometers both in longitudinal and transverse directions. The locations of the settlement gauges in plan view are indicated in Fig. 5.3. The positions of centrally located gauges (numbers 9 to 18) are shown in Fig. 5.1.

5.3.2 Observed Differential Settlement Cracks

The settlement records for the period from May, 1965 to October, 1966, taken from the construction reports, are plotted in Fig. 5.4. Each settlement line in Fig. 5.4 corresponds to the particular date indicated, and the corresponding level of fill is shown on the longitudinal section in Fig. 5.1. The settlement records clearly indicate a significant shift of the maximum settlement towards the left or east abutment. Although the maximum settlement agreed with the anticipated settlement in magnitude, its shift towards the left side was rather unexpected. These large differential movements resulted in transverse cracks in an area located on the upstream side of the dam and between the left abutment and settlement gauge No. 18. The extent of the area of visible cracking shown in Figs. 5.1 and 5.3 is between Sections 2 and 3 with the centre of the area located approximately 440 feet along

the crest from the left abutment.

5.3.3 Sequence of Appearance of Cracks

The cracks did not all appear simultaneously and at the same level of construction of dam. The sequence of cracking is illustrated in Fig. 5.5. Cracking was first observed on August 14, 1966 on the upstream slope of the dam, about 210 feet from the centre line. Within a week the number of cracks increased with new ones appearing closer to the centre line of the dam, as indicated between Sections A and C in Fig. 5.5. It is of interest to note that during this particular week (August 15-22) the increment of settlement recorded by gauges Nos. 16 and 17 was about half a foot. As the settlement of the foundation continued and with the addition of some fill subsequent to August 14, 1966, further cracks appeared in the same zone in October, 1966. This time the cracking was located between Sections B and C as shown in Fig. 5.5. The approximate zones of cracks, as revealed by exploratory trenches and test shafts, and their sequence of development is shown in Fig. 5.6 along with the settlement of the base of dam in the transverse direction on August 14, 1966 and on October 28, 1966. The cracks revealed by the test shafts varied from one to three inches in width and extended downwards approximately to El. 1810.00, intercepting many large voids of about 10 inches in width.

Gordon and Dugid (1970) have described the measures subsequently adopted to control the cracking. These measures

essentially consisted of preloading the area to the west of the cracked zone with a surcharge of 260,000 cubic yards of material to induce as much settlement as possible ahead of placing core and core-abutment tie, sluicing the gravel shell material with water to close all the previous cracks, increasing the capacity of gravel blanket and drains on the downstream side of the dam to handle more leakage, and changing the section of the dam in this area. The impervious core was brought closer to the upstream face where it could be placed as late as possible. An additional benefit of the surface core was its better accessibility for reworking any cracked area that might result from the settlement continuing at a substantial but decreasing rate for a number of years. The core material was made more plastic by mixing it with about 6% bentonite. This increased the plasticity index of core material from 4 to approximately 20. The downstream slope of the upper fill was flattened from 2:1 to 3:1 to increase the slope stability as a precaution against the saturation due to leakage through possible future cracks. The adoption of these measures and careful inspection since construction has resulted in satisfactory operation without any leakage.

5.4 Analysis of Cracking

The analysis presented here is concerned only with the period up to the end of October, 1966. The core material of Duncan Dam is a glacial till with the following characteristics (Gordon and Dugid, 1970):

Liquid limit	17.6%
Plasticity index	4.3
Proctor optimum moisture content	9.8%
Proctor maximum dry density	128 lbs./cft.

The grain size distribution is shown in Fig. 5.11. There is a considerable similarity between Duncan Till and Mica Till (Section 2.8.1). From the tensile studies conducted on Mica Till it can be concluded that a low plastic till such as Duncan Till will have a negligible tensile strength especially at water contents wet of optimum. The low tensile strength of the core material of Duncan Dam suggests the reasonable assumption that the cracks have appeared when one of the principal stresses became tensile. The problem of assessing the suitability of the finite element method for the prediction of cracking is one of calculating the zones of tension and comparing them with the zones of cracking observed in the actual structure.

A three dimensional finite element analysis has been used as it is more relevant in this present case than a two dimensional analysis. Nevertheless for the sake of comparison a two dimensional analysis has also been performed. During construction, the deformations and stresses in a fill dam result from the compression of the foundation and the gravity loading of the embankment itself. The effect of foundation settlement, which was the dominating factor in the case of Duncan Dam has been introduced into the analysis by specifying the incremental settlements derived from Fig.

5.4 at the base of the dam for various levels of construction as shown in Fig. 5.1. This represents a boundary condition of known displacements. The gravity loading was introduced by specifying the self-weight of only the newly added material of the fill. The analysis was performed in 5 lifts as shown in Fig. 5.1 with each lift analyzed twice. The three dimensional finite element idealization used is shown in Fig. 5.1 in the longitudinal direction and in Fig. 5.7 in the transverse direction. A total of 310 elements and 426 nodes were used. The material idealization consisting of core, pervious, semi-pervious, and common pervious types is also shown in Fig. 5.7.

The non-linear stress-strain relationships were introduced into the analysis in digital form as described in Chapter III. The triaxial test data used in the analysis for the materials are shown in Figs. 5.8, 5.9 and 5.10. Consolidated undrained test results were used for the impervious and the semi-pervious materials because it was thought that such data would be the most representative of the field conditions. These are somewhat in between the two extreme limits of unconsolidated-undrained and consolidated-drained conditions. This is partly because of the rapid loading during the embankment construction and partly due to the low pore pressures generally developed in the core and the semi-pervious zone. However it is recognized that the approach can only be approximate as the partial consolidation that occurs in the field cannot be represented accurately by the

conventional consolidated undrained tests.

The stress-strain data used for core and semi-pervious zone in the analysis were derived from the available tri-axial test results of Duncan Dam materials obtained prior to the construction of the dam. These tests were performed on samples comprising materials below 3/4" size. The test specimens were prepared in a 4" diameter by 8" high, 3 part split mould. Soil was compacted in five equal layers of approximately 1.7" thicknesses. Twenty-five blows of a standard 5.5 lb. hammer with a 12" drop were applied to each layer. Tests were performed on samples prepared at optimum water content and 3% greater than optimum. Since the placement water content was approximately at 1% to 2% greater than the optimum the stress-strain data used in the analysis was derived from the available test data by averaging the stress-strain relationships. Stress-strain data were not available for the pervious and the common-pervious material used in Duncan Dam, therefore drained triaxial test results of a gravelly material having similar gradations as at Duncan was used in the present analysis. The stress-strain relationships (Figs. 5.9 and 5.10) used in the analysis for the pervious and the common-pervious materials were derived from the available extensive triaxial test data obtained in connection with the design of Mica Dam for different gradations of sand and gravel. The test results were partly reported by Skermer and Hillis (1970). The tests were performed on 6" x 12" samples, at different cell pressures ranging up to 450 psi.

The corresponding gradations of pervious and common pervious material, for which the stress-strain relationships were derived, are shown in Fig. 5.11. The average gradation curves of pervious, semi-pervious and core material of the Duncan Dam are also shown in Fig. 5.11.

As discussed in Chapter III Poisson's ratio was limited to a maximum value of 0.49. "No tension" analysis was not performed for the reasons given in Section 4.10. The calculation of the elastic parameters in terms of K and G was done using the procedure described in Section 3.9.

The two dimensional analysis was performed assuming plane strain conditions along the central longitudinal section, the idealization of which is shown in Fig. 5.14. The analysis used 235 nodes and 388 constant strain triangular elements. The number of lifts and the construction levels were kept the same as for the three dimensional analysis (Fig. 5.1).

5.5 Results of Analyses

5.5.1 Three Dimensional Analysis

The aim of the analysis was to compare the locations of the tensile stresses computed for the idealized analytical model of the dam with the location of the cracks observed in the real structure. The zone of cracking, as noted earlier, was confined between transverse sections 2 and 3 (Figs. 5.3 and 5.5). It is convenient to deal with the development of

the cracks between these sections by considering an intermediate section located at a distance of 440 feet from the left abutment (Fig. 5.5). This section is located approximately in the centre of the cracked area. To facilitate the comparison of progressive development of cracks along the transverse direction and height of the dam, vertical lines I, II, III and IV in Figs. 5.5 and 5.6 are considered. These are the vertical lines at which the sections A, B, C and D intersect the intermediate section, referred to above.

The distributions of minimum principal element stresses and strains along the vertical lines I, II, III and IV have been computed by three dimensional analysis for two different time instances, August 14 and October 28, which correspond to two different levels of filling and settlement of foundation. The results of the present three dimensional analysis along with those of a previous three dimensional analysis (Eisenstein et al., 1972) are shown in Fig. 5.12. The previous analysis differs from the present one only in the following respects:

- (1) Because of the limitation on the number of material types that could be handled by the previous computer program only three types of material namely the pervious, core, and semi-pervious materials were considered in the previous analysis. The common-pervious material considered in the present analysis was assumed to be the same as the semi-pervious material. The zone represented by the common-pervious material of the present analysis

is in general stiffer than the corresponding zone of the previous analysis.

- (2) The elastic moduli were calculated directly from the conventional plots of triaxial test data, instead of the stress invariant approach, used in the present analysis. The reference confining stress was assumed to be average of the minor and intermediate principal stresses that occur in an element. Whenever a principal stress assumed a negative value it was considered to be zero in calculating the confining stress needed for the derivation of moduli. When both the minor and intermediate principal stresses were negative, the confining stress was assumed to be zero.

The results by the previous and the present analysis are discussed below.

On August 14, 1966 the first cracks appeared in the area upstream of vertical line I and in its vicinity. The analytical results obtained for this stage show that the only tensile stress found is along the vertical line I and above an elevation of about 1830 feet. All other parts of the dam remain in compression at this time with regard to stresses, although principal tensile strains are common. Within a week, more cracks developed extending towards the centre line. However no analysis has been performed for conditions at this date (August 22, 1966).

In October, 1966 a new distinct crack was observed within the same transverse section but now extending between

sections B and C (Fig. 5.5). The stresses calculated along vertical lines II and III clearly indicate tension between sections B and C for the conditions existing at the end of October. Tension is not indicated along vertical line IV and no cracks were detected in its vicinity. Therefore, the calculations indicate reasonably well the sequence of cracking along the transverse section. It is interesting to note that the previous and present analysis, although introducing slightly different elastic parameters into the computations, lead to the same conclusions as regards the sequence of cracking. This indicates that the most dominant factor in the analysis of cracking at Duncan Dam is the effect of the settlement of the foundation.

In order to verify the location of the cracks in the longitudinal direction, the distribution of minimum principal stresses and strains along centre line and section B are shown in Fig. 5.13. The stresses and strains are plotted for surface elements for two dates namely, August 14, 1966 and October 28, 1966. Since these stresses and strains obtained by the previous and the present analyses are almost the same (Fig. 5.12), the results of only the present analysis are shown in Fig. 5.13. From this figure, it can be seen that the analysis indicates the location of the cracks along the longitudinal section of the dam with reasonable accuracy. Some tensile stresses are also indicated adjacent to the right abutment and, indeed, limited cracking was observed in this area as well.

5.5.2 Two Dimensional Analysis

The distributions of minimum principal stress and strain along the central longitudinal section (Fig. 5.14) for two dimensional analysis are shown in Fig. 5.15. It can be seen that the location of the transverse section along which cracks appeared is predicted properly by the two dimensional analysis. However, the sequence of cracking and the distribution of cracks along the transverse section cannot be predicted as a plane strain condition is not satisfied on sections A, B and D (Fig. 5.5).

5.6 Summary

Duncan Dam, constructed on an extremely compressible foundation, was subjected to severe cracking due to large differential foundation settlement. Accurate and detailed observations of settlements and cracks at Duncan Dam constitute an important case history. Advantage of this was taken to test the usefulness of finite element analysis for assessing the cracking potential of earth structures.

The stresses and strains in Duncan Dam were computed using a three dimensional finite element program including the realistic boundary conditions, the non-linear stress-strain relationships and the actual construction step sequence. Two dimensional finite element analysis has also been performed assuming a plane strain condition along the central longitudinal section. The results of the three dimensional analysis predict reasonably well both the location and sequ-

ence of development of the cracks. The two dimensional analysis predicts reasonably well the location of cracks along the longitudinal section, although the sequence of development of cracks along the transverse section cannot be predicted. The agreement found between analysis and observation is noteworthy since it is unlikely that the stress-strain relationships used in the analysis are wholly representative of the in-situ behaviour. One might anticipate that sometimes the agreement between the observed and predicted displacements will be less impressive compared to the agreement between stresses. This is due to the fact that displacements are, in general, more sensitive to the variation of elastic parameters used in the analysis than are stresses. From the results of the finite element analyses performed on Duncan Dam, it may be concluded that the finite element method has a considerable potential in the analysis of cracking of earth dams. Reasonable predictions regarding the cracking of earth dams appear to be possible even with the use of simple, isotropic elastic theory in the analysis.

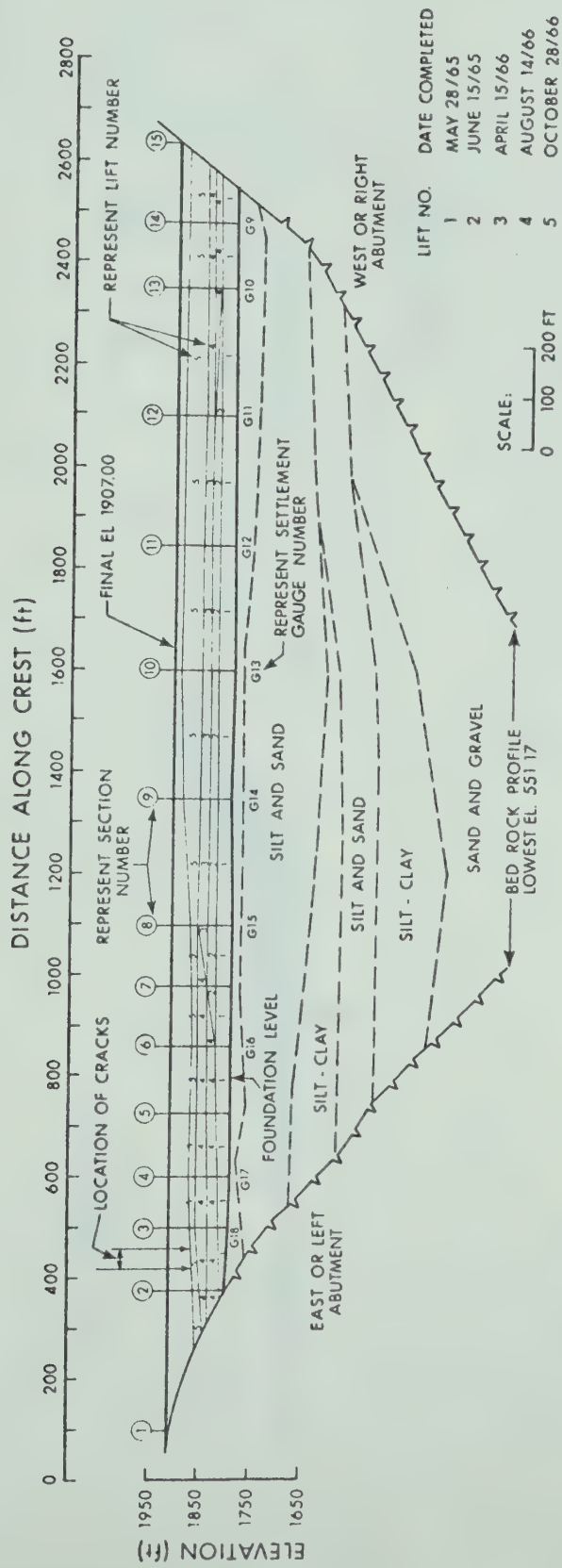


FIG. 5.1 LONGITUDINAL SECTION OF DUNCAN DAM SHOWING CONSTRUCTION SEQUENCE AND LOCATION OF CRACKS

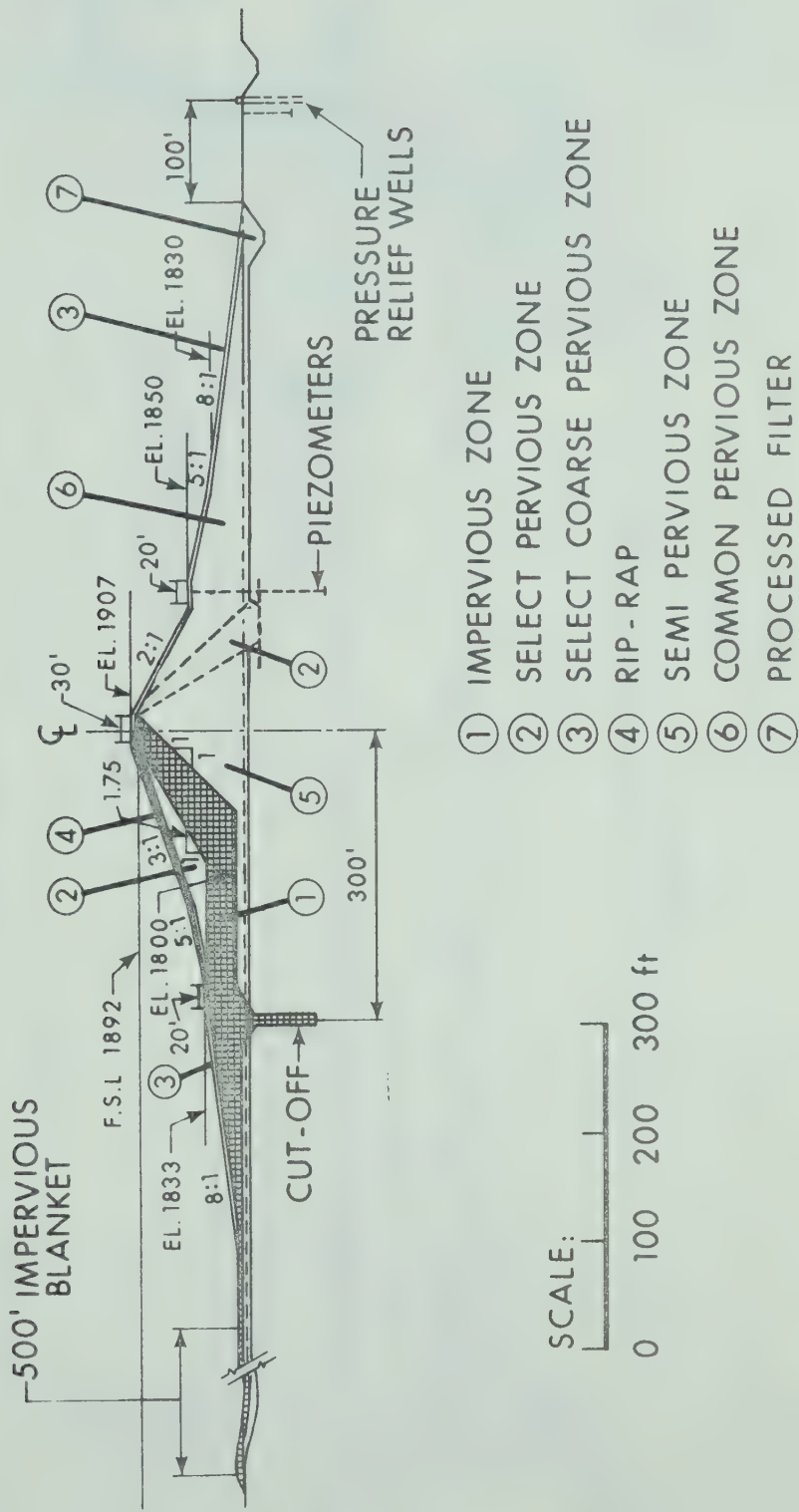


FIG. 5.2 A TYPICAL CROSS SECTION OF DUNCAN DAM [AFTER GORDON AND DUGUID, 1970]

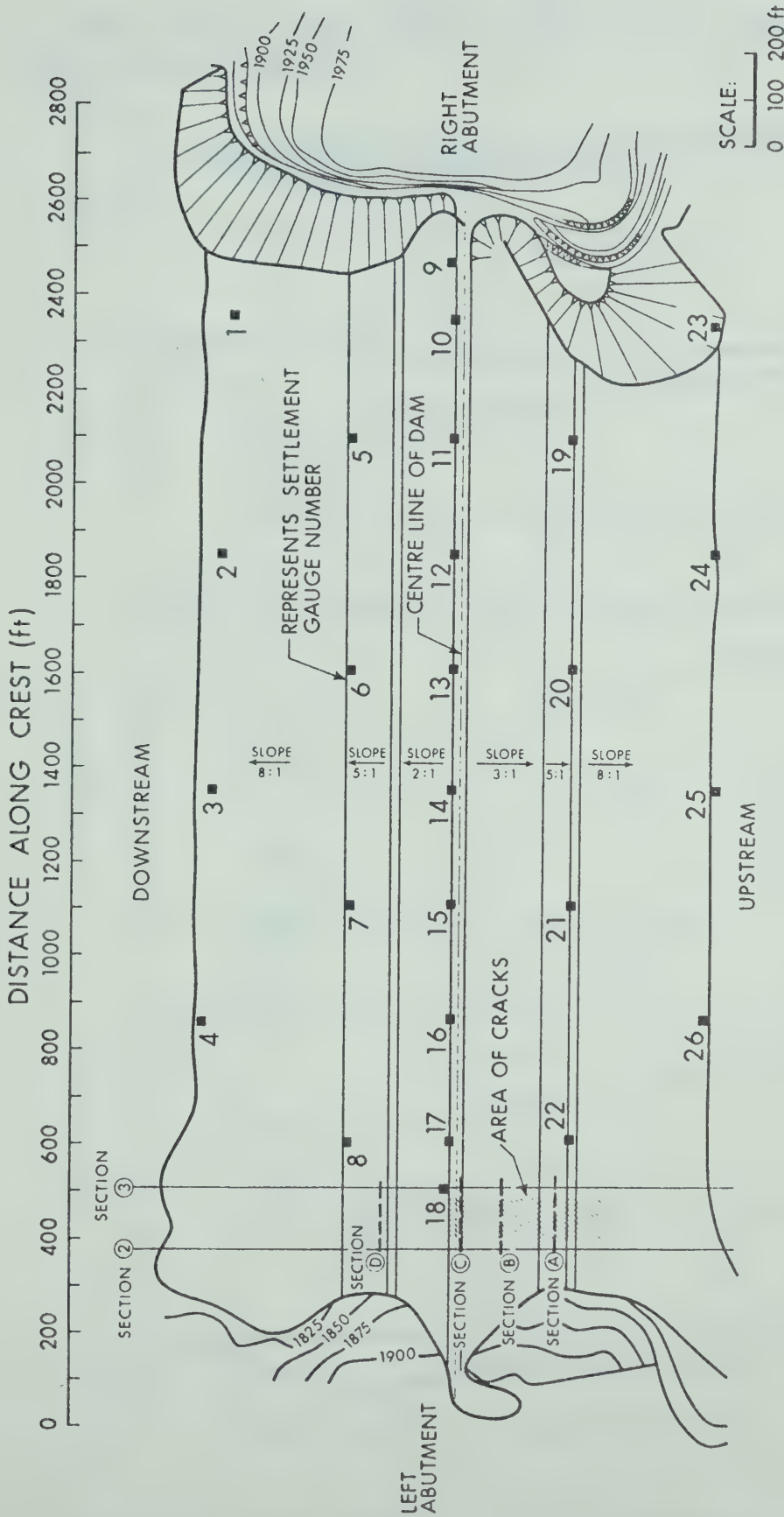


FIG. 5.3 PLAN VIEW OF DUNCAN DAM SHOWING LOCATION OF SETTLEMENT GAUGES AND AREA OF CRACKS

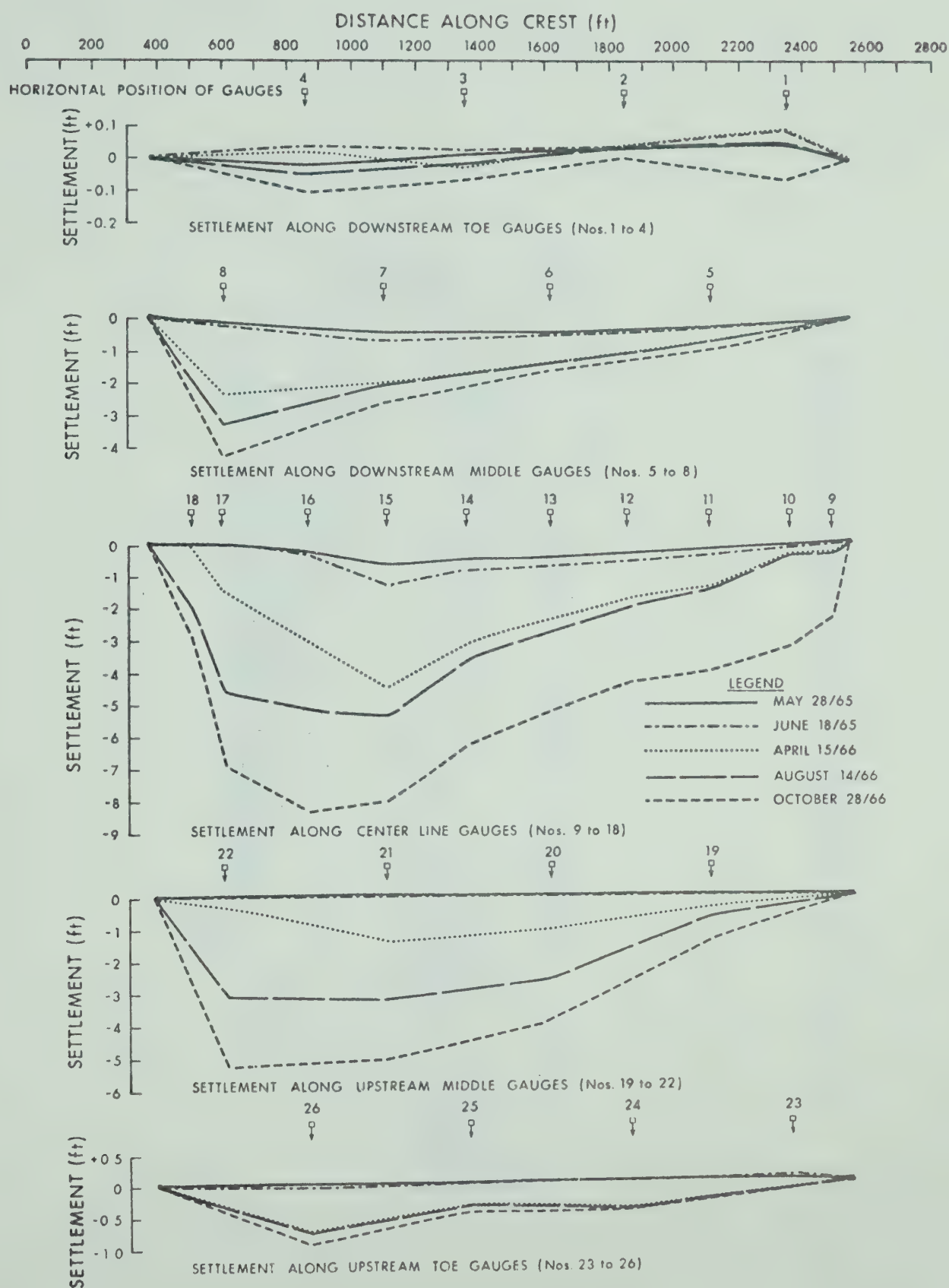


FIG. 5.4 SETTLEMENT ALONG LONGITUDINAL SECTIONS

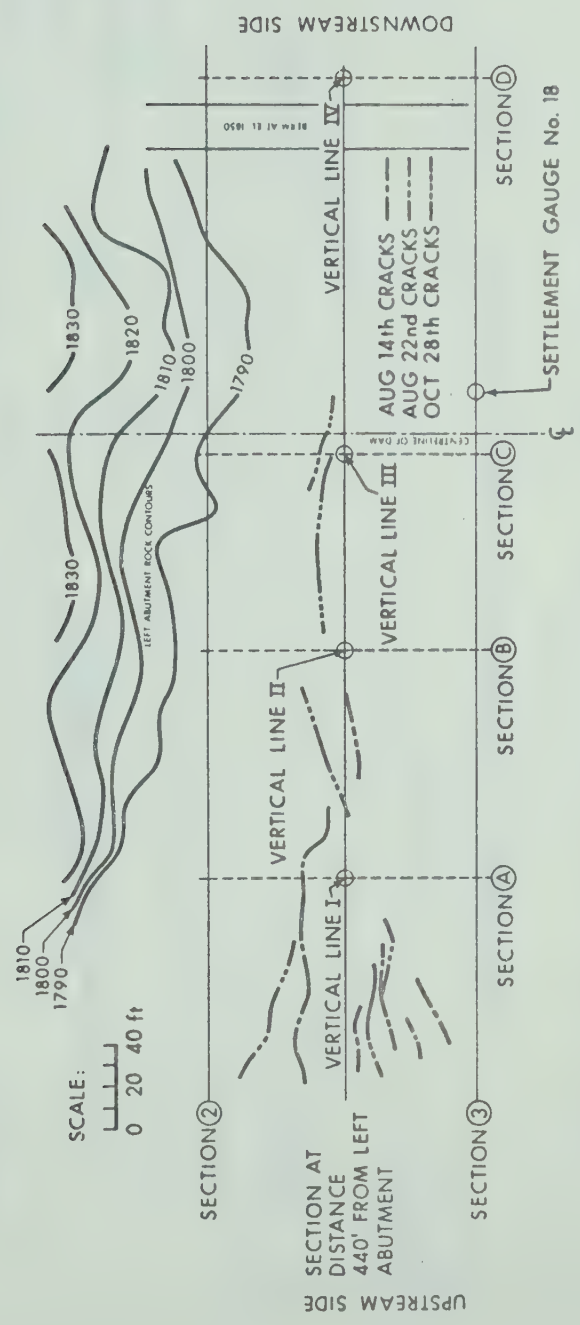


FIG. 5.5 SEQUENCE OF DEVELOPMENT OF CRACKS

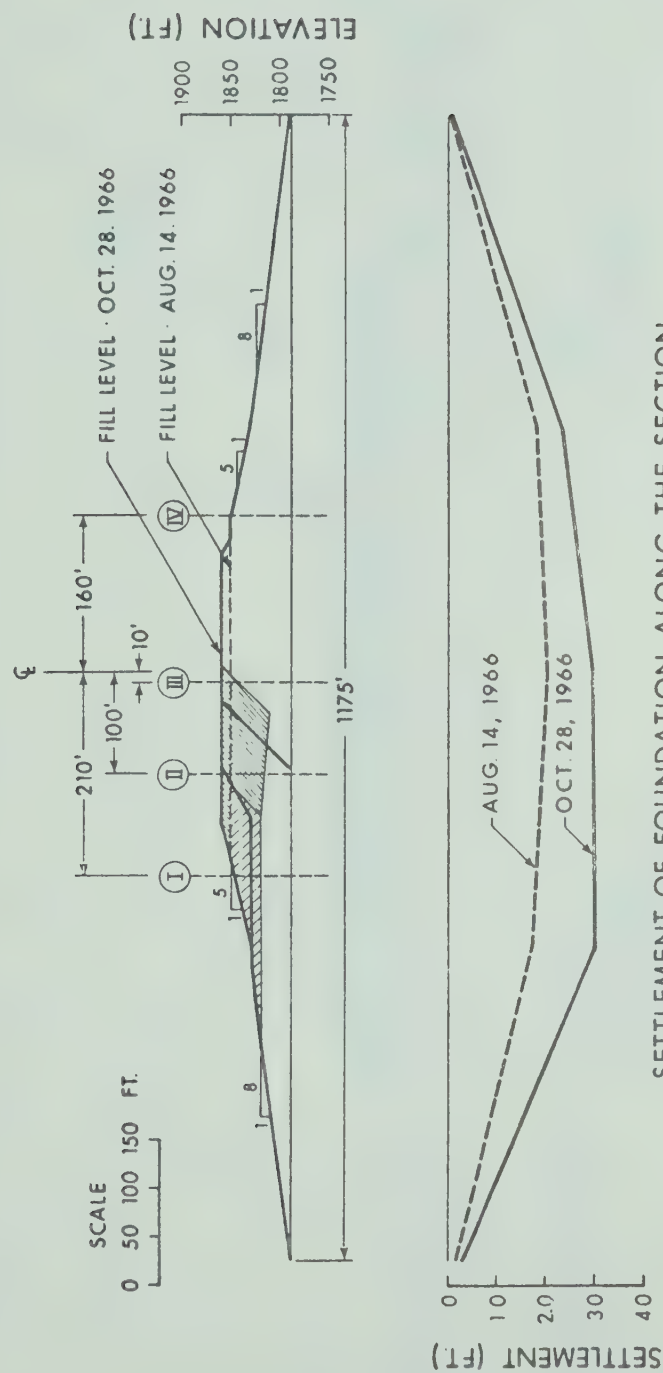


FIG. 5.6 SECTION OF DAM AT A DISTANCE OF 440 FEET FROM LEFT ABUTMENT SHOWING APPROXIMATE ZONES IN WHICH CRACKS DEVELOPED PROGRESSIVELY

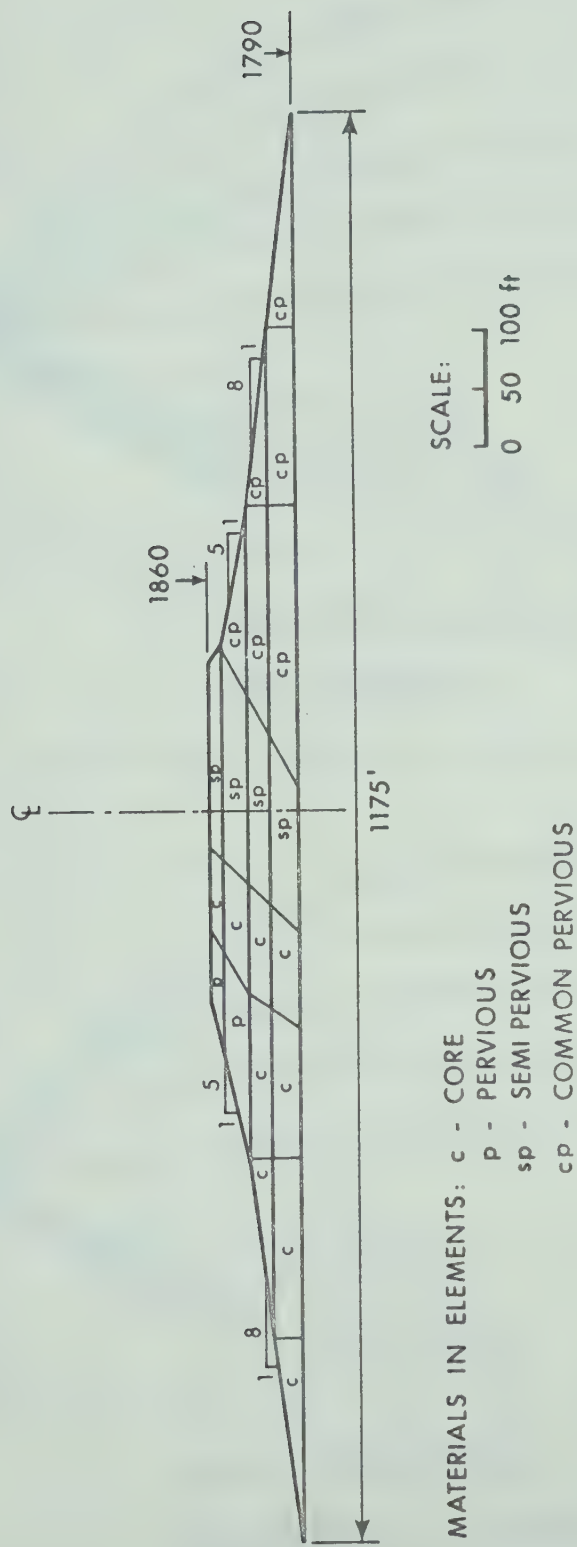


FIG. 5.7 FINITE ELEMENT IDEALIZATION AT SECTION 3 FOR THREE DIMENSIONAL ANALYSIS

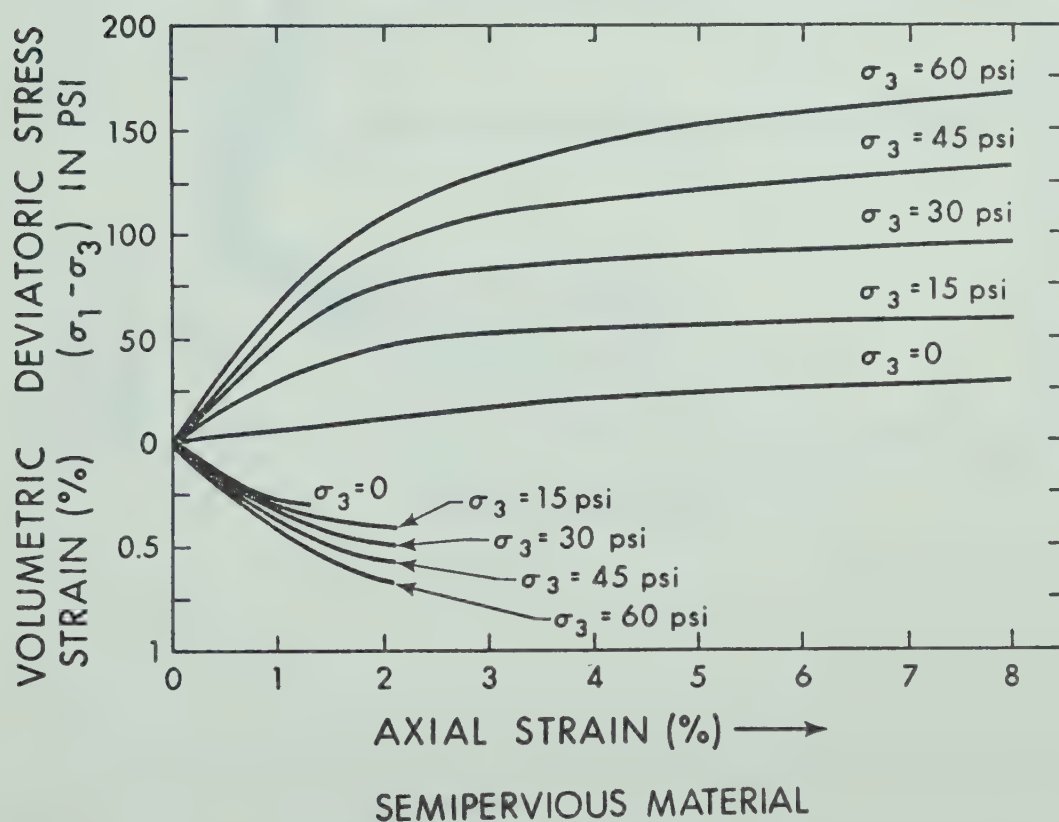
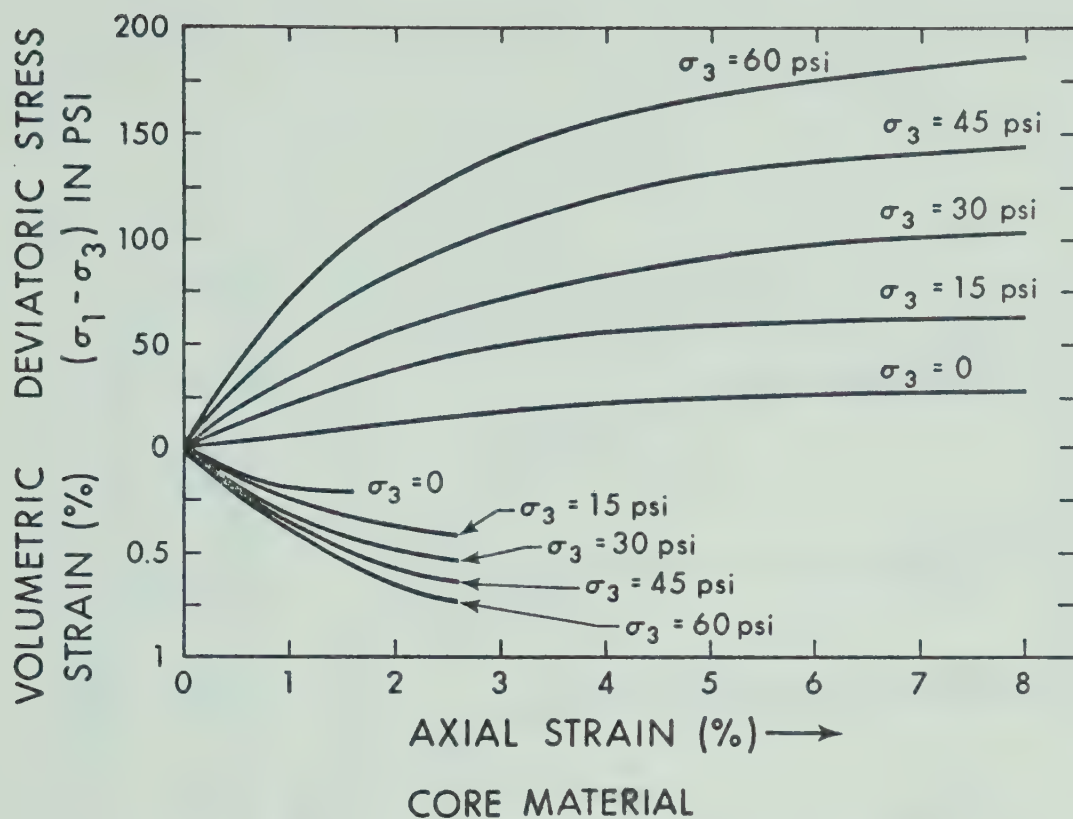


FIG. 5.8 CONSOLIDATED UNDRAINED TRIAXIAL STRESS-STRAIN RELATIONSHIPS FOR THE CORE AND SEMIPIERVOUS MATERIAL OF DUNCAN DAM

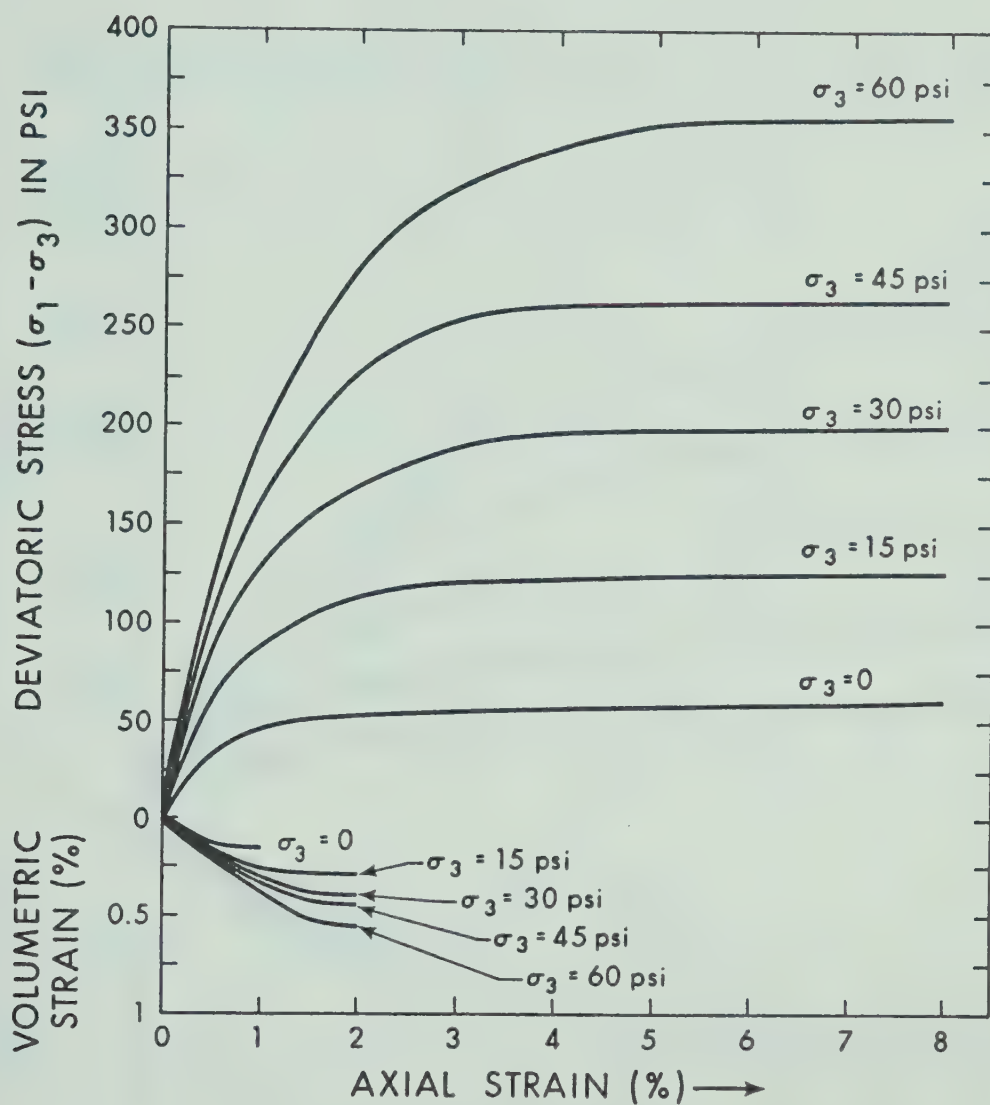


FIG. 5.9 CONSOLIDATED DRAINED TRIAXIAL STRESS-STRAIN RELATIONSHIPS FOR PVIOUS MATERIAL

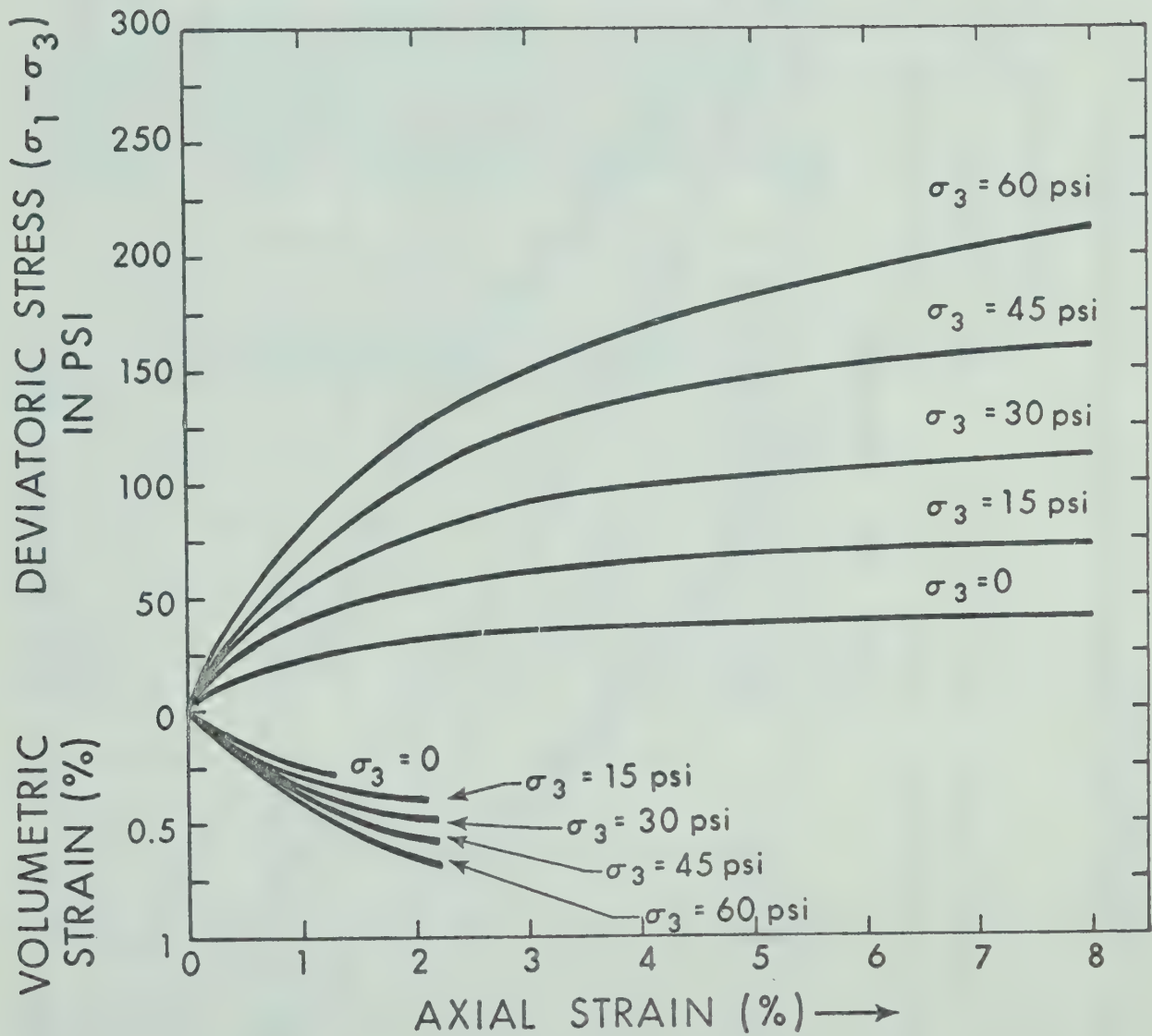


FIG. 5.10 CONSOLIDATED DRAINED TRIAXIAL STRESS-STRAIN RELATIONSHIPS FOR COMMON PERVIOUS MATERIAL

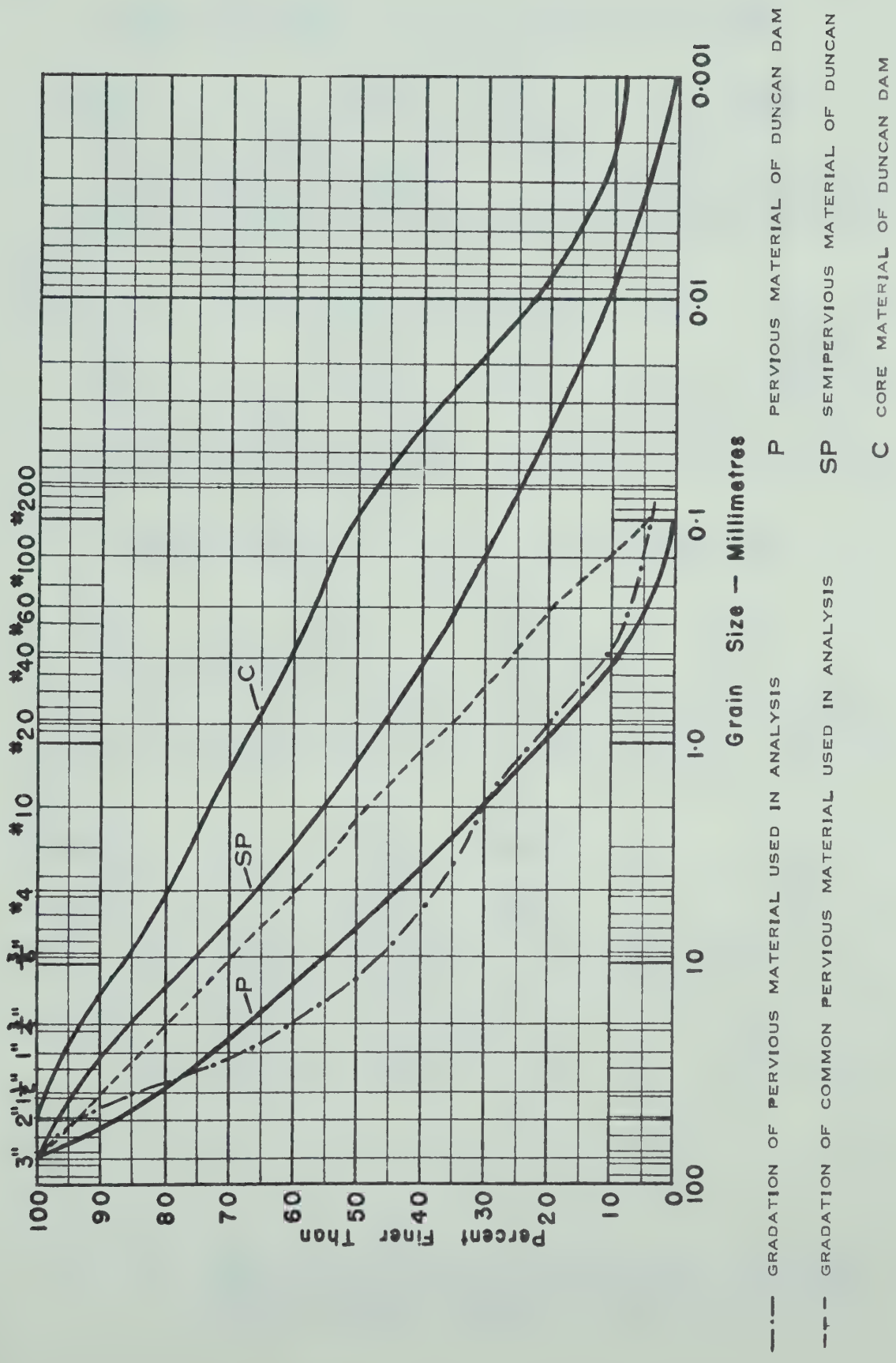


FIG. 5.11 GRAIN SIZE DISTRIBUTION CURVES FOR MATERIALS OF DUNCAN DAM

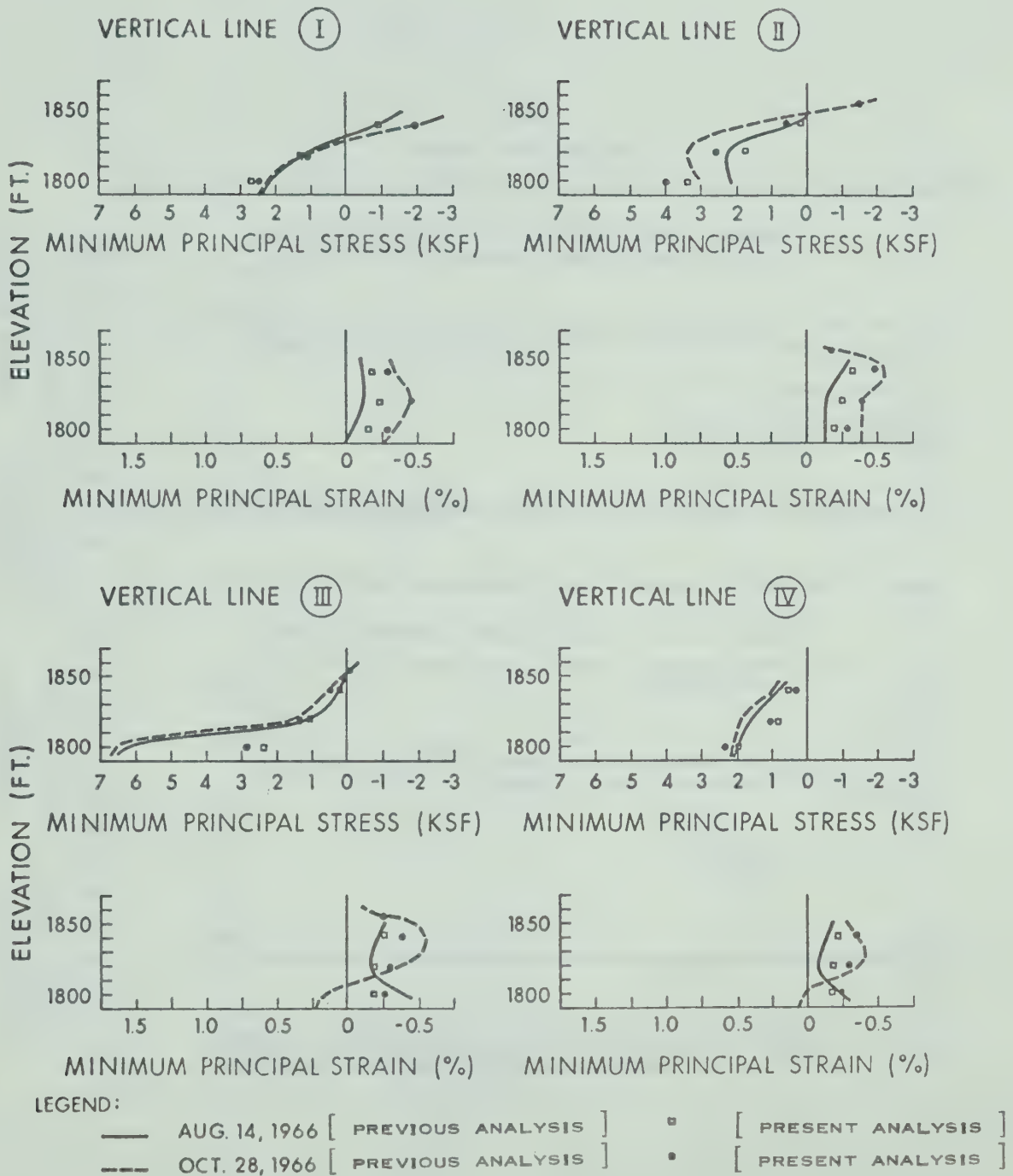


FIG. 5.12 DISTRIBUTION OF MINIMUM PRINCIPAL STRESSES AND STRAINS ALONG VERTICAL LINES I, II, III, AND IV

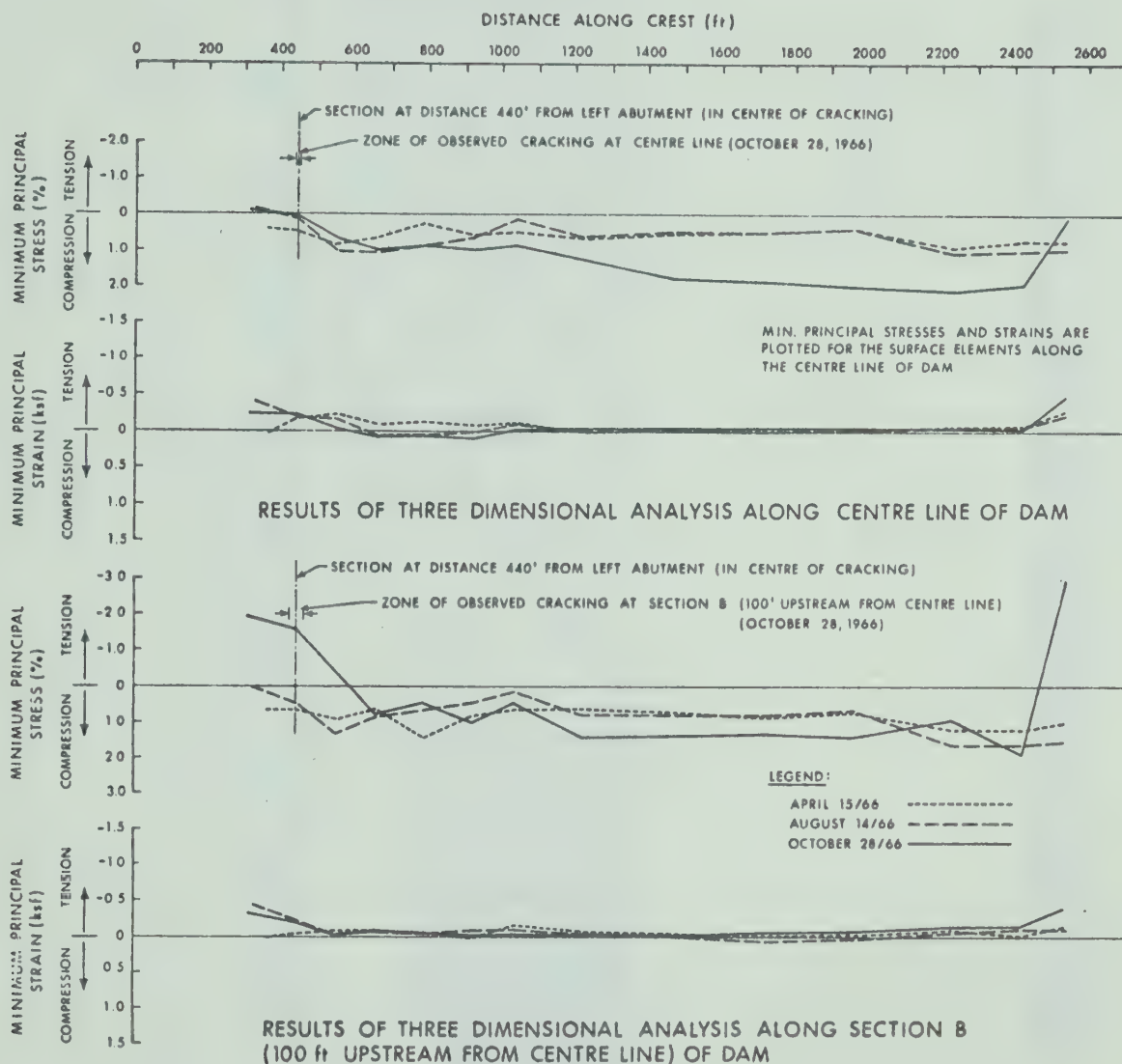


FIG. 5.13 MINIMUM PRINCIPAL STRESSES AND STRAINS ALONG TWO LONGITUDINAL SECTIONS FOR THREE DIMENSIONAL ANALYSIS

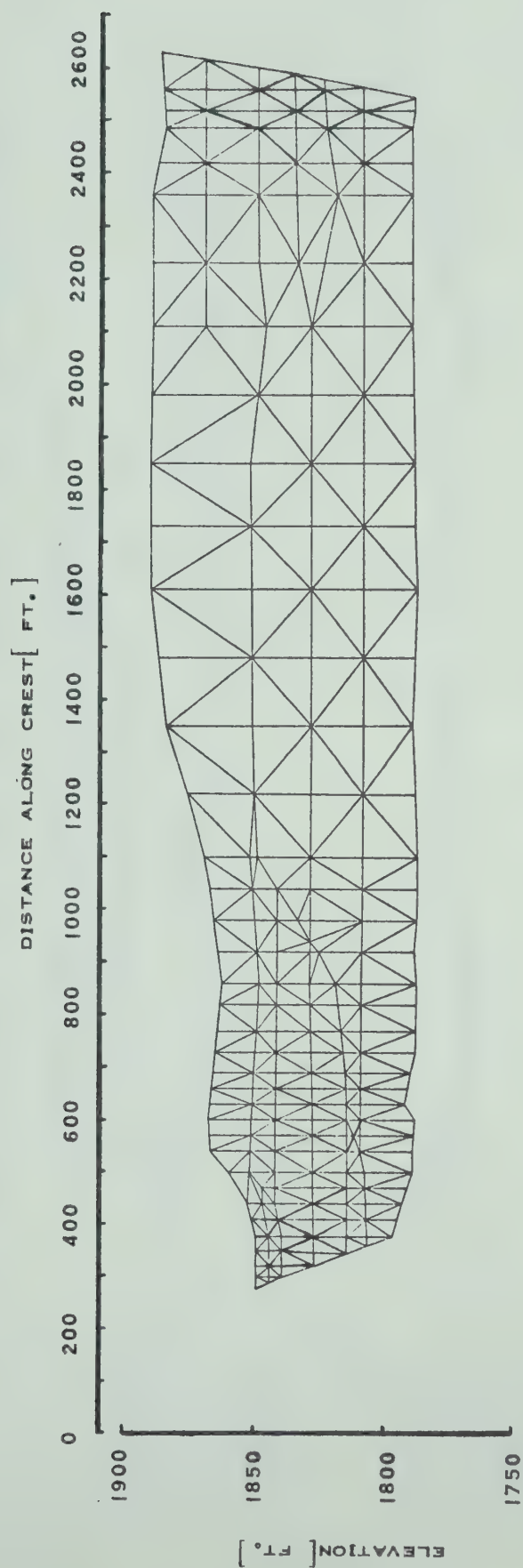


FIG. 5.14 FINITE ELEMENT IDEALIZATION ALONG CENTRAL LONGITUDINAL SECTION FOR TWO DIMENSIONAL ANALYSIS

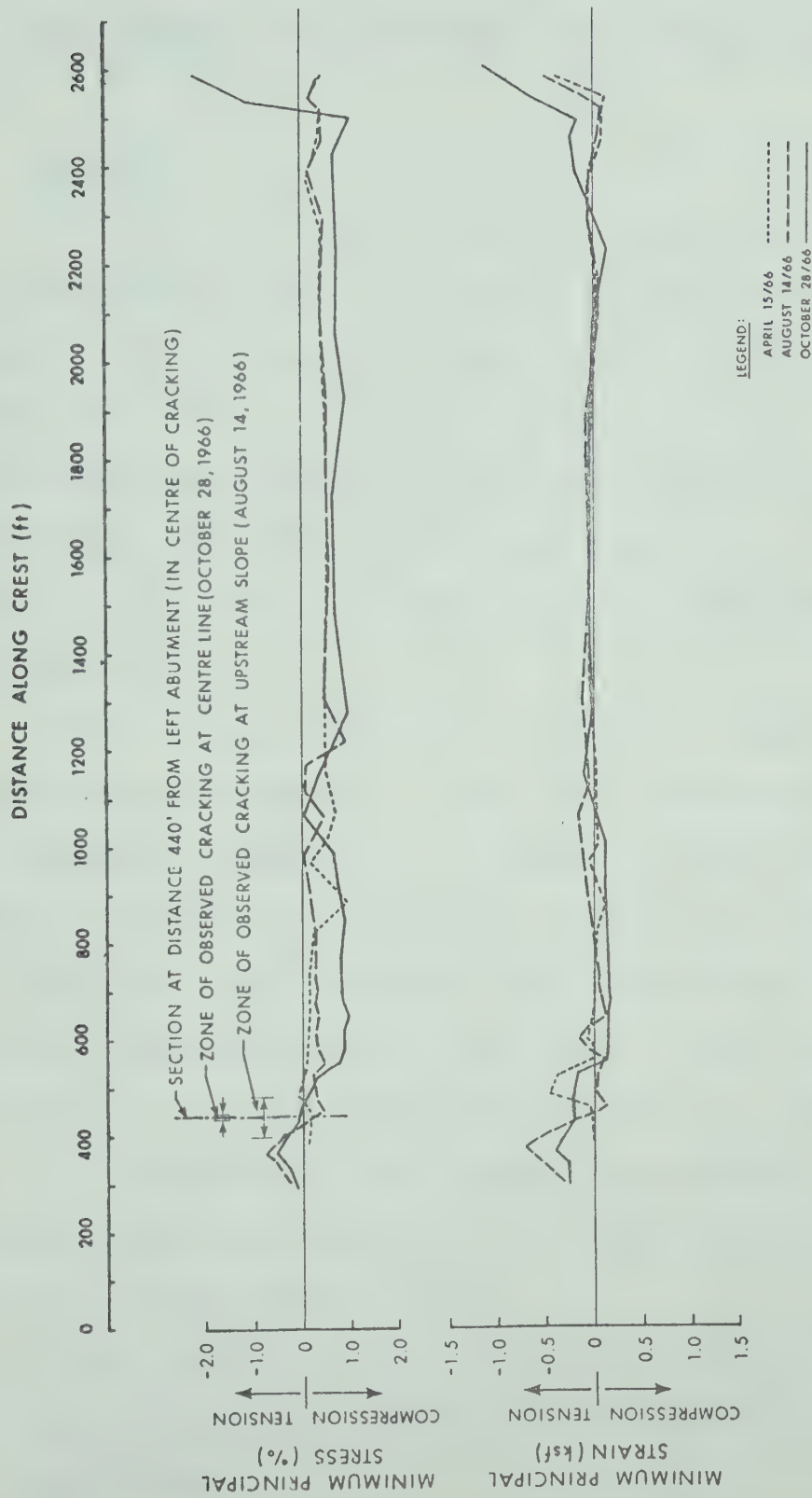


FIG. 5.15 MINIMUM PRINCIPAL STRESSES AND STRAINS ALONG THE CENTRAL LONGITUDINAL SECTION FOR TWO DIMENSIONAL ANALYSIS

CHAPTER VI

CONCLUSIONS AND SUGGESTIONS FOR FURTHER RESEARCH

6.1 General

The finite element method is a very useful and versatile tool for the analysis of cracking of earth dams. To obtain results that are useful in the prediction of cracking of earth dams during and at the end of the period of their construction, the geometry of the dam, the displacement boundary conditions, the construction step sequence, and the stress-strain relationships of soil are to be simulated properly in the analysis.

For a proper simulation of certain complex geometries and boundary conditions of the dam a three dimensional analysis becomes a necessity. In general a three dimensional analysis requires a considerable amount of computer memory and computer time. However, with the availability of large capacity computers three dimensional finite element analyses for large structures such as earth dams, are now feasible.

Any procedure, that attempts to simulate the real stress-strain behaviour of a soil, can only be approximate for the following main reasons:

- (1) A satisfactory theory which can completely account for the deformational behaviour of soils is not presently available.
- (2) The limitations that usually exist in the field and

laboratory test procedures make it difficult to obtain the necessary parameters to describe the deformation of soils under different conditions of loading.

Assuming piecewise linearity, isotropic elastic theory has been used in the present analysis of cracking of earth dams. Though the theory cannot account for the dilatancy effect of soils, it is simple and the parameters needed for its application to the analysis are easily obtained from the conventional laboratory tests. The acceptable agreement obtained in this work between the results of analysis and the field observations at Duncan Dam suggests that the theory used in the analysis is satisfactory for the prediction of cracking of earth dams.

6.2 Criterion for Failure of Soil in Tension

Soils are extremely weak in tension. From the results of the tensile studies conducted on a low plastic glacial till (Chapter II) it can be concluded that when the placement water content is above optimum the tensile strength of soil is practically equal to zero. Hence, a criterion for tensile failure, based on zero tensile strength for the core of the dam, appears to be appropriate. When the analysis is aimed at evolving a suitable design for an earth dam against tensile cracking it is prudent to neglect the tensile strength of the material of core. A criterion based on tensile strain at failure has been suggested (e.g., Narain, 1962). This has the following disadvantages when compared to the criterion

based on zero tensile strength:

- (1) The tensile strain at failure for a soil is a sensitive parameter depending on factors such as type of soil, water content, rate of strain, type and the amount of compaction, state of stress in the directions normal to the direction of tensile stress, and the type of tension test used. In comparison to the compression tests, tension tests are more difficult to perform as routine soil tests. The tensile strains are usually observed over large distances along the crest of dam whereas the laboratory tensile strains are observed on comparatively small specimens tested under certain particular stress states. As such the correlation achieved between the field and laboratory tensile failure strains can only be approximate.
- (2) In general when compared to the strains the stresses computed in an analysis are less sensitive to the changes in elastic moduli. Because of the present limitations that exist in simulating the stress-strain behaviour of soil using laboratory test data it is unlikely that the stress-strain relationships used in the analysis would be wholly representative of the field behaviour of soil. Under these circumstances it appears reasonable to place more reliance on the computed stresses rather than on the computed strains.
- (3) There is a possibility for a principal strain to be tensile while the three principal stresses remain com-

pressive. This situation does not lead to a tensile crack. The analysis of cracking at Duncan Dam (Chapter V) indicated the observed tensile cracks only occurred at locations where one of the principal stresses and the corresponding strain were tensile. This indicates that the criterion based on tensile strain alone is inadequate for the analysis of cracking. When the tensile strength of the soil is assumed to be zero no reliance on tensile tests need be made in the analysis.

Laboratory tensile tests are, however, useful for making comparative studies on tensile characteristics of soils. Such studies are useful in specifying the type of core material and its placement conditions for an effective control of cracking. In spite of the limitations outlined previously the laboratory tensile failure strains still provide useful information to aid in the interpretation of the field tensile strain measurement data.

6.3 Tensile Characteristics of Soil

The indirect tension test procedure, used in the present work for evaluating the tensile characteristics of a typical till, was found to be satisfactory. The test procedure can be used for soils with low to medium plasticity to ensure a brittle failure. A procedure to obtain the tensile stress-strain relationship for soils with different moduli in tension and compression is indicated.

Based on the laboratory tests performed on Mica Till

with and without the addition of small amounts of bentonite the following conclusions are drawn:

- (1) When the water content is above optimum the flexibility of a soil increases rapidly with the water content whereas the tensile strength decreases with the water content. The percentage decrease in tensile strength, with a given percentage increase in water content above optimum, is more in a low plastic soil compared to that of a soil with high plasticity. Hence the addition of highly plastic bentonite to a low plastic till aids in achieving the required flexibility without much reduction in the tensile strength.
- (2) Rate of loading has considerable effect on the tensile stress and strain at failure. From the results obtained on Mica Till and from those reported by Tschebotarioff et al. (1953) and Narain (1962) there appears to exist, for compacted soils, a critical rate of loading that mobilizes the minimum tensile stress and strain at failure. A knowledge of the critical rate of loading is useful in obtaining the minimum tensile strain at failure for a given soil at a given water content.
- (3) An increase in compactive effort decreased the flexibility and increased the tensile strength of till when the water content is well below the Proctor optimum. For water contents near and above the Proctor optimum the tensile strength decreased with the compactive effort. For the type of soil tested, over compaction at water

contents greater than the Proctor optimum hardly improves the tensile strength of soil.

6.4 Factors Affecting the Development of Tensile Zones in Earth Dams During Construction

The results of a finite element analysis, concerning the development of tensile zones in an earth dam during its construction depends on the simulation of a number of factors in the analysis. To evaluate the influence of different factors parametric studies were conducted. From the results of these parametric studies the following conclusions are offered.

6.4.1 Single Step and Incremental Loading

One of the important factors to be considered in the simulation of the construction of an earth dam in the analysis is the construction step sequence. While a single step analysis is simpler and less time consuming than an incremental analysis, it results in unrealistic displacements and exaggerated tensile zones. For a proper simulation of the construction step sequence an incremental analysis becomes a necessity. The optimum number of increments needed for an analysis is governed by the cost of computation and the accuracy of the results required. After a given number of load increments, the results become practically insensitive to further increments. In the case of a three dimensional analysis, because of its high cost of computation, the

limitations on the number of increments becomes more severe than a two dimensional analysis.

6.4.2 Linear and Non-Linear Analyses

A non-linear analysis, which simulates the non-linear stress-strain behaviour of soils, is more realistic than a linear analysis. Comparison of linear and non-linear analyses showed that the tensile stresses obtained by a linear analysis are higher than those computed by a non-linear analysis. The non-linear behaviour of a soil can be simulated conveniently in an incremental analysis. A procedure to determine the elastic parameters from the laboratory test data, converted to a stress invariant form, is suggested.

The use of this procedure offers the following advantages:

- (1) An assumption regarding the third principal stress is not necessary.
- (2) Approximations in representing the laboratory stress-strain relationships are eliminated because the experimental data is supplied in digital form.

A close agreement between the experimental stress-strain relationship and those obtained in the analysis is possible if each step is analyzed twice. The "average moduli" approach used in the analyses here is found to be satisfactory.

6.4.3 "No Tension" Analysis

In an incremental non-linear analysis the tensile stresses computed in the zones of tension are of small magni-

tude. Hence the local stress redistribution, that occurs due to the removal of tensile stresses from the tensile zones, does not alter the development of tensile zones computed subsequently in the upper layers. As a "no tension" analysis involves an iterative procedure considerable savings in the cost of computation can be effected in a three dimensional analysis by not removing the tensile stresses.

6.4.4 Three Dimensional Effects

The plane strain condition, generally assumed in the analysis of cracking of earth dams, is satisfied only for homogeneous dams with a symmetrical cross section. The non-homogeneity of the materials and complexity of the geometry of the dam are often the main reasons necessitating a three dimensional analysis. Where the material of core differs from that of the shell significant errors arise from a two dimensional analysis. The tensile stresses are under-estimated when shell is more flexible than core and they are over-estimated when shell is less flexible than core.

6.5 Control of Cracking by Non-Homogeneous Modelling

As indicated in Chapter IV (Section 4.9) a considerable reduction in tensile stresses is possible by changing the placement specifications of the fill in critical tensile zones. To derive suitable placement specifications, the finite element method can be used to a considerable advantage in analyzing the effect of changing the flexibility of core

in the zones of computed tensile stresses.

6.6 Applicability of the Analysis of Cracking to a Real Structure

A three dimensional finite element analysis when applied to a case study of cracking at Duncan Dam, showed a reasonably good agreement between the computed and the observed tensile zones. This indicates, with proper simulation of the various factors (Section 6.3) in the analysis, the finite element method can be used with reliance for the analysis of cracking of earth dams during and at the end of their construction. Finite element analytical procedure may also be used as a design tool to control cracking in earth dams (Section 6.5).

6.7 Suggestions for Further Research

Based on the work presented here, the following further research and field studies on deformation and cracking of earth dams are suggested:

- (1) The stress-strain relationships used in the analysis should be such that they enable a proper simulation to be made of the deformational behaviour of soil under different conditions of loading. To obtain such stress-strain relationships suitable laboratory test procedures should be evolved. A theory, which also considers the dilatancy effect of soils, is desirable, especially for problems involving large strains and failures due to shear.

- (2) The analysis of cracking of earth dams presented here is limited to the period of construction of dam. It is desirable to consider other critical conditions such as the first filling of reservoir and earthquake loading.
- (3) The tensile tests presented give, in broad terms, the behaviour of a typical low plastic core material under tension. Information obtained by more extensive tensile testing on different types of soil is useful in readily recognizing the soils susceptible to tensile cracking. In addition to obtaining information on the tensile behaviour of soils, it is highly desirable that research aimed at determining the factors contributing to the tensile strength of a soil be conducted. This will provide a better insight into the problem of tensile cracking.
- (4) Effectiveness of different preventative measures, taken against cracking and subsequent erosion failure in earth dams, should be evaluated. Laboratory tests, aimed at determining the erodability of soil through cracks, the self-healing properties of soil, and the dependability of filters in prevention of erosion failures are of value.
- (5) Information concerning stresses, deformations, development of tensile cracks, and erosion failures, obtained by reliable field observations is of a great value in testing the usefulness of the analytical and laboratory procedures developed for the analysis of cracking of

earth dams. In addition to recording the movements of the surface monuments, stress and strain observations should be obtained from the instruments located within the suspected, critical zones of tension. Such observations greatly contribute to the evaluation of the conditions responsible for tensile cracking.

REFERENCES

- Akazawa, T. (1953), "Tension Test Method for Concrete", Bulletin No. 16, International Association of Testing and Research Laboratories, Paris, November, 1953, pp. 11-23.
- Alberro, J. (1972), "Stress-Strain Analysis of El Infiernillo Dam", ASCE Speciality Conference on Performance of Earth and Earth-Supported Structures, June, 1972, Purdue University, Lafayette, Indiana, Vol. 1, Part 1, pp. 837-852.
- ASCE Committee on Earth and Rockfill Dams (1967), "Progress Report: Problems in Design and Construction of Earth and Rockfill Dams", Journal of the Soil Mechanics and Foundations Division, ASCE, Vol. 93, No. SM3, May, 1967, pp. 129-136.
- Bendel, H. (1962), "Die Berechnung von Spannungen und Verschiebungen in Erddammen", Mitt. Versuchsanstalt f. Wasserbau und Erdbau, No. 55, ETH, Zurich.
- Bishop, A.W. (1952), "The Stability of Earth Dams", Ph.D. Thesis, University of London, London.
- Bishop, A.W. and Henkel, D.J. (1962), The Measurement of Soil Properties in the Triaxial Test, Second Edition, Edward Arnold, London, p. 72.
- Bjerrum, L. (1967), Discussion, Ninth International Congress on Large Dams, Istanbul, Vol. VI, p. 456.
- Bofinger, H.E. (1970), "The Measurement of the Tensile Properties of Soil-Cement", Ministry of Transport, Road Research Laboratory Report LR365, Crownthorne, Berkshire.
- Breen, J.J. and Stephens, J.E. (1966), "Split Cylinder Test Applied to Bituminous Mixtures at Low Temperatures", Journal of Materials, Vol. 1, No. 1, American Society for Testing and Materials, March, 1966.
- Brown, C.B. and King, I.P. (1966), "Automatic Embankment Analysis: Equilibrium and Instability Conditions", Geotechnique, Vol. 16, No. 3, September, 1966, pp. 209-219.
- Carniero, F.L.L.B. and Barcellos, A. (1953), "Concrete Tensile Strength", Bulletin No. 13, International Association of Testing and Research Laboratories for Materials and Structures, Paris, March, 1953, pp. 97-127.

- Casagrande, A. (1950), "Notes on the Design of Earth Dams", Journal of the Boston Society of Civil Engineers, Vol. 37, No. 4, October, 1950. (Reprinted in Contributions to Soil Mechanics 1941-1953, Boston Society of Civil Engineers, Boston, Mass., 1953, pp. 231-255).
- Chang, C.Y. and Duncan, J.M. (1970), "Analysis of Soil Movements Around Deep Excavation", Journal of the Soil Mechanics and Foundations Division, ASCE, Vol. 96, No. SM5, September, 1970, pp. 1655-1681.
- Chang, T.Y., Ko, H.Y., Scott, R.F. and Westman, R.A. (1967), "An Integrated Approach to the Stress Analysis of Granular Materials", Report of the Soil Mechanics Laboratory, California Institute of Technology, Pasadena, California.
- Chen, W.F. (1970), "Extensibility of Concrete and Theorems of Limit Analysis", Journal of Engineering Mechanics Division, ASCE, Vol. 96, No. EM3, June, 1970, pp. 341-352.
- Clough, G.W. and Duncan, J.M. (1970), "Finite Element Analyses of Port Allen and Old River Locks", Report No. TE69-3, Office of Research Services, University of California, Berkeley.
- Clough, R.W. and Woodward, R.J., III (1967), "Analysis of Embankment Stresses and Deformations", Journal of the Soil Mechanics and Foundations Division, ASCE, Vol. 93, No. SM4, July, 1967, pp. 529-549.
- Clough, R.W. (1969), "Comparison of Three Dimensional Finite Elements", Proc. of Symp. on Application of Finite Element Methods in Civil Engineering, ASCE, Nashville, November, 1969, pp. 1-26.
- Colback, P.S.B. (1966), "An Analysis of Brittle Fracture Initiation and Propagation in the Brazilian Test", Proc. Congr. Intern. Soc. Rock Mech., 1 st., Lisbon, pp. 385-391.
- Covarrubias, S.W. (1969), "Cracking of Earth and Rockfill Dams", Harvard Soil Mechanics Series, No. 82, April, 1969.
- Desai, C.S. and Reese, L.C. (1970), "Analysis of Footings on Layered Soils", Journal of the Soil Mechanics and Foundations Division, ASCE, Vol. 96, No. SM4, July, 1970, pp. 1289-1310.

- Desai, C.S. (1971), "Non-Linear Analyses Using Spline Functions", Journal of the Soil Mechanics and Foundations Division, ASCE, Vol. 97, No. SM10, October, 1971, pp. 1461-1480.
- Dolezalova, M. (1970), "Effect of Steepness of Rocky Canyons Slopes on Cracking of Clay Cores of Rock-and-Earthfill Dams", Trans. Tenth Congress on Large Dams, Vol. 1, June, 1970, pp. 215-224.
- Duncan, J.M. and Dunlop, P. (1969), "Slopes in Stiff-Fissured Clays and Shales", Journal of the Soil Mechanics and Foundations Division, ASCE, Vol. 95, No. SM2, March, 1969, pp. 467-492.
- Duncan, J.M. and Chang, C.Y. (1970), "Non-Linear Analysis of Stress and Strain in Soils", Journal of the Soil Mechanics and Foundations Division, ASCE, Vol. 96, No. SM5, September, 1970, pp. 1629-1654.
- Duncan, J.M. and Chang, C.Y. (1972), Discussion Closure of "Non-Linear Analysis of Stress and Strain in Soils", by Duncan, J.M. and Chang, C.Y., Journal of the Soil Mechanics and Foundations Division, ASCE, Vol. 98, No. SM5, May, 1972, pp. 495-498.
- Duncan, J.M. (1972), "Finite Element Analyses of Stresses and Movements in Dams, Excavations and Slopes", State of the Art Report, WES Symp. on Appl. of Finite Element Method in Geotechnical Engg., Vicksburg, Miss., May, 1972.
- Eisenstein, Z., Krishnayya, A.V.G. and Morgenstern, N.R. (1972), "An Analysis of Cracking at Duncan Dam", ASCE Speciality Conference on Performance of Earth and Earth-Supported Structures, June, 1972, Purdue University, Lafayette, Indiana, Vol. 1, Part 1, pp. 765-777.
- Fang, H.Y. and Chen, W.F. (1971), "New Method for Determination of Tensile Strength of Soils", Preprint of Paper Presented at the 50th Annual Meeting of the Highway Research Board, Washington, D.C., January, 1971.
- Felippa, C.A. (1966), "Refined Finite Element Analysis of Linear and Non-Linear Two Dimensional Structures", Ph.D. Thesis, University of California, Berkeley, California.
- Finn, W.D.L. (1967), "Static and Seismic Behaviour of an Earth Dam", Canadian Geotechnical Journal, Vol. 4, No. 1, February, 1967, pp. 28-37.

- Frazier, G.A. (1969), "Vibrational Characteristics of Three-Dimensional Solids, with Applications to Earth Dams", Ph.D. Thesis, Montana State University, Bozman, Montana.
- Frocht, M.M. (1957), Photoelasticity, Vol. 2, John Wiley and Sons, Inc., New York.
- Gates, R.H. (1968), "Inelastic Analysis of Slopes by the Finite Element Method", Ph.D. Thesis, University of Illinois.
- Girijavallabhan, C.V. and Reese, L.C. (1968), "Finite Element Method for Problems in Soil Mechanics", Journal of the Soil Mechanics and Foundations Division, ASCE, Vol. 94, No. SM2, March, 1968, pp. 473-496.
- Gordon, J.L. and Duguid, D.R. (1970), "Experiences with Cracking at Duncan Dam", Trans. Tenth Congress on Large Dams, Vol. 1, June, 1970, pp. 469-486.
- Haefeli, R. (1951), "Investigation and Measurements of the Shear Strength of Saturated Cohesive Soils", Geotechnique, Vol. 2, No. 3, pp. 186-208.
- Harr, M.E. (1966), Foundations of Theoretical Soil Mechanics, McGraw-Hill Book Co., New York.
- Hasegawa, H. and Ikeuti, M. (1966), "On the Tensile Strength of Disturbed Soils", Symposium on Rheology and Soil Mechanics, Edited by J. Kravtchenko and P.M. Sirieys, Springer, Berlin, pp. 405-412.
- Herrmann, L.R. (1964), "Elasticity Equations for Incompressible and Nearly Incompressible Materials by a Variational Theorem", A.I.A.A. Journal, Vol. 3, No. 10, pp. 1896-1900.
- Hertz, H. (1883), "Über die Verteilung der Druckkräfte in einem elastischen Kreiscylinder", Zeitschrift für Mathematik und Physik, Vol. 28.
- Hondros, G. (1959), "The Evaluation of Poisson's Ratio and the Modulus of Materials of a Low Tensile Resistance by the Brazilian (Indirect Tensile) Test with Particular Reference to Concrete", Australian Journal of Applied Science, Vol. 10, No. 3, pp. 243-268.
- Ingles, O.G. and Frydman, S. (1963), "An Examination of Some Methods for Strength Measurement in Soils", Proc. Fourth Australia-New Zealand Conference on Soil Mechanics and Foundation Engineering, August, 1963, Adelaide, pp. 213-219.

- Jurgensen, L. (1934), "The Application of the Theories of Elasticity and Plasticity to Foundation Problems", Reprinted in Contributions to Soil Mechanics, 1925-1940, Boston Society of Civil Engineers, 1940, pp. 148-183.
- Kjaernsli, B. and Torblaa, I. (1968), "Leakage Through Horizontal Cracks in the Core of Hyttejuvet Dam", Papers on Earth and Rockfill Dams in Norway, Publication No. 80, Norwegian Geotechnical Institute, Oslo, pp. 39-47.
- Kulhawy, F.H., Duncan, J.M. and Seed, H.B. (1969), "Finite Element Analyses of Stresses and Movements in Embankments during Construction", Report No. TE69-4, Office of Research Services, University of California, Berkeley.
- Kulhawy, F.H. and Duncan, J.M. (1970), "Non-Linear Finite Element Analysis of Stresses and Movements in Oroville Dam", Report No. TE70-2, Office of Research Services, University of California, Berkeley.
- Lee, K.L. and Shen, C.K. (1968), "Horizontal Movements Related to Subsidence", Journal of the Soil Mechanics and Foundations Division, ASCE, Vol. 94, No. SM6, pp. 139-146.
- Lefebvre, G. and Duncan, J.M. (1971), "Three Dimensional Finite Element Analyses of Dams", Contract Report S-71-6, U.S. Army Engineer Waterways Experiment Station, Vicksburg, Miss., May, 1971.
- Leonards, G.A. and Narain, J. (1963), "Flexibility of Clay and Cracking of Earth Dams", Journal of the Soil Mechanics and Foundations Division, ASCE, Vol. 89, No. SM2, Part 1, March, 1963, pp. 47-98.
- Lowe III, J. (1970), "Recent Development in Design and Construction of Earth and Rockfill Dams", Transactions 10th Congress on Large Dams, Montreal, Vol. 5, Q. 36, pp. 1-60.
- Lowe III, J. (1972), Report, Session II: Earth and Earth-Rock Dams, ASCE Speciality Conference on Performance of Earth and Earth-Supported Structures, June, 1972, Purdue University, Lafayette, Indiana, Vol. 2, pp. 55-70.
- Marsal, R.J. and Ramirez de Arellano, L. (1967), "Performance of El Infiernillo Dam, 1963-1966", Journal of the Soil Mechanics and Foundations Division, ASCE, Vol. 93, No. SM4, July, 1967, pp. 265-298.

- Mellor, M. and Hawkes, I. (1971), "Measurement of Tensile Strength by Diametral Compression of Discs and Annuli", *Engineering Geology*, Vol. 5, No. 3, October, 1971, pp. 173-225.
- Narain, J. (1962), "Flexibility of Compacted Clay", Ph.D. Thesis, Purdue University, Lafayette, Indiana.
- Narain, J. and Rawat, P.C. (1970), "Tensile Strength of Compacted Soils", *Journal of the Soil Mechanics and Foundations Division, ASCE*, Vol. 96, No. SM6, November, 1970, pp. 2185-2190.
- Nobari, E.S. and Duncan, J.M. (1972), "Movements in Dams Due to Reservoir Filling", *ASCE Speciality Conference on Performance of Earth and Earth-Supported Structures*, June, 1972, Purdue University, Lafayette, Indiana, Vol. 1, Part 1, pp. 797-815.
- Nonveiller, E. and Anagnosti, P. (1961), "Stresses and Deformation in Cores of Rockfill Dams", *Proc. Fifth International Conference on Soil Mechanics and Foundation Engineering*, Vol. II, Duroid, Paris, pp. 673-680.
- Palmerton, J.B. (1972), "Application of Three Dimensional Finite Element Analysis", *WES Symp. on Appl. of Finite Element Method in Geotechnical Engg.*, Vicksburg, Miss., May, 1972.
- Patrick, J.G. (1967), "Post-Construction Behaviour of Round Butte Dam", *Journal of the Soil Mechanics and Foundations Division, ASCE*, Vol. 93, No. SM4, July, 1967, pp. 251-263.
- Pope, R.J. (1967), "Evaluation of Cougar Dam Embankment Performance", *Journal of the Soil Mechanics and Foundations Division, ASCE*, Vol. 93, SM4, July, 1967, pp. 231-250.
- Schober, W. (1967), "Behaviour of Gepatsch Rockfill Dam", *Proc. Ninth International Conference on Large Dams*, Vol. III, Question 34, Istanbul, pp. 667-699.
- Scott, R.F. (1963), *Principles of Soil Mechanics*, Addison Wesley, Reading, Mass.
- Scott, R.F. and Ko, H.Y. (1969), "State of the Art Report on Deformation and Strength Characteristics", *State of Art Volume, Seventh International Conference on Soil Mechanics and Foundation Engineering*, Mexico, pp. 1-47.
- Sherard, J.L. (1952), "Influence of Soil Properties and Construction Methods on the Performance of Homogeneous Earth Dams", Ph.D. Thesis, Harvard University, Cambridge, Mass.

- Sherard, J.L., Decker, R.S. and Ryker, N.L. (1972), "Hydraulic Fracturing in Low Dams of Dispersive Clay", Paper Presented to the ASCE Speciality Conference on Performance of Earth and Earth-Supported Structures, June, 1972, Purdue University, Lafayette, Indiana, Vol. 1, Part 1, pp. 653-689.
- Skermmer, N.A. and Hillis, S.F. (1970), "Gradation and Shear Characteristics of Four Cohesionless Soils", Canadian Geotechnical Journal, Vol. 7, pp. 62-68.
- Smith, I.M. and Kay, S. (1971), "Stress Analysis of Contractive or Dilative Soil", Journal of the Soil Mechanics and Foundations Division, ASCE, Vol. 97, No. SM7, July, 1971, pp. 981-997.
- Strohm, W.E., Jr. and Johnson, S.J. (1971), "The Influence of Construction Step Sequence and Non-Linear Material Behaviour on Cracking of Earth and Rockfill Dams", Miscellaneous Paper S-71-10, U.S. Army Engineer Waterways Experiment Station, Vicksburg, Mississippi.
- Tamez, E. and Springall, G. (1960), "The Use of Soils as Construction Materials for Earth Dams", Proc. First Pan-American Conference of Soil Mechanics and Foundation Engineering, Vol. III, Mexico, pp. 1269-1286.
- Terzaghi, K. (1943), Theoretical Soil Mechanics, John Wiley and Sons, Inc., New York.
- Thompson, M.R. (1965), "The Split-Tensile Strength of Lime-Stabilized Soils", Lime Stabilization, Highway Research Record, No. 92, Highway Research Board, pp. 69-79.
- Timoshenko, S. and Goodier, J.N. (1951), "Concentrated Force at a Point of a Straight Boundary", Theory of Elasticity, Second Edition, McGraw-Hill, New York, p. 85.
- Tschebotarioff, G.P., Ward, E.R. and DePhillippe, A.A. (1953), "The Tensile Strength of Disturbed and Recompacted Soils", Proc. Third International Conference on Soil Mechanics and Foundation Engineering, Vol. I, Zurich, pp. 207-210.
- Vaughan, P.R., Kluth, D.J., Leonard, M.W. and Pradoura, H.H.M. (1970), "Cracking and Erosion of the Rolled Clay Core of Balderhead Dam and the Remedial Works Adopted for Its Repair", Trans. Tenth Congress on Large Dams, Vol. 1, pp. 73-93.

- Wilson, E.L. (1963), "Finite Element Analysis of Two-Dimensional Structures", Structural Engineering Laboratory Report No. 63-2, University of California, Berkeley, California, (June, 1963).
- Wilson, E.L. (1966), "Analysis of Plane Stress Structures", Computing Programming Series, University of California, Berkeley, California.
- Wright, P.J.F. (1955), "Comments on an Indirect Tensile Test on Concrete Cylinders", Magazine of Concrete Research, Vol. 7, No. 20, London, July, 1955, pp. 87-96.
- Zienkiewicz, O.C., Valliappan, S. and King, I.P. (1968), "Stress Analysis of Rock as a 'No-Tension' Material", Geotechnique, Vol. 18, pp. 56-66.
- Zienkiewicz, O.C., Irons, B.M., Ergatoudis, J., Ahmad, S. and Scott, F.C. (1969), "Isoparametric and Associated Element Families for Two and Three Dimensional Analysis", Proc. Course on Finite Element Methods in Stress Analysis, Edited by Holand, I. and Bell, K., Trondheim Tech. University.

APPENDIX A

COMPUTER PROGRAM FOR TWO DIMENSIONAL
FINITE ELEMENT ANALYSISA.1 Scope

This appendix contains a description of the computer program used for two dimensional finite element analyses and a listing of the program.

A.2 Language, Code and Limitations

Language. The computer program presented here was written in FORTRAN IV language and run on an IBM 360/67 computer with an MTS operating system at the University of Alberta, Edmonton.

Code. The title of the code is Finite Element Non-Linear Analysis in Two Dimensional Problems (FENA2D).

Limitations. The program in the present form can handle a problem less than or equal to the following size:

Number of elements	=	400
Number of nodes	=	250
Number of read elements	=	150
Number of read nodes	=	250
Number of boundary nodes	=	50
Number of materials	=	5
Number of cell pressures at which triaxial data is supplied	=	10

Number of axial strain points at which triaxial data is supplied	=	20
--	---	----

If the size of a problem exceeds the above limits the dimensions have to be increased accordingly. The minimum required dimension for each array is given in A.4.1.

A.3 Development and the Main Features of Program

The program in its original form was developed by E.L. Wilson (University of California, 1962) to perform a two dimensional finite element analysis either for plane strain or plane stress condition using constant strain triangular elements. The analysis had to be linear and the loads were to be applied in a single step. The equations of equilibrium were solved by Gauss-Seidel iterative procedure.

Z. Eisenstein (University of Alberta, 1969) added to the above program the automatic generation of nodes and elements. The author (1970) modified the program to its present form, given in the listing, to perform, in addition to the linear single step analysis, a non-linear two dimensional analysis in a number of steps with an option to analyze each step once or twice. An option for a "no tension" analysis is possible. A facility to generate a uniform element pattern (detailed in A.5) in addition to the existing generation of non-uniform pattern is available.

The program consists of a Main and a Subroutine called TESTD. Only the main features of the program are given below since a detailed description appears in A.5.

- (1) The input data regarding elements, nodes, boundary conditions, type of generation, number of materials and type of analysis are read.
- (2) The nodes and elements are generated in the prescribed manner and the appropriate elastic parameters are assigned to each element. In the case of a non-linear analysis the triaxial test data are converted to the stress-invariant form by the subroutine TESTD. The elastic parameters for each element are determined from the converted form of the test data. The stresses considered for calculation of the initial moduli are those corresponding to the "at-rest" condition.
- (3) The information regarding the number of steps, whether each step to be analyzed once or twice, whether "no tension" analysis to be performed or not is read. The number of elements, nodes and the boundary conditions for the particular step are also read.
- (4) The element stiffness is formed for all the elements in the particular step, the equilibrium equations are set up and solved by Gauss-Seidel iterative procedure.
- (5) The displacements, stresses and strains are computed and the elastic moduli are calculated from the test data in case of a non-linear analysis. If the step has to be repeated once more the "average moduli" are used. "No tension" analysis is performed if it is opted for.
- (6) In the multiple step analysis the stresses, strains and displacements are accumulated. When a particular step

is to be repeated the added stresses, strains and displacements of that step are deducted from the total values before the analysis is repeated with the "average moduli".

A.4 Nomenclature

In Section A.4.1 that follows the variables that need a change in their dimension declaration according to the size of the problem are designated by parentheses after the variable name. The description and the minimum required size of the variable are also indicated. The variables defining the minimum sizes are given as input to the program.

A.4.1 Description and Size of Variables

<u>Name</u>	<u>Description</u>	<u>Minimum Size When Applicable</u>
ACOE()	Shear strength parameter associated with cohesion given by $2c \cos \phi / (1 - \sin \phi)$	(NUMAT)
AJ()	X-distance between nodes i and j of an element	(NUMEL)
AK()	X-distance between nodes i and k of an element	(NUMEL)
BCOE()	Shear strength parameter associated with σ_3 given by $2 \sin \phi / (1 - \sin \phi)$	(NUMAT)
BJ()	Y-distance between nodes i and j of an element	(NUMEL)
BK()	Y-distance between nodes i and k of an element	(NUMEL)

<u>Name</u>	<u>Description</u>	<u>Minimum Size When Applicable</u>
COED()	Coefficient of thermal expansion assigned for each read or generated element	(NUMEL)
COEDR()	Coefficient of thermal expansion assigned for each read element	(NUREL)
CONFAC	Conversion factor used to convert the triaxial test results to the units in which analysis is performed	
DSX()	Displacement in X-direction given as input for already generated nodes	(NUMNP)
DSXQ()	Total displacement in X-direction	(NUMNP)
DSXR()	Displacement in X-direction given as input only for read nodes	(NURNP)
DSY()	Displacement in Y-direction given as input for already generated nodes	(NUMNP)
DSYQ()	Total displacement in Y-direction	(NUMNP)
DSYR()	Displacements in Y-direction given as input only for read nodes	(NURNP)
DT()	Temperature change in a read or generated element	(NUMEL)
DTR()	Temperature change in a read element	(NUREL)
EBREAD()	Bulk modulus read for each material type	(NUMAT)
EBULK()	Bulk modulus assigned for each element	(NUMEL)
EMAX()	Percent maximum principal strain in each element	(NUMEL)
EMIN()	Percent minimum principal strain in each element	(NUMEL)
EPXV()	Percent total X-strain in each element	(NUMEL)
EPYV()	Percent total Y-strain in each element	(NUMEL)

<u>Name</u>	<u>Description</u>	<u>Minimum Size When Applicable</u>
ESHEAR()	Shear modulus assigned for each element	(NUMEL)
ESREAD()	Shear modulus read for each material type	(NUMAT)
ET()	Young's modulus assigned for a read or generated element	(NUMEL)
ETR()	Young's modulus assigned for a read element	(NUREL)
GAMV()	Total percent shear strain in each element	(NUMEL)
GOCT()	Percent octahedral shear strain	(NSTRN, NCELP,NUMAT)
HEAD()	Heading for the identification of the problem	18
IANLYS	Code to identify whether the analysis is for plane stress or for plane strain condition	
IGEN	Code to identify whether the element generation is of uniform or non-uniform pattern	
ITOPT	Code to identify whether a step is to be analyzed once or twice.	
KOPT	Code to identify whether "no tension" analysis is to be performed or not	
M	Element or nodal number	
MAT()	Material number assigned to each element	(NUMEL)
MATN	Number of elements to which material number other than 1 is to be assigned	
N	Element or nodal number	
NANLYS	Code to identify whether the analysis is linear or non-linear	

<u>Name</u>	<u>Description</u>	<u>Minimum Size When Applicable</u>
NAP()	A vector to store the adjacent nodal points from a given node	(NUMNP)
NBOUN	Number of nodes at which the boundary displacements are specified in a particular step	
NCELP	Number of confining pressures at which triaxial test data is supplied as input	
NCPIN	Cycle interval for the print of the force unbalance	
NCYCM	Maximum number of iterations permitted in one step	
NFIX()	Code to indicate the type of boundary displacement conditions prescribed	(NUMBC)
NLOAD	Number of nodes at which the loads are specified in a particular step	
NOBSET	Number of sets of elements for which the overburden factor is prescribed	
NOPIN	Cycle interval for the print of displacements and stresses	
NP()	A vector used in the process of inversion of nodal point stiffness and modification of boundary flexibility	(NUMNP,10)
NPB()	Nodal number at which the type of boundary displacement is specified	(NUMBC)
NPI()	Nodal number for node i of a read or generated element	(NUMEL)
NPIR()	Nodal number for node i of a read element	(NUMER)
NPJ()	Nodal number for node j of a read or generated element	(NUMEL)
NPJR()	Nodal number for node j of a read element	(NUMER)

<u>Name</u>	<u>Description</u>	<u>Minimum Size When Applicable</u>
NPK()	Nodal number for node k of a read or generated element	(NUMEL)
NPKR()	Nodal number for node k of a read element	(NUMER)
NPNUM()	Nodal number of the read or generated nodes	(NUMNP)
NPNUR()	Nodal number of the read nodes only	(NURNP)
NSET	Number of elements excluding the one read for which the same overburden factor has to be assigned	
NSTEP	Number of steps for the analysis	
NSTRN	Number of axial strain points at which the triaxial data is supplied	
NTENS	Code to identify whether shear failure is to be considered or not	
NUMAT	Number of material types present in the given problem	
NUMBC	Number of boundary points at which displacements are prescribed in the problem	
NUMBCS	Number of boundary points at which displacements are specified in the step considered	
NUME()	Element number for read or generated elements	(NUMEL)
NUMEL	Number of elements in the problem	
NUMELS	Number of elements in the step considered	
NUMER()	Element number for read elements only	(NUREL)
NUMNP	Number of nodal points in the problem	
NUMNPS	Number of nodal points in the step considered	
NUREL	Number of read elements	

<u>Name</u>	<u>Description</u>	<u>Minimum Size When Applicable</u>
NURNP	Number of read nodal points	
OBFAC()	Overburden factor	(NUMEL)
PA()	Angle of inclination in degrees of the major principal stress with x-axis in an element	
RO()	Density of the material in read or generated elements	(NUMEL)
ROR()	Density of the material in read elements only	(NUREL)
ROREAD()	Density of the material read for each material type	(NUMAT)
SD()	Deviatoric stresses read from test data	(NSTRN, NCELP, NUMAT)
SIGINT()	A vector used in the conversion of data from triaxial form to stress invariant form	(NCELP, NUMAT)
SIGINV()	A vector used in the conversion of data from triaxial form to stress invariant form	(NSTRN, NCELP, NUMAT)
SL()	Number of triaxial cell pressure values at which data is supplied	(NCELP, NUMAT)
SLOPE()	Slope of the boundary along which a boundary point moves	NUMBC
ST()	Number of percent axial strain values at which triaxial data is supplied	(NSTRN, NUMAT)
SXX()	Vector used in the inversion of stiffness	(NUMNP,9)
SXY()	Vector used in the inversion of stiffness	(NUMNP,9)
SYX()	Vector used in the inversion of stiffness	(NUMNP,9)
SY Y()	Vector used in the inversion of stiffness	(NUMNP,9)

<u>Name</u>	<u>Description</u>	<u>Minimum Size When Applicable</u>
TAD()	A vector used to identify the nodes at which displacements are specified	(NUMNP)
TAL()	A vector used to identify the nodes at which loads are specified	(NUMNP)
THERM()	Thermal stress in an element	(NUMEL)
TOCTD()	Octahedral shear stress	(NSTRN, NCELP,NUMAT)
VS()	Volumetric strain obtained from triaxial test	(NSTRN, NCELP,NUMAT)
VSTN()	A vector used in the conversion of the triaxial test data to stress invariant form	(NSTRN, NCELP,NUMAT)
XMAX()	Maximum principal stress in an element	(NUMEL)
XMIN()	Minimum principal stress in an element	(NUMEL)
XLDR()	X-load at read nodes only	(NURNP)
XLOAD()	X-load at read or generates nodes	(NUMNP)
XORD()	X-coordinate for read or generated nodes	(NUMNP)
XORDR()	X-coordinate for read nodes only	(NURNP)
XU()	Poisson's ratio assigned to read or generate elements	(NUMEL)
XUR()	Poisson's ratio assigned to read elements	(NUREL)
XYV()	Total shear stress in an element	(NUMEL)
XV()	Total x-stress in an element	(NUMEL)
YLDR()	Y-load at read nodes only	(NURNP)
YLOAD()	Y-load at read or generated nodes	(NUMNP)
YORD()	Y-coordinate for read or generated nodes	(NUMNP)

<u>Name</u>	<u>Description</u>	<u>Minimum Size When Applicable</u>
YORDR()	Y-coordinate for read nodes only	(NURNP)
YV()	Total y-stress in an element	(NUMEL)

A.5 Input Data Procedure

A.4.1 has to be referred for the explanations of the name of variables used in this section.

(1) Control cards (Number of Cards = 2)

(a) Card 1 (18A4)

1-72 HEAD Title card for identification of the problem

(b) Card 2 (9I5)

1-5 NUMEL

6-10 NUREL

11-15 NUMNP

16-20 NURNP

21-25 NUMBC

25-30 NUMAT

31-35 NANLYS Equal to zero for linear analysis;
equal to 1 for non-linear analysis

36-40 IANLYS Equal to zero for plane strain analysis;
equal to 1 for plane stress analysis

41-45 IGEN Equal to zero for non-uniform pattern of generation of element;
equal to 1 for uniform pattern of generation of elements. The patterns are given below.

Uniform Pattern:

Non-Uniform Pattern:

(2) Element data cards (Number of cards = NUREL) (4I5)

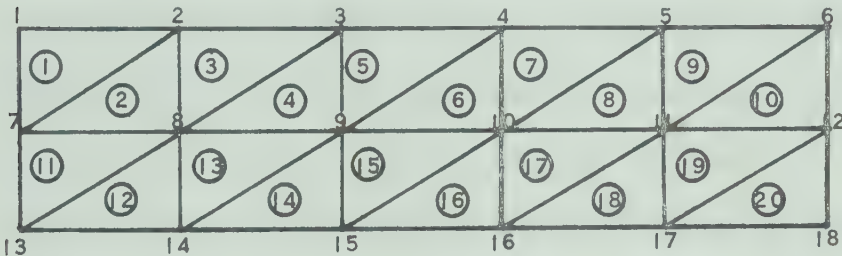
1-5 NUMER()

5-10 NPIR()

11-15 NPJR()

16-20 NPKR()

Example for uniform element pattern generation:

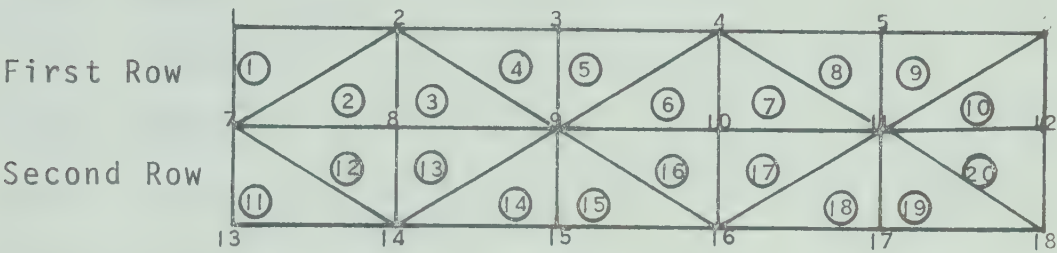


The element numbers have been circled. To generate the above mesh pattern it is necessary to supply the information regarding the first and the last element in each row. Here for example elements 1, 10, 11 and 20 are to be read in. The nodes i, j and k for these elements are to be given in the anticlock wise direction as shown below:

<u>Name of Element</u>	<u>Node i</u>	<u>Node j</u>	<u>Node k</u>
1	2	1	7
10	6	11	12
11	8	7	13
20	12	17	18

NUREL for this example is 4 and NUMEL is 20.

Example for non-uniform element pattern generation:



The element numbers have been circled. To generate the above mesh pattern it is necessary to supply information regarding the first and last elements in the first row and the first three elements and the last element in the second row. This is due to the difference between the orientation of the element 11 and the element 1. The following gives the nodal data to be supplied in the anticlock wise direction.

<u>Name of Element</u>	<u>Node i</u>	<u>Node j</u>	<u>Node k</u>
1	2	1	7
10	6	11	12
11	7	13	14
12	7	14	8
13	9	8	14
20	11	18	12

NUREL for this example is 6 while NUMEL is 20.

The intermediate elements will be assigned the same values of modulus, density, etc. as those read for the end elements.

(3) Nodal data cards (Number of cards = NURNP) (I5,4F10.0,
2F12.8)

1-5 NPNUR()
6-15 XORDR()
16-25 YORDR()
26-35 XLDR()
36-45 YLDR()
46-57 DSXR()
58-69 DSYR()

When the intermediate nodes between the two extreme nodes are equally spaced in one coordinate direction with the distance in other coordinate direction being the same, the intermediate nodes are generated with equal distances between them, each distance being equal to the total distance between the extreme nodes read divided by the difference between the nodal numbers. The intermediate nodes are assigned the proper nodal numbers. The other quantities like displacements, loads, etc. for the intermediate nodes will be the same as those read for the extreme nodes.

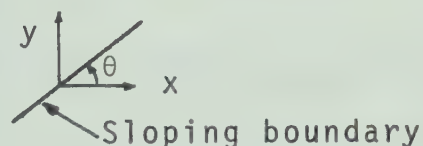
(4) Boundary point displacement cards (Number of cards = NUMBC) (2I5,F8.3)

1-5 NPB()
6-10 NFIX()
11-18 SLOPE()

The following codes have been used to define the mode of displacement at a given boundary point.

x-direction	y-direction	Sloping Boundary	NFIX()	SLOPE()
Zero displacement	Zero displacement		0	0
Zero displacement			1	0
	Zero displacement		2	0
		Free to move along a slop- ing boundary	2	$\tan \theta$

Sloping boundary is as shown:



(5) Material type generation card (1 card) (I5)

1-5 MATN If there is only one material a blank card is required and the material number cards given in (6) below are omitted. All elements are automatically assigned a material number equal to 1.

(6) Material number cards (Number of cards = MATN) (2I5)

1-5 M Element number

6-10 MAT(M) Assigned material number

(7) Material properties cards (Number of cards = NUMAT) (5F10.0)

1-10 ROREAD()

11-20 EBREAD() Normally assigned in a linear analysis

21-30 ESREAD() Normally assigned in a linear analysis

31-40 ACOEF() Needed if shear failure has to be considered

41-50 BCOEF() Needed if shear failure has to be considered

(8) Overburden factor control card (1 card) (I5)

1-5 NOBSET If the analysis is linear NOBSET = 0 and (9) is omitted

(9) Overburden factor cards (Number of cards = NOBSET)

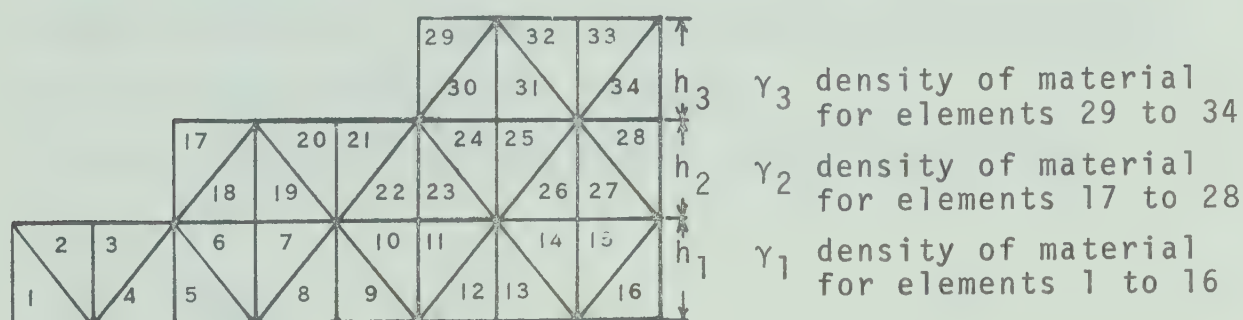
(2I5,F10.0)

1-5 M Element number

6-10 NSET

11-20 OBFAC() To be given only if value is not equal to one.

The following example provides an explanation for (8) and (9).



When a non-linear analysis has to be performed for gravity loaded structures the initial moduli are computed for each element considering the overburden pressure at the mid height of the element. In the sketch shown above there are 34 elements to be considered in a particular step. The overburden pressure at the mid height of a certain element say 16 is $(\gamma_1 h_1/2 + \gamma_2 h_2 + \gamma_3 h_3)$ where γ_1 , γ_2 and γ_3 are the densities of the materials and h_1 , h_2 and h_3 are the heights as shown. Now the overburden factor can be defined for the element 16 as follows:

$$\text{OBFAC}(16) = (\gamma_1 h_1/2 + \gamma_2 h_2 + \gamma_3 h_3) / (\gamma_1 h_1/2).$$

If for example $h_1 = h_2 = h_3 = h$ and $\gamma_1 = \gamma_2 = \gamma_3 = \gamma$ then the overburden factor control card and the overburden factor cards will be as given below.

NOBSET = 3

<u>M</u>	<u>NSET</u>	<u>OBFAC(M)</u>
5	5	3.0
11	5	5.0
23	5	3.0

OBFAC(M) = 1.0 is automatically set in the program and hence need not be supplied in the data. In the present example elements 1 to 4, 17 to 22 and 29 to 34 will have an overburden factor equal to unity.

(10) Triaxial test data control card (1 card) (2I5,F10.0)

1-5 NCELP

6-10 NSTRN

11-20 CONFAC

If the analysis is linear a blank card for (10) has to be substituted and (11), (12), (13) are to be omitted.

(11) Cell pressure card (1 card) (10F5.0)

If the test results are to be supplied say at 0, 5, 10, 30 and 40 psi cell pressure values, the input is as follows:

1-5 0.0

6-10 5.0

11-15 10.0

16-20 30.0

21-25 40.0

(12) Axial strain and deviatoric stress cards (Number of cards = NSTRN) (11F5.0)

Each card will have the axial strain punched in the first

five columns and the deviatoric stresses corresponding to the various cell pressures (given in (11)) at that particular axial strain are punched in the subsequent columns.

- (13) Axial strain and volumetric strain cards (Number of cards = NSTRN) (11F5.0)

Each card will have the axial strain punched in the first five columns and the volumetric strain corresponding to the various cell pressures (given in (11)) at that particular axial strain are punched in the subsequent columns. Volume expansion has to be neglected while giving the volumetric strain input.

- (14) Option for "no tension" analysis (1 card) (I5)

1-5 KOPT Equal to zero when "no tension" analysis is not needed and equal to one when it is needed

- (15) Option for analyzing each step once or twice (1 card) (I5)

1-5 ITOPT Equal to zero for analysis once and equal to one for analysis twice. If the analysis is linear ITOPT = 0.

- (16) Number of steps and option for consideration of shear failure (1 card) (2I5)

1-5 NSTEP For a single step analysis NSTEP = 1

6-10 NTENS If shear failure is to be considered NTENS = 1, otherwise NTENS = 0

- (17) Nodal loads control card (1 card) (I5)

1-5 NLOAD If NLOAD is equal to zero (18) is omitted

- (18) Nodal loads specified in the step considered (Number of cards = NLOAD) (I5,2F10.0)

1-5 N Nodal number

6-15 YLOAD(N)

16-25 XLOAD(N)

(19) Nodal displacements control card (1 card) (I5)

1-5 NBOUN If NBOUN is equal to zero (20) is omitted

(20) Nodal displacements specified in the step considered
(as many as the number NBOUN) (I5,2F10.0)

1-5 M Nodal Number

6-15 DSY(M)

16-25 DSX(M)

A.6 Output of Results

The following results are obtained as output:

- (1) The complete nodal and element data with the initial values of the elastic parameters assigned to each element.
- (2) Cumulative nodal displacements, element stresses, and strains for each step of the analysis.
- (3) Element principal stresses and strains for each step of the analysis.
- (4) Elastic parameters assigned to each element in each step of the analysis.

A.7 Listing of Program

A listing of the two dimensional program follows.


```

6      C
7      C
8      C TWO DIMENSIONAL FINITE ELEMENT PROGRAM WITH CONSTANT STRAIN TRIANGULAR
9      C
10     C ELEMENTS OF 6 DEGREES OF FREEDOM FOR EACH ELEMENT.PLANE STRAIN/ STRESS.
11     C
12     C LINEAR/ NONLINEAR, SINGLE/ MULTIPLE STEP ANALYSIS (WITH OPTION FOR
13     C
14     C REMOVAL OF TENSILE STRESSES) CAN BE PERFORMED.
15     C
16     C
17     C
18     C ORIGINAL PROGRAM DEVELOPED BY E.L.WILSON (UNIVERSITY OF CALIFORNIA,1962)
19     C
20     C PROGRAM MODIFIED BY Z.EISENSTEIN (UNIVERSITY OF ALBERTA,1969) AND
21     C
22     C A.V.G. KRISHNAYYA (UNIVERSITY OF ALBERTA, 1970)
23     C
24     C
25     C
26     C      MAIN PROGRAM
27     C
28     C
29     C
30     C      DIMENSION AND COMMON STATEMENTS
31     C
32     C
33     C      DIMENSION EBULK(400),ESHEAR(400),OBFAC(400),HEAD(18),
34     C      1DSX(250),DSY(250),XLOAD(250),YLOAD(250),NP(250,10),SXX(250,9),
35     C      2SXY(250,9),SYX(250,9),SYY(250,9),NAP(250),PA(400),
36     C      3NPNUR(250),XORDR(250),YORDR(250),XLDR(250),YLDR(250),DSXR(250),
37     C      4DSYR(250),TAD(250),MAT(400),TAL(250),          ET(400),
38     C      5XU(400),RO(400),COED(400),DT(400),THERM(400),AJ(400),
39     C      6BJ(400),AK(400),BK(400),GAMV(400),
40     C      7SLOPE(50),NUMER(150),NPIR(150),NPJR(150),NPKR(150),ETR(150),
41     C      8 ROR(150),XUR(150),COEDR(150),DTR(150),NPB(50),NFI(50),LM(3),
42     C      9A(6,6),B(6,6),S(6,6),THETA(50)
43     C      COMMON/AREA1/SXX,SXY,SYX,SYY
44     C      COMMON/AREA2/
45     C      1 XORD(250),YORD(250),NPI(400),NPJ(400),NPK(400),NPNUM(250),
46     C      1NUME(400),NUMNP,NUMEL
47     C      DIMENSION DSXQ(250),DSYQ(250),          XV(400),
48     C      1YV(400),XYV(400),EPXV(400),EPYV(400),XMAX(400),XMIN(400),EMAX(400)
49     C      2,EMIN(400)
50     C      COMMON/AREA3/
51     C      1 ST(20,5),SL(20,5),SD(20,10,5),VS(20,10,5),NUMAT,
52     C      2NCELP,CONFAC,NSTRN
53     C      DIMENSION ROREAD( 5),EBREAD( 5),ESREAD( 5),ACOE( 5),BCOE( 5)
54     C
55     C
56     C READ PROBLEM CONTROL CARDS
57     C
58     C
59     C      150 READ(5,100)HEAD
60     C      WRITE(6,99)
61     C      WRITE(6,100)HEAD

```



```

62      READ(5,1) NUMEL,NUREL,NUMNP,NURNP,NUMBC,NUMAT,NANLYS,IANLYS,IGEN
63      WRITE(6,101) NUMEL
64      WRITE(6,125) NUREL
65      WRITE(6,102) NUMNP
66      WRITE(6,124) NURNP
67      WRITE(6,103) NUMBC
68      WRITE(6,2000) NUMAT
69      C
70      C
71      C READ ELEMENT DATA
72      C
73      C
74      READ(5,9) (NUMER(N),NPIR(N),NPJR(N),NPKR(N),N=1,NUREL)
75
76
77      C READ NODAL DATA
78      C
79      C
80      READ(5,3)
81      1      (NPNUR(M),XORDR(M),YORDR(M),XLDR(M),YLDR(M),
82      2DSXR(M),DSYR(M),M=1,NURNP)
83      C
84      C GENERATION OF NOT READ ELEMENTS
85      C
86      DO 161 N=1,NUREL
87      M=N+1
88      IF(M-NUREL) 162,162,163
89      162 I=NUMER(M)-NUMER(N)
90      IF(I-1) 163,163,164
91      164 L=NUMER(N)
92      NPA=NPIR(N)
93      NPC=NPKR(N)
94      K=0
95      KO=2*K
96      KE=1
97      IO=I+1
98      IF(IGEN.EQ.0) GO TO 3000
99      DO 3166 JO=1,IO
100     J=JO-1
101     LJ=L+J
102     NUME(LJ)=NUMER(N)+J
103     IF(2-KE) 3168,3168,3167
104     3167 NPI(LJ)=NPA+KO
105     NPJ(LJ)=NPA-1+KO
106     NPK(LJ)=NPC+KO
107     GO TO 3174
108     3168 NPI(LJ)=NPA+KO
109     NPJ(LJ)=NPC+KO
110     NPK(LJ)=NPC+1+KO
111     K=K+1
112     KO=K
113     KE=0
114     3174 ET(LJ)=ETR(N)
115     RO(LJ)=ROR(N)
116     XU(LJ)=XUR(N)
117     COED(LJ)=COEDR(N)
118     DT(LJ)=DTR(N)
119     KE=KE+1
120     3166 CONTINUE
121     GO TO 161

```



```

122      3000 DO 166 JO=1,10
123          J=JO-1
124          LJ=L+J
125          NUME(LJ)=NUMER(N)+J
126          IF(2-KE)169,168,167
127      167 NPI(LJ)=NPA+KO
128          NPJ(LJ)=NPA-1+KO
129          NPK(LJ)=NPC+KO
130          GO TO 174
131      168 NPI(LJ)=NPA+KO
132          NPJ(LJ)=NPC+KO
133          NPK(LJ)=NPC+1+KO
134          GO TO 174
135      169 IF(3-KE)172,171,166
136      171 NPI(LJ)=NPA+KO
137          NPJ(LJ)=NPC+1+KO
138          NPK(LJ)=NPC+2+KO
139          GO TO 174
140      172 NPI(LJ)=NPA+KO
141          NPJ(LJ)=NPC+2+KO
142          NPK(LJ)=NPA+1+KO
143          K=K+1
144          KO=2*K
145          KE=0
146      174 ET(LJ)=ETR(N)
147          RO(LJ)=ROR(N)
148          XU(LJ)=XUR(N)
149          COED(LJ)=COEDR(N)
150          DT(LJ)=DTR(N)
151          KE=KE+1
152      166 CONTINUE
153          GO TO 161
154      163 L=NUMER(N)
155          NUME(L)=NUMER(N)
156          NPI(L)=NPIR(N)
157          NPJ(L)=NPJR(N)
158          NPK(L)=NPKR(N)
159          ET(L)=ETR(N)
160          RO(L)=ROR(N)
161          XU(L)=XUR(N)
162          COED(L)=COEDR(N)
163          DT(L)=DTR(N)
164      161 CONTINUE
165 C
166 C
167 C      GENERATION OF NOT READ NODAL POINTS
168 C
169          DO 151 M=1,NURNP
170          N=M+1
171          IF(N-NURNP) 152,152,186
172      152 I=NPNUM(N)-NPNUM(M)
173          GO TO 154
174      186 I=0
175      154 L=NPNUM(M)
176          IO=I+1
177          DO 156 JO=1,10
178          J=JO-1
179          LJ=L+J
180          NPNUM(LJ)=NPNUM(M)+J
181          IF(I=0) 188,188,189

```



```

182      188 XORD(LJ)=XORDR(M)
183      YORD(LJ)=YORDR(M)
184      GO TO 191
185      189 XORD(LJ)=XORDR(M)+((XORDR(N)-XORDR(M))/I)*J
186      YORD(LJ)=YORDR(M)+((YORDR(N)-YORDR(M))/I)*J
187      191 IF(J-0) 158,158,159
188      159 IF(J-I) 157,153,156
189      158 XLOAD(LJ)=XLDR(M)
190      YLOAD(LJ)=YLDR(M)
191      DSX(LJ)=DSXR(M)
192      DSY(LJ)=DSYR(M)
193      GO TO 156
194      153 XLOAD(LJ)=XLDR(N)
195      YLOAD(LJ)=YLDR(N)
196      DSX(LJ)=DSXR(N)
197      DSY(LJ)=DSYR(N)
198      GO TO 156
199      157 XLOAD(LJ)=0
200      YLOAD(LJ)=0
201      DSX(LJ)=0
202      DSY(LJ)=0
203      156 CONTINUE
204      151 CONTINUE
205  C
206  C      INITIALIZE TOTAL DISPLACEMENTS AND STRESSES AND STRAINS
207      606 DO 10 J=1,NUMNP
208      DSX0(J)=0.0
209      DSY0(J)=0.0
210      10 CONTINUE
211      DO 11 J=1,NUMEL
212      XV(J)=0.
213      YV(J)=0.
214      XYV(J)=0.
215      EPXV(J)=0.
216      EPYV(J)=0.
217      11 CONTINUE
218      WRITE(6,111)
219      WRITE(6,109) (NPNUM(M),XORD(M),YORD(M),XLOAD(M),YLOAD(M),
220      1DSX(M),DSY(M),M=1,NUMNP)
221  C
222  C
223  C      READ BOUNDARY CONDITIONS.
224  C
225  C
226      READ(5,4) (NPB(L),NFI(X(L),SLOPE(L),          L=1,NUMBC)
227  C
228  C
229      WRITE(6,112)
230      WRITE(6,4) (NPB(L),NFI(X(L),SLOPE(L),          L=1,NUMBC)
231  C      ASSIGN PROPER MATERIAL NUMBER IF NECESSARY
232      DO 854 I=1,NUMEL
233      854 MAT(I)=1
234      READ(5,6) MATN
235      IF(MATN.EQ.0) GO TO 56
236      DO 55 I=1,MATN
237      55 READ(5,20) M,MAT(M)
238  C
239  C      ACDEF=2.*COS(PHI)/(1.-SIN(PHI)),BCDEF=2.*SIN(PHI)/(1-SIN(PHI))
240  C
241  C

```



```

242 C READ MATERIAL PROPERTIES.
243 C
244 C
245 56 DO 850 I=1,NUMAT
246 READ(5,2010) ROREAD(I),EBREAD(I),ESREAD(I),ACOE(I),BCOE(I)
247 WRITE(6,2020)ROREAD(I),EBREAD(I),ESREAD(I),ACOE(I),BCOE(I)
248 850 CONTINUE
249 DO 57 N=1,NUMEL
250 I=MAT(N)
251 RO(N)=ROREAD(I)
252 EBULK(N)=EBREAD(I)
253 ESHEAR(N)=ESREAD(I)
254 OBFAC(N)=1.0
255 57 CONTINUE
256 C
257 C
258 C READ OVERBURDEN FACTOR
259 C
260 C
261 READ (5,6) NOBSET
262 IF(NOBSET.EQ.0) GO TO 48
263 DO 771 I=1,NOBSET
264 READ (5,753) M,NSET,OBFAC(M)
265 IF (NSET.EQ.0) GO TO 771
266 DO 772 J=1,NSET
267 M=M+1
268 772 OBFAC(M)=OBFAC(M-1)
269 771 CONTINUE
270 C
271 C
272 C READ TRIAXIAL TEST DATA CONTROL CARD.
273 C
274 C
275 48 READ(5,2021) NCELP,NSTRN,CONFAC
276 IF(NCELP.EQ.0) GO TO 44
277 CALL TESTD
278 C
279 C
280 C INTERPOLATE INITIAL MODULI FOR ALL ELEMENTS
281 C
282 C
283 DO 600 M=1,NUMEL
284 IF(RO(M).LE.0.0) GO TO 600
285 I=NPI(M)
286 J=NPJ(M)
287 K=NPJ(M)
288 Y1=ABS(YORD(I)-YORD(J))
289 Y2=ABS(YORD(J)-YORD(K))
290 Y3=ABS(YORD(K)-YORD(I))
291 DEPTH=0.0
292 IF(Y1.GT.DEPH) DEPTH=Y1
293 IF(Y2.GT.DEPH) DEPTH=Y2
294 IF(Y3.GT.DEPH) DEPTH=Y3
295 DEPTH=DEPTH/2.
296 NCOUNT=0
297 N=MAT(M)
298 OBP=DEPTH*RO(M)*OBFAC(M)
299 AVGSIG=OBP*.5
300 18 NCOUNT=NCOUNT+1
301 SIGM1=OBP

```



```

302      SIGM2=AVGSIG
303      SIGM3=AVGSIG
304      SIGOCT=(SIGM1+SIGM2+SIGM3)/3.
305      SIGIN=SIGM1*SIGM2*SIGM3
306      CONF5=SIGIN/(SIGOCT**2)
307      DIVOCT=SQRT((SIGM1-SIGM2)**2+(SIGM2-SIGM3)**2+(SIGM3-SIGM1)**2)
308      DIVOCT=DIVOCT/3.
309      DO 720 J=1,NCELP
310      JLS=J
311      IF( CONF5-SL(J,N)) 721,720,720
312 720 CONTINUE
313 721 CONTINUE
314      DO 790 K=1,NSTRN
315      JS1=K
316      IF(DIVOCT-SD(K,JLS-1,N)) 791,790,790
317 790 CONTINUE
318 791 CONTINUE
319      DO 50 K=1,NSTRN
320      JS2=K
321      IF(DIVOCT-SD(K,JLS,N)) 51,50,50
322 50 CONTINUE
323 51 CONTINUE
324      PR1=1.061*(VS(JS1,JLS-1,N)-VS(JS1-1,JLS-1,N))/(ST(JS1,N)-ST(JS1-1,
325      IN))-1.0
326      IF(PR1.GT.0.49) PR1=0.49
327      PR2=1.061*(VS(JS2,JLS,N)-VS(JS2-1,JLS,N))/(ST(JS2,N)-ST(JS2-1,
328      IN))-1.0
329      IF(PR2.GT.0.49) PR2=0.49
330      PR3=PR1+((PR2-PR1)*(CONF5-SL(JLS-1,N))/(SL(JLS,N)-SL(JLS-1,N)))
331      IF(PR3.GT.0.49) PR3=0.49
332      CONST=PR3/(1.-PR3)
333      HPR=OBP*CONST
334      HPR=(HPR+AVGSIG)/2.
335      CSTRS=ABS(HPR-AVGSIG)
336      IF(NCOUNT.GE.21) GO TO 52
337      IF(ABS(HPR-AVGSIG).LT.0.01) GO TO 52
338      AVGSIG=HPR
339      GO TO 18
340 52 WRITE(6,125) M,NCOUNT,HPR,CSTRS,PR3
341      DIF1=SD(JS1,JLS-1,N)-SD(JS1-1,JLS-1,N)
342      ETP1=DIF1/(ST(JS1,N)-ST(JS1-1,N))
343      GTP1=ETP1/(0.9428*(1.+PR1))
344      DIF2=SD(JS2,JLS,N)-SD(JS2-1,JLS,N)
345      ETP2=DIF2/(ST(JS2,N)-ST(JS2-1,N))
346      GTP2=ETP2/(0.9428*(1.+PR2))
347      GTP=GTP1+(GTP2-GTP1)*(CONF5-SL(JLS-1,N))/(SL(JLS,N)-SL(JLS-1,N))
348      GTP=100.*GTP
349      EBULK(M)=GTP*2.*(1.+PR3)/(3.*(1.-2.*PR3))
350      ESHEAR(M)=GTP
351 600 CONTINUE
352      IF(NCELP.NE.0) GO TO 46
353 44 IF(NANLYS.EQ.0) GO TO 46
354 46 WRITE(6,110)
355 C
356 C
357 C PRINT ELEMENT DATA
358 C
359 C
360      WRITE(6,2055){NUME(N),NPI(N),NPJ(N),NPK(N),EBULK(N),RO(N),ESHEAR(N
361      1),MAT(N),N=1,NUMEL)

```



```

362      C
363      C
364      C  READ PARTICULARS  OF CURRENT STEP.
365      C
366      C
367          READ(5,6) KOPT
368          READ(5,6) ITOPT
369          READ(5,20) NSTEP,NTENS
370          DO 500 JM = 1,NSTEP
371          READ(5,13) NUMELS,NUMNPS,NUMBCS,NCPIN,NOPIN,NCYCM,TOLER,XFAC,LNUM
372          NUMEL=NUMELS
373          NUMNP=NUMNPS
374          NUMBC=NUMBCS
375          DO 761 N=1,NUMNP
376          TAD(N)=0.0
377          TAL(N)=0.0
378      761  CONTINUE
379      C
380      C
381      C  READ BOUNDARY LOADS FOR CURRENT STEP
382      C
383      C
384          READ(5,5) NLOAD
385          IF(NLOAD.EQ.0) GO TO 4050
386          DO 4051 I=1,NLOAD
387          READ(5,602) N,YLOAD(N),XLOAD(N)
388          IF(YLOAD(N).NE.0.0) TAL(N)=2.0
389          IF(XLOAD(N).NE.0.0) TAL(N)=1.0
390      4051  CONTINUE
391      C
392      C
393      C  READ BOUNDARY DISPLACEMENTS FOR CURRENT STEP
394      C
395      C
396      4050  READ(5,6) NBOUN
397          IF(NBOUN.EQ.0) GO TO 41
398          DO 601 N=1,NBOUN
399          READ(5,602) M,DSY(M),DSX(M)
400          IF(DSY(M).NE.0.0) TAD(M)=2.0
401          IF(DSX(M).NE.0.0) TAD(M)=1.0
402      601  CONTINUE
403      41  WRITE (6,101) NUMEL
404          WRITE(6,102) NUMNP
405          WRITE(6,103) NUMBC
406          WRITE(6,104) NCPIN
407          WRITE(6,105) NOPIN
408          WRITE(6,106) NCYCM
409          WRITE(6,107) TOLER
410          WRITE(6,108) XFAC
411          WRITE(6,117) LNUM
412          NITER=0
413          IF(NSTEP.EQ.1) GO TO 160
414          IF(NCELP.EQ.0) GO TO 160
415          WRITE(6,110)
416          WRITE(6,2055) (NUME(N),NPI(N),NPJ(N),NPK(N),EBULK(N),RO(N),ESHEAR(N
417          1), MAT(N),      N=1,NUMEL)
418          WRITE(6,111)
419          WRITE(6,109) (NPNUM(M),XORD(M),YORD(M),XLOAD(M),YLOAD(M),
420          1DSX(M),DSY(M),M=1,NUMNP)
421      C

```



```

422      C      INITIALIZATION
423      C
424      160 NCYCLE=0
425      NITER=NITER+1
426      NUMPT=NCPIN
427      NUMOPT=NOPI
428      DO 175 L=1,NUMNP
429      DO 170 M=1,9
430      SXX(L,M)=0.0
431      SXY(L,M)=0.0
432      SYX(L,M)=0.0
433      SYY(L,M)=0.0
434      170 NP(L,M)=0
435      NP(L,10)=0
436      175 NP(L,1)=L
437      C
438      C      MODIFICATION OF LOADS AND ELEMENT DIMENSIONS
439      C
440      NERROR=0
441      DO 180 N=1,NUMEL
442      ET(N)=0.0
443      COED(N)=0.0
444      DT(N)=0.0
445      XU(N)=0.0
446      I=NP I(N)
447      J=NP J(N)
448      K=NP K(N)
449      AJ(N)=XORD(J)-XORD(I)
450      AK(N)=XORD(K)-XORD(I)
451      BJ(N)=YORD(J)-YORD(I)
452      BK(N)=YORD(K)-YORD(I)
453      176 AREA=(AJ(N)*BK(N)-BJ(N)*AK(N))/2.
454      IF (AREA) 701,701,177
455      177 THERM(N)=ET(N)*COED(N)*DT(N)/(XU(N)-1.)
456      DL=AREA*RO(N)/3.
457      XLOAD(I)=THERM(N)*(BK(N)-BJ(N))/2.+XLOAD(I)
458      XLOAD(J)=-THERM(N)*BK(N)/2.+XLOAD(J)
459      XLOAD(K)=THERM(N)*BJ(N)/2.+XLOAD(K)
460      YLOAD(I)=THERM(N)*(AJ(N)-AK(N))/2.+YLOAD(I)-DL
461      YLOAD(J)=THERM(N)*AK(N)/2.+YLOAD(J)-DL
462      YLOAD(K)=-THERM(N)*AJ(N)/2.+YLOAD(K)-DL
463      IF (AREA.GT.0.0) GO TO 180
464      701 WRITE(6,711)N
465      NERROR=NERROR+1
466      180 CONTINUE
467      IF (NERROR.GT.0) GO TO 925
468      C
469      C      FORMATION OF STIFFNESS ARRAY
470      C
471      DO 200 N=1,NUMEL
472      AREA=(AJ(N)*BK(N)-AK(N)*BJ(N))+.5
473      COMM=0.25/AREA
474      A(1,1)=BJ(N)-BK(N)
475      A(1,2)=0.0
476      A(1,3)=BK(N)
477      A(1,4)=0.0
478      A(1,5)=-BJ(N)
479      A(1,6)=0.0
480      A(2,1)=0.0
481      A(2,2)=AK(N)-AJ(N)

```



```

482      A(2,3)=0.0
483      A(2,4)=-AK(N)
484      A(2,5)=0.0
485      A(2,6)=AJ(N)
486      A(3,1)=AK(N)-AJ(N)
487      A(3,2)=BJ(N)-BK(N)
488      A(3,3)=-AK(N)
489      A(3,4)=BK(N)
490      A(3,5)=AJ(N)
491      A(3,6)=-BJ(N)
492      IF(IANLYS.EQ.0) COM1=EBULK(N)+ESHEAR(N)*(4./3.)
493      IF(IANLYS.EQ.0) COM2=EBULK(N)-ESHEAR(N)*(2./3.)
494      IF(IANLYS.GT.0) COM1=4.*ESHEAR(N)*(EBULK(N)+ESHEAR(N)/3.)/(EBULK(N)
495      I)+(4./3.)*ESHEAR(N)
496      IF(IANLYS.GT.0) COM2=2.*ESHEAR(N)*(EBULK(N)-(2./3.)*ESHEAR(N))/(EB
497      IULK(N)+(4./3.)*ESHEAR(N))
498      B(1,1)=      COMM*COM1
499      B(1,2)=COMM*COM2
500      B(1,3)=0.0
501      B(2,1)=COMM*COM2
502      B(2,2)=COMM*COM1
503      B(2,3)=0.0
504      B(3,1)=0.0
505      B(3,2)=0.0
506      B(3,3)=COMM*ESHEAR(N)
507  C
508      DO 182 J=1,6
509      DO 182 I=1,3
510      S(I,J)=0.0
511      DO 182 K=1,3
512      182 S(I,J)=S(I,J)+B(I,K)*A(K,J)
513      DO 183 J=1,6
514      DO 183 I=1,3
515      183 B(J,I)=S(I,J)
516      DO 184 J=1,6
517      DO 184 I=1,6
518      S(I,J)=0.0
519      DO 184 K=1,3
520      184 S(I,J)=S(I,J)+B(I,K)*A(K,J)
521  C
522      LM(1)=NPI(N)
523      LM(2)=NPJ(N)
524      LM(3)=NPK(N)
525      DO 200 L=1,3
526      DO 200 M=1,3
527      LX=LM(L)
528      MX=0
529      185 MX=MX+1
530      IF(NP(LX,MX)-LM(M)) 190,195,190
531      190 IF(NP(LX,MX)) 185,195,185
532      195 NP(LX,MX)=LM(M)
533      IF(MX-10) 196,702,702
534      196 SXX(LX,MX)=SXX(LX,MX)+S(2*L-1,2*M-1)
535      SXY(LX,MX)=SXY(LX,MX)+S(2*L-1,2*M)
536      SYX(LX,MX)=SYX(LX,MX)+S(2*L,2*M-1)
537      200 SYY(LX,MX)=SYY(LX,MX)+S(2*L,2*M)
538  C
539  C      COUNT OF ADJACENT NODAL POINTS
540  C
541      DO 206 M=1,NUMNP

```



```

542      MX=1
543      205 MX=MX+1
544      IF (NP(M,MX)) 206,206,205
545      206 NAP(M)=MX-1
546      C
547      C      INVERSION OF NODAL POINT STIFFNESS
548      C
549      DO 210 M=1,NUMNP
550      COMM=SXX(M,1)*SYY(M,1)-SXY(M,1)*SYX(M,1)
551      TEMP=SYY(M,1)/COMM
552      SYY(M,1)=SXX(M,1)/COMM
553      SXX(M,1)=TEMP
554      SXY(M,1)=-SXY(M,1)/COMM
555      SYX(M,1)=-SYX(M,1)/COMM
556      210 CONTINUE
557      C
558      C      MODIFICATION OF BOUNDARY FLEXIBILITIES
559      C
560      DO 240 L=1,NUMBC
561      M=NPB(L)
562      NP(M,1)=0
563      IF(NFIX(L)-1) 225,220,215
564      215 C=(SXX(M,1)*SLOPE(L)+SXY(M,1))/(SYX(M,1)*SLOPE(L)-SYY(M,1))
565      R=1.-C*SLOPE(L)
566      SXX(M,1)=(SXX(M,1)-C*SYX(M,1))/R
567      SXY(M,1)=(SXY(M,1)-C*SYY(M,1))/R
568      SYX(M,1)=SXX(M,1)*SLOPE(L)
569      SYY(M,1)=SXY(M,1)*SLOPE(L)
570      GO TO 240
571      220 SYY(M,1)=SYY(M,1)-SYX(M,1)*SXY(M,1)/SXX(M,1)
572      GO TO 230
573      225 SYY(M,1)=0.0
574      230 SXX(M,1)=0.0
575      235 SXY(M,1)=0.0
576      SYX(M,1)=0.0
577      240 CONTINUE
578      C
579      C      ITERATION OF NODAL POINT DISPLACEMENTS
580      C
581      KOUNT=0
582      243 WRITE(6,119)
583      KOUNT=KOUNT+1
584      244 SUM=0.0
585      DO 290 M=1,NUMNP
586      NUM=NAP(M)
587      IF (SXX(M,1)+SYY(M,1)) 275,290,275
588      275 FRX=XLOAD(M)
589      FRY=YLOAD(M)
590      DO 280 L=2,NUM
591      N=NP(M,L)
592      FRX=FRX-SXX(M,L)*DSX(N)-SXY(M,L)*DSY(N)
593      280 FRY=FRY-SYX(M,L)*DSX(N)-SYY(M,L)*DSY(N)
594      DX=SXX(M,1)*FRX+SXY(M,1)*FRY-DSX(M)
595      DY=SYX(M,1)*FRX+SYY(M,1)*FRY-DSY(M)
596      DSX(M)=DSX(M)+XFAC*DX
597      DSY(M)=DSY(M)+XFAC*DY
598      IF(NP(M,1)) 285,290,285
599      285 SUM=SUM+ABS(DX/SXX(M,1))+ABS(DY/SYY(M,1))
600      290 CONTINUE
601      C

```



```

602      C      CYCLE COUNT AND PRINT CHECK
603      C
604          NCYCLE=NCYCLE+1
605          IF (NCYCLE-NUMPT) 305,300,300
606      300  NUMPT=NUMPT+NCPIN
607          WRITE(6,120)NCYCLE,SUM
608      305  IF (SUM-TOLER) 400,400,310
609      310  IF (NCYCM-NCYCLE) 400,400,315
610      315  IF (NCYCLE-NUMOPT) 244,320,320
611      320  NUMOPT=NUMOPT+NOPIN
612      C
613      C      PRINT OF DISPLACEMENTS AND STRESSES
614      C
615      400  CONTINUE
616          IF (SUM-TOLER) 440,440,430
617      430  IF (NCYCM-NCYCLE) 440,440,243
618      440  WRITE(6,975)SUM,TOLER
619      975  FORMAT(5H0SUM=1E15.6,6HTOLER=1E15.6)
620          DO 421 N=1,NUMEL
621              I=NPI(N)
622              J=NPJ(N)
623              K=NPK(N)
624              EPX=(BJ(N)-BK(N))*DSX(I)+BK(N)*DSX(J)-BJ(N)*DSX(K)
625              EPY=(AK(N)-AJ(N))*DSY(I)-AK(N)*DSY(J)+AJ(N)*DSY(K)
626              GAM=(AK(N)-AJ(N))*DSX(I)-AK(N)*DSX(J)+AJ(N)*DSX(K)
627              I+(BJ(N)-BK(N))*DSY(I)+BK(N)*DSY(J)-BJ(N)*DSY(K)
628              COMM=1./((AJ(N)*BK(N)-AK(N)*BJ(N))
629              IF (IANLYS.EQ.0) CCM1=EBULK(N)+ESHEAR(N)*(4./3.)
630              IF (IANLYS.EQ.0) COM2=EBULK(N)-ESHEAR(N)*(2./3.)
631              IF (IANLYS.GT.0) COM1=4.*ESHEAR(N)*(EBULK(N)+ESHEAR(N)/3.)/(EBULK(N)
632              I)+(4./3.)*ESHEAR(N))
633              IF (IANLYS.GT.0) CCM2=2.*ESHEAR(N)*(EBULK(N)-(2./3.)*ESHEAR(N))/(EB
634              ULK(N)+(4./3.)*ESHEAR(N))
635              COM3=ESHEAR(N)
636              X=COMM*(COM1*EPX+COM2*EPY)+THERM(N)
637              Y=COMM*(COM2*EPX+COM1*EPY)+THERM(N)
638              XY=COMM*COM3*GAM
639              XV(N)=XV(N)+X
640              YV(N)=YV(N)+Y
641              XYV(N)=XYV(N)+XY
642              EPXV(N)=EPXV(N)+(EPX*100.)/((AJ(N)*BK(N)-AK(N)*BJ(N))
643              EPYV(N)=EPYV(N)+(EPY*100.)/((AJ(N)*BK(N)-AK(N)*BJ(N))
644              GAMV(N)=GAMV(N)+GAM*100.*COMM
645              C=(XV(N)+YV(N))/2.0
646              R=SQRT(((YV(N)-XV(N))/2.0)**2+XYV(N)**2)
647              XMAX(N)=C+R
648              XMIN(N)=C-R
649              PA(N)=0.5*57.29578*ATAN(2.*XYV(N)/(YV(N)-XV(N)))
650              IF (2.*XV(N)-XMAX(N)-XMIN(N))405,420,420
651      405  IF (PA(N)) 410,420,415
652      410  PA(N)=PA(N)+90.0
653          GO TO 420
654      415  PA(N)=PA(N)-90.0
655      420  ANG=PA(N)*11./630.
656          CC=COS(ANG)**2
657          SS=SIN(ANG)**2
658          SC=COS(ANG)*SIN(ANG)
659          EMAX(N)=EPXV(N)*CC+EPYV(N)*SS-SC*GAMV(N)
660          EMIN(N)=EPXV(N)*SS+EPYV(N)*CC+SC*GAMV(N)
661          IF (ITOPT.EQ.0) GO TO 421

```



```

662      IF(NITER.EQ.2) GO TO 421
663      WRITE(6,124) NUME(N),XV(N),YV(N),XYV(N),XMAX(N),XMIN(N),PA(N),
664      1EPXV(N),EPYV(N),EMAX(N),EMIN(N)
665      XV(N)=XV(N)-X
666      YV(N)=YV(N)-Y
667      XYV(N)=XYV(N)-XY
668      EPXV(N)=EPXV(N)-{(EPX*100.)/(AJ(N)*BK(N)-AK(N)*BJ(N))}
669      EPYV(N)=EPYV(N)-{(EPY*100.)/(AJ(N)*BK(N)-AK(N)*BJ(N))}
670      GAMV(N)=GAMV(N)-GAM*100.*CGMM
671      421 CONTINUE
672      C
673      C
674      C FIND THE MAXIMUM AND MINIMUM PRINCIPAL STRESSES
675      SIG1=0.0
676      SIG2=0.0
677      M1=0
678      M2=0
679      DO 630 M=1,NUMEL
680      IF(XMAX(M).LT.SIG1) GO TO 631
681      SIG1=XMAX(M)
682      M1=M
683      631 IF(XMIN(M).GT.SIG2) GO TO 630
684      SIG2=XMIN(M)
685      M2=M
686      630 CONTINUE
687      WRITE(6,117) JM
688      WRITE (6,633) (SIG1,M1,SIG2,M2)
689      C
690      DO 650 J=1,NUMNP
691      IF(ITOPT.EQ.1.AND.NITER.EQ.1) GO TO 770
692      XLOAD(J)=0.0
693      YLOAD(J)=0.0
694      XORD(J)=XORD(J)+DSX(J)
695      YORD(J)=YORD(J)+DSY(J)
696      DSXQ(J)=DSX(J)+DSXQ(J)
697      DSYQ(J)=DSY(J)+DSYQ(J)
698      DSX(J)=0.0
699      DSY(J)=0.0
700      GO TO 650
701      770 DSXQ(J)=DSX(J)+DSXQ(J)
702      DSYQ(J)=DSY(J)+DSYQ(J)
703      WRITE (6,122) NPNUM(J),DSXQ(J),DSYQ(J)
704      DSXQ(J)=DSXQ(J)-DSX(J)
705      DSYQ(J)=DSYQ(J)-DSY(J)
706      IF(TAD(J).EQ.1.0) DSY(J)=0.0
707      IF(TAD(J).EQ.2.0) DSX(J)=0.0
708      IF(TAD(J).NE.0.0) GO TO 5001
709      DSX(J)=0.0
710      DSY(J)=0.0
711      5001 IF(TAL(J).EQ.1.0) YLOAD(J)=0.0
712      IF(TAL(J).EQ.2.0) XLOAD(J)=0.0
713      IF(TAL(J).NE.0.0) GO TO 650
714      XLOAD(J)=0.0
715      YLOAD(J)=0.0
716      650 CONTINUE
717      IF(KOPT.EQ.0) GO TO 664
718      IF(ITOPT.GT.0.AND.NITER.EQ.1.AND.KOPT.GT.0) GO TO 664
719      IF(KOUNT.GT.1) GO TO 681
720      WRITE(6,121)
721      WRITE(6,122)(NPNUM(M),DSXQ(M),DSYQ(M),M=1,NUMNP)

```



```

722      WRITE(6,123)
723      WRITE(6,124) (NUME(N),XV(N),YV(N),XYV(N),XMAX (N),XMIN (N),PA (N),
724      IEPXV(N),EPYV(N),EMAX (N),EMIN (N),N=1,NUMEL)
725      681 IF(NSTEP.EQ.1) GO TO 925
726      IF(JM.EQ.NSTEP) GC TO 925
727      IF(SIG1.LE.0.005) GO TO 664
728      C  TENSILE STRESS REMOVED
729      DO 660 M=1,NUMEL
730      IF(XMAX(M).LE.0.0) GO TO 660
731      ANG=PA(M)*11./630.
732      I=NPI(M)
733      J=NPJ(M)
734      K=NPK(M)
735      AJ(M)=XORD(J)-XORD(I)
736      AK(M)=XORD(K)-XORD(I)
737      BJ(M)=YORD(J)-YCRD(I)
738      BK(M)=YORD(K)-YORD(I)
739      AJ1=AJ(M)*COS(ANG)+BJ(M)*SIN(ANG)
740      BJ1=-AJ(M)*SIN(ANG)+BJ(M)*COS(ANG)
741      AK1=AK(M)*COS(ANG)+BK(M)*SIN(ANG)
742      BK1=-AK(M)*SIN(ANG)+BK(M)*COS(ANG)
743      R1I=XMAX(M)*(BK1-BJ1)/2.
744      R1I=-R1I
745      R1J=-XMAX(M)*BK1/2.
746      R1J=-R1J
747      R1K=XMAX(M)*BJ1/2.
748      R1K=-R1K
749      XMAX(M)=0.0
750      XV(M)=XMIN(M)*(SIN(ANG)**2)
751      YV(M)=XMIN(M)*(COS(ANG)**2)
752      XYV(M)=XMIN(M)*SIN(ANG)*COS(ANG)
753      IF(XMIN(M).LE.0.0) GO TO 661
754      R2I=XMIN(M)*(AJ1-AK1)/2.
755      R2I=-R2I
756      R2J=XMIN(M)*AK1/2.
757      R2J=-R2J
758      R2K=-XMIN(M)*AJ1/2.
759      R2K=-R2K
760      XMIN(M)=0.0
761      XV(M)=0.0
762      YV(M)=0.0
763      XYV(M)=0.0
764      XLOAD(I)=COS(ANG)*R1I+XLOAD(I)-SIN(ANG)*R2I
765      XLOAD(J)=COS(ANG)*R1J+XLOAD(J)-SIN(ANG)*R2J
766      XLOAD(K)=COS(ANG)*R1K+XLOAD(K)-SIN(ANG)*R2K
767      YLOAD(I)=SIN(ANG)*R1I+YLOAD(I)+COS(ANG)*R2I
768      YLOAD(J)=SIN(ANG)*R1J+YLOAD(J)+COS(ANG)*R2J
769      YLOAD(K)=SIN(ANG)*R1K+YLOAD(K)+COS(ANG)*R2K
770      GO TO 660
771      661 XLOAD(I)=COS(ANG)*R1I+XLOAD(I)
772      XLOAD(J)=COS(ANG)*R1J+XLOAD(J)
773      XLOAD(K)=COS(ANG)*R1K+XLOAD(K)
774      YLOAD(I)=SIN(ANG)*R1I+YLOAD(I)
775      YLOAD(J)=SIN(ANG)*R1J+YLOAD(J)
776      YLOAD(K)=SIN(ANG)*R1K+YLOAD(K)
777      660 CONTINUE
778      WRITE(6,6)KOUNT
779      GO TO 243
780      664 IF(ITOPT.GT.0.AND.NITER.EQ.1) GO TO 764
781      WRITE (6,121)

```



```

782      WRITE(6,122)(NPNUM(M),DSXQ(M),DSYQ(M),M=1,NUMNP)
783      WRITE(6,123)
784      WRITE(6,124) (NUME(N),XV(N),YV(N),XYV(N),XMAX (N),XMIN (N),PA (N),
785      1EPXV(N),EPYV(N),EMAX (N),EMIN (N),N=1,NUMEL)
786  C
787  C
788  C   INTERPOLATE MODULI
789  C
790  C
791      764 DO 501 JJ=1,NUMEL
792          NCOUN=0
793          IF(ITOPT.EQ.0) RO(JJ)=0.0
794          IF(NITER.EQ.2) RO(JJ)=0.0
795          IF (NANLYS.EQ.0) GO TO 500
796          IF(KOPT.GT.0.AND.ITOPT.EQ.1.AND.NITER.EQ.1.AND.XMAX(JJ).GE.0.0) GO
797      1 TO 501
798          AVGSIG=ABS(XMAX(JJ))
799          IF(XMAX(JJ).GE.0.0) AVGSIG=0.0
800          DIVS=ABS(XMIN(JJ))-AVGSIG
801          DIVS=ABS(DIVS)
802          N=MAT(JJ)
803          DIVSF=ACOE(N)+BCOE(N)*ABS(XMAX(JJ))
804          IF(XMAX(JJ).GE.0.0) DIVSF=ACOE(N)
805          IF(NCELP.EQ.0) GO TO 852
806          SIGM1=ABS(XMIN(JJ))
807          SIGM2=(AVGSIG+SIGM1)/2.
808          SIGM3=AVGSIG
809          IF(IANLYS.GT.0) SIGM2=0.0
950      NCOUN=NCOUN+1
811          SIGOCT=(SIGM1+SIGM2+SIGM3)/3.
812          SIGIN=SIGM1*SIGM2*SIGM3
813          CONFS=SIGIN/(SIGOCT**2)
814          DIVOCT=SQRT((SIGM1-SIGM2)**2+(SIGM2-SIGM3)**2+(SIGM3-SIGM1)**2)
815          DIVOCT=DIVOCT/3.
816          DO 26 J=1,NCELP
817              JLS=J
818              IF( CONFS-SL(J,N)) 27,26,26
819      26 CONTINUE
820      27 CONTINUE
821          DO 28 K=1,NSTRN
822              JS1=K
823              IF(DIVOCT-SD(K,JLS-1,N)) 29,28,28
824      28 CONTINUE
825      29 CONTINUE
826          DO 751 K=1,NSTRN
827              JS2=K
828              IF(DIVOCT-SD(K,JLS,N)) 752,751,751
829      751 CONTINUE
830      752 CONTINUE
831          PR1=1.061*(VS(JS1,JLS-1,N)-VS(JS1-1,JLS-1,N))/(ST(JS1,N)-ST(JS1-1,
832      1N))-1.0
833          IF(PR1.GT.0.49) PR1=0.49
834          PR2=1.061*(VS(JS2,JLS ,N)-VS(JS2-1,JLS ,N))/(ST(JS2,N)-ST(JS2-1,
835      1N))-1.0
836          IF(PR2.GT.0.49) PR2=0.49
837          PR3=PR1+((PR2-PR1)*( CONFS-SL(JLS-1,N))/(SL(JLS,N)-SL(JLS-1,N)))
838          IF(PR3.GT.0.49 ) PR3=0.49
839          DIF1=SD(JS1,JLS-1,N)-SD(JS1-1,JLS-1,N)
840          ETP1=DIF1/(ST(JS1,N)-ST(JS1-1,N))
841          GTP1=ETP1/(0.9428*(1.+PR1))

```



```

842      DIF2=SD(JS2,JLS,N)-SD(JS2-1,JLS,N)
843      ETP2=DIF2/(ST(JS2,N)-ST(JS2-1,N))
844      GTP2=ETP2/(0.9428*(1.+PR2))
845      GTP=GTP1+ (GTP2-GTP1)*((CONFS -SL(JLS-1,N))/(SL(JLS,N)-SL(JLS-1,N))
846      GTP=100.*GTP
847      BULKM   =GTP*2.*(1.+PR3)/(3.*(1.-2.*PR3))
848      SHEARM=GTP
849      IF(IANLYS.GT.0) GO TO 852
850      SIGMM2=PR3*(SIGM1+SIGM3)
851      SIGMM2=(SIGMM2+SIGM2)/2.
852      STRS=ABS(SIGMM2-SIGM2)
853      IF(NCOUN.GE.11) GO TO 851
854      IF(ABS(SIGMM2-SIGM2).LT.0.01) GO TO 851
855      SIGM2=SIGMM2
856      GO TO 950
851  WRITE(6,125)  JJ,NCOUN,SIGM2,STRS,PR3
852  CONTINUE
      IF(NITER.EQ.1)TEBULK=BULKM
860      IF(NITER.EQ.2)EBULK(JJ)=BULKM
861      IF(ITOPT.GT.0.AND.NITER.EQ.1)EBULK(JJ)=(EBULK(JJ)+TEBULK)/2.
862      IF(ITOPT.EQ.0.AND.NITER.EQ.1)EBULK(JJ)=TEBULK
863      IF(NITER.EQ.1)TSHEAR=SHEARM
864      IF(NITER.EQ.1.AND.DIVS.GE.DIVSF.AND.NTENS.GT.0) TSHEAR=EBULK(JJ)/5
865      10.
866      IF(NITER.EQ.2)ESHEAR(JJ)=SHEARM
867      IF(NITER.EQ.2.AND.DIVS.GE.DIVSF.AND.NTENS.GT.0) ESHEAR(JJ)=EBULK(J
868      1J)/50.
869      IF(ITOPT.GT.0.AND.NITER.EQ.1)ESHEAR(JJ)=(ESHEAR(JJ)+TSHEAR)/2.
870      IF(ITOPT.EQ.0.AND.NITER.EQ.1)ESHEAR(JJ)=TSHEAR
871      IF(ESHEAR(JJ).GT.(1.45*EBULK(JJ)))ESHEAR(JJ)=1.45*EBULK(JJ)
872      IF(ESHEAR(JJ).LT.(EBULK(JJ)/50.))ESHEAR(JJ)=EBULK(JJ)/50.
873  501  CONTINUE
874      WRITE(6,110)
875      WRITE(6,2055)(NUME(N),NPI(N),NPJ(N),NPK(N),EBULK(N),RO(N),ESHEAR(N
876      1),MAT(N),N=1,NUMEL)
877      IF(ITOPT.EQ.0) GO TO 500
878      IF(NITER.EQ.1) GO TO 160
879  500  CONTINUE
880  C
881      GO TO 925
882  C
883  C   PRINT OF ERRORS IN INPUT DATA
884  C
885  702  WRITE(6,712)LX
886  C
887  C
888  C   FORMAT STATEMENTS
889  C
890  C
891      1  FORMAT (9I5)
892      2  FORMAT(1I5,3I4,4E12.4,1F8.4)
893      3  FORMAT(1I5,4F10.0,2F12.8)
894      4  FORMAT (2I5,1F8.3)
895      5  FORMAT (3E15.8)
896      6  FORMAT(1I5)
897      7  FORMAT(1I4,6F8.0)
898      8  FORMAT(2I4,2F8.0)
899      9  FORMAT(4I5)
900      13  FORMAT(6I5,2F10.0,15)
901      20  FORMAT (2I5)

```



```

902      21  FORMAT(7F5.0)
903      23  FORMAT (1X,'LATSTRESS',6X, 6F8.3/)
904      24  FORMAT (1X,'STRAIN',3X,1F6.2, 6F8.3/)
905      40  FORMAT(12F6.0)
906      99  FORMAT (1H1)
907      100 FORMAT(18A4)
908      101 FORMAT (30HNUMBER OF ELEMENTS           =114/)
909      102 FORMAT (30H NUMBER OF NODAL POINTS       =114/)
910      103 FORMAT (30H NUMBER OF BOUNDARY POINTS    =114/)
911      104 FORMAT (30H CYCLE PRINT INTERVAL        =114/)
912      105 FORMAT (30H OUTPUT INTERVAL OF RESULTS  =114/)
913      106 FORMAT (30H CYCLE LIMIT                 =114/)
914      107 FORMAT (30H TOLERANCE LIMIT              =1E12.4/)
915      108 FORMAT (30H OVER RELAXATION FACTOR      =1F6.3)
916      117 FORMAT (30H LIFT NUMBER                  =114/)
917      109 FORMAT (118,4F12.6,2F12.8)
918      110 FORMAT (74H1EL.  I  J  K      EBULK      DENSITY      ESHEAR
919      1MAT NO.                )
920      111 FORMAT(80H1      NP      X-ORD      Y-ORD      X-LOAD      Y-LOAD
921      1      X-DISP      Y-DISP      )
922      112 FORMAT(20H BOUNDARY CONDITIONS)
923      119 FORMAT(34H0      CYCLE      FORCE UNBALANCE)
924      120 FORMAT (11I2,1E20.6)
925      121 FORMAT(42H0NODAL POINT X-DISPLACEMENT Y-DISPLACEMENT)
926      122 FORMAT (11I2,2E15.6)
927      123 FORMAT(5H1ELNO 4X,8HX-STRESS 4X,8HY-STRESS 3X,9HXY-STRESS 2X,10HMA
928      1X-STRESS 2X,10HMIN-STRESS 2X,9HDIRECTION 3X,8HX-STRAIN 3X,8HY-STRA
929      2IN 1X,10HMAX-STRAIN 1X,10HMIN-STRAIN)
930      124 FORMAT(11I5,5E12.5,5E11.4)
931      125 FORMAT(2I5,3E12.5)
932      126 FORMAT(11I4,2E12.5)
933      602  FORMAT(1I5,2F10.0)
934      633  FORMAT ('0')
935      1'MAX. PRINCIPAL STRESS=',F10.5,'AND OCCURS IN ELEM.',I6//
936      2'MIN. PRINCIPAL STRESS=',F10.5,'AND OCCURS IN ELEM.',I6//)
937      711  FORMAT(32H0ZERO OR NEGATIVE AREA, EL.NO. =114)
938      712  FORMAT(33H0OVER 8 N.P. ADJACENT TO N.P. NO.114)
939      670  FORMAT(//4I5,6F12.6)
940      753  FORMAT(2I5,F10.0)
941      823  FORMAT(5H1NODE 4X,8HX-STRESS 4X,8HY-STRESS 3X,9HXY-STRESS)
942      824  FORMAT (30H NUMBER OF READ NODAL POINTS =114/)
943      825  FORMAT (30H NUMBER OF READ ELEMENTS      =114/)
944      1010 FORMAT(1I5,6F5.0)
945      1020 FORMAT(1I5,4F15.6)
946      1030 FORMAT(3I5)
947      2000 FORMAT('0','NUMBER OF THE MATERIAL=',I5/)
948      2010 FORMAT(5F10.0)
949      2020 FORMAT('0',10X,'DENSITY=',F15.6//,10X,'BULK MODULUS=',F15.6//,10X,
950      1'SHEAR MODULUS=',F15.6//,10X,'ACOEFF.=',F15.6//,10X,'BCOEFF.=',F15.6)
951      2021 FORMAT(2I5,F10.0)
952      2051 FORMAT(10F5.0)
953      2052 FORMAT(11F5.0)
954      2053 FORMAT('0',10X,'STRESS-STRAIN RELATIONSHIPS FOR MATERIAL='I5//)
955      2055 FORMAT(1I5,3I4,3E12.4,I5)
956      C
957      C
958      925  STOP
959      C
960      END
961      C

```



```

962      C
963      C
964      C
965      SUBROUTINE TESTD
966      C
967      C
968      C
969      C CONVERSION OF TRIAXIAL TEST DATA FROM CONVENTIONAL FORM TO STRESS
970      C INVARIANT FORM AND INTERPOLATION
971      C
972      C
973      C
974      DIMENSION SL(10,5),SD(20,10,5),VS(20,10,5),SIGINV(20,10,5),
975      1VSTN(20,10,5)
976      COMMON/AREA3/
977      1      ST(20,5),SIGINT(20,5),TOCTD(20,10,5),GOCT(20,10,5),NUMAT,
978      1NCELP,CONFAC,NSTRN
979      C
980      C
981      C
982      C READ CELL PRESSURE DATA FOR GIVEN MATERIALS
983      C
984      C
985      DO 10 N=1,NUMAT
986      READ(5,1010) (SL(J,N),J=1,NCELP)
987      DO 15 J=1,NCELP
988      SL(J,N)=SL(J,N)*CONFAC
989      SIGINT(J,N)=SL(J,N)
990      15 CONTINUE
991      C
992      C
993      C READ DEVIATORIC STRESS DATA FOR GIVEN MATERIALS
994      C
995      C
996      DO 20 K=1,NSTRN
997      READ(5,1020) ST(K,N),(SD(K,J,N),J=1,NCELP)
998      DO 25 J=1,NCELP
999      SD(K,J,N)=SD(K,J,N)*CONFAC
1000      25 CONTINUE
1001      20 CONTINUE
1002      WRITE (6,1030) N
1003      WRITE(6,1040) (SL(J,N),J=1,NCELP)
1004      C
1005      C
1006      C READ VOLUMETRIC STRAIN DATA FOR GIVEN MATERIALS
1007      C
1008      C
1009      DO 30 K=1,NSTRN
1010      READ (5,1020) ST(K,N),(VS(K,J,N),J=1,NCELP)
1011      WRITE(6,1050) ST(K,N),(VS(K,J,N),J=1,NCELP)
1012      30 CONTINUE
1013      DO 35 K=1,NSTRN
1014      WRITE(6,1050) ST(K,N),(SD(K,J,N),J=1,NCELP)
1015      35 CONTINUE
1016      10 CONTINUE
1017      DO 40 N=1,NUMAT
1018      DO 45 J=1,NCELP
1019      DO 50 K=1,NSTRN
1020      PROD= (SL(J,N)**2)*(SC(K,J,N)+SL(J,N))
1021      SIGOCT=SL(J,N)+(SD(K,J,N))/3.

```



```

1022         IF(J.EQ.1.AND.K.EQ.1) GO TO 51
1023         SIGINV(K,J,N)=PROD/(SIGOCT**2)
1024     51     IF(J.EQ.1.AND.K.EQ.1) SIGINV(K,J,N)=0.0
1025     50     CONTINUE
1026     45     CONTINUE
1027         DO 70 I=1,NCELP
1028         DO 55 K=1,NSTRN
1029         DO 60 J=1,NCELP
1030             JLS=J
1031             IF(SIGINT(I,N)-SIGINV(K,J,N))61,60,60
1032     60     CONTINUE
1033     61     CONTINUE
1034             TOCTD(K,I,N)=SD(K,JLS-1,N)+(SD(K,JLS,N)-SD(K,JLS-1,N))*(SIGINT(I,N
1035             1)-SIGINV(K,JLS-1,N))/(SIGINV(K,JLS,N)-SIGINV(K,JLS-1,N))
1036             TOCTD(K,I,N)=TOCTD(K,I,N)*0.4714
1037             VSTN(K,I,N)=VS(K,JLS-1,N)+(VS(K,JLS,N)-VS(K,JLS-1,N))*(SIGINT(I,N
1038             1-SIGINV(K,JLS-1,N))/(SIGINV(K,JLS,N)-SIGINV(K,JLS-1,N))
1039             GOCT(K,I,N)=0.4714*(3.*ST(K,N) -VSTN(K,I,N))
1040     55     CONTINUE
1041     70     CONTINUE
1042             WRITE(6,1031) N
1043             WRITE (6,1041) (SIGINT(I,N),I=1,NCELP)
1044             DO 75 K=1,NSTRN
1045     75     WRITE(6,1050) ST(K,N),(TOCTD(K,I,N),I=1,NCELP)
1046             DO 80 K=1,NSTRN
1047     80     WRITE(6,1050) ST(K,N),(GOCT(K,J,N),J=1,NCELP)
1048     40     CONTINUE
1049     1000  FORMAT(3I5,F10.0)
1050     1010  FORMAT(10F5.0)
1051     1020  FORMAT(11F5.0)
1052     1030  FORMAT('0',' DATA IN CONVENTIONAL FORM FOR MATERIAL NO. ',I5/)
1053     1031  FORMAT('0',' DATA IN STRESS INVARIANT FORM FOR MATERIAL NO. ',I5/)
1054     1040  FORMAT(1X,'LATSTRESS',6X,10F8.3/)
1055     1041  FORMAT(1X,'J3/(SIGOCT)**2',1X,10F8.3/)
1056     1050  FORMAT(1X,'STRAIN',3X,F6.2,10F8.3/)
1057     1060  FORMAT(I5)
1058     1070  FORMAT(3F10.0)
1059     1071  FORMAT(3F8.3,4F12.4)
1060         RETURN
1061     C
1062         END
1063     C
END OF FILE

```


APPENDIX B
COMPUTER PROGRAM FOR THREE DIMENSIONAL
FINITE ELEMENT ANALYSIS

B.1 Scope

This appendix contains a description of the computer program used for three dimensional finite element analysis and a listing of the program.

B.2 Language, Code and Limitations

Language: The computer program presented here was written in FORTRAN IV language and run on an IBM 360/67 computer with an MTS operating system at the University of Alberta, Edmonton.

Code: The title of the code is Finite Element Non-Linear Analysis for Three Dimensional Problems (FENA3D).

Limitations: The program as presented in this appendix is dependent on the MTS system subroutines and can handle a problem less than or equal to the following size:

Number of elements	=	350
Number of nodes	=	450
Number of materials	=	5
Number of cell pressures at which triaxial data is supplied	=	10
Number of axial strain points at which tri- axial data is supplied	=	20

If the size of a problem exceeds the above limits the dimen-

sions have to be increased accordingly. The minimum required dimension for each array is given in B.4.1.

One of the main limitations of a three dimensional analysis is the requirement of a large computer storage. In the present program the equation solver solves the equations in blocks using a core storage of $(2*MBAND*(MBAND+1))$ locations, MBAND being the half-band width. The core storage needed increases rapidly with the half-band width. On a computer with an available capacity of 1000K a maximum band width of about 320 can be handled with the use of the present program. Also it is to be noted that the computation time increases very rapidly with the half-band width. So it is normally preferable to limit the half-band width to about 250 while using the present program.

B.3 Development, The Main Features of Program and Computation Time

B.3.1 Development

The development of the present program was based on the ideas used by E.L. Wilson (University of California, 1966) in coding a two dimensional finite element program with a solver that solves the equations by Gaussian elimination in blocks. The program was developed by the author in the year 1971.

B.3.2 Main Features

The program consists of eight subroutines and a main

program. Eight other system-dependent subroutines are referenced in this program. These are:

TIME,ADROF,RCALL,SETDSN,WRITE,READ,NOTE,POINT

the details of which can be obtained from the manual of the MTS system subroutines. Fig. B.1 shows the sequence of calling the different subroutines written for the present program. The function of the Main Program and each subroutine is described here in brief.

Main Program. Variables whose dimensions are prescribed depending on the half-band width computed for the current analysis, are passed to other subroutines. These variables change the dimensions of certain arrays appearing in certain DIMENSION statements of other subroutines.

Subroutine MSUB. This is the master subroutine which calls other subroutines necessary for the analysis. In this subroutine the coefficients needed for integration by Gaussian quadrature are computed, and the elastic parameters needed for each step in the non-linear analysis are calculated.

Subroutine READIN. This subroutine reads all the data pertaining to nodes, elements, materials, loads, and boundary conditions and interpolates the initial moduli needed in the non-linear analysis for all elements. It also calculates the half-band width for the current problem.

Subroutine TESTD. This subroutine reads the triaxial test data and converts it into the stress-invariant form.

Subroutine ASTIF. This subroutine assembles the load vector, and the total stiffness matrix from the element stiff-

ness obtained by calling the subroutine ELSTIF. It calls the subroutine MODIFY in order to modify the total stiffness matrix, and load vector to suit the given displacement boundary conditions. Formation and modification of the total stiffness matrix, and the load vector are done in blocks of size $MBAND*(MBAND+1)$ and the information is written on a temporary sequential disc file.

Subroutine ELSTIF. This subroutine forms the element stiffness matrix for each element and returns to ASTIF. An isoparametric, eight-node hexahedral element has been used for the present program. The same element is specialized to represent triangular prisms or tetrahedra. The subroutine also forms the element stress matrix, computes the element stresses, and returns them to the subroutine STRESS.

Subroutine MODIFY. This subroutine modifies the total stiffness matrix, and the load vector according to the prescribed boundary displacement conditions and returns them to the subroutine ASTIF.

Subroutine BAND1. This is an equation solver which solves the equations by the direct method of Gaussian elimination. The equations are solved in single precision and in blocks by transferring parts of stiffness matrix, and load vector from sequential files to core and vice versa. Two temporary sequential disc files of sufficient size are used. The required size of sequential files in terms of the number of tracks (NTRACK) can be determined as follows:

Let each track of the file correspond to NBYTES
(about 7000)

Let the number of equations to be solved be NEQ

Let the half-band width be MBAND

Number of blocks needed to write information into a file is obtained from $NBLOCK = (NEQ/MBAND) + 1$

Number of tracks needed for the file can be obtained from $NTRACK = (NBLOCK) * (MBAND) * (MBAND + 1) / (NBYTES) + 1$.

File 2 is used to write the total stiffness matrix, and the load vector as formed in the subroutine ASTIF and File 1 is used to write information regarding the reduced equations obtained in the process of Gaussian elimination.

Subroutine STRESS. This subroutine computes the stresses and strains related to elements and nodes by calling the subroutine ELSTIF for the formation of the element stress matrix.

B.3.3 Computation Time

It has been observed that considerable savings on the cost of computation (even up to 50%) can be effected by introducing an efficient method of data transfer between core and sequential files. In the present program such transfers are effected by calling certain system-subroutines and by making suitable EQUIVALENCE statements. Table B.1 compares the computation time needed for solving 738 equations with a half-band width of 171 by using different methods of handling the transfer of data between core and files. The example considered here was concerned with a three dimensional finite element analysis of an earth dam. Total computation time for the complete analysis of the problem and the percent reductions in time have been presented in Table B.1. In the present

program, Method 5 indicated in Table B.1, has been used as it effects the maximum reduction of the computation time.

B.3.3.1 Estimation of Computation (CPU) Time

It is generally useful to estimate before hand the approximate computation time spent in the assembly of the total stiffness matrix and the solution of equations for a given problem. The cost of computation sometimes dictates the size of the problem in terms of the number of nodes and elements. By knowing the number of nodes, the half-band width and the number of elements for a given problem the computation time needed for the solution of equations may be estimated by referring to Fig. B.2. This figure shows the relationship between the half-band width (MBAND) and the computation time for solution of equations equal to MBAND in number, in each block. This relationship has been obtained by solving problems of different sizes using the three dimensional program. The computation time needed for the solution of equations in a problem is obtained by multiplying the number of blocks with the computation time per block, read from Fig. B.2 at the given half-band width. The time needed for the assembly of the total stiffness matrix is estimated between 0.8 sec. and 1.2 sec. per element depending on whether a two-point or three-point integration formula is used for the formation of the element stiffness. This time multiplied by the number of elements gives the time for the formation of the total stiffness matrix.

Since the time required for solution of a given number of equations at a given half-band width depends on the number of displacement boundary conditions imposed, the time given by Fig. B.2 should be considered as approximate.

B.4 Nomenclature

In Section B.4.1 that follows, the variables that need a change in their dimension declaration according to the size of the problem are designated by parentheses after the variable name. The description and the minimum required size of the variable are also indicated. The variables defining the minimum sizes are given as input to the program.

B.4.1 Description and Size of Variables

<u>Name</u>	<u>Description</u>	<u>Minimum Size When Applicable</u>
ACOE()	Shear strength parameter associated with cohesion given by $2c \cos \phi / (1 - \sin \phi)$	(NUMAT)
BCOE()	Shear strength parameter associated with σ_3 given by $2 \sin \phi / (1 - \sin \phi)$	(NUMAT)
CONFAC	Conversion factor used to convert the triaxial test results to the units in which analysis is performed	
DISPX()	Total displacement of a node in x-direction	(NUMNP)
DISPY()	Total displacement of a node in y-direction	(NUMNP)
DISPZ()	Total displacement of a node in z-direction	(NUMNP)
EBREAD()	Bulk modulus read for each material type	(NUMAT)

<u>Name</u>	<u>Description</u>	<u>Minimum Size When Applicable</u>
EBULK()	Bulk modulus assigned to each element	(NUMEL)
EDEV()	Shear modulus assigned to each element	(NUMEL)
ESREAD()	Shear modulus read for each material type	(NUMAT)
GOCT()	Percent octahedral shear strain	(NSTRN, NCELP,NUMAT)
HED()	Heading for the identification of the problem	(18)
ITOPT	Code to identify whether a step is to be analyzed once or twice	
KODE()	Code for each node to identify the type of boundary displacement condition	(NUMNP)
KOEL()	Code for each element to identify the type of integration formula to be used	(NUMEL)
KOUNT()	Counter used for computing the nodal stresses	(NUMNP)
KTERMI	Code to identify whether the execution to be stopped after the generation of the element and nodal data	
M	Element or nodal number	
MAT()	Material number assigned to each element	(NUMEL)
MATN	Number of elements to which material number has to be changed	
MBAND	Half-band width as calculated in program	
N	Element or nodal number	
NANLYS	Code to identify whether the analysis is linear or non-linear	

<u>Name</u>	<u>Description</u>	<u>Minimum Size When Applicable</u>
NBOUN	Number of nodes at which the boundary displacements or loads are specified in a particular step	
NCELP	Number of confining pressures at which triaxial test data is supplied as input	
NOBSET	Number of sets of elements for which the overburden factor is prescribed	
NP()	Vector to store the eight nodes of each element	(8,NUMEL)
NSET	Number of elements (excluding the one read) for which the same overburden factor has to be assigned	
NSHEAR	Code to identify whether shear failure is to be considered or not	
NSTEP	Number of steps for the analysis	
NSTRN	Number of axial strain points at which the triaxial data is supplied	
NUM1	Number of sets of nodes for which codes other than zero are to be assigned	
NUM2	Number of nodes (excluding the one read) for which the same code has to be assigned	
NUMAT	Number of material types present in the given problem	
NUMCE	Number of sets of hexahedra and base triangular prisms to be generated	
NUMEL	Number of elements in the problem	
NUMELS	Number of elements in a particular step	
NUMJK	Number of hexahedra or base triangular prisms (excluding the one read) to be generated	

<u>Name</u>	<u>Description</u>	<u>Minimum Size When Applicable</u>
NUMNP	Number of nodes in the problem	
NUMTH	Number of tetrahedra in the problem	
NUMTP	Number of triangular prisms in the problem	
OBFAC()	Overburden factor	(NUMEL)
RO()	Density of the material in an element	(NUMEL)
ROREAD()	Density of the material read for each material type	(NUMAT)
SD()	Deviatoric stresses read from test data	(NSTRN, NCELP,NUMAT)
SGTEL	Total element stresses	(NUMEL,6)
SGTNP	Total nodal stresses	(NUMNP,6)
SGTPS()	Principal stresses and strains in an element	(NUMEL,7)
SIGA()	Nodal stresses in a particular step	(NUMNP,6)
SIGINT()	A vector used in the conversion of data from triaxial form to stress invariant form	(NCELP, NUMAT)
SIGINV()	A vector used in the conversion of data from triaxial form to stress invariant form	(NSTRN, NCELP,NUMAT)
SL()	Number of triaxial cell pressure values at which data is supplied	(NCELP, NUMAT)
ST()	Number of percent axial strain values at which triaxial data is supplied	(NSTRN, NUMAT)
STN()	Percent nodal strains in a particular step	(NUMNP,3)
STNT()	Percent total nodal strains	(NUMNP,3)
STRNT()	Percent total element strains	(NUMEL,6)
TOCTD()	Octahedral shear stress	(NSTRN, NCELP,NUMAT)

<u>Name</u>	<u>Description</u>	<u>Minimum Size When Applicable</u>
U()	Force or displacement in x-direction given as input at a nodal point	(NUMNP)
V()	Force or displacement in y-direction given as input at a nodal point	(NUMNP)
VS()	Volumetric strain obtained from tri- axial test	(NSTRN, NCELP,NUMAT)
VSTN()	A vector used in the conversion of the triaxial test data to stress invariant form	(NSTRN, NCELP,NUMAT)
W()	Force or displacement in z-direction given as input at a nodal point	(NUMNP)
X()	x-coordinate of a nodal point	(NUMNP)
Y()	y-coordinate of a nodal point	(NUMNP)
Z()	z-coordinate of a nodal point	(NUMNP)

B.5 Input Data Procedure

B.3.4.1 has to be referred for the explanation of the name of variables used in this section.

(1) Problem Control Cards (2 cards)

(a) Problem Identification Card (1 card) (18A4)

1-72 HED

(b) Preliminary Information Card (1 card) (7I6)

1-6 NUMNP

7-12 NUMEL

13-18 NUMAT

19-24 NUMCE

25-30 NUMTP

31-36 NUMTH

37-42 NANLYS Zero for linear analysis and one
for non-linear analysis

Figs. B.3 and B.4 show an example of a three dimensional idealization of a model dam representing different types of elements as given below:

<u>Type of Elements</u>	<u>Element Numbers</u>
Hexahedra	2,3,5,10
Base triangular prisms	7,8
Triangular prisms	1,4,9 (for element 9 back-face is inclined)
Tetrahedra	6

The preliminary information card for this problem would be as follows:

```

NUMNP  =   23
NUMEL  =   10
NUMAT  =    1  (number of material types equal to one
                for this example)
NUMCE  =    4
NUMTP  =    3
NUMTH  =    1
NANLYS =    0  (analysis is linear)

```

(2) Nodal Point Data Cards (Number of cards less than or equal to NUMNP) (2I5,6F5.0)

```

1-5    N
6-10   KODE( )
11-15  X( )
16-20  Y( )
21-25  Z( )

```


26-30 U()

31-35 V()

36-40 W()

In an earth dam problem the nodes can seldom be arranged with equal spacing. However in problems where nodes can be spaced equally with the other two coordinate distances being constant only the extreme nodes need to be given as input. The intermediate nodes are generated with nodal displacements and loads equal to zero and nodal code equal to zero. The following nodal codes are used to represent the various boundary displacement conditions.

<u>KODE(N)</u>	<u>X-Displacement Specified</u>	<u>Y-Displacement Specified</u>	<u>Z-Displacement Specified</u>
0	NO	NO	NO
1	NO	NO	YES
2	NO	YES	NO
3	YES	NO	NO
4	YES	NO	YES
10	YES	YES	NO
11	NO	YES	YES
12	YES	YES	YES

(3) Nodal Code Change Control Card (1 card) (I5)

1-5 NUM1 (If no changes are needed NUM1 is equal to zero and (4) is omitted)

As mentioned before the intermediate nodes are generated with zero nodal codes. However if some of them happen to have codes other than zero it becomes necessary to

assign the proper codes. NUM1 gives the number of sets of nodes to which the proper codes are to be assigned.

(4) Nodal Code Change Cards ($2 \times \text{NUM1}$ cards)

(a) Number of nodes in a set excluding the one read (I5)

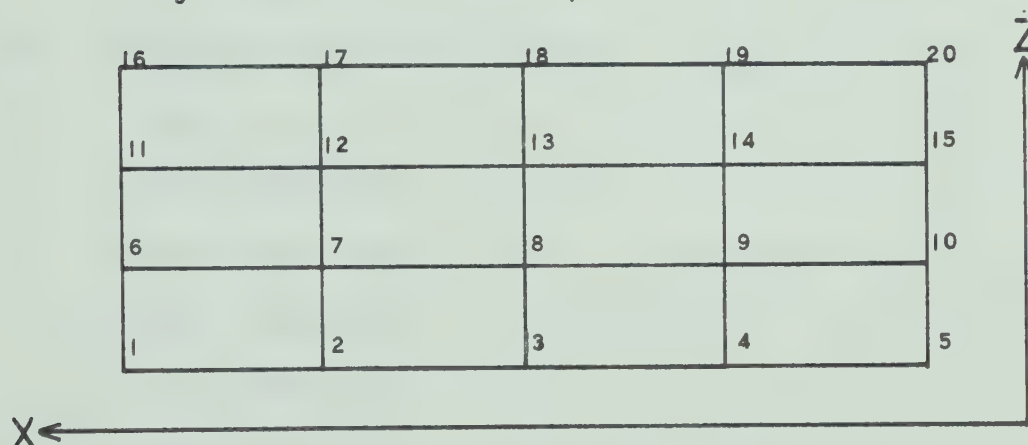
1-5 NUM2

(b) Nodal Number and the Code (2I5)

1-5 N

6-10 KODE(N)

As an example for (3) let it be assumed that the nodal points shown in the sketch below are spaced equally in x and z directions for a particular value of y and have a code equal 2.



If the intermediate nodes namely 2,3,4,7,8,9,12,13, 14,17,18 and 19 are generated with the extreme nodes as input they will be generated with a code equal to zero. Since the proper code to be assigned to the intermediate nodes is 2, the following input cards are necessary.

4 (NUM1) (I5)


```

2      (NUM2) (I5)
2  2   (N,KODE(N)) (2I5)
2      (NUM2) (I5)
7  2   (N,KODE(N)) (2I5)
2      (NUM2) (I5)
12  2   (N,KODE(N)) (2I5)
2      (NUM2) (I5)
17  2   (N,KODE(N)) (2I5)

```

(5) Cards for Generation of Hexahedra and Base Triangular Prisms (2*NUMCE cards)

(a) Number of elements (excluding the one given as input) to be generated (I5)

1-5 NUMJK

(b) Element data card (11I5)

```

1-5   M
6-10  KOEL(M)
11-15 NP(1,M)
16-20 NP(2,M)
21-25 NP(3,M)
26-30 NP(4,M)
31-35 NP(5,M)
36-40 NP(6,M)
41-45 NP(7,M)
46-50 NP(8,M)
51-55 MAT(M)

```

Considering the example in Fig. B.3 the sets of base triangular prisms and hexahedra to be generated are 4 which is given by the number NUMCE. Each set

is represented by two cards. The first card gives the value NUMJK and the second card gives the details of the element from which the other elements equal to NUMJK in numbers are generated in that particular set. The element code to be given as input indicates the type of integration formula (two or three point) to be used for that particular element. If the element is a regular body, e.g., a rectangular prism or a triangular prism, a two point integration formula is used and in the case of a skewed element a three point integration formula is used for better accuracy. In addition, the code indicates whether the given element is a hexahedron or not. If the element is not a hexahedron, the evaluation of stresses at the corners of the element (for the purpose of computing the nodal stresses) has to be done very close to the corner (but not at the corner) to avoid a division by zero. The following element codes are used in the present program:

<u>Element Code</u>	<u>Integration Formula Used</u>	<u>Type of Element</u>
0	Two point Gaussian quadrature	Regular hexahedron
1	Two point Gaussian quadrature	Regular element other than a hexahedron
2	Three point Gaussian quadrature	Skewed element other than a hexahedron
3	Three point Gaussian quadrature	Skewed hexahedron

The following gives the set-up of cards for the generation of the hexahedra and the base triangular prisms for the example given in Fig. B.3 and Fig. B.4.

1(NUMJK(I5)

2,0,12,3,2,11,15,6,5,14,1(M,KOEL(M),(NP(KK,M),KK=1,8),
MAT(M))(11I5)

0(NUMJK(I5)

5,0,16,7,6,15,18,9,8,17,1(M,KOEL(M),(NP(KK,M),
KK=1,8),MAT(M))(11I5)

1(NUMJK)(I5)

7,1,12,12,11,11,20,15,14,19,1(M,KOEL(M),(NP(KK,M),
KK=1,8),MAT(M))(11I5)

0(NUMJK)(I5)

10,3,21,16,15,20,23,18,17,22,1(M,KOEL(M),(NP(KK,M),
KK=1,8),MAT(M))(11I5)

The elements 3 and 8 will be generated accordingly with the same element code and material numbers given for elements 2 and 7 respectively.

- (6) Cards for the Generation of Triangular Prisms (NUMTP cards) (11I5)

If NUMTP is zero (6) is to be omitted.

1-5 M

6-10 KOEL(M)

11-15 NP(1,M)

16-20 NP(2,M)

21-25 NP(3,M)

26-30 NP(4,M)

31-35 NP(5,M)

36-40 NP(6,M)

41-45 NP(7,M)

46-50 NP(8,M)

51-55 MAT(M)

In the example shown in Fig. B.2, NUMTP=3. The cards set up would be as follows:

1,1,11,2,1,10,14,5,5,14,1(M,KOEL(M),(NP(KK,M),KK=1,8),
MAT(M))(11I5)

4,1,15,6,5,14,17,8,8,17,1(M,KOEL(M),(NP(KK,M),KK=1,8),
MAT(M))(11I5)

9,2,20,15,14,19,22,17,17,22,1(M,KOEL(M),(NP(KK,M),
KK=1,8),MAT(M))(11I5)

(7) Cards for the Generation of Tetrahedra (NUMTH cards)
(11I5)

If NUMTH is zero (7) will be omitted.

1-5 M

6-10 KOEL(M)

11-15 NP(1,M)

16-20 NP(2,M)

21-25 NP(3,M)

26-30 NP(4,M)

31-35 NP(5,M)

36-40 NP(6,M)

41-45 NP(7,M)

46-50 NP(8,M)

51-55 MAT(M)

In the example shown in Fig. B.3 NUMTH=1. The card set up would be as follows:

6,2,11,11,10,10,19,14,14,19,1(M,KOEL(M),(NP(KK,M),
KK=1,8),MAT(M))(11I5)

(8) Cards for Changing the Material Numbers for Certain Elements

(a) Control Card to Change Material Numbers (1 card) (I5)

1-5 MATN

(b) Cards to Change Material Numbers (MATN cards) (2I5)

1-5 M

6-10 MAT(M)

As the material number for the generated elements will be the same as that assigned to the element given as input, it would sometimes be necessary to alter the material number in some of the generated elements. When these changes are not necessary MATN is equal to zero and (b) is omitted.

(9) Overburden Factor Control Card (1 card) (I5)

1-5 NOBSET (If the analysis is linear NOBSET=0 and (10) is omitted)

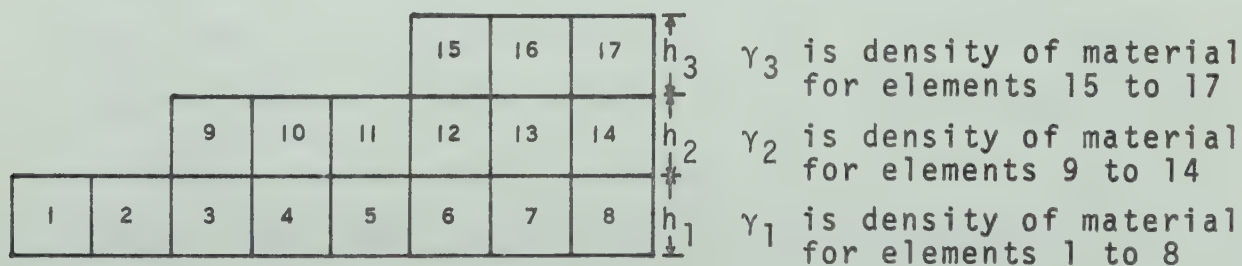
(10) Overburden Factor Cards (Number of cards = NOBSET)
(2I5,F10.0)

1-5 M Element number

6-10 NSET

11-20 OBFAC() To be given only if the value is not equal to one

The following example provides an explanation for (9) and (10)



When a non-linear analysis has to be performed for gravity loaded structures the initial moduli are computed for each element considering the overburden pressure at the mid height of the element. In the sketch shown above there are 17 elements to be considered in a particular step. The overburden pressure at the mid height of a certain element say 8 is $(\gamma_1 h_1/2 + \gamma_2 h_2 + \gamma_3 h_3)$ where γ_1 , γ_2 and γ_3 are the densities of the materials and h_1 , h_2 and h_3 are the heights as shown. Now the overburden factor can be defined for the element 8 as follows:

$$\text{OBFAC}(8) = (\gamma_1 h_1/2 + \gamma_2 h_2 + \gamma_3 h_3)/\gamma_1 h_1/2).$$

If for example $h_1 = h_2 = h_3 = h$ and $\gamma_1 = \gamma_2 = \gamma_3 = \gamma$, then the overburden factor control card and the overburden factor cards will be as given below:

NOBSET=3

<u>M</u>	<u>NSET</u>	<u>OBFAC(M)</u>
3	2	3.0
6	2	5.0
12	2	3.0

OBFAC(M)=1.0 is automatically set in the program and hence need not be supplied in the data. In the present example elements 1,2,9,10,11,15,16 and 17 will have an overburden factor equal to unity.

(11) Triaxial Test Data Control Card (1 card) (2I5,F10.0)

1-5 NCELP

6-10 NSTRN

11-20 CONFAC

If the analysis is linear a blank card for (11) to be supplied and (12), (13), (14) are omitted.

(12) Cell Pressure Card (1 card) (10F5.0)

If the test results are to be supplied say at 0,5,10,30 and 40 psi cell pressure values the input is as follows:

1-5	0.0
6-10	5.0
11-15	10.0
16-20	30.0
21-25	40.0

(13) Axial Strain and Deviatoric Stress Cards (Number of cards = NSTRN) (11F5.0)

Each card will have the axial strain punched in the first five columns and the deviatoric stresses corresponding to the various cell pressures (given in (12)) at that particular axial strain are punched in the subsequent columns.

(14) Axial Strain and Volumetric Strain Cards (Number of cards = NSTRN) (11F5.0)

Each card will have the axial strain punched in the first five columns and the volumetric strain corresponding to the various cell pressures (as given by (12)) at that particular axial strain are punched in the subsequent columns. Volume expansion is to be neglected while giving the volumetric strain input.

(15) Card for the Termination of Execution After the Generation of Element and Nodal Data (1 card) (I5)

1-5 KTERMI (KTERMI=1 terminates execution and
KTERMI=0 does not terminate execution)

When the data is run for the first time it is preferable to terminate the execution after the generation of element and nodal data so that the correctness of generation can be verified. Also the correct value of MBAND computed during this first run can be utilized in setting the dimensions of certain vectors in MAIN PROGRAM as described in (21).

(16) Card to Control Iteration Option (1 card) (I5)

1-5 ITOPT (ITOPT=1 causes each step to be analyzed twice and ITOPT=0 causes each step to be analyzed only once. In the case of a linear analysis ITOPT=0)

(17) Card to Indicate the Number of Steps and the Option for the Consideration of Shear Failure (1 card) (2I5)

1-5 NSTEP

6-10 NSHEAR (NSHEAR=1 causes the shear failure to be considered and if NSHEAR=0 shear failure is not considered)

(18) Card to Read the Number of Elements Involved in a Particular Step (1 card) (I5)

1-5 NUMELS

(19) Card to Read the Number of Nodal Points at Which Incremental Loads or Displacements are Prescribed in a Given Step (1 card) (I5)

1-5 NBOUN

(20) Cards that Input Incremental Nodal Loads or Displacements (NBOUN cards) (I5,3F10.0)

1-5 N

6-15 U(N)

16-25 V(N)

26-35 W(N)

U(), V() and W() could be either the prescribed forces

or the prescribed displacements in x, y and z directions. In a particular coordinate direction if a displacement boundary condition is specified then the read quantity becomes a prescribed displacement in that direction; otherwise it is taken as a prescribed force in that direction. It is not possible to prescribe a force and a displacement simultaneously in a given direction at a given nodal point.

(21) Procedure to Set the Dimensions of the Arrays in the MAIN PROGRAM

The dimensions of these arrays are based on the half-band width and the number of equations which in turn depend on the problem. So it is necessary to know the value of the half-band width and the number of equations for the problem on hand to set the dimensions of arrays in MAIN PROGRAM. Because of the facility provided to terminate the execution of the program after the generation of the element and nodal data, and the calculation of the half-band width (MBAND) in subroutine READIN, it is not necessary to know the correct value of MBAND beforehand. An arbitrary value of say 100 can be assumed during the first run for setting the dimensions of arrays in MAIN PROGRAM. The dimension of these arrays do not effect the execution up to the generation of nodes and elements. After obtaining the correct value of MBAND the dimensions of the arrays in MAIN PROGRAM are reset for the final run. The number of equations (NE1) is given as three times the total number of nodes involved in the problem

on hand. The dimensioning of arrays is as follows:

```
DIMENSION B(NE1),A(MBAND,2*MBAND),BL(MBAND),BR(MBAND),
AL(MBAND**2),AR(MBAND**2)
```

```
EQUIVALENCE (B(1),BL(1)),(B(MBAND+1),BR(1)),(A(1,1),
AL(1)),(A(1,MBAND+1),AR(1))
```

```
NE1=3*NUMNP
```

```
MB1=MBAND
```

The quantities that appear in MAIN PROGRAM of the listing given in Section B.8 correspond to the value of MBAND equal to 114 and NE1 equal to 405.

B.6 Control Cards to Create Sequential Files and to Run Data

The following control cards were used to create the sequential files and to run the data:

```
$CREATEØ-TØTYPE=SEQØSIZE=nT
```

```
$CREATEØ-TEMP2ØTYPE=SEQØSIZE=nT
```

```
$RUNØ-LOAD#Ø1=-TØ2=-TEMP2
```

The value n representing the number of tracks was obtained using the procedure given in Section B.3.2

B.7 Output of the Results

The following results are obtained as output:

- (1) The complete nodal and element data with the initial values of the elastic parameters assigned to each element.
- (2) Cumulative nodal displacements, stress and strains for elements and nodes for each step of the analysis.
- (3) Element principal stress and strains for each step of the analysis.

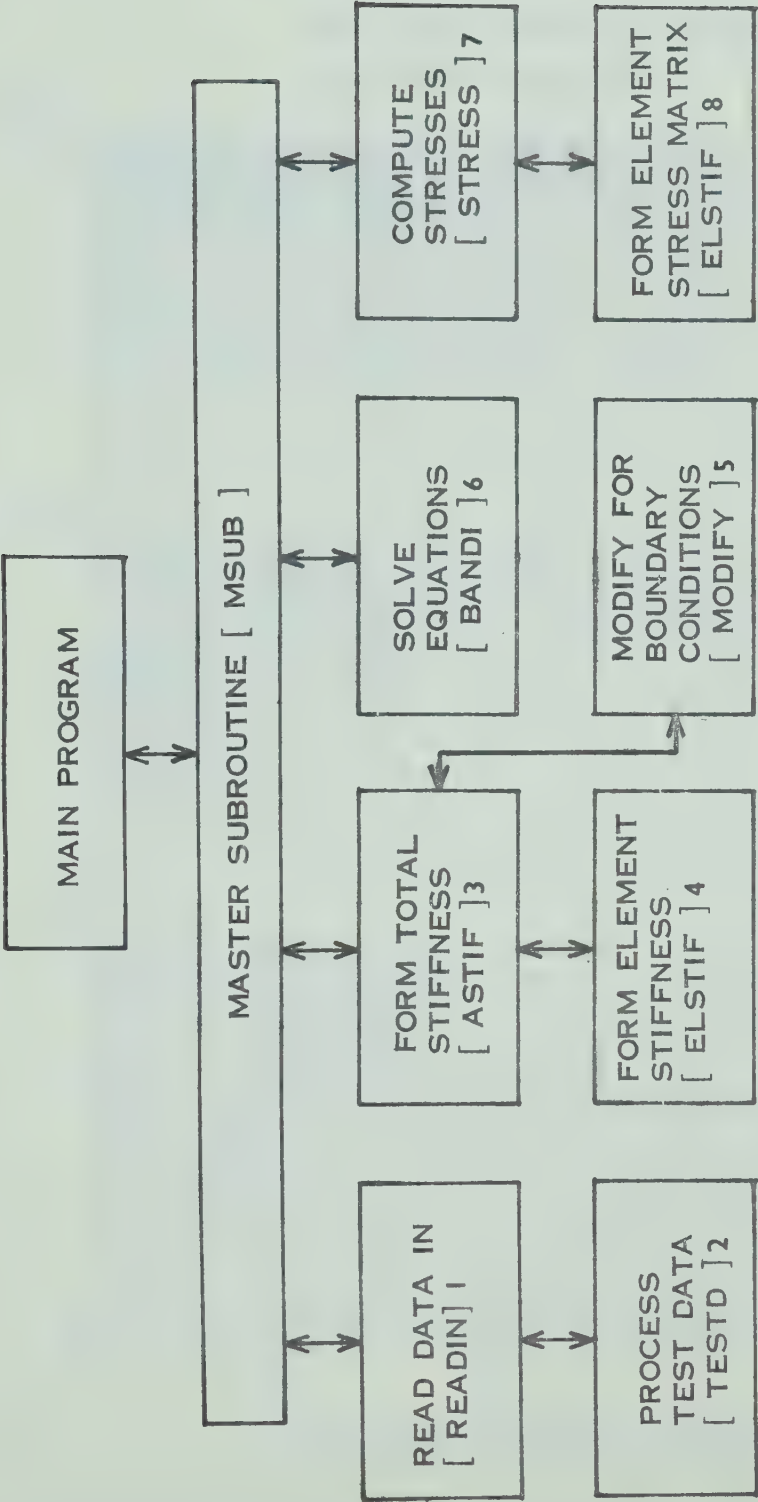
- (4) Elastic parameters assigned to each element in each step of the analysis.

B.8 Listing of Program

A listing of the computer program appears after the Fig. B.4.

TABLE B.1
COMPARISON OF THE COMPUTATION TIME WITH DIFFERENT METHODS OF DATA TRANSFERS

In all the following methods a three dimensional finite element analysis of an earth dam, consisting of 738 equations with a half-band width of 171 has been performed in single precision		Type of write and read statements used.				Percent reduction of total CPU time %	
NO.	METHOD USED					CPU time for solution of equations (sec.)	Total CPU time for the analysis (sec.)
1	Two sequential files are created. Transfers between core and files are effected by FORTRAN read and write statements in subscripted form. For back substitution the file 1 is over-read every time from the beginning to the proper block.	File 1: WRITE(1)(N81,B(N),(A(M,N),M=2,MBAND),N=1,MBAND) File 1: READ(1)(N81,B(N),(A(M,N),M=2,MBAND),N=1,MBAND) File 2: WRITE(2)(B1),(A(J,I),J=1,MBAND),I=1,MBAND File 2: READ(2)(B(N),(A(M,N),N=1,MBAND),N=MBAND,2*MBAND)				99.00	173.44
2	One sequential file for File 2 and a line file for File 1 are created. Direct access is made available for File 1. Transfers between core and files are effected as in (1) except that over-reading is eliminated by direct access read and write statements.	File 1: WRITE(1)'IDx1000'(B(N),(A(M,N),M=2,MBAND),N=1,MBAND) File 1: READ(1)'IDx1000'(B(N),(A(M,N),M=2,MBAND),N=1,MBAND) File 2: WRITE(2)(Same as in (1)) File 2: READ(2)(Same as in (1))				84.90	159.77
3	Two sequential files are created. Transfers between core and files are effected as in (1) and (2). Direct access with sequential file 1 is obtained by calling subroutines NOTE and POINT.	File 1: WRITE(1)(Same as in (1)) called NOTE File 1: READ(1)(Same as in (1)) called POINT File 2: WRITE(2)(Same as in (1)) File 2: READ(2)(Same as in (1))				72.86	147.30
4	Two sequential files are created. Transfers between core and file are effected by FORTRAN unsubscripted read and write statements made possible by equivalence statements. Direct access with sequential file 1 is same as in (3).	File 1: WRITE(1) AL,B1 File 1: READ(1) AL,BL File 2: WRITE(2) AL,BL File 2: READ(2) AR,BR Called NOTE and POINT, made EQUIVALENCE statements				39.61	101.53
5	Two sequential files are created. Transfers between core and file are effected by calling subroutines READ and WRITE with same equivalence statements as in (4). Direct access with sequential file 1 is made available as in (3) and (4).	File 1: CALL WRITE(AL(LL),LEN,0.1,FDUB,&550) File 1: CALL READ(AL(LL),LEN,0.1,2,FDUB,&550) File 2: CALL WRITE(AL(LL),LEN,0.1,2,&550) File 2: CALL READ(AR(LL),LEN,0.1,2,&550) Similar statements for BL and BR Called NOTE and POINT and made EQUIVALENCE statements				21.48	77.00
							55.50



NUMBERS INDICATE THE ORDER OF CALLING DIFFERENT SUBROUTINES

NAME OF SUBROUTINE APPEARS WITHIN BRACKETS

3 TO 8 IS REPEATED FOR EVERY STEP OF THE INCREMENTAL ANALYSIS

FIG. B.1 SEQUENCE OF CALLING DIFFERENT SUBROUTINES

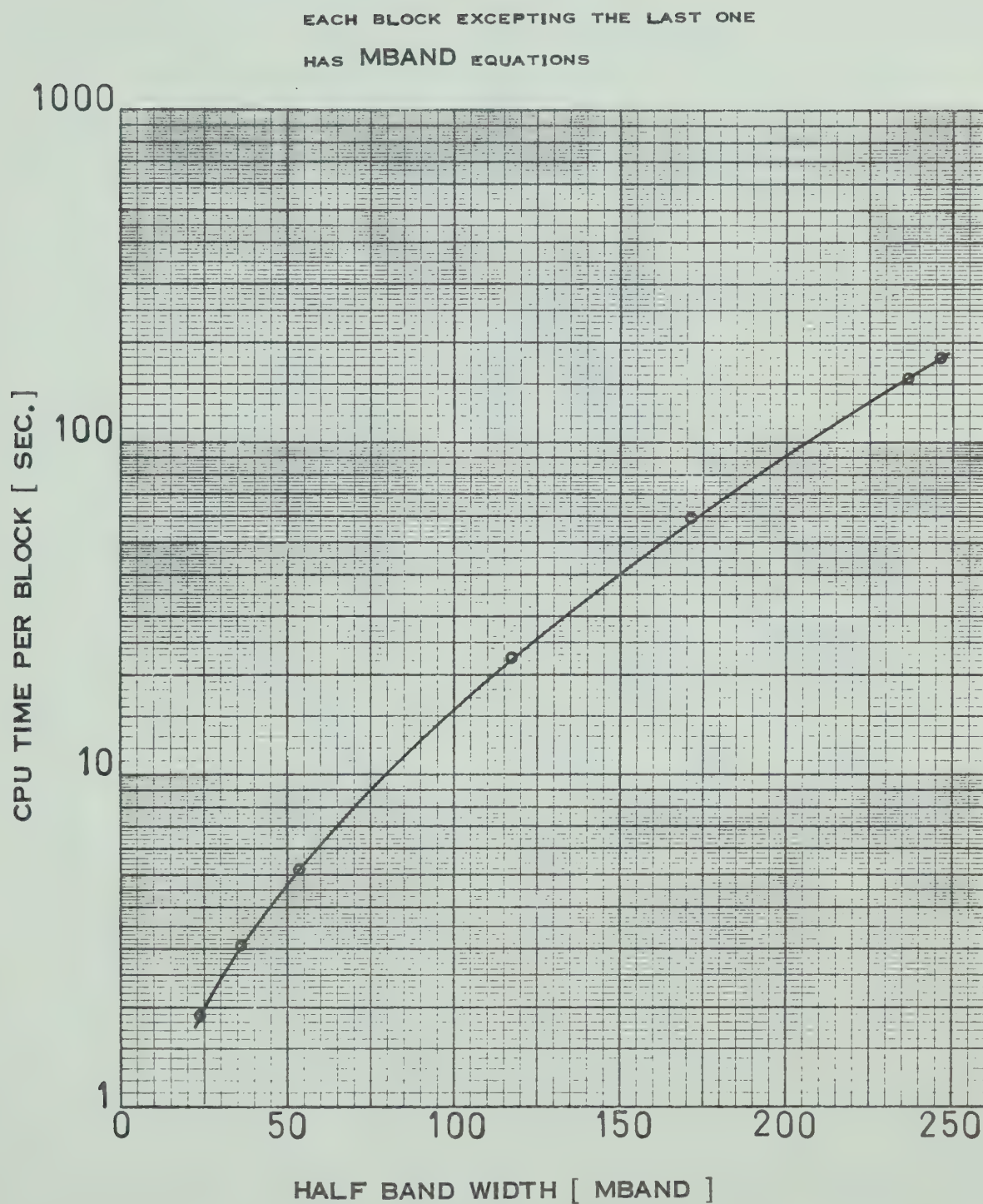


FIG. B.2 APPROXIMATE CPU TIME FOR SOLUTION
OF EQUATIONS IN 3-D PROGRAM

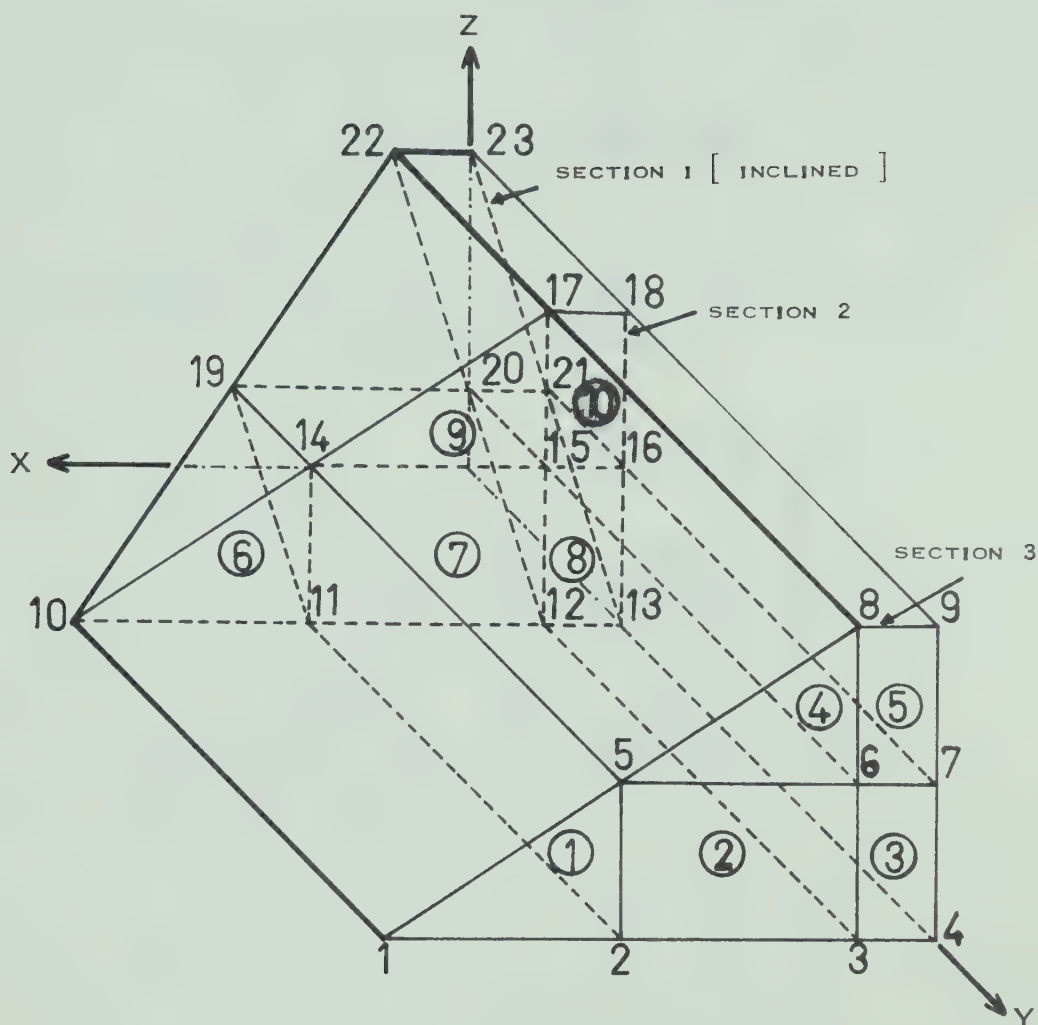


FIG. B.3 THREE DIMENSIONAL VIEW OF A MODEL DAM [ELEMENT NUMBERS ARE CIRCLED]

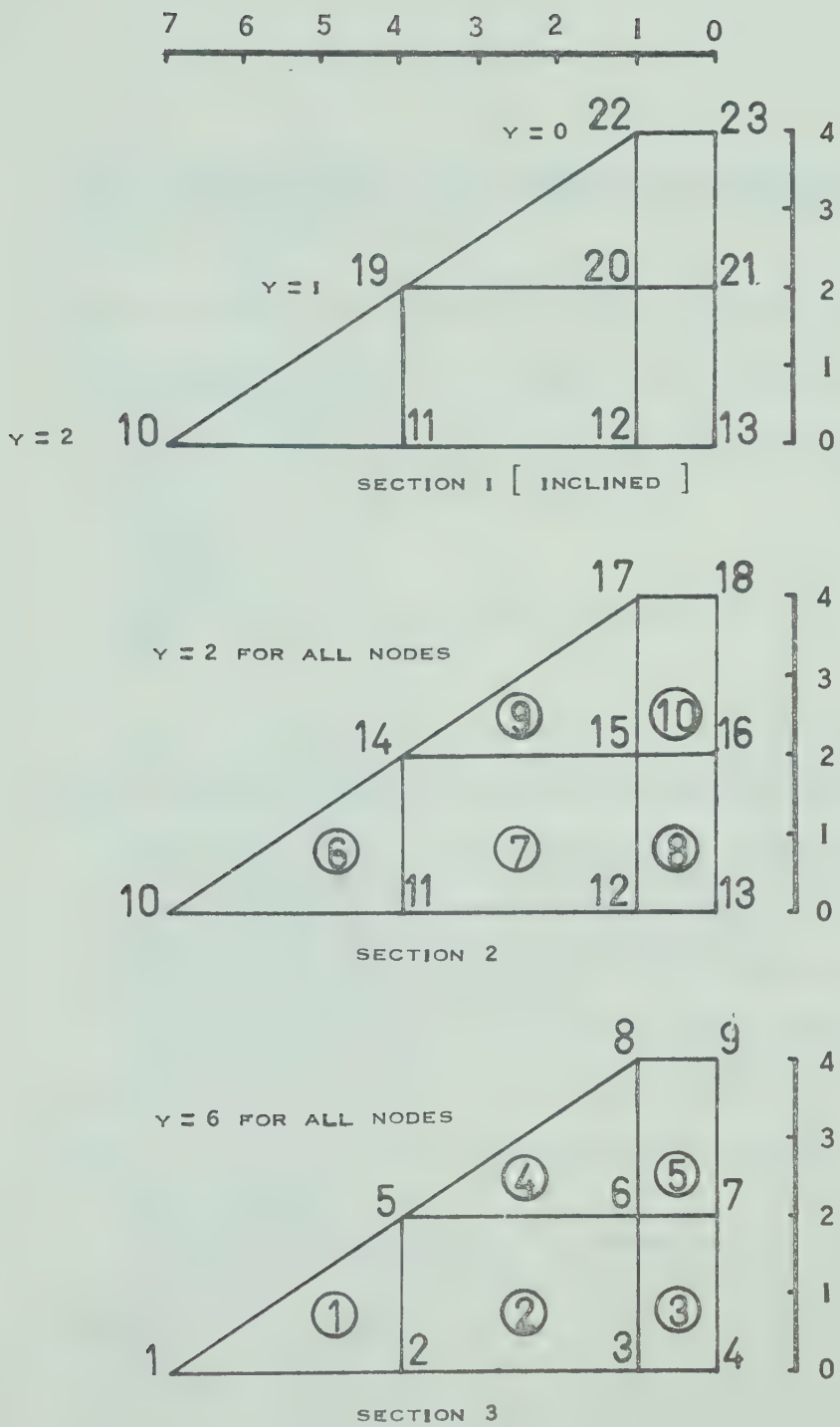


FIG. B.4 SECTIONAL VIEWS OF MODEL DAM
 [ELEMENT NUMBERS ARE CIRCLED]


```

6      C THREE DIMENSIONAL FINITE ELEMENT PROGRAM USING ISOPARAMETRIC HEXAHEDRA
7      C WITH 24 DEGREES OF FREEDOM PER EACH ELEMENT. EQUATIONS ARE SOLVED BY
8      C GAUSSIAN ELIMINATION IN BLOCKS.
9      C
10     C
11     C
12     C DEVELOPED & CODED BY A.V.G.KRISHNAYYA, CIVIL ENG. DEPT., U OF A, 1971.
13     C
14     C
15     C MAIN PROGRAM THAT CHANGES THE DIMENSIONS AND EQUIVALENCE STATEMENTS
16     C ACCORDING TO THE SIZE OF THE PROBLEM
17     C
18         DIMENSION B(405), A(114,228), BL(114), BR(114), AL(12996), AR(12996)
19         EQUIVALENCE (B(1),BL(1)),(B(115),BR(1)),(A(1,1),AL(1)),(A(1,115),
20         1AR(1))
21         NE1=405
22         MB1=114
23         MB2=2*MB1
24         LA=MB1**2
25         LA2=LA
26         CALL MSUB(B,A,BL,BR,AL,AR,MB1,MB2,LA,LA2,NE1)
27         STOP
28         END
29     C
30     C
31         SUBROUTINE MSUB(AP,STIF,APL,APR,STIFL,STIFR,MB1,MB2,LA,LA2,NE1)
32     C
33     C THIS IS THE MASTER SUBROUTINE WHICH CALLS OTHER SUBROUTINES REQUIRED
34     C FOR ANALYSIS. IT INTERPOLATES THE ELASTIC PARAMETERS FOR EACH STEP.
35     C
36         COMMON NANLYS,KSHIFT, RO(350),X(450),Y(450),Z(450),U(450),V(450),
37         1W(450),SGTEL(350,6),SGTPS(350,7),STRNT(350,6),STNT(450,3),
38         2 ECMI(3,3),STRN(6),ESTIF(24,24),ECM(6,6),EBM(6,24),ESM(6,24),WT
39         COMMON NUMNP,NUMEL, NE2, KODE( 450),SGTNP(450,6),
40         1NP(8, 350),MAT( 350),MBAND,NEQ,M,LM(24),KOEL( 350),
41         2PSY(52),ETA(52),ZTA(52),AQ(43),PP(24),ELDISP(24),
42         3KOUNT( 450),SIGA( 450,6),STN( 450,3),SIGEL(6),SIGP(7),NUMBLK,
43         4 DISPX(450),DISPY(450),DISPZ(450)
44         COMMON EBULK(350),EDEV(350),NITER,ITOPT,ACOE( 5),BCOE( 5),STP(3)
45         COMMON/AREA1/ST(20,5),SL(10,5),SD(20,10,5),VS(20,10,5),NUMAT,NCELP
46         1,CONFAC,NSTRN
47         DIMENSION AP(NE1),STIF(MB1,MB2),APL(MB1),APR(MB1),STIFL(LA2),
48         1STIFR(LA)
49     C
50     C COORDINATES OF PARENT ELEMENT ARE STORED IN THREE VECTORS
51         CALL TIME (0)
52         EXTERNAL GETFD
53         INTEGER ADROF,FDUB
54         CALL RCALL(GETFD,2,0,ADROF(' -T '),1,FDUB,&100)
55         CALL SETDSN(1,' -T ',FDUB,&100)
56         GO TO 101
57         100 WRITE(6,600)
58         600 FORMAT(' FILE ERROR')
59         STOP
60         101 CONTINUE
61         NE2=NE1

```



```

62      DO 88 I=1,5,4
63      J1=I+1
64      DO 89 K=1,J1
65      PSY(K)=-1.
66      PSY(K+2)=+1.
67      89 CONTINUE
68      88 CONTINUE
69      DO 90 I=1,5,4
70      ETA(I)=-1.
71      ETA(I+1)=1.
72      ETA(I+2)=1.
73      90 ETA(I+3)=-1.
74      DO 91 I=1,4
75      ZTA(I)=-1.
76      91 ZTA(I+4)= 1.
77      DO 60 I= 45,49,4
78      J1=I+1
79      DO 61 K=1,J1
80      PSY(K)=-0.99
81      PSY(K+2)=0.99
82      61 CONTINUE
83      60 CONTINUE
84      DO 62 I=45,49,4
85      ETA(I)=-0.99
86      ETA(I+1)=0.99
87      ETA(I+2)=0.99
88      62 ETA(I+3)=-0.99
89      DO 63 I=45,48
90      ZTA(I)=-0.99
91      63 ZTA(I+4)=0.99
92      C ARGUMENTS AND WEIGHTING FACTORS ARE STORED IN FOUR VECTORS
93      C TWO POINT FORMULA
94      T1=-0.57735027
95      T2=-(T1)
96      DO 79 I=9,12
97      PSY(I)=T1
98      79 PSY(I+4)=T2
99      DO 81 I=9,13,4
100     ETA(I)=T1
101     ETA(I+1)=T1
102     ETA(I+2)=T2
103     81 ETA(I+3)=T2
104     DO 82 I=9,15,2
105     ZTA(I)=T1
106     82 ZTA(I+1)=T2
107     C THREE POINT FORMULA
108     T3=-0.77459667
109     T4=0.0
110     T5=-(T3)
111     A1=0.55555556
112     A2=0.888888889
113     DO 85 I=17,25
114     PSY(I)=T3
115     PSY(I+9)=T4
116     85 PSY(I+18)=T5
117     DO 86 I=17,35,9
118     J1=I+2
119     DO 87 K=1,J1
120     ETA(K)=T3
121     ETA(K+3)=T4

```



```

122      ETA(K46)=T5
123      87 CONTINUE
124      86 CONTINUE
125      DO 92 I=17,41,3
126      ZTA(I)=T3
127      ZTA(I+1)=T4
128      ZTA(I+2)=T5
129      92 CONTINUE
130      AQ(17)=(A1**3)
131      AQ(19)=(A1**3)
132      AQ(23)=(A1**3)
133      AQ(25)=(A1**3)
134      AQ(35)=(A1**3)
135      AQ(37)=(A1**3)
136      AQ(41)=(A1**3)
137      AQ(43)=(A1**3)
138      DO 95 I=18,28,2
139      95 AQ(I)=(A1**2)*A2
140      DO 96 I=32,42,2
141      96 AQ(I)=(A1**2)*A2
142      AQ(21)=(A2**2)*A1
143      AQ(27)=(A2**2)*A1
144      AQ(29)=(A2**2)*A1
145      AQ(31)=(A2**2)*A1
146      AQ(33)=(A2**2)*A1
147      AQ(39)=(A2**2)*A1
148      AQ(30)=(A2**3)
149      CALL READIN(AP,STIF,APL,APR,STIFL,STIFR,ME1,M82,LA,LA2)
150      CALL TIME(1,1)
151      CKTERMI>0 TERMINATES EXECUTION AFTER GENERATION OF NODAL & ELEMENT DATA
152      C***** READ STATEMENT *****
153      READ(5,1015) KTERMI
154      IF(KTERMI.GT.0) GO TO 28
155      C ITOPT=0 PAST STRESS SOLUTION
156      C ITOPT=1 AVERAGE STRESS SOLUTION
157      C***** READ STATEMENT *****
158      READ(5,1015) ITOPT
159      C
160      C INITIALIZE THE TOTAL ELEMENT AND NODAL STRESSES, STRAINS AND
161      C NODAL DISPLACEMENTS
162      DO 10 I=1,NUMNP
163      DISPX(I)=0.0
164      DISPY(I)=0.0
165      DISPZ(I)=0.0
166      DO 10 J=1,6
167      10 SGYNP(I,J)=0.0
168      DO 15 I=1,NUMNP
169      DO 15 J=1,3
170      15 STNT(I,J)=0.0
171      DO 30 I=1,NUMEL
172      DO 30 J=1,6
173      30 SGTEL(I,J)=0.0
174      DO 31 I=1,NUMEL
175      DO 31 J=1,6
176      31 STRNT(I,J)=0.0
177      DO 35 I=1,NUMEL
178      DO 35 J=1,7
179      35 SGTPS(I,J)=0.0
180      C NSTEP=NUMBER OF INCREMENTS
181      C NSHEAR=0 SHEAR FAILURE NOT CONSIDERED

```



```

182      C NSHEAR=1 SHEAR FAILURE CONSIDERED
183      C ***** READ STATEMENT *****
184          READ (5,1000) NSTEP,NSHEAR
185          DO 20 IJK=1,NSTEP
186      C NUMEL= NUMBER OF ELEMENTS CONSIDERED IN CURRENT INCREMENT
187      C ***** READ STATEMENT *****
188          READ (5,1015) NUMELS
189          WRITE(6,1015) IJK
190          WRITE(6,1015) NUMELS
191          NUMEL=NUMELS
192      C
193      C
194      C
195      C ***** READ STATEMENT *****
196          READ(5,1015) NBOUN
197          IF(NBOUN.EQ.0) GO TO 222
198          WRITE(6,2003)
199          DO 206 J=1,NBOUN
200      C ***** READ STATEMENT *****
201          READ(5,2020) N,U(N),V(N),W(N)
202          WRITE(6,2002) N,U(N),V(N),W(N)
203      206      CONTINUE
204      222      NITER=0
205      205      NITER=NITER+1
206          CALL ASTIF(AP,STIF,AFL,APR,STIFL,STIFR,MB1,MB2,LA,LA2)
207          CALL TIME(1,1)
208      C
209          CALL BAND1(AP,STIF,AFL,APR,STIFL,STIFR,MB1,MB2,LA,LA2,FDUR)
210          WRITE (6,2003)
211          DO 25 N=1,NUMNP
212              DISPX(N)=DISPX(N)+AP(3*N-2)
213              DISPY(N)=DISPY(N)+AP(3*N-1)
214              DISPZ(N)=DISPZ(N)+AP(3*N)
215      25      WRITE (6,2002) N,DISPX(N),DISPY(N),DISPZ(N)
216              CALL TIME(1,1)
217              IF(ITOPT.EQ.0) GO TO 255
218              IF(NITER.EQ.2) GO TO 255
219              DO 251 N=1,NUMNP
220                  DISPX(N)=DISPX(N)-AP(3*N-2)
221                  DISPY(N)=DISPY(N)-AP(3*N-1)
222                  DISPZ(N)=DISPZ(N)-AP(3*N)
223      251      CONTINUE
224      C
225      255      CALL STRESS(AP,STIF,AFL,APR,STIFL,STIFR,MB1,MB2,LA,LA2)
226          CALL TIME(1,1)
227          IF(NSTEP.EQ.1.AND.ITOPT.EQ.0) GO TO 28
228          DO 26 M=1,NUMEL
229              MTYPE=MAT(M)
230              IF(ITOPT.EQ.0) RO(M)=0.0
231              IF(NITER.EQ.2) RO(M)=0.0
232              IF(NANLYS.EQ.0) GO TO 26
233              AVGSIG=ABS(SGTPS(M,1))
234              IF(SGTPS(M,1).GE.0.0)AVGSIG=0.0
235              DIVS=ABS(SGTPS(M,3))-AVGSIG
236              DIVS=ABS(DIVS)
237              VSTR=ABS(SGTPS(M,3))
238              N=MAT(M)
239              DIVSF=ACOE(N)+BCOE(N)+ABS(SGTPS(M,1))
240              IF(SGTPS(M,1).GE.0.0) DIVSF=ACOE(N)
241              IF(NCELP.EQ.0) GO TO 450

```



```

242      SIGM1=ABS(SGTPS(M,3))
243      SIGM2=ABS(SGTPS(M,2))
244      IF(SGTPS(M,2).GE.0.0) SIGM2=0.0
245      SIGM3=ABS(SGTPS(M,1))
246      IF(SGTPS(M,1).GE.0.0) SIGM3=0.0
247      SIGOCT=(SIGM1+SIGM2+SIGM3)/3.
248      SIGIN=SIGM1+SIGM2+SIGM3
249      CONF5=SIGIN/(SIGOCT**2)
250      DIVOCT=SQRT(((SIGM1-SIGM2)**2+((SIGM2-SIGM3)**2+((SIGM3-SIGM1)**2)
251      DIVOCT=DIVOCT/3.
252      DO 41 J=1,NCELP
253      JLS=J
254      IF(CONF5-SL(J,N)) 42,41,41
255      41 CONTINUE
256      42 CONTINUE
257      DO 43 K=1,NSTRN
258      JS1=K
259      IF (DIVOCT-SD(K,JLS-1,N)) 44,43,43
260      43 CONTINUE
261      44 CONTINUE
262      DO 300 K=1,NSTRN
263      JS2=K
264      IF(DIVOCT-SD(K,JLS,N)) 301,300,300
265      300 CONTINUE
266      301 CONTINUE
267      PR1=1.061*(VS(JS1,JLS-1,N)-VS(JS1-1,JLS-1,N))/(ST(JS1,N)-ST(JS1-1,
268      IN))-1.0
269      IF(PR1.GT.0.49) PR1=0.49
270      PR2=1.061*(VS(JS2,JLS,N)-VS(JS2-1,JLS,N))/(ST(JS2,N)-ST(JS2-1,
271      IN))-1.0
272      IF(PR2.GT.0.49) PR2=0.49
273      PR3=PR1+((PR2-PR1)*(CONF5-SL(JLS-1,N))/(SL(JLS,N)-SL(JLS-1,N)))
274      IF(PR3.GT.0.49) PR3=0.49
275      DIF1=SD(JS1,JLS-1,N)-SD(JS1-1,JLS-1,N)
276      ETP1=DIF1/(ST(JS1,N)-ST(JS1-1,N))
277      GTP1=ETP1/(0.9428*(1.+PR1))
278      DIF2=SD(JS2,JLS,N)-SD(JS2-1,JLS,N)
279      ETP2=DIF2/(ST(JS2,N)-ST(JS2-1,N))
280      GTP2=ETP2/(0.9428*(1.+PR2))
281      GTP=GTP1+(GTP2-GTP1)*(CONF5-SL(JLS-1,N))/(SL(JLS,N)-SL(JLS-1,N))
282      GTP=100.*GTP
283      BULKM =GTP*2.*(1.+PR3)/(3.*(1.-2.*PR3))
284      SHEARM=GTP
285      IF(NCELP.NE.0) GO TO 455
286      450 CONTINUE
287      C DETERMINE MODULI FROM OTHER THAN TRIAXIAL DATA
288      455 CONTINUE
289      IF(NITER.EQ.1) TEBULK=BULKM
290      IF(NITER.EQ.2) EBULK(M)=BULKM
291      IF(ITOPT.GT.0.AND.NITER.EQ.1) EBULK(M)=(TEBULK+EBULK(M))/2.
292      IF(ITOPT.EQ.0.AND.NITER.EQ.1) EBULK(M)=TEBULK
293      IF(NITER.EQ.1) TEDEV=SHEARM
294      IF(NITER.EQ.1.AND.DIVS.GE.DIVSF.AND.NSHEAR.GT.0) TEDEV=EBULK(M)/50.
295      IF(NITER.EQ.2) EDEV(M)=SHEARM
296      IF(NITER.EQ.2.AND.DIVS.GE.DIVSF.AND.NSHEAR.GT.0) EDEV(M)=EBULK(M)/5
297      10.
298      IF(ITOPT.GT.0.AND.NITER.EQ.1) EDEV(M)=(TEDEV+EDEV(M))/2.
299      IF(ITOPT.EQ.0.AND.NITER.EQ.1) EDEV(M)=TEDEV
300      IF(EDEV(M).GT.(1.45*EBULK(M))) EDEV(M)=1.45*EBULK(M)
301      IF(EDEV(M).LT.(EBULK(M)/50.)) EDEV(M)=EBULK(M)/50.

```



```

302      26 CONTINUE
303      WRITE(6,2010) (M,EBULK(M),EDEV(M),RO(M),M=1,NUMEL)
304      IF(ITOPT.EQ.0) GO TO 20
305      IF(NITER.EQ.1) GO TO 205
306      CALL TIME(1.1)
307      20 CONTINUE
308  C
309      1000 FORMAT(2I5)
310      1015 FORMAT(I5)
311      1050 FORMAT(2F15.6)
312      2002 FORMAT (I4,3E15.5)
313      2003 FORMAT('1',10X,'NODAL DISPLACEMENTS'//,'NODE      X_DISP
314      1Y-DISP      Z-DISP'//)
315      2005 FORMAT(///,1H ,10X, 21H MATERIAL PROPERTIES //
316      11X, 8HELE. NO.,4X, 9HBULK MOD.,4X,14HSHEAR MODULUS,4X,11HUNIT WEI
317      2GHT,//)
318      2010 FORMAT(1H ,15,F17.4,F15.3,F17.4)
319      2020 FORMAT(15,3F10.0)
320      28 RETURN
321      END
322  C
323  C
324      SUBROUTINE READIN(AP,STIF,APL,APR,STIFL,STIFR,MB1,MB2,LA,LA2)
325  C
326  C THIS SUBROUTINE READS AND PRINTS MATERIAL DATA, NODAL DATA, ELEMENT DATA.
327  C IT GENERATES COORDINATES OF INTERMEDIATE NODAL POINTS AND CALCULATES
328  C THE BAND WIDTH AND NUMBER OF EQUATIONS
329  C
330  C
331  C
332      COMMON NANLYS,KSHIFT, RO(350),X(450),Y(450),Z(450),U(450),V(450),
333      1W(450),SGTEL(350,6),SGTPS(350,7),STRNT(350,6),STNT(450,3),
334      2 ECMI(3,2),STRN(6) ,ESTIF(24,24),ECM(6,6),EBM(6,24),ESM(6,24),WT
335      COMMON NUMNP,NUMEL, NE2, KODE( 450),SGTNP(450,6),
336      1NP(8, 350),MAT( 350),MBAND,NEQ,M,LM(24),KOEL( 350),
337      2PSY(52),ETA(52),ZTA(52),AQ(43),PP(24),ELDISP(24),
338      3KOUNT( 450),SIGA( 450,6),STN( 450,3),SIGEL(6),SIGP(7),NUMBLK,
339      4 DISPX(450),DISPY(450),DISPZ(450)
340      COMMON EBULK(350),EDEV(350),NITER,ITOPT,ACOE( 5),BCOE( 5),STP(3)
341      COMMON/AREA1/ST(20,5),SL(10,5),SD(20,10,5),VS(20,10,5),NUMAT,NCELP
342      1,CONFAC,NSTRN
343      DIMENSION AP(NE2),STIF(MB1,MB2),APL(MB1),APR(MB1),STIFL(LA2),
344      1STIFR(LA)
345  C
346      DIMENSION HED(18),OBFAC(350),ROREAD( 5),EBREAD( 5),ESREAD( 5)
347  C READ PRELIMINARY INFORMATION
348  C NANLYS TO BE ZERO WHEN NUMAT=1 AND ANALYSIS IS LINEAR
349  C***** READ STATEMENT *****
350      READ (5,1000) HED,NUMNP,NUMEL,NUMAT,NUMCE,NUMTP,NUMTH,NANLYS
351      WRITE (6,2000) HED,NUMNP,NUMEL,NUMAT,NUMCE,NUMTP,NUMTH
352  C
353  C READ AND WRITE MATERIAL PROPERTIES
354  C
355  C READ AND WRITE NODAL DATA AND GENERATE INTERMEDIATE NODAL DATA
356  C
357      32 WRITE(6,2015)
358      L=1
359  C***** READ STATEMENT *****
360      READ(5,1020) N,KODE(N),X(N),Y(N),Z(N),U(N),V(N),W(N)
361      GO TO 40

```



```

362      C
363      20 READ(5,1020) N,KODE(N),X(N),Y(N),Z(N),U(N),V(N),W(N)
364          DN = N-L
365          DX =(X(N)-X(L))/DN
366          DY =(Y(N)-Y(L))/DN
367          DZ =(Z(N)-Z(L))/DN
368      25  L=L+1
369      C
370          IF(N-L) 50,40,30
371      30  X(L) = X(L-1)+DX
372          Y(L) = Y(L-1)+DY
373          Z(L)=Z(L-1)+DZ
374          KODE(L)= 0
375          U(L) = 0
376          V(L)= 0
377          W(L)=0
378          GO TO 25
379      C
380      40  IF(NUMNP-N)750,60,20
381      750 WRITE (6,2025) N
382          CALL EXIT
383      C
384      C ASSIGN PROPER CODE FOR NODES GENERATED BEFORE WITH KODE(N)=0
385      C
386      C***** READ STATEMENT *****
387      60  READ (5,1037) NUM1
388          IF(NUM1.EQ.0) GO TO 83
389          DO 81 I=1,NUM1
390      C***** READ STATEMENT *****
391      READ (5,1037) NUM2
392      C***** READ STATEMENT *****
393      READ (5,1016) N,KCODE(N)
394          IF (NUM2.EQ.0) GO TO 81
395          DO 82 J=1,NUM2
396          N=N+1
397          KODE(N)=KCODE(N-1)
398      82  CONTINUE
399      81  CONTINUE
400      83  WRITE(6,2020)(N,KODE(N),X(N),Y(N),Z(N),U(N),V(N),W(N),N=1,NUMNP)
401      C
402      C
403      C READ AND WRITE ELEMENT DATA
404      C
405      C GENERATE THE HEXAHEDRA AND BASE TRIANGULAR PRISMS IF ANY
406          WRITE (6,2030)
407          DO 70 IJ=1,NUMCE
408      C***** READ STATEMENT *****
409      READ (5,1037) NUMJK
410          WRITE(6,1037) NUMJK
411      C***** READ STATEMENT *****
412      READ (5,1036) M,KOEL(M),(NP(KK,M),KK=1,8),MAT(M)
413          WRITE(6,1036) M,KOEL(M),(NP(KK,M),KK=1,8),MAT(M)
414          IF (NUMJK.EQ.0) GO TO 70
415          DO 71 JK=1,NUMJK
416          M=M+1
417          KOEL(M)=KOEL(M-1)
418          MAT(M)=MAT(M-1)
419          NP(1,M)=NP(1,M-1)+1
420          NP(2,M)=NP(2,M-1)+1
421          NP(3,M)=NP(3,M-1)+1

```



```

422      NP(4,M)=NP(4,M-1)+1
423      NP(5,M)=NP(5,M-1)+1
424      NP(6,M)=NP(6,M-1)+1
425      NP(7,M)=NP(7,M-1)+1
426      NP(8,M)=NP(8,M-1)+1
427      WRITE(6,1036) M,KOEL(M),(NP(KK,M),KK=1,8),MAT(M)
428      71 CONTINUE
429      70 CONTINUE
430      IF(NUMTP.EQ.0) GO TO 74
431      C READ THE TRIANGULAR PRISMS
432      DO 84 I=1,NUMTP
433      C***** READ STATEMENT *****
434      READ (5,1036) M,KOEL(M),(NP(KK,M),KK=1,8),MAT(M)
435      WRITE(6,1036) M,KOEL(M),(NP(KK,M),KK=1,8),MAT(M)
436      84 CONTINUE
437      74 IF (NUMTH.EQ.0) GO TO 75
438      C READ THE TETRAHEDRA
439      DO 73 I=1,NUMTH
440      C***** READ STATEMENT *****
441      READ (5,1036) M,KOEL(M),(NP(KK,M),KK=1,8),MAT(M)
442      WRITE(6,1036) M,KOEL(M),(NP(KK,M),KK=1,8),MAT(M)
443      73 CONTINUE
444      75 IF(NUMAT.EQ.1) GO TO 510
445      C ASSIGN PROPER MAT(M) FOR ELEMENTS WHOSE MAT(M).NE.1
446      C***** READ STATEMENT *****
447      READ(5,1037) MATN
448      IF(MATN.EQ.0) GO TO 510
449      C***** READ STATEMENT *****
450      DO 2 I=1,MATN
451      2 READ(5,1016) M,MAT(M)
452      510 DO 200 I=1,NUMAT
453      C
454      C ACDEF=2.*COS(PHI)/(1.-SIN(PHI)),BCDEF=2.*SIN(PHI)/(1-SIN(PHI))
455      C
456      C***** READ STATEMENT *****
457      READ (5,2057) ROREAD(I),EBREAD(I),ESREAD(I),ACDEF(I),BCDEF(I)
458      WRITE(6,2059) ROPEAC(I),EBREAD(I),ESREAD(I),ACDEF(I),BCDEF(I)
459      200 CONTINUE
460      DO 140 N=1,NUMEL
461      I=MAT(N)
462      PO(N)=ROREAD(I)
463      EBULK(N)=EBREAD(I)
464      EDEV(N)=ESREAD(I)
465      OBFAC(N)=1.0
466      140 CONTINUE
467      C***** READ STATEMENT *****
468      READ (5,1037) NOBSET
469      IF(NOBSET.EQ.0) GO TO 150
470      DO 145 I=1,NOBSET
471      C***** READ STATEMENT *****
472      READ (5,1050) M,NSET,OBFAC(M)
473      IF(NSET.EQ.0) GO TO 145
474      DO 155 J=1,NSET
475      M=M+1
476      155 OBFAC(M)=OBFAC(M-1)
477      145 CONTINUE
478      C***** READ STATEMENT *****
479      150 READ(5,1050) NCELP,NSTRN,CONFAC
480      IF(NCELPEQ.0) GO TO 100
481      CALL TESTD

```



```

482      DO 600 M=1,NUMEL
483      IF(RO(M).LE.0.0) GO TO 600
484      N=MAT(M)
485      NCOUNT=0
486      DEPTH=(ABS(Z(NP(5,M))-Z(NP(1,M)))+ABS(Z(NP(6,M))-Z(NP(2,M)))
487      1+ABS(Z(NP(7,M))-Z(NP(3,M)))+ABS(Z(NP(8,M))-Z(NP(4,M))))*0.125
488      OBP=DEPTH*RO(M)*OBFAC(M)
489      AVGSIG=OBP*0.5
490      18      NCOUNT=NCOUNT+1
491      SIGM1=OBP
492      SIGM2=AVGSIG
493      SIGM3=AVGSIG
494      SIGOCT=(SIGM1+SIGM2+SIGM3)/3.
495      SIGIN=SIGM1*SIGM2*SIGM3
496      CONFS=SIGIN/(SIGOCT**2)
497      DIVOCT=SQRT((SIGM1-SIGM2)**2+(SIGM2-SIGM3)**2+(SIGM3-SIGM1)**2)
498      DIVOCT=DIVOCT/3.
499      DO 720 J=1,NCELP
500      JLS=J
501      IF( CONFS-SL(J,N)) 721,720,720
502      720      CONTINUE
503      721      CONTINUE
504      DO 790 K=1,NSTRN
505      JS1=K
506      IF(DIVOCT-SD(K,JLS-1,N)) 791,790,790
507      790      CONTINUE
508      791      CONTINUE
509      DO 50 K=1,NSTRN
510      JS2=K
511      IF(DIVOCT-SD(K,JLS,N)) 51,50,50
512      50      CONTINUE
513      51      CONTINUE
514      PR1=1.061*(VS(JS1,JLS-1,N)-VS(JS1-1,JLS-1,N))/(ST(JS1,N)-ST(JS1-1,
515      1N))-1.0
516      IF(PR1.GT.0.49) PR1=0.49
517      PR2=1.061*(VS(JS2,JLS ,N)-VS(JS2-1,JLS ,N))/(ST(JS2,N)-ST(JS2-1,
518      1N))-1.0
519      IF(PR2.GT.0.49) PR2=0.49
520      PR3=PR1+((PR2-PR1)*( CONFS-SL(JLS-1,N))/(SL(JLS,N)-SL(JLS-1,N)))
521      IF(PR3.GT.0.49 ) PR3=0.49
522      CONST=PR3/(1.-PR3)
523      HPR=OBP*CONST
524      HPR=(HPR+AVGSIG)/2.
525      CSTRS=ABS(HPR-AVGSIG)
526      IF(NCOUNT.GE.21) GO TO 52
527      IF(ABS(HPR-AVGSIG).LT.0.01) GO TO 52
528      AVGSIG=HPR
529      GO TO 18
530      52      WRITE(6,125) M,NCOUNT,HPR,CSTRS,PR3
531      DIF1=SD(JS1,JLS-1,N)-SD(JS1-1,JLS-1,N)
532      ETP1=DIF1/(ST(JS1,N)-ST(JS1-1,N))
533      GTP1=ETP1/(0.9428*(1.+PR1))
534      DIF2=SD(JS2,JLS,N)-SD(JS2-1,JLS,N)
535      ETP2=DIF2/(ST(JS2,N)-ST(JS2-1,N))
536      GTP2=ETP2/(0.9428*(1.+PR2))
537      GTP=GTP1+ (GTP2-GTP1)*(CONFS -SL(JLS-1,N))/(SL(JLS,N)-SL(JLS-1,N))
538      GTP=100.*GTP
539      EBULK(M)=GTP*2.*(1.+PR3)/(3.*(1.-2.*PR3))
540      EDEV(M)=GTP
541      600      CONTINUE

```



```

542         IF(NCELP.NE.0) GO TO 310
543     100 IF(NANLYS.EQ.0) GO TO 310
544 C ASSIGN MODULI FROM OTHER THAN TRIAXIAL DATA
545     310 DO 76 M=1,NUMEL
546         76 WRITE(6,1036) M,KCEL(M),(NP(KN,M),KN=1,8),MAT(M)
547         WRITE(6,2005)
548         WRITE(6,2010) (M,EBULK(M),EDEV(M),RO(M),M=1,NUMEL)
549 C
550 C     DETERMINE BAND WIDTH AND NUMBER OF EQUATIONS
551 C
552     L=0
553     DO 80 M=1,NUMEL
554     DO 80 I=1,7
555     II=I+1
556     DO 80 J=II,8
557     K= IABS(NP(I,M)-NP(J,M))
558     IF (K.GT.L) L=K
559 80 CONTINUE
560     WRITE(6,3000)
561 C
562     MBAND=3*(L+1)
563     NEQ1=3*NUMNP
564 C
565     WRITE(6,2040)MBAND,NEQ1
566     IF(MBAND.LE.300)GO TO 90
567     CALL EXIT
568 C
569 3000 FORMAT( ' READIN COMPLETED ' ///)
570 90 RETURN
571 C
572 C FORMAT STATEMENTS
573     125 FORMAT(2I5,2E15,6,F8,5)
574     1000 FORMAT(18A4/ 7I6)
575     1016 FORMAT(2I5)
576     1036 FORMAT(11I5)
577     1037 FORMAT(15)
578     2000 FORMAT(1H1,10X,18A4,////
579         1 1H ,      26H NUMBER OF NODAL POINTS = ,I6/
580         2 1H ,      26H NUMBER OF ELEMENTS      = ,I6/
581         3 1H ,      26H NUMBER OF MATERIALS,      = ,I6/
582         4 1H ,      26H NUMBER OF HEXA. READ      = ,I6/
583         5 1H ,      26H NUMBER OF PRISMS          = ,I6/
584         6 1H ,      26H NUMBER OF TETRAEDRA       = ,I6)
585     2005 FORMAT(///,1H ,10X, 21H MATERIAL PROPERTIES //
586         11X, 8HELE. NO.,4X, 9HBULK MOD.,4X,14HSHEAR MODULUS,4X,11HUNIT WEI
587         2GHT,///)
588     1010 FORMAT(6X,F12,0,2F6,0)
589     2010 FORMAT(1H ,15,F17,4,F15,3,F17,4)
590     2012 FORMAT (F17,4,F15,3,F17,4)
591     2015 FORMAT('1',10X,'NODAL POINT INPUT'//,'NODE   CODE       XCOORD       Y
592         1 COORD      Z COORD      X FORCE      Y FORCE      Z FORCE'//)
593     1020 FORMAT(2I5,6F5,0)
594     2020 FORMAT(14,I6,6F12,3)
595     2025 FORMAT(1H0,26H ERROR IN NODAL DATA,NODE = ,I4)
596     2030 FORMAT('1',10X,'ELEMENT DATA'//,'ELEM EL.CODE N1   N2   N3   N4
597         1 N5   N6   N7   N8 MAT.NUM.'//)
598     1035 FORMAT (6I6,F6,0)
599     2040 FORMAT(///10X,' BAND WIDTH              =',I6/
600         1          10X,'NUMBER OF EQUATIONS =' ,I6)
601     2050 FORMAT(///10X, 33H PROBLEM EXCEEDS SPECIFIED LIMITS )

```



```

602      2051 FORMAT(5F5.0)
603      2052 FORMAT(6F5.0)
604      2053 FORMAT('0',10X,'STRESS - STRAIN RELATIONSHIPS FOR MATERIAL',16//)
605      2055 FORMAT(1X,'LATSTRESS',6X,5F8.3/)
606      2056 FORMAT(1X,'STRN.',3X,F6.2,5F8.3/)
607      2057 FORMAT(5F10.0)
608      2059 FORMAT(5F15.6)
609      1050 FORMAT(215,F10.0)
610      2060 FORMAT(5F10.2)
611      C
612      END
613      C
614      SUBROUTINE TESTD
615      C
616      C THIS SUBROUTINE CONVERTS TRIAXIAL TEST DATA FROM CONVENTIONAL FORM
617      C TO INVARIANT FORM.
618      C
619      C
620      DIMENSION SL(10,5),SD(20,10,5),VS(20,10,5),SIGINV(20,10,5),
621      IVSTN(20,10,5),
622      COMMON/AREA1/
623      1      ST(20,5),SIGINT(10,5),TOCTD(20,10,5),GOCT(20,10,5),NUMAT,
624      INCPLP,CONFAC,NSTRN
625      DO 10 N=1,NUMAT
626      C*****READ STATEMENT *****
627      READ(5,1010) (SL(J,N),J=1,NCPLP)
628      DO 15 J=1,NCPLP
629      SL(J,N)=SL(J,N)*CONFAC
630      SIGINT(J,N)=SL(J,N)
631      15 CONTINUE
632      DO 20 K=1,NSTRN
633      C***** READ STATEMENT *****
634      READ(5,1020) ST(K,N),(SD(K,J,N),J=1,NCPLP)
635      DO 25 J=1,NCPLP
636      SD(K,J,N)=SD(K,J,N)*CONFAC
637      25 CONTINUE
638      20 CONTINUE
639      WRITE (6,1030) N
640      WRITE(6,1040) (SL(J,N),J=1,NCPLP)
641      DO 30 K=1,NSTRN
642      C***** READ STATEMENT *****
643      READ (5,1020) ST(K,N),(VS(K,J,N),J=1,NCPLP)
644      WRITE(6,1050) ST(K,N),(VS(K,J,N),J=1,NCPLP)
645      30 CONTINUE
646      DO 35 K=1,NSTRN
647      WRITE(6,1050) ST(K,N),(SD(K,J,N),J=1,NCPLP)
648      35 CONTINUE
649      10 CONTINUE
650      DO 40 N=1,NUMAT
651      DO 45 J=1,NCPLP
652      DO 50 K=1,NSTRN
653      PROD= (SL(J,N)**2)*(SD(K,J,N)+SL(J,N))
654      SIGOCT=SL(J,N)+(SD(K,J,N))/3.
655      IF(J.EQ.1.AND.K.EQ.1) GO TO 51
656      SIGINV(K,J,N)=PROD/(SIGOCT**2)
657      51 IF(J.EQ.1.AND.K.EQ.1) SIGINV(K,J,N)=0.0
658      50 CONTINUE
659      45 CONTINUE
660      DO 70 I=1,NCPLP
661      DO 55 K=1,NSTRN

```



```

662      DO 60 J=1,NCELP
663      JLS=J
664      IF (SIGINT(I,N)-SIGINV(K,J,N))61,60,60
665 60 CONTINUE
666 61 CONTINUE
667      TOCTD(K,I,N)=SD(K,JLS-1,N)+(SD(K,JLS,N)-SD(K,JLS-1,N))*((SIGINT(I,N)
668 1)-SIGINV(K,JLS-1,N))/(SIGINV(K,JLS,N)-SIGINV(K,JLS-1,N))
669      TOCTD(K,I,N)=TOCTD(K,I,N)*0.4714
670      VSTN(K,I,N)=VS(K,JLS-1,N)+(VS(K,JLS,N)-VS(K,JLS-1,N))*((SIGINT(I,N)
671 1-SIGINV(K,JLS-1,N))/(SIGINV(K,JLS,N)-SIGINV(K,JLS-1,N))
672      GOCT(K,I,N)=0.4714*(3.*ST(K,N) -VSTN(K,I,N))
673 55 CONTINUE
674 70 CONTINUE
675      WRITE(6,1031) N
676      WRITE (6,1041) (SIGINT(I,N),I=1,NCELP)
677      DO 75 K=1,NSTRN
678 75 WRITE(6,1050)ST(K,N),(TOCTD(K,I,N),I=1,NCELP)
679      DO 80 K=1,NSTRN
680 80 WRITE(6,1050) ST(K,N),(GOCT(K,J,N),J=1,NCELP)
681 40 CONTINUE
682 1000 FORMAT(3I5,F10.0)
683 1010 FORMAT(10F5.0)
684 1020 FORMAT(11F5.0)
685 1030 FORMAT('0','DATA IN CONVENTIONAL FORM FOR MATERIAL NO.',I5/)
686 1031 FORMAT('0',' DATA IN STRESS INVARIANT FORM FOR MATERIAL NO. ',I5/)
687 1040 FORMAT(1X,'LATSTRESS',6X,10F8.3/)
688 1041 FORMAT(1X,'J3/(SIGOCT)**2',1X,10F8.3/)
689 1050 FORMAT(1X,'STRAIN',3X,F6.2,10F8.3/)
690 1060 FORMAT(I5)
691 1070 FORMAT(3F10.0)
692 1071 FORMAT(3F8.3,4F12.4)
693      RETURN
694      END
695 C
696      SUBROUTINE ASTIF(AP,STIF,AFL,APR,STIFL,STIFR,MB1,MB2,LA,LA2)
697 C
698 C THIS SUBROUTINE TAKES EACH ELEMENT IN TURN AND FORMS THE ELEMENT STIFFNESS
699 C MATRIX (BY CALLING ELSTIF).IT ASSEMBLES THE ELEMENT STIFFNESSES INTO
700 C TOTAL STIFFNESS MATRIX . ASSEMBLES THE APPLIED LOAD VECTOR & MODIFIES
701 C THE ASSEMBLAGES FOR DISPLACEMENT BOUNDARY CONDITIONS ( BY CALLING
702 C MODIFY).
703 C
704      COMMON NANLYS,KSHIFT, RO(350),X(450),Y(450),Z(450),U(450),V(450),
705 1W(450),SGTEL(350,6),SGTPS(350,7),STRNT(350,6),STNT(450,3),
706 2 ECMI(3,3),STRN(6) ,ESTIF(24,24),ECM(6,6),EBM(6,24),FSM(6,24),WT
707      COMMON NUMNP,NUMEL, NE2, KODE( 450),SGTNP(450,6),
708 1NP(8, 350),MAT( 350),MBAND,NEQ,M,LM(24),KOEL( 350),
709 2PSY(52),ETA(52),ZTA(52),AQ(43),PP(24),ELDISP(24),
710 3KOUNT( 450),SIGA( 450,6),STN( 450,3),SIGEL(6),SIGP(7),NUMBLK,
711 4 DISPX(450),DISPY(450),DISPZ(450)
712      COMMON EBULK(350),EDEV(350),NITER,ITOPT,ACDEF( 5),BCDEF( 5),STP(3)
713      COMMON/AREAL/ST(20,5),SL(10,5),SD(20,10,5),VS(20,10,5),NUMAT,NCELP
714 1,CONFAC,NSTRN
715      DIMENSION AP(NE2),STIF(MB1,MB2),APL(MB1),APR(MB1),STIFL(LA2),
716 1STIFR(LA)
717 C
718      INTEGER*2 LEN
719      NBYTES=MBAND*MBAND*4
720      FNUMRC=FLOAT(NBYTES)/32000
721      NUMREC=NBYTES/32000

```



```

722      IF ((FNUMRC-NUMREC).GT.0.0) NUMREC=NUMREC+1
723      600 FORMAT( 'FILE ERROR IN ASTIF*')
724      C
725      C      INITIALIZATION
726      C
727      REWIND 2
728      NB=MBAND/3
729      ND=3*NB
730      NEO=2*ND
731      NUMBLK=0
732      C
733      DO 10 I=1,NEO
734      AP(I)=0.0
735      DO 10 J=1,ND
736      10 STIF(J,I)=0.0
737      DO 21 I=1,6
738      DO 21 J=1,6
739      ECM(I,J)=0.0
740      21 CONTINUE
741      C
742      C      FORM ELEMENT CONSTITUTIVE MATRIX (ECM) IF NUMAT=1)
743      IF(NUMAT.NE.1) GO TO 20
744      IF(NANLYS.NE.0) GO TO 20
745      C
746      COM1=EBULK(1)+1.33333*EDEV(1)
747      COM2=EBULK(1)-0.666667*EDEV(1)
748      COM3=EDEV(1)
749      ECM(1,1)=COM1
750      ECM(2,2)=COM1
751      ECM(3,3)=COM1
752      ECM(4,4)=COM3
753      ECM(5,5)=COM3
754      ECM(6,6)=COM3
755      ECM(1,2)=COM2
756      ECM(1,3)=COM2
757      ECM(2,1)=COM2
758      ECM(2,3)=COM2
759      ECM(3,1)=COM2
760      ECM(3,2)=COM2
761      DET=COM1**3+2.*COM2**3-3.*COM1*COM2**2
762      COM4=(COM1**2-COM2**2)/DET
763      COM5=(COM2**2-COM1*(COM2))/DET
764      ECMI(1,1)=COM4
765      ECMI(2,2)=COM4
766      ECMI(3,3)=COM4
767      ECMI(1,2)=COM5
768      ECMI(1,3)=COM5
769      ECMI(2,1)=COM5
770      ECMI(2,3)=COM5
771      ECMI(3,1)=COM5
772      ECMI(3,2)=COM5
773      C
774      C      FORM STIFFNESS MATRIX IN BLOCKS
775      20 NUMBLK=NUMBLK+1
776      NH=NB*(NUMBLK+1)
777      NM=NH-NB
778      NL=NM-NB+1
779      WRITE(6,1001) NUMBLK,NL,NM
780      KSHIFT=3*NL-3
781      DO 110 M=1,NUMBLK

```



```

782      IF(MAT(M))110,110,25
783      25 DO 35 I=1,8
784      IF(NP(I,M)-NL)35,30,30
785      30 IF(NP(I,M)-NM)40,40,35
786      35 CONTINUE
787      GO TO 110
788  C
789      40 CALL ELSTIF(AP,STIF,APL,APR,STIFL,STIFR,MB1,MB2,LA,LA2,I)
790      MAT(M)=-MAT(M)
791  C      ASSEMBLE ESTIF INTO TOTAL STIFFNESS MATRIX
792      DO 75 I=1,8
793      I2=3*I
794      LM(I2)=3*NP(I,M)
795      LM(I2-1)=LM(I2)-1
796      75 LM(I2-2)=LM(I2)-2
797  C
798      DO 100 I=1,24
799      II=LM(I)-KSHIFT
800      DO 100 J=1,24
801      JJ=LM(J)-II+1-KSHIFT
802      IF(JJ.LE.0) GO TO 100
803      STIF(JJ,II)=STIF(JJ,II)+ESTIF(I,J)
804      100 CONTINUE
805  C      ADD GRAVITY LOADS IN TO AP VECTOR
806      DO 46 I=3,24,3
807      II=LM(I)-KSHIFT
808      46 AP(II)=AP(II)-WT
809      110 CONTINUE
810      WRITE(6,1000)
811      WRITE(6,1002) (M,MAT(M),M=1,NUMEL)
812  C      ADD NODAL LOADS INTO AP VECTOR
813      DO 51 N=NL,NM
814      N2=3*N-KSHIFT
815      AP(N2)=AP(N2)+W(N)
816      AP(N2-1)=AP(N2-1)+V(N)
817      51 AP(N2-2)=AP(N2-2)+U(N)
818  C      MODIFY STIFFNESS AND LOAD VECTOR FOR DISPLACEMENTS
819      DO 102 N=NL,NM
820      IF(N=NUMNP) 111,111,102
821      111 N2=3*N-KSHIFT
822      IF (KODE(N)-10)82,72,62
823      62 IF(KODE(N).EQ.12)GO TO 61
824      IK=N2-1
825      CALL MODIFY(AP,STIF,APL,APR,STIFL,STIFR,MB1,MB2,LA,LA2,IK,N)
826      CALL MODIFY(AP,STIF,APL,APR,STIFL,STIFR,MB1,MB2,LA,LA2,N2,N)
827      GO TO 102
828      61 II=N2-2
829      IK=N2-1
830      CALL MODIFY(AP,STIF,APL,APR,STIFL,STIFR,MB1,MB2,LA,LA2,IK,N)
831      CALL MODIFY(AP,STIF,APL,APR,STIFL,STIFR,MB1,MB2,LA,LA2,N2,N)
832      CALL MODIFY(AP,STIF,APL,APR,STIFL,STIFR,MB1,MB2,LA,LA2,II,N)
833      GO TO 102
834      72 II=N2-2
835      IK=N2-1
836      CALL MODIFY(AP,STIF,APL,APR,STIFL,STIFR,MB1,MB2,LA,LA2,II,N)
837      CALL MODIFY(AP,STIF,APL,APR,STIFL,STIFR,MB1,MB2,LA,LA2,IK,N)
838      GO TO 102
839      82 IF(KODE(N)-1)102,78,101
840      78 CALL MODIFY(AP,STIF,APL,APR,STIFL,STIFR,MB1,MB2,LA,LA2,N2,N)
841      GO TO 102

```



```

842      101 IF(KODE(N)-3) 105,106,107
843      106 II=N2-2
844          CALL MODIFY(AP,STIF,APL,APR,STIFL,STIFR,MB1,MB2,LA,LA2,II,N)
845          GO TO 102
846      105 IK=N2-1
847          CALL MODIFY(AP,STIF,APL,APR,STIFL,STIFR,MB1,MB2,LA,LA2,IK,N)
848          GO TO 102
849      107 II=N2-2
850          CALL MODIFY(AP,STIF,APL,APR,STIFL,STIFR,MB1,MB2,LA,LA2,II,N)
851          CALL MODIFY(AP,STIF,APL,APR,STIFL,STIFR,MB1,MB2,LA,LA2,N2,N)
852      102 CONTINUE
853  C
854  C      WRITE BLOCK OF EQUATIONS ON DISC AND SHIFT UP LOWER BLOCK
855      LEN=32000
856      LL=1
857      DO 400 L=1,NUMREC
858          IF(L.EQ.NUMREC)LEN=NBYTES-((NUMREC-1)*32000)
859          CALL WRITE(STIFL(LL),LEN,0,1,2,6401)
860          WRITE(6,1005) LL,LEN,STIFL(LL)
861          LL=LL+8000
862          GO TO 400
863      401 WRITE(6,600)
864          STOP
865      400 CONTINUE
866      LEN=MBAND*4
867      CALL WRITE(APL,LEN,0,1,2,6401)
868      WRITE(6,1005) MBAND,LEN,APL(1)
869      1005 FORMAT(2I10,E20,7)
870      DO 270 I=1,ND
871          K=I+ND
872          AP(I)=AP(K)
873          AP(K)=0.0
874          DO 270 J=1,ND
875              STIF(J,I)=STIF(J,K)
876      270 STIF(J,K)=0.0
877  C
878  C      CHECK FOR LAST BLOCK
879  C
880      IF(NM-NUMNP)20,280,280
881      280 CONTINUE
882      RETURN
883      1000 FORMAT( /10X,'ELEMENT STIFFNESS FORMED FOR ELEMENTS WITH -VE MAT(M
884      1)IN THE FOLLOWING: '/')
885      1001 FORMAT( /10X,'BLOCK NUMBER=',I5/10X,'LOWEST NODE NUMBER=',I5/10X,
886      1'HIGHEST NODE NUMBER=',I5/)
887      1002 FORMAT (26I5)
888      END
889  C
890      SUBROUTINE ELSTIF(AP,STIF,APL,APR,STIFL,STIFR,MB1,MB2,LA,LA2,KOP)
891  C      THIS SUBROUTINE FORMS THE ELEMENT STIFFNESS MATRIX (ESTIF) OR
892  C      ELEMENT STRESS MATRIX (ESM)
893  C
894      COMMON NANLYS,KSHIFT, RO(350),X(450),Y(450),Z(450),U(450),V(450),
895      1W(450),SGTEL(350,6),SGTPS(350,7),STRNT(350,6),STNT(450,3),
896      2 ECMI(3,3),STRN(6),ESTIF(24,24),ECM(6,6),EBM(6,24),ESM(6,24),WT
897      COMMON NUMNP,NUMEL, NE2, KODE( 450),SGTNP(450,6),
898      1NP(8, 350),MAT( 350),MBAND,NEQ,M,LM(24),KOEL( 350),
899      2PSY(52),ETA(52),ZTA(52),AQ(43),PP(24),ELDISP(24),
900      3KOUNT( 450),SIGA( 450,6),STN( 450,3),SIGEL(6),SIGP(7),NUMBLK,
901      4 DISPX(450),DISPY(450),DISPZ(450)

```



```

902      COMMON EBULK(350),EDEV(350),NITER,ITOPT,ACOE( 5),BCOE( 5),STP(3)
903      COMMON/AREA1/ST(20,5),SL(10,5),SD(20,10,5),VS(20,10,5),NUMAT,NCELP
904      1,CONFAC,NSTRN
905      DIMENSION AP(NE2),STIF(MB1,MB2),APL(MB1),APR(MB1),STIFL(LA2),
906      1STIFR(LA)
907      DO 70 I=1,24
908      DO 70 J=1,24
909      70 ESTIF(I,J)=0.0
910      VOL=0.0
911      L1=NP(1,M)
912      L2=NP(2,M)
913      L3=NP(3,M)
914      L4=NP(4,M)
915      L5=NP(5,M)
916      L6=NP(6,M)
917      L7=NP(7,M)
918      L8=NP(8,M)
919      C FORM CONSTITUTIVE MATRIX
920      IF(NANLYS.NE.0) GO TO 2
921      IF(NUMAT.EQ.1) GO TO 17
922      2 COM1=EBULK(M)+1.33333*EDEV(M)
923      COM2=EBULK(M)-0.6666667*EDEV(M)
924      COM3=EDEV(M)
925      ECM(1,1)=COM1
926      ECM(2,2)=COM1
927      ECM(3,3)=COM1
928      ECM(4,4)=COM3
929      ECM(5,5)=COM3
930      ECM(6,6)=COM3
931      ECM(1,2)=COM2
932      ECM(1,3)=COM2
933      ECM(2,1)=COM2
934      ECM(2,3)=COM2
935      ECM(3,1)=COM2
936      ECM(3,2)=COM2
937      DET=COM1**3+2.*COM2**3-3.*COM1*COM2**2
938      COM4=(COM1**2-COM2**2)/DET
939      COM5=(COM2**2-COM1*COM2)/DET
940      ECMI(1,1)=COM4
941      ECMI(2,2)=COM4
942      ECMI(3,3)=COM4
943      ECMI(1,2)=COM5
944      ECMI(1,3)=COM5
945      ECMI(2,1)=COM5
946      ECMI(2,3)=COM5
947      ECMI(3,1)=COM5
948      ECMI(3,2)=COM5
949      C
950      17 IF(KOP.EQ.2) GO TO 14
951      IF(KOEL(M).LE.1) GO TO 11
952      IF(KOEL(M).GE.2) GO TO 12
953      11 DO 21 LN1=9,16
954      L=LN1
955      GO TO 13
956      12 DO 22 LN2=17,43
957      L=LN2
958      GO TO 13
959      14 IF(KOEL(M).EQ.1) GO TO 81
960      IF(KOEL(M).EQ.2) GO TO 81
961      DO 20 LN3=1,8

```



```

962         L=LN3
963         GO TO 13
964     81     DO 25 LN4=45,52
965         L=LN4
966         GO TO 13
967     15     L=44
968         PSY(44)=0.0
969         ETA(44)=0.0
970         ZTA(44)=0.0
971     C FORMULATE DERIVATIVE MATRIX
972     13     PEP1=-(1./8.)*(1.-ETA(L))*(1.-ZTA(L))
973         PEP2=-(1./8.)*(1.+ETA(L))*(1.-ZTA(L))
974         PEP3=(1./8.)*(1.+ETA(L))*(1.-ZTA(L))
975         PEP4=(1./8.)*(1.-ETA(L))*(1.-ZTA(L))
976         PEP5=-(1./8.)*(1.-ETA(L))*(1.+ZTA(L))
977         PEP6=-(1./8.)*(1.+ETA(L))*(1.+ZTA(L))
978         PEP7=+(1./8.)*(1.+ETA(L))*(1.+ZTA(L))
979         PEP8=+(1./8.)*(1.-ETA(L))*(1.+ZTA(L))
980         PET1=-(1./8.)*(1.-PSY(L))*(1.-ZTA(L))
981         PET2=+(1./8.)*(1.-PSY(L))*(1.-ZTA(L))
982         PET3=+(1./8.)*(1.+PSY(L))*(1.-ZTA(L))
983         PET4=-(1./8.)*(1.+PSY(L))*(1.-ZTA(L))
984         PET5=-(1./8.)*(1.-PSY(L))*(1.+ZTA(L))
985         PET6=+(1./8.)*(1.-PSY(L))*(1.+ZTA(L))
986         PET7=+(1./8.)*(1.+PSY(L))*(1.+ZTA(L))
987         PET8=-(1./8.)*(1.+PSY(L))*(1.+ZTA(L))
988         PZT1=-(1./8.)*(1.-PSY(L))*(1.-ETA(L))
989         PZT2=-(1./8.)*(1.-PSY(L))*(1.+ETA(L))
990         PZT3=-(1./8.)*(1.+PSY(L))*(1.+ETA(L))
991         PZT4=-(1./8.)*(1.+PSY(L))*(1.-ETA(L))
992         PZT5=+(1./8.)*(1.-PSY(L))*(1.-ETA(L))
993         PZT6=+(1./8.)*(1.-PSY(L))*(1.+ETA(L))
994         PZT7=+(1./8.)*(1.+PSY(L))*(1.+ETA(L))
995         PZT8=+(1./8.)*(1.+PSY(L))*(1.-ETA(L))
996     C FORM THE JACOBIAN MATRIX
997         X1J=PEP1*X(L1)+PEP2*X(L2)+PEP3*X(L3)+PEP4*X(L4)+PEP5*X(L5)+
998         1PEP6*X(L6)+PEP7*X(L7)+PEP8*X(L8)
999         X2J=PET1*X(L1)+PET2*X(L2)+PET3*X(L3)+PET4*X(L4)+PET5*X(L5)+
1000         1PET6*X(L6)+PET7*X(L7)+PET8*X(L8)
1001         X3J=PZT1*X(L1)+PZT2*X(L2)+PZT3*X(L3)+PZT4*X(L4)+PZT5*X(L5)+
1002         1PZT6*X(L6)+PZT7*X(L7)+PZT8*X(L8)
1003         Y1J=PEP1*Y(L1)+PEP2*Y(L2)+PEP3*Y(L3)+PEP4*Y(L4)+PEP5*Y(L5)+
1004         1PEP6*Y(L6)+PEP7*Y(L7)+PEP8*Y(L8)
1005         Y2J=PET1*Y(L1)+PET2*Y(L2)+PET3*Y(L3)+PET4*Y(L4)+PET5*Y(L5)+
1006         1PET6*Y(L6)+PET7*Y(L7)+PET8*Y(L8)
1007         Y3J=PZT1*Y(L1)+PZT2*Y(L2)+PZT3*Y(L3)+PZT4*Y(L4)+PZT5*Y(L5)+
1008         1PZT6*Y(L6)+PZT7*Y(L7)+PZT8*Y(L8)
1009         Z1J=PEP1*Z(L1)+PEP2*Z(L2)+PEP3*Z(L3)+PEP4*Z(L4)+PEP5*Z(L5)+
1010         1PEP6*Z(L6)+PEP7*Z(L7)+PEP8*Z(L8)
1011         Z2J=PET1*Z(L1)+PET2*Z(L2)+PET3*Z(L3)+PET4*Z(L4)+PET5*Z(L5)+
1012         1PET6*Z(L6)+PET7*Z(L7)+PET8*Z(L8)
1013         Z3J=PZT1*Z(L1)+PZT2*Z(L2)+PZT3*Z(L3)+PZT4*Z(L4)+PZT5*Z(L5)+
1014         1PZT6*Z(L6)+PZT7*Z(L7)+PZT8*Z(L8)
1015     C INVERT THE JACOBIAN MATRIX
1016         DETJ=X1J*(Y2J*Z3J-Z2J*Y3J)-Y1J*(X2J*Z3J-Z2J*X3J)+Z1J*(X2J*Y3J-Y2J*
1017         1X3J)
1018         IF(DE TJ.LE.0.0) GO TO 75
1019         X1I=(1./DETJ)*(Y2J*Z3J-Z2J*Y3J)
1020         X2I=(1./DETJ)*(Y3J*Z1J-Z3J*Y1J)
1021         X3I=(1./DETJ)*(Y1J*Z2J-Z1J*Y2J)

```



```

1022      Y1I=(1./DETJ)*(Z2J*X3J-X2J*Z3J)
1023      Y2I=(1./DETJ)*(Z3J*X1J-X3J*Z1J)
1024      Y3I=(1./DETJ)*(Z1J*X2J-X1J*Z2J)
1025      Z1I=(1./DETJ)*(X2J*Y3J-Y2J*X3J)
1026      Z2I=(1./DETJ)*(X3J*Y1J-Y3J*X1J)
1027      Z3I=(1./DETJ)*(X1J*Y2J-Y1J*X2J)
1028      PP(1)=X1I*PEP1+X2I*PET1+X3I*PZT1
1029      PP(2)=Y1I*PEP1+Y2I*PET1+Y3I*PZT1
1030      PP(3)=Z1I*PEP1+Z2I*PET1+Z3I*PZT1
1031      PP(4)=X1I*PEP2+X2I*PET2+X3I*PZT2
1032      PP(5)=Y1I*PEP2+Y2I*PET2+Y3I*PZT2
1033      PP(6)=Z1I*PEP2+Z2I*PET2+Z3I*PZT2
1034      PP(7)=X1I*PEP3+X2I*PET3+X3I*PZT3
1035      PP(8)=Y1I*PEP3+Y2I*PET3+Y3I*PZT3
1036      PP(9)=Z1I*PEP3+Z2I*PET3+Z3I*PZT3
1037      PP(10)=X1I*PEP4+X2I*PET4+X3I*PZT4
1038      PP(11)=Y1I*PEP4+Y2I*PET4+Y3I*PZT4
1039      PP(12)=Z1I*PEP4+Z2I*PET4+Z3I*PZT4
1040      PP(13)=X1I*PEP5+X2I*PET5+X3I*PZT5
1041      PP(14)=Y1I*PEP5+Y2I*PET5+Y3I*PZT5
1042      PP(15)=Z1I*PEP5+Z2I*PET5+Z3I*PZT5
1043      PP(16)=X1I*PEP6+X2I*PET6+X3I*PZT6
1044      PP(17)=Y1I*PEP6+Y2I*PET6+Y3I*PZT6
1045      PP(18)=Z1I*PEP6+Z2I*PET6+Z3I*PZT6
1046      PP(19)=X1I*PEP7+X2I*PET7+X3I*PZT7
1047      PP(20)=Y1I*PEP7+Y2I*PET7+Y3I*PZT7
1048      PP(21)=Z1I*PEP7+Z2I*PET7+Z3I*PZT7
1049      PP(22)=X1I*PEP8+X2I*PET8+X3I*PZT8
1050      PP(23)=Y1I*PEP8+Y2I*PET8+Y3I*PZT8
1051      PP(24)=Z1I*PEP8+Z2I*PET8+Z3I*PZT8
1052      C FORM ELEMENT B MATRIX
1053      DO 10 I=1,6
1054      DO 10 J=1,24
1055      10 EBM(I,J)=0.0
1056      DO 30 J=1,22,3
1057      EBM(4,J)=PP(J+1)
1058      EBM(6,J)=PP(J+2)
1059      30 EBM(1,J)=PP(J)
1060      DO 31 J=2,23,3
1061      EBM(4,J)=PP(J-1)
1062      EBM(5,J)=PP(J+1)
1063      31 EBM(2,J)=PP(J)
1064      DO 32 J=3,24,3
1065      EBM(5,J)=PP(J-1)
1066      EBM(6,J)=PP(J-2)
1067      32 EBM(3,J)=PP(J)
1068      C FORM ELEMENT STRESS MATRIX
1069      DO 50 I=1,6
1070      DO 50 J=1,24
1071      ESM(I,J)=0.0
1072      DO 50 K=1,6
1073      50 ESM(I,J)=ESM(I,J)+ECM(I,K)*EBM(K,J)
1074      IF (KOP.EQ.1) GO TO 51
1075      IF (L.NE.44) GO TO 16
1076      DO 52 I=1,6
1077      SIGEL(I)=0.0
1078      DO 52 J=1,24
1079      52 SIGEL(I)=SIGEL(I)+ESM(I,J)*ELDISP(J)
1080      DO 510 I=1,6
1081      STRN(I)=0.0

```



```

1082      DO 500 J=1,24
1083      500 STRN(I)=STRN(I)+EBM(I,J)*ELDISP(J)
1084      STRN(I)=STRN(I)*100.
1085      510 CONTINUE
1086      GO TO 80
1087      16 IF(KOEL(M).EQ.0) GO TO 82
1088      IF(KOEL(M).EQ.3) GO TO 82
1089      N=NP(L-44,M)
1090      KOUNT(N)=KOUNT(N)+1
1091      DO 83 I=1,6
1092      DO 83 J=1,24
1093      83 SIGA(N,I)=SIGA(N,I)+ESM(I,J)*ELDISP(J)
1094      DO 84 I=1,3
1095      DO 84 J=1,24
1096      84 STN(N,I)=STN(N,I)+EBM(I,J)*ELDISP(J)
1097      25 CONTINUE
1098      GO TO 15
1099      82 N=NP(L,M)
1100      KOUNT(N)=KOUNT(N)+1
1101      DO 35 I=1,6
1102      DO 35 J=1,24
1103      35 SIGA(N,I)=SIGA(N,I)+ESM(I,J)*ELDISP(J)
1104      DO 36 I=1,3
1105      DO 36 J=1,24
1106      36 STN(N,I)=STN(N,I)+EBM(I,J)*ELDISP(J)
1107      20 CONTINUE
1108      GO TO 15
1109      51 IF(KOEL(M).LE.1) GO TO 55
1110      C FORM ELEMENT STIFFNESS MATRIX THREE POINT INTEGRATION
1111      DO 61 I=1,24
1112      DO 61 J=1,24
1113      DO 61 K=1,6
1114      61 ESTIF(I,J)=ESTIF(I,J)+AQ(L)*EBM(K,I)*ESM(K,J)*DETJ
1115      VOL=VOL+AQ(L)*DETJ
1116      WT=VOL*RO( M)/8.
1117      22 CONTINUE
1118      GO TO 80
1119      C FORM ELEMENT STIFFNESS MATRIX TWO POINT INTEGRATION
1120      55 DO 60 I=1,24
1121      DO 60 J=1,24
1122      DO 60 K=1,6
1123      60 ESTIF(I,J)=ESTIF(I,J)+EBM(K,I)*ESM(K,J)*DETJ
1124      VOL=VOL+DETJ
1125      WT=VOL*RO( M)/8.
1126      21 CONTINUE
1127      GO TO 80
1128      75 WRITE(6,1000)M
1129      CALL EXIT
1130      RETURN
1131      C
1132      C
1133      1000 FORMAT (1H1, 18H VOLUME OF ELEMENT ,I4, 18H IS LESS THAN ZERO)
1134      END
1135      C
1136      SUBROUTINE STRESS(AP,STIF,APL,APR,STIFL,STIFR,MB1,MB2,LA,LA2)
1137      C
1138      C THIS SUBROUTINE FORMS THE ELEMENT STRESS MATRIX (ESM),MULTIPLIES BY
1139      C THE ELEMENT DISPLACEMENT VECTOR (ELDISP)AND RECORDS THE STRESSES IN
1140      C SIGEL (BY CALLING ELSTIF). IT THEN COMPUTES PRINCIPAL STRESSES AND
1141      C STRAINS FOR ELEMENTS AND NODAL STRESSES.

```



```

1142      C
1143      COMMON NANLYS,KSHIFT, R0(350),X(450),Y(450),Z(450),U(450),V(450),
1144      1W(450),SGTEL(350,6),SGTPS(350,7),STRNT(350,6),STNT(450,3),
1145      2 ECMI(3,3),STRN(6),ESTIF(24,24),ECM(6,6),EBM(6,24),ESM(6,24),WT
1146      COMMON NUMNP,NUMEL, NE2, KODE(450),SGTNP(450,6),
1147      1NP(8,350),MAT(350),MBAND,NEQ,M,LM(24),KOEL(350),
1148      2PSY(52),ETA(52),ZTA(52),AQ(43),PP(24),ELDISP(24),
1149      3KOUNT(450),SIGA(450,6),STN(450,3),SIGEL(6),SIGP(7),NUMBLK,
1150      4 DISPX(450),DISPY(450),DISPZ(450)
1151      COMMON FBULK(350),EDEV(350),NITER,ITOPT,ACDEF(5),BCDEF(5),STP(3)
1152      COMMON/AREA1/ST(20,5),SL(10,5),SD(20,10,5),VS(20,10,5),NUMAT,NCELP
1153      1,CONFAC,NSTRN
1154      DIMENSION AP(NE2),STIF(MB1,MB2),APL(MB1),APR(MB1),STIFL(LA2),
1155      1STIFR(LA)
1156      C
1157      DO 5 N=1,NUMNP
1158      KOUNT(N)=0
1159      DO 5 J=1,6
1160      5 SIGA(N,J)=0.0
1161      DO 6 N=1,NUMNP
1162      DO 6 J=1,3
1163      6 STN(N,J)=0.0
1164      C
1165      SIG1=0.0
1166      SIG2=0.0
1167      SIG3=0.0
1168      M1=0
1169      M2=0
1170      M3=0
1171      C
1172      WRITE(6,2000)
1173      DO 100 M=1,NUMEL
1174      C COMPUTE ELEMENT DISPLACEMENTS
1175      C
1176      DO 10 I=1,8
1177      I2=3*I
1178      LMI2=3*NP(I,M)
1179      ELDISP(I2)=AP(LMI2)
1180      ELDISP(I2-1)=AP(LMI2-1)
1181      10 ELDISP(I2-2)=AP(LMI2-2)
1182      C
1183      C COMPUTE ELEMENT STRESSES
1184      C
1185      MAT(M)=IABS(MAT(M))
1186      CALL ELSTIF(AP,STIF,APL,APR,STIFL,STIFR,MB1,MB2,LA,LA2,2)
1187      DO 15 I=1,6
1188      15 SGTEL(M,I)=SGTEL(M,I)+SIGEL(I)
1189      C
1190      DO 500 I=1,6
1191      500 STRNT(M,I)=STRNT(M,I)+STRN(I)
1192      WRITE(6,2010)M,(SGTEL(M,I),I=1,6), (STRNT(M,I),
1193      1I=1,3)
1194      C
1195      C COMPUTE ELEMENT PRINCIPAL STRESSES AND PRINCIPAL STRAINS
1196      C
1197      T1=SGTEL(M,1)+SGTEL(M,2)+SGTEL(M,3)
1198      T2=SGTEL(M,1)*SGTEL(M,2)+SGTEL(M,2)*SGTEL(M,3)+SGTEL(M,3)*SGTEL(M,
1199      11)-SGTEL(M,4)**2-SGTEL(M,5)**2-SGTEL(M,6)**2
1200      T3=SGTEL(M,1)*SGTEL(M,2)*SGTEL(M,3)+2.*SGTEL(M,4)*SGTEL(M,5)*
1201      1SGTEL(M,6)-SGTEL(M,1)*(SGTEL(M,5)**2-SGTEL(M,2)*(SGTEL(M,6)**2)

```



```

1202      2-SGTEL(M,3)*(SGTEL(M,4)**2)
1203      CSOLUTION OF CUBIC EQUATION BY NEWTON METHOD
1204      IF (ABS(T3).LE.1.E-50) GO TO 36
1205      S=0.0
1206      DO 31 I=1,20
1207      FS=S**3-T1*(S**2)+T2*S-T3
1208      FPR=3.*(S**2)-2.*T1*S+T2
1209      IF (ABS(FPR).LE.1.E-30) GO TO 12
1210      GO TO 11
1211      12 WRITE(6,2060) FPR
1212      FPR=1.0
1213      11 X1=S-FS/FPR
1214      IF (ABS(X1-S).LT.1.E-6) GO TO 32
1215      31 S=X1
1216      32 T4=(T1-X1)/2.
1217      T5=SQRT(((T1-X1)**2)/4.-T3/X1)
1218      36 IF (ABS(T3).LE.1.E-50) T4=T1/2.
1219      IF (ABS(T3).LE.1.E-50) T5=SQRT((T1**2)/4.-T2)
1220      IF (ABS(T3).LE.1.E-50) X1=0.0
1221      X2=T4+T5
1222      X3=T4-T5
1223      SIGP(1)=X1
1224      SIGP(2)=X2
1225      SIGP(3)=X3
1226      C PRINCIPAL STRESSES ARRANGED IN ORDER
1227      DO 33 I=1,2
1228      JJ=3-I
1229      DO 34 J=1,JJ
1230      IF (SIGP(J).LT.SIGP(J+1)) GO TO 35
1231      GO TO 34
1232      35 X4=SIGP(J)
1233      X5=SIGP(J+1)
1234      SIGP(J+1)=X4
1235      SIGP(J)=X5
1236      34 CONTINUE
1237      33 CONTINUE
1238      C COMPUTE MAXIM. SHEAR STRESS
1239      SIGP(4)=(SIGP(1)-SIGP(3))/2.
1240      DO 20 I=1,4
1241      20 SGTPS(M,I)=SIGP(I)
1242      T1=STRNT(M,1)+STRNT(M,2)+STRNT(M,3)
1243      T2=STRNT(M,1)*STRNT(M,2)+STRNT(M,2)*STRNT(M,3)+STRNT(M,3)*STRNT(M,
1244      11)-0.25*(STRNT(M,4)**2+STRNT(M,5)**2+STRNT(M,6)**2)
1245      T3=STRNT(M,1)*STRNT(M,2)*STRNT(M,3)+0.25*(STRNT(M,4)*STRNT(M,5)*ST
1246      1RNT(M,6)-STRNT(M,1)*(STRNT(M,5)**2)-STRNT(M,2)*(STRNT(M,6)**2)-
1247      2STRNT(M,3)*(STRNT(M,4)**2))
1248      IF (ABS(T3).LE.1.E-50) GO TO 536
1249      S=0.0
1250      DO 531 I=1,20
1251      FS=S**3-T1*(S**2)+T2*S-T3
1252      FPR=3.*(S**2)-2.*T1*S+T2
1253      IF (ABS(FPR).LE.1.E-30) GO TO 512
1254      GO TO 511
1255      512 WRITE(6,2060) FPR
1256      FPR=1.0
1257      511 X1=S-FS/FPR
1258      IF (ABS(X1-S).LT.1.E-6) GO TO 532
1259      531 S=X1
1260      532 T4=(T1-X1)/2.
1261      T5=SQRT(((T1-X1)**2)/4.-T3/X1)

```



```

1262      536 IF(ABS(T3).LE.1.E-50) T4=T1/2.
1263      IF(ABS(T3).LE.1.E-50) T5=SQRT((T1**2)/4.-T2)
1264      IF(ABS(T3).LE.1.E-50) X1=0.0
1265      X2=T4+T5
1266      X3=T4-T5
1267      STP(1)=X1
1268      STP(2)=X2
1269      STP(3)=X3
1270      C PRINCIPAL STRAINS ARRANGED IN ORDER
1271      DO 533 I=1,2
1272      JJ=3-I
1273      DO 534 J=1,JJ
1274      IF(STP(J).LT.STP(J+1)) GO TO 535
1275      GO TO 534
1276      535 X4=STP(J)
1277      X5=STP(J+1)
1278      STP(J+1)=X4
1279      STP(J)=X5
1280      534 CONTINUE
1281      533 CONTINUE
1282      DO 520 I=1,3
1283      J=I+4
1284      520 SGTPS(M,J)=STP(I)
1285      IF(ITOPT.EQ.0) GO TO 350
1286      IF(NITER.EQ.2) GO TO 350
1287      DO 200 I=1,6
1288      200 SGTEL(M,I)=SGTEL(M,I)-SIGEL(I)
1289      DO 201 I=1,6
1290      201 STRNT(M,I)=STRNT(M,I)-STRN(I)
1291      C
1292      C FIND MAXIMUM ELEMENT STRESSES
1293      350 IF(SGTPS(M,1).LT.SIG1) GO TO 115
1294      SIG1=SGTPS(M,1)
1295      M1=M
1296      115 IF(SGTPS(M,3).GT.SIG2) GO TO 120
1297      SIG2=SGTPS(M,3)
1298      M2=M
1299      120 IF(SGTPS(M,4).LT.SIG3) GO TO 100
1300      SIG3=SGTPS(M,4)
1301      M3=M
1302      100 CONTINUE
1303      WRITE(6,2040) SIG1,M1,SIG2,M2,SIG3,M3
1304      WRITE(6,2001)
1305      WRITE(6,2002) (M,(SGTPS(M,I),I=1,7),M=1,NUMEL)
1306      C
1307      C FIND AVERAGE NODAL STRESSES AND STRAINS (%)
1308      DO 110 N=1,NUMNP
1309      RK=KOUNT(N)
1310      IF(RK.EQ.0.0) GO TO 110
1311      DO 116 I=1,6
1312      SIGA(N,I)= SIGA(N,I)/RK
1313      116 CONTINUE
1314      110 CONTINUE
1315      DO 111 N=1,NUMNP
1316      RP=KOUNT(N)
1317      IF(RP.EQ.0.0) GO TO 111
1318      DO 117 I=1,3
1319      STN(N,I)=100.*STN(N,I)/RP
1320      117 CONTINUE
1321      111 CONTINUE

```



```

1322      WRITE(6,2050)
1323      DO 27 N=1,NUMNP
1324      IF(KOUNT(N).EQ.0) GO TO 27
1325      DO 25 I=1,6
1326      25  SGTNP(N,I)=SGTNP(N,I)+SIGA(N,I)
1327      DO 26 J=1,3
1328      26  STNT(N,J)=STNT(N,J)+STN(N,J)
1329      WRITE(6,2055) N,SGTNP(N,1),SGTNP(N,2),SGTNP(N,3),SGTNP(N,4),SGTNP(
1330      N,5),SGTNP(N,6),STNT(N,1),STNT(N,2),STNT(N,3)
1331      IF(ITOPT.EQ.0) GO TO 27
1332      IF(NITER.EQ.2) GO TO 27
1333      DO 250 I=1,6
1334      250  SGTNP(N,I)=SGTNP(N,I)-SIGA(N,I)
1335      DO 251 J=1,3
1336      251  STNT(N,J)=STNT(N,J)-STN(N,J)
1337      27  CONTINUE
1338      RETURN
1339  C
1340      2000 FORMAT('1',10X,'ELEMENT STRESSES'////,'ELEM  SIGMA X      SIGMA Y
1341      1  SIGMA Z      SIGMAXY      SIGMAZY      SIGMAZX      STRAINXX      ST
1342      2RAINYY      STRAINZZ'///)
1343      2010 FORMAT(I4, 9E12.5)
1344      2001 FORMAT('1',10X,'PRINCIPAL STRESSES'////,'ELEM  SIGMA 3      SIGMA 2
1345      1  SIGMA 1      MAXSHEAR      STRAIN3  1 STRAIN2      STRAIN1'///)
1346      2002 FORMAT(I4,7E12.5)
1347      2040 FORMAT(1H1,
1348      1 27H MAXIMUM PRINCIPAL STRESS = ,E15.5,19H AND OCCURS IN ELEM,I6//
1349      2 27H MINIMUM PRINCIPAL STRESS = ,E15.5,19H AND OCCURS IN ELEM,I6//
1350      3 27H MAXIMUM SHEAR STRESS   = ,E15.5,19H AND OCCURS IN ELEM,I6//
1351      2050 FORMAT('1',10X,'AVERAGE NODAL STRESS'////,'NODE  SIGMA X      SIGMA
1352      1Y      SIGMA Z      SIGMA XY      SIGMA YZ      SIGMA ZX      STRAINX
1353      2  STRAINY      STRAINZ'///)
1354      2055 FORMAT(I4,9E12.5)
1355      2060 FORMAT(E12.5)
1356  C
1357      END
1358  C
1359  C
1360      SUBROUTINE MODIFY (AP,STIF,APL,APR,STIFL,STIFR,MB1,MB2,LA,LA2,I,N)
1361  C
1362  C THIS SUBROUTINE MODIFIES THE TOTAL STIFFNESS MATRIX AND LOAD VECTOR
1363  C FOR DISPLACEMENT BOUNDARY CONDITIONS.
1364  C
1365      COMMON NANLYS,KSHIFT, RO(350),X(450),Y(450),Z(450),U(450),V(450),
1366      1W(450),SGTEL(350,6),SGTPS(350,7),STRNT(350,6),STNT(450,3),
1367      2 ECMI(3,3),STRN(6),ESTIF(24,24),ECM(6,6),EBM(6,24),ESM(6,24),WT
1368      COMMON NUMNP,NUMEL, NE2, KODE( 450),SGTNP(450,6),
1369      1NP(8, 350),MAT( 350),MBAND,NEQ,M,LM(24),KOEL( 350),
1370      2PSY(52),ETA(52),ZTA(52),AQ(43),PP(24),ELDISP(24),
1371      3KOUNT( 450),SIGA( 450,6),STN( 450,3),SIGEL(6),SIGP(7),NUMBLK,
1372      4  DISPX(450),DISPY(450),DISPZ(450)
1373      COMMON EBULK(350),EDEV(350),NITER,ITOPT,ACOE( 5),BCOEF( 5),STP(3)
1374      COMMON/AREA1/ST(20,5),SL(10,5),SD(20,10,5),VS(20,10,5),NUMAT,NCELP
1375      1,CONFAC,NSTRN
1376      DIMENSION AP(NE2),STIF(MB1,MB2),APL(MB1),APR(MB1),STIFL(LA2),
1377      1STIFR(LA)
1378  C
1379      DISP=U(N)
1380      IF((I-3*N+1+KSHIFT).EQ.0) DISP=V(N)
1381      IF((I-3*N+KSHIFT).EQ.0) DISP=W(N)

```



```

1382      C
1383      DO 50 J=2,MBAND
1384      IL=I+J-1
1385      IU=I-J+1
1386      IF(IU.LE.0)GO TO 10
1387      AP(IU)=AP(IU)-STIF(J,IU)*DISP
1388      STIF(J,IU)=0.0
1389      10  IF(IL.GT.NEQ) GO TO 50
1390      AP(IL)=AP(IL)-STIF(J,I)*DISP
1391      STIF(J,I)=0.0
1392      50  CONTINUE
1393      AP(I)=DISP
1394      STIF(1,I)=1.0
1395      RETURN
1396      C
1397      END
1398      C
1399      C
1400      SUBROUTINE BAND1(E,A,BL,BR,AL,AR,MB1,MB2,LA,LA2,FDUB)
1401      C
1402      C THIS SUBROUTINE SOLVES EQUATIONS IN BLOCKS USING GAUSSIAN ELIMINATION.
1403      C SYSTEM SUBROUTINES READ AND WRITE ARE CALLED FOR DATA TRANSFERS BETWEEN
1404      C CORE AND FILES. SYSTEM SUBROUTINES NOTE AND POINT ARE CALLED FOR BACK
1405      C SPACEING DATA IN FILE 1 DURING BACK SUBSTITUTION.
1406      C
1407      COMMON NANLYS,KSHIFT, RO(350),X(450),Y(450),Z(450),U(450),V(450),
1408      1W(450),SGTEL(350,6),SGTPS(350,7),STRNT(350,6),STNT(450,3),
1409      2 ECMI(3,3),STRN(6),ESTIF(24,24),ECM(6,6),EBM(6,24),ESM(6,24),WT
1410      COMMON NUMNP,NUMEL, NE2, KODE( 450),SGTNP(450,6),
1411      1NP(8, 350),MAT( 350),MM ,NEQ,M,LM(24),KOEL( 350),
1412      2PSY(52),ETA(52),ZTA(52),AQ(43),PP(24),ELDISP(24),
1413      3KOUNT( 450),SIGA( 450,6),STN( 450,3),SIGEL(6),SIGP(7),NUMBLK,
1414      4 DISPX(450),DISPY(450),DISPZ(450)
1415      COMMON EBULK(350),EDEV(350),NITER,ITOPT,ACOE( 5),BCOE( 5),STP(3)
1416      COMMON/AREA1/ST(20,5),SL(10,5),SD(20,10,5),VS(20,10,5),NUMAT,NCELP
1417      1,CONFAC,NSTRN
1418      DIMENSION INFO(4),INDEX(20)
1419      DIMENSION B(NE2),A(MB1,MB2),BL(MB1),BR(MB1),AL(LA2),AR(LA)
1420      INTEGER*2 LEN
1421      NBYTES=MM*MM*4
1422      FNUMRC=FLOAT(NBYTES)/32000
1423      NUMREC=NBYTES/32000
1424      IF((FNUMRC-NUMREC).GT.0.0) NUMREC=NUMREC+1
1425      600  FORMAT('ERROR FILE IN BAND1')
1426      NN=NEQ/2
1427      C
1428      C
1429      REWIND 1
1430      REWIND 2
1431      NB=0
1432      WRITE(6,1002)MM,NUMREC
1433      1002  FORMAT(2I10,E20.7)
1434      GO TO 50
1435      C
1436      C SHIFT BLOCK OF EQUATIONS
1437      C
1438      10  NB=NB+1
1439      DO 20 N=1,NN
1440      NM=NN+N
1441      B(N)=B(NM)

```



```

1442      B(NM)=0.0
1443      DO 20 M=1,MM
1444      A(M,N)= A(M,NM)
1445      A(M,NM)=0.0
1446 20 C
1447 C      READ EQUATIONS IN TO CORE
1448 C
1449      IF(NUMBLK-NB)50,60,50
1450 50 LL=1
1451      DO 500 L=1,NUMREC
1452      CALL READ(AR(LL),LEN,0,LD,2,C550)
1453      WRITE(6,1003) LEN,LL,MM,NUMREC,AR(LL)
1454      LL=LL+8000
1455      GO TO 500
1456 550 WRITE(6,600)
1457      STOP
1458 500 CONTINUE
1459      CALL READ (BR,LEN,0,LD,2,C550)
1460      WRITE(6,1002) LEN,NN,BR(1)
1461 1003 FORMAT(4I10,E20,7)
1462      IF(NB)60,10,60
1463 C
1464 C      REDUCE BLOCK OF EQUATIONS
1465 C
1466 60 DO 100 N=1,NN
1467      IF(A(1,N))65,100,C5
1468 65 B(N)=B(N)/A(1,N)
1469      DO 90 L=2,MM
1470      IF(A(L,N))70,90,70
1471 70 C=A(L,N)/A(1,N)
1472      I=N+L-1
1473      J=0
1474      DO 80 K=L,MM
1475      J=J+1
1476 80 A(J,I)=A(J,I)-C*A(K,N)
1477      B(I)=B(I)-A(L,N)*B(N)
1478      A(L,N)=C
1479 90 CONTINUE
1480 100 CONTINUE
1481      WRITE(6,1000) NB
1482      CALL TIME(1,1)
1483 C
1484 C      WRITE BLOCK OF REDUCED EQUATIONS
1485 C
1486      IF(NUMBLK-NB)110,120,110
1487 110 CONTINUE
1488      CALL NOTE(FDUB,INFO)
1489      INDEX(NB)=INFO(2)
1490      LEN=32000
1491      LL=1
1492      DO 700 L=1,NUMREC
1493      IF(L.EQ.NUMREC)LEN=NBYTES-((NUMREC-1)*32000)
1494      CALL WRITE(AL(LL),LEN,0,1,FDUB,C550)
1495      WRITE(6,1002) LL,LEN,AL(LL)
1496      LL=LL+8000
1497 700 CONTINUE
1498      LEN=MM*4
1499      CALL WRITE(BL,LEN,0,1,FDUB,C550)
1500      WRITE(6,1002) LL,LEN,BL(1)
1501      GO TO 10

```



```

1502      C
1503      C      BACK SUBSTITUTION
1504      C
1505      120  DO 140 M=1,NN
1506           N=NN+1-M
1507           DO 130 K=2,MM
1508              L=N+K-1
1509      130  B(N)=B(N)-A(K,N)*B(L)
1510           NM=N+NN
1511           B(NM)=B(N)
1512      140  A(NB,NM)=B(N)
1513           WRITE(6,1001) NB
1514           CALL TIME(1,1)
1515           NB=NB-1
1516           IF(NB)150,160,150
1517      150  CONTINUE
1518           INFO(1)=INDEX(NB)
1519           CALL POINT(FDUB,INFO,1)
1520           LL=1
1521           DO 800 L=1,NUMREC
1522              CALL READ(AL(LL),LEN,0,LZ,FDUB,&550)
1523              WRITE(6,1002) LL,LEN,AL(LL)
1524              LL=LL+8000
1525      800  CONTINUE
1526              CALL READ(BL,LEN,0,LZ,FDUB,&550)
1527              WRITE(6,1002) LL,LEN,BL(1)
1528              GO TO 120
1529      C
1530      C      ORDER UNKNOWNNS IN B ARRAY
1531      C
1532      160  K=0
1533           NUMEQ=3*NUMNP
1534           DO 180 NB=1,NUMBLK
1535              DO 180 N=1,NN
1536                 NM=N+NN
1537                 K=K+1
1538                 IF(K.GT.NUMEQ) GO TO 190
1539      180  B(K)=A(NB,NM)
1540      190  RETURN
1541      C
1542      1000  FORMAT(//10X,'EQUATIONS REDUCED IN BLOCK NUMBER=',I5//)
1543      1001  FORMAT(//10X,'BACK SUBSTITUTION COMPLETED IN BLOCK NUMBER=',I5//)
1544      END
END OF FILE

```


APPENDIX C

ELEMENT STIFFNESS FORMULATION FOR
ISOPARAMETRIC HEXAHEDRONC.1 Scope

This appendix contains the element stiffness formulation for an isoparametric, eight-node hexahedral element with 24 degrees of freedom. The formulation given here is essentially based on the one described by Clough (1969).

C.2 Interpolation Functions

An isoparametric element is the one in which the displacements and the geometry of the element are described by the same interpolation functions. It can be shown that such an element with a proper choice of the interpolation functions, satisfies the necessary requirements for the convergence of the finite element solution to the correct answer (Zienkiewicz et al., 1969). For the eight node hexhedron shown in Fig. C.1 the relationship between the local coordinates (ξ, η, ζ) of the parent element and the global cartisian coordinates (x, y, z) of the element is provided by a set of linear interpolation functions as:

$$\begin{Bmatrix} x \\ y \\ z \end{Bmatrix} = \begin{bmatrix} N & 0 & 0 \\ 0 & N & 0 \\ 0 & 0 & N \end{bmatrix} \begin{Bmatrix} \bar{x} \\ \bar{y} \\ \bar{z} \end{Bmatrix} \quad (C.1)$$

in which \bar{x} , \bar{y} , and \bar{z} are the coordinates of the eight nodes of the element (Fig. C.1(b)) expressed in Cartesian global coordinate system as:

$$\begin{aligned}\bar{x}^T &= \langle x_1 x_2 \quad \dots \quad x_i \quad \dots \quad x_8 \rangle \\ \bar{y}^T &= \langle y_1 y_2 \quad \dots \quad y_i \quad \dots \quad y_8 \rangle \\ \bar{z}^T &= \langle z_1 z_2 \quad \dots \quad z_i \quad \dots \quad z_8 \rangle ,\end{aligned}$$

and

$$N = \langle N_1 N_2 \quad \dots \quad N_i \quad \dots \quad N_8 \rangle .$$

The linear interpolation functions are expressed in terms of the local coordinates of the parent element as:

$$N_i = 1/8(1 + \xi\xi_i)(1 + \eta\eta_i)(1 + \zeta\zeta_i) , \quad (C.2)$$

in which ξ_i , η_i and ζ_i are the coordinates of the eight nodes of the parent element as shown in Fig. C.1(a). According to the definition of an isoparametric element the displacements $(u,v,w,)$ of the element should be expressed by the same interpolation functions used to describe the geometry. By analogy with Eq. C.1 the displacements are expressed as:

$$\begin{Bmatrix} u \\ v \\ w \end{Bmatrix} = \begin{bmatrix} N & 0 & 0 \\ 0 & N & 0 \\ 0 & 0 & N \end{bmatrix} \begin{Bmatrix} \bar{u} \\ \bar{v} \\ \bar{w} \end{Bmatrix} \quad (C.3)$$

where \bar{u} , \bar{v} , \bar{w} are the nodal displacement vectors expressed as:

$$\begin{aligned}\bar{u}^T &= \langle u_1 u_2 \quad \dots \quad u_i \quad \dots \quad u_8 \rangle \\ \bar{v}^T &= \langle v_1 v_2 \quad \dots \quad v_i \quad \dots \quad v_8 \rangle \\ \bar{w}^T &= \langle w_1 w_2 \quad \dots \quad w_i \quad \dots \quad w_8 \rangle .\end{aligned}$$

C.3 Element Stiffness Evaluation

The element strains are expressed in terms of the nodal displacements by performing the appropriate differentiation on Eq. C.3. The resulting expression is:

$$\left\{ \begin{array}{c} \epsilon_{xx} \\ \epsilon_{yy} \\ \epsilon_{zz} \\ \gamma_{xy} \\ \gamma_{yz} \\ \gamma_{zx} \end{array} \right\} = \left[\begin{array}{ccc} \frac{\partial N}{\partial x} & 0 & 0 \\ 0 & \frac{\partial N}{\partial y} & 0 \\ 0 & 0 & \frac{\partial N}{\partial z} \\ \frac{\partial N}{\partial y} & \frac{\partial N}{\partial x} & 0 \\ 0 & \frac{\partial N}{\partial z} & \frac{\partial N}{\partial y} \\ \frac{\partial N}{\partial z} & 0 & \frac{\partial N}{\partial x} \end{array} \right] \left\{ \begin{array}{c} \bar{u} \\ \bar{v} \\ \bar{w} \end{array} \right\} \quad (C.4)$$

Eq. C.4 can be expressed in the abbreviated form as:

$$\{\epsilon\} = [B] \{\bar{r}\} . \quad (C.5)$$

The derivatives needed in the strain matrix of Eq. C.4 are obtained from:

$$\begin{Bmatrix} \frac{\partial N}{\partial x} \\ \frac{\partial N}{\partial y} \\ \frac{\partial N}{\partial z} \end{Bmatrix} = [J]^{-1} \begin{Bmatrix} \frac{\partial N}{\partial \xi} \\ \frac{\partial N}{\partial \eta} \\ \frac{\partial N}{\partial \zeta} \end{Bmatrix} \quad (C.6)$$

where $[J]$ is the Jacobian matrix which can in turn be obtained from:

$$[J] = \begin{bmatrix} \frac{\partial x}{\partial \xi} & \frac{\partial y}{\partial \xi} & \frac{\partial z}{\partial \xi} \\ \frac{\partial x}{\partial \eta} & \frac{\partial y}{\partial \eta} & \frac{\partial z}{\partial \eta} \\ \frac{\partial x}{\partial \zeta} & \frac{\partial y}{\partial \zeta} & \frac{\partial z}{\partial \zeta} \end{bmatrix} = \begin{Bmatrix} \frac{\partial N}{\partial \xi} \\ \frac{\partial N}{\partial \eta} \\ \frac{\partial N}{\partial \zeta} \end{Bmatrix} [\bar{x} \ \bar{y} \ \bar{z}] \quad (C.7)$$

By inverting $[J]$ obtained from Eq. C.7 and using Eq. C.6 and Eq. C.4 the strain matrix $[B]$ is evaluated. As the strain matrix is expressed in local coordinates, the integration necessary to evaluate the element stiffness has to be performed in the same local coordinates using the relationship for the elemental volume:

$$dv = dx \ dy \ dz = \det[J] \ d\xi \ d\eta \ d\zeta \quad (C.8)$$

The element stiffness can now be evaluated from:

$$[K] = \int_V [B]^T [C][B]dv = \int_{-1}^1 \int_{-1}^1 \int_{-1}^1 [B]^T [C][B] \det[J] d\xi d\eta d\zeta \quad (C.9)$$

where $[C]$ the constitutive matrix given by:

$$[C] = \frac{E}{(1+\nu)(1-2\nu)} \begin{bmatrix} 1-\nu & \nu & \nu & 0 & 0 & 0 \\ \nu & 1-\nu & \nu & 0 & 0 & 0 \\ \nu & \nu & 1-\nu & 0 & 0 & 0 \\ 0 & 0 & 0 & \frac{1-2\nu}{2} & 0 & 0 \\ 0 & 0 & 0 & 0 & \frac{1-2\nu}{2} & 0 \\ 0 & 0 & 0 & 0 & 0 & \frac{1-2\nu}{2} \end{bmatrix} \quad (C.10)$$

The integrations are performed numerically using Gaussian quadrature formulae.

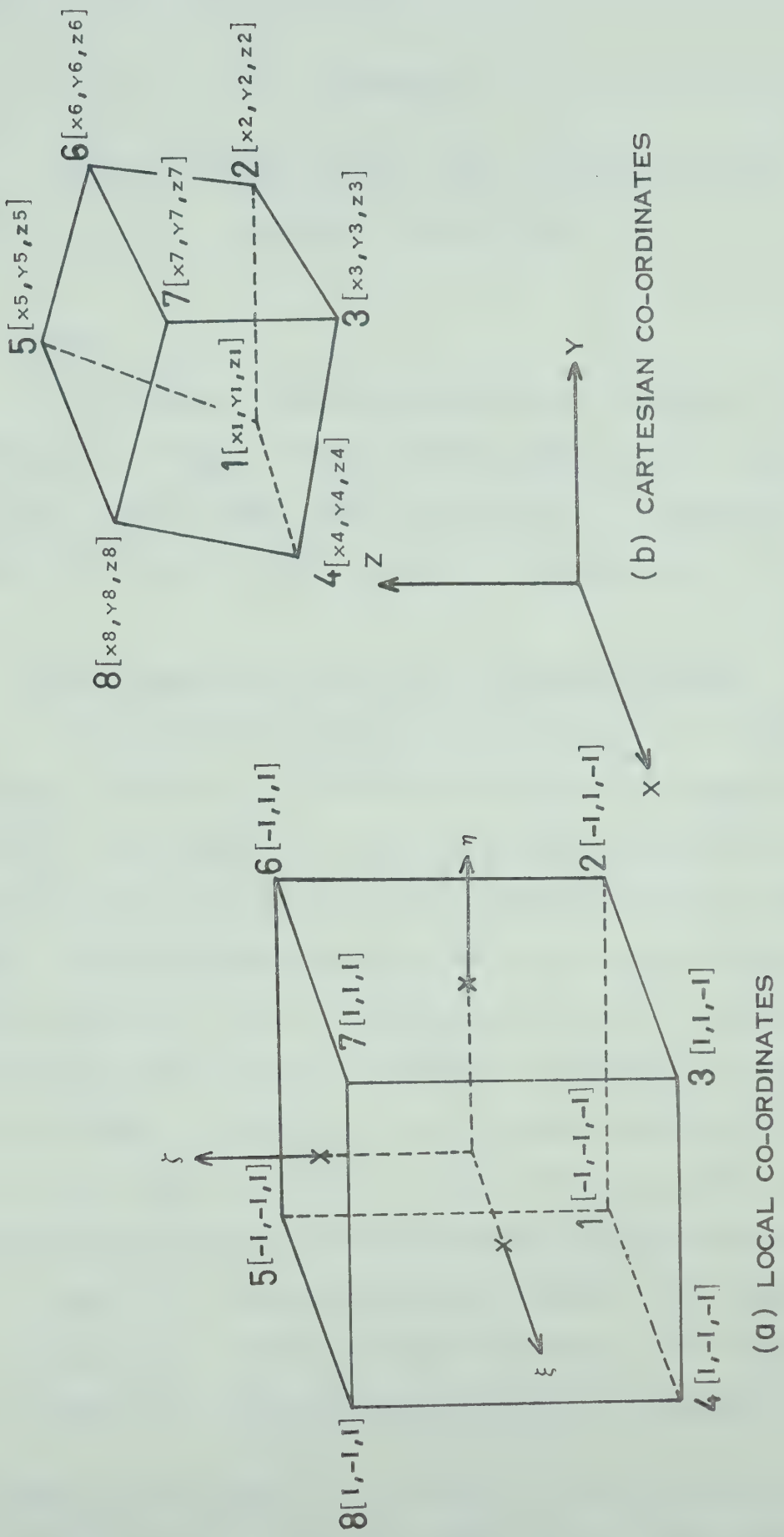


FIG. C.1 EIGHT NODE HEXAHEDRON REPRESENTATION IN LOCAL AND CARTESIAN CO-ORDINATES

APPENDIX D

FINITE ELEMENT METHOD FOR THE ANALYSIS OF
INDIRECT TENSION TESTD.1 Scope

This appendix describes the main features of a two dimensional finite element method used for the analysis of an indirect tension test when the material is assumed to be bilinear, having different moduli in compression and tension.

D.2 Basic Considerations for a Bilinear Material

A finite element method for solving two dimensional problems involving a bilinear material was suggested by Wilson (1963). The method that uses a successive approximation technique can be handled very conveniently by the two dimensional finite element program that uses an iterative equation solver (Wilson, 1963). The program given in Appendix A was modified by the author, following the procedure suggested by Wilson (1963), to consider the bilinear property of material.

A bilinear material has the following three possible stress-strain relationships depending on the stress state:

- Type I - Both principal stresses are compressive
- Type II - Both principal stresses are tensile
- Type III - One principal stress is compressive while the other is tensile.

For Type I and Type II the stress-strain relationship in x-y coordinate system is of the normal form. For Type III the

stress-strain relationship is a function of the angle of inclination of the major principal stress with the x-axis. In terms of the principal coordinate system the stress-strain relationship is written as:

$$\{\bar{\sigma}\} = [\bar{c}] \{\bar{\epsilon}\} \quad (D.1)$$

where $[\bar{c}]$ is given by Eq. 2.7 of Chapter II. If $\{\sigma\}$ and $\{\epsilon\}$ represent stresses and strains in x-y coordinate system then

$$\{\bar{\epsilon}\} = [T]^T \{\epsilon\} \quad (D.2)$$

$$\{\sigma\} = [T] \{\bar{\sigma}\} \quad (D.3)$$

with $[T]$, the transformation matrix, given by:

$$[T] = \begin{bmatrix} \cos^2 \theta & \sin^2 \theta & 2 \sin \theta \cos \theta \\ \sin^2 \theta & \cos^2 \theta & -2 \sin \theta \cos \theta \\ -\sin \theta \cos \theta & \sin \theta \cos \theta & \cos^2 \theta - \sin^2 \theta \end{bmatrix} \quad (D.4)$$

Since $\{\sigma\} = [c] \{\epsilon\}$ the constitutive matrix in x-y coordinate system for a bilinear material is given as:

$$[C] = [T] [\bar{c}] [T]^T \quad (D.5)$$

In the finite element program the constitutive matrix for

Type III as given by Eq. D.5 is computed for an element considering the angle θ obtained from the previous solution.

D.3 Analysis of Indirect Tension Test

The finite element idealization of a quadrant of the circular section analyzed is shown in Fig. D.1. To start with the solution was obtained for $E_c/E_t = 1$ and for the assigned value of G/E_c . Before the next solution was attempted each element was assigned the appropriate constitutive matrix depending on the type to which it belongs. For Type III the constitutive matrix was obtained from Eq. D.5. The solution thus obtained for $E_c/E_t = 1$ was used to perform the necessary modifications for obtaining the next solution. The solution procedure was repeated until the stresses and displacements obtained in two successive solutions closely agree with each other. For the analyses performed the final solution could be obtained after 10 to 15 repetitions.

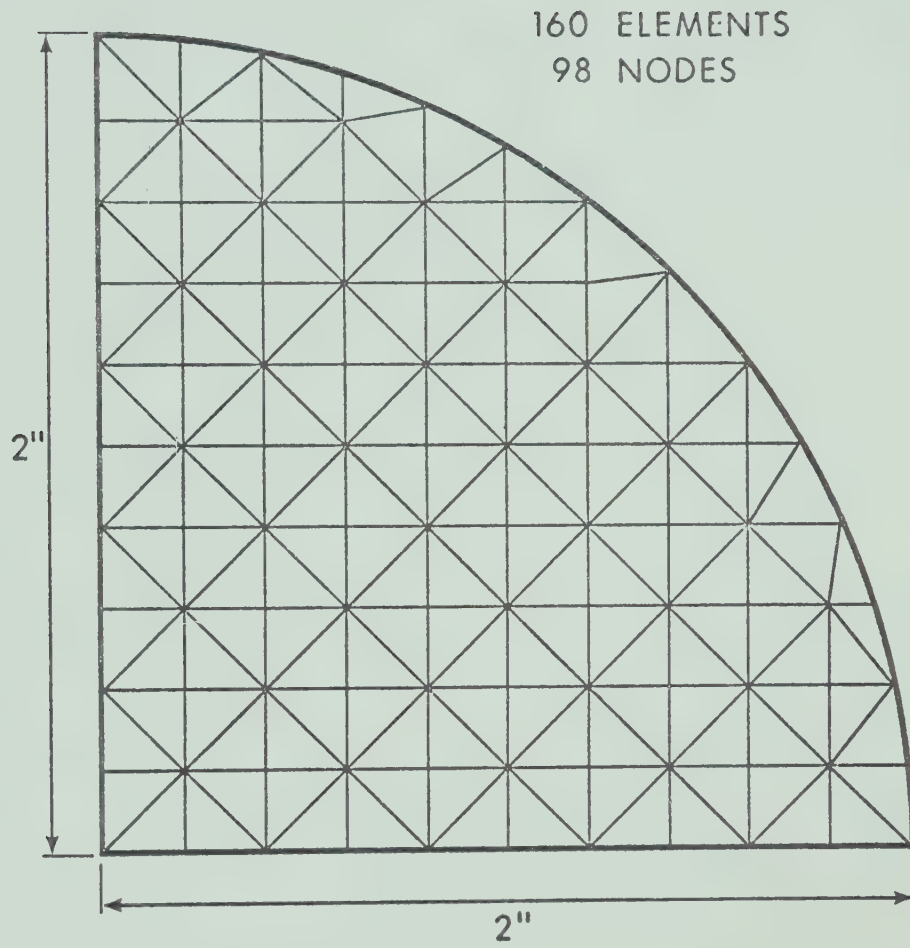


FIG. D.1 FINITE ELEMENT IDEALIZATION OF A QUADRANT
OF THE CIRCULAR SECTION ANALYSED

B30054